Hydrothermal synthesis and mineralogy of the alkali amphiboles

George Rowbotham

HYDROTHERMAL SYNTHESIS AND MINERALOGY OF THE ALKALI AMPHIBOLES

by: George Rowbotham,

Department of Geology,

Science Laboratories,

University of Durham.

Submitted for the degree of Doctor of Philosophy

at the University of Durham

December, 1973

Grey College

TABLE OF CONTENTS

Page

CHAPTER FOUR

CHEMISTRY OF THE ALKALI AMPHIBOLES

Page

CHAPTER FIVE

ALKALI AMPHIBOLES FROM THE ILÍMAUSSAQ INTRUSION, S.W. GREENLAND

CHAPTER SIX

ELECTRON MICROPROBE INVESTIGATIONS OF ALKALI AMPHIBOLES

APPENDICES

LIST OF FIGURES

LIST OF TABLES

LIST OF PLATES

ABSTRACT

The mineralogy of the alkali amphiboles is reviewed. Various suggestions are put forward to rationalise the nomenclature of these minerals.

Several alkali amphibole compositions have been successfully synthesized for the first time using hydrothermal synthesis techniques. The compositions of these minerals correspond to richterite-K, eckermannite-K and sundiusite-K. In addition five amphiboles of intermediate composition have been synthesized. Two of these minerals have compositions between richterite and tremolite indicating only partial 'A' site occupation.

Attempts to synthesize amphiboles of miyashiroite-K composition have failed to yield amphibole and the condensed product is a phyllosilicate.

A survey of all the available alkali amphibole analyses has revealed only two possible miscibility gaps in the alkali amphiboles, one in the area of the miyashiroite composition and the other in the ferroeckermannite field. Many of the analyses in the literature are of a suspect quality and various suggestions have been made to decide on the quality of an analysis.

A method of representing alkali amphiboles of intermediate composition has been found by using the substitutions in the Y sites which are balanced by substitutions in the Z and X sites. This method has revealed that there is complete solid solution between riebeckite and arfvedsonite, magnesioarfvedsonite and magnesioriebeckite, and richterite and eckermannite. A suggested nomenclature for these compositions has also been proposed.

Alkali amphiboles from the celebrated nepheline syenite of Ilímaussaq, S.W. Greenland have been analysed and these analyses reveal a compositional trend from close to katophorite to arfvedsonite. Electron microprobe analyses of alkali amphiboles from the saturated rocks of Tugtutôq, S.W. Greenland show a trend in compositions from ferrorichterite to riebeckite-arfvedsonite.

Arfvedsonites from the late-stage lujavrites of Ilímaussaq contain high concentrations of potassium. This element has been shown to be exchanged between amphibole and nepheline in these rocks.

Electron microprobe studies have shown the chemical variations within continuously and discontinuously zoned alkali amphiboles and in addition a study of co-existing glaucophane and hornblende has demonstrated that glaucophane develops around the hornblende as the rock retrogresses from the eclogite facies to the glaucophane schist facies.

X-ray diffraction studies of synthetic and natural alkali amphiboles demonstrate that the $a_o \sin\beta$ parameter is controlled by the occupants of the 'A' site and the octahedral sites. The b_o axis depends upon the M(4) and M(2) occupancy; and the β angle shows a strong positive correlation with the M(4) occupant and to a lesser extent the magnesium and potassium contents. The c_o axes of alkali amphiboles are longest in iron-rich compositions.

Infra-red spectroscopic studies indicate that it is possible to "fingerprint" the various alkali amphibole sub-groups. The presence of K^+ or Na^+ in the 'A' sites of synthetic alkali amphiboles raises the stretching frequency of adjacent OH groups by about 60 cm^{-1}. In natural amphiboles, however, the increase in frequency is only 20-40 cm^{-1}, due probably to the effects of substitutions such as F^- for OH^- and the presence of trivalent cations in M(1) and M(3).

ACKNOWLEDGEMENTS

Professors G. M. Brown and K. C. Dunham are gratefully acknowledged for the use of facilities provided by the Department of Geological Sciences at the University of Durham.

Mr. R. Phillips is sincerely thanked for his supervision and for reading the manuscript of this thesis. Dr. C. H. Emeleus and Dr. D. M. Hirst are also thanked for reading several chapters of the thesis.

Professor G. M. Brown and Dr. C. H. Emeleus are also thanked for their encouragement, advice, and help with several aspects of the research.

Various members of academic staff are thanked for help with the techniques used in the Department of Geological Sciences; Dr. J. G. Holland (X-ray fluorescence), Dr. C. H. Emeleus (electron microprobe), Mr. R. Brown (Chemistry Department - infra-red spectroscopy). Professor MacKenzie (Manchester University) is gratefully acknowledged for permission to use the high pressure apparatus at Manchester University and Dr. D. L. Hamilton is sincerely thanked for training in High Pressure techniques. Dr. D. Williams (Leeds University) and Dr. S. W. Richardson (Edinburgh) also ran some experiments at high temperatures. Dr. V. C. Farmer (Macauley Institute, Aberdeen) is thanked for some of the infra-red spectrograms.

The technical staff are also thanked for their help during the course of this work especially Mr. R. Lambert (Geochemistry Laboratory) and Mrs. Margaret Watson.

The following people are thanked for donating specimens:- Dr. D. C. Almond (Kingston Polytechnic), Dr. T. W. Bloxam (University

College, Swansea), Dr. J. R. Butler (Imperial College, London), Dr. J. J. de Cilliers, Dr. R. G. Coleman (U.S. Geological Survey), Dr. C. H. Emeleus, Professor W. G. Ernst (U.C.L.A.), Mr. P. G. Embrey (British Museum), Mr. P. B. Greenwood (I.G.S., London), Dr. A. A. Hodgson (Cape Asbestos Co. Ltd.), Dr. N. Holgate (University of Glasgow), Professor C. Klein (Harvard University), Dr. von Knorring (Leeds University), Dr. R. Macdonald (University of Lancaster), Dr. C. Milton (U.S. Geological Survey), Professor H. Neumann (Oslo University), Dr. S. Roy (Jadavpur University, Calcutta), Professor H. Sørenson (University of Copenhagen), Dr. V. Timbrell (Medical Research Council, Penarth), Dr. B. G. J. Upton (University of Edinburgh), Dr. J. Wadsworth (Manchester University), Dr. A. J. R. White (Australian National University).

Mrs. G. C. Robinson is sincerely thanked for her efficient typing of the manuscript.

Finally the Natural Environment Research Council is thanked for a research studentship.

CHAPTER ONE

INTRODUCTION

1-1. General remarks.

The word "amphibole" comes from the Greek "amphibolos" meaning ambiguous and was first coined by Haüy in 1801. Tschermak in 1871 first described the relationship between the amphiboles and the pyroxene group of minerals. Both Penfield (1890) and Schaller (1916) recognized that water was a part of the structure of tremolite and the latter was the first to derive the correct formula for this mineral.

The amphiboles have a very variable chemistry and this reflects a complex arrangement of cation sites of differing size and shape. These minerals can readily accommodate cations of ionic radii between about 0.40 and 1.40Å. All major elements of the earth's crust and mantle fall into this range but the cations enter the amphibole structure in an orderly manner.

Amphiboles are common rock-forming minerals and this group together with the pyroxenes form 17% by volume of the total of the minerals in the earth's crust. The amphiboles are ubiquitous and occur in igneous, metamorphic, metasomatic, and authigenic deposits and have recently been described from a meteoritic body, and from the Apollo XI rocks.

1-2. Aims of the present research.

The first aim was to attempt the synthesis of several alkali amphibole compositions which had previously not been investigated, and to determine the physical parameters of these phases. During the course of the research both hydroxy- and fluor-alkali amphiboles were synthesized.

These synthetic phases, together with previously published results, were used to determine the variations of the cell dimensions with crystal

chemistry. In addition many analysed alkali amphiboles from various parageneses were used to correlate cell parameters with crystal chemistry.

The chemistry of the alkali amphiboles is imperfectly known and all the analyses from the literature together with those of the author were plotted to locate any miscibility gaps in the alkali amphiboles. The various substitutions postulated by different authors were also tested.

The chemistry and physical parameters of alkali amphiboles from the celebrated Ilímaussaq intrusion, S.W. Greenland were determined, together with amphiboles from other plutonic bodies in the area.

The electron microprobe has been used to elucidate the relationships between co-existing and zoned amphiboles and infra-red spectroscopy has revealed the effect of alkali ions in the 'A' site of the amphiboles upon the hydroxyl stretching frequency.

Work on the amphibole group of minerals has greatly increased over the last decade but many gaps still exist in our knowledge of these minerals. Attempts have been made during this research to fill a few of these gaps relating to the alkali amphiboles. Physical and chemical data on the amphiboles has expanded so rapidly that it is necessary to give a comprehensive review of the state of knowledge of these minerals at the time of writing.

1-3. Structure of the amphiboles.

Penfield and Stanley (1908) from careful and detailed chemical analysis of certain amphiboles came to the conclusion that the amphibole group had a basic ring structure and they argued that it would be reasonable to speak of this structure in the same way as the benzene ring in organic chemistry. They thought of the structure as an amphibole acid and suggested a possible formula:-

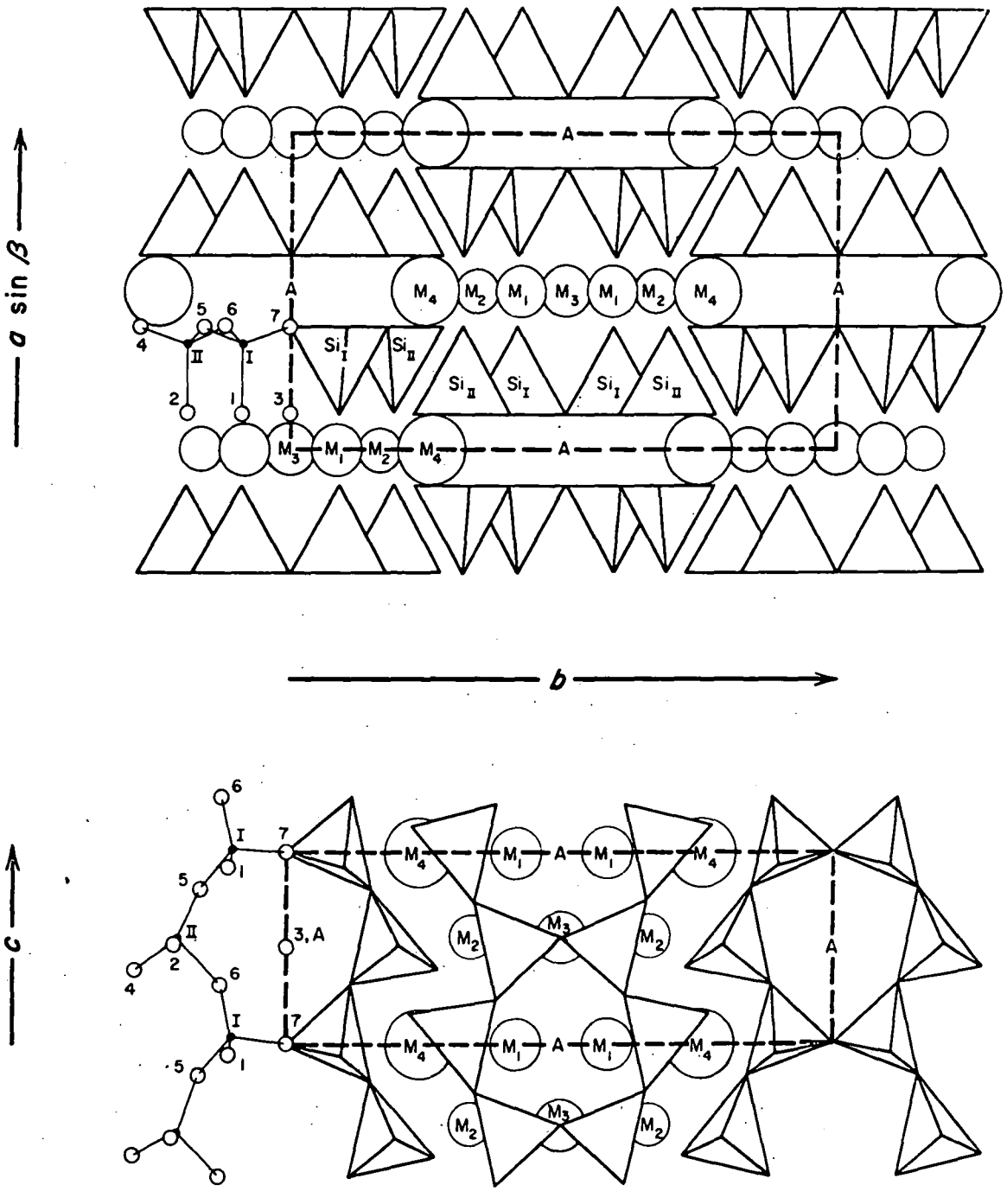

Fig. 1-1 Schematic diagram of the structure of the amphiboles, (after Ernst, 1968).

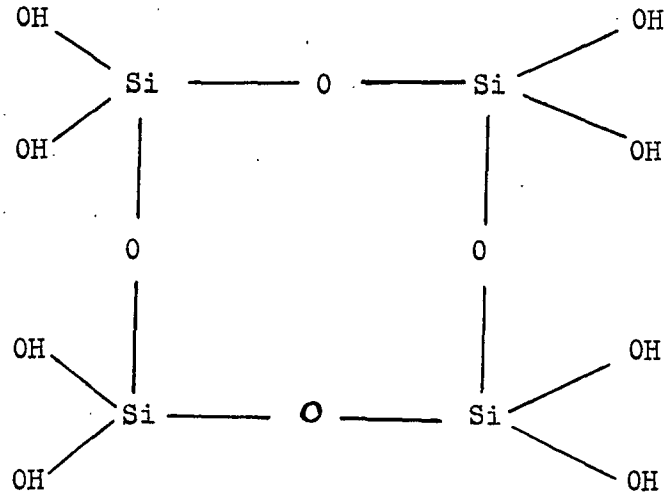

They were uncertain of the number of silicon atoms and hydroxyl ions in the structure.

Despite the work of Schaller (1916) the formula for tremolite was taken as $CaMg_3(SiO_4)_3$ and Winchell (1924) argued that the pyroxenes and amphiboles were so similar in their physical properties that you would expect the same "molecules" to occur in both groups.

Warren (1929) and Warren and Modell (1930) derived the structure of tremolite, the other monoclinic amphiboles and anthophyllite (an orthorhombic amphibole) from X-ray structure analysis. This structure was derived from that of diopside which Warren and Bragg (1928) had evaluated and diopside and tremolite were related thus:-

Diopside	Tremolite
$a_o = 9.71\text{Å}$	$a_o = 9.78\text{Å}$
$b_o = 8.89\text{Å}$	$b_o = 17.80\text{Å}$
$c_o = 5.24\text{Å}$	$c_o = 5.26\text{Å}$
$\beta = 105°50'$	$\beta = 106°02'$

Therefore the b_o dimension of tremolite is twice that of diopside.

The structure of the amphiboles is shown schematically in Fig. 1-1 from Ernst (1968). The structure consists of double chains of tetrahedrally

co-ordinated cations of infinite length parallel to the 'c' crystallographic axis. The tetrahedra share alternately two and three oxygens between consecutive tetrahedrally co-ordinated cations in the chains. The chain consists of six membered rings surrounding a central void.

Oxygens shared by pairs of fourfold co-ordinated cations are termed bridging oxygens. The backs of the chains consist of nearly co-planar oxygens. These oxygens were stated to be co-planar by Warren but subsequent three dimensional structure analyses have noted that this is not so (Papike and Clark, 1968; Papike, Ross, and Clark, 1969). These are designated as non-bridging O(4) and bridging O(5), O(6) and O(7). The latter three are bonded to tetrahedral cations only, but O(4) is located at the periphery of the double chain and is bonded to a cation of six-eight fold co-ordination.

Apical oxygens are also almost a co-planar anionic layer consisting of the non-bridging O(1) and O(2) and bonded on one side to fourfold co-ordinated cations and on the other by six-eight fold co-ordinated cations. Directly over the void in the chain is an anion designated O(3) bonded only to octahedrally co-ordinated cations and is typically monovalent, either hydroxyl, fluorine or more rarely chlorine and on occasions may be oxygen.

1-3-1. Cation Structural Sites.

These sites are made up of the tetrahedrally co-ordinated Si(I) and Si(II) (named by Warren because in tremolite only silicon was present in these sites); octahedrally co-ordinated M(1), M(2) and M(3); six-eight fold co-ordinated M(4); and finally the 'A' site which is twelvefold co-ordinated.

The metal ions are co-planar and the double chain is slightly folded outwards away from the metal ions either side of the centre line (07) (Whittaker, 1949). The metal sites are located between two layers of apical

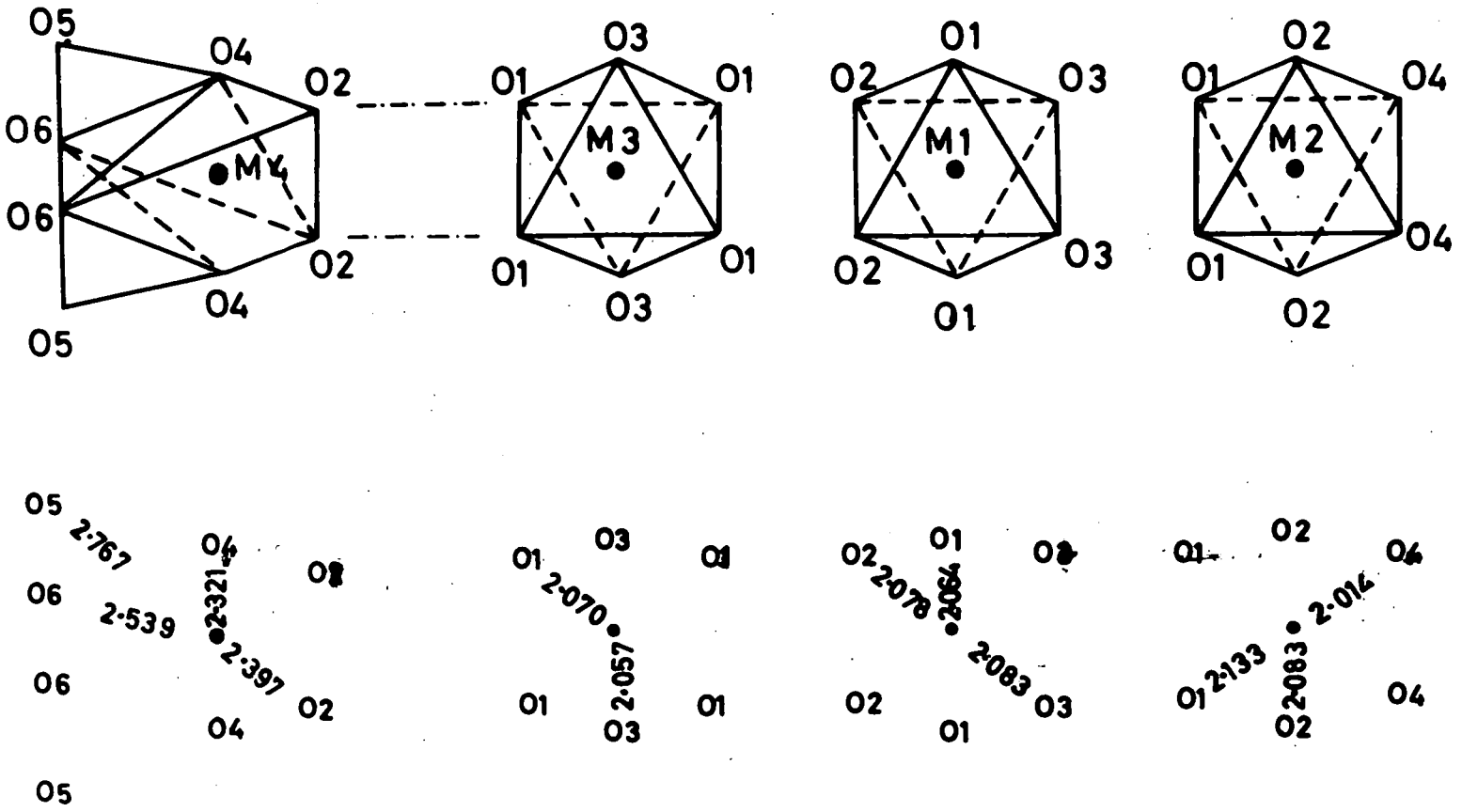

Bond lengths for Tremolite from Papike et.al. 1969.

Fig.1-2 Schematic diagram of the cation positions in the monoclinic amphiboles.

oxygens; M(2) and M(4) are situated at the peripheries of adjacent opposite facing chains and these provide bonds which bind the chains together parallel to the 'a' and 'b' axes. The relative positions of the co-planar cations can be seen in the upper portion of Fig. 1-1 which is a section normal to the 'c' axis. The lower part of the diagram, a projection normal to $a_o \sin\beta$ shows the arrangement of the chains and how the M(2) and M(4) cations bind the chains together laterally, i.e. parallel to the 'b' crystallographic axis.

The M(2) and M(4) sites are equivalent to the six-eight fold M sites in the pyroxenes and M(1) and M(3) are equivalent the octahedral sites in the micas. Therefore one can look upon the amphiboles as an intermediate stage in polymerisation between pyroxenes and micas.

A large cavity arises from the superposition of the voids of adjacent back to back double chains and is designated the structural 'A' site. The position of this site is in the void below the O(3) anion (see Fig. 1-1).

In Fig. 1-2 a schematic diagram of the metal sites in the monoclinic amphiboles is shown. M(1), M(2), and M(3) are shown as regular octahedral sites but M(2) is slightly more distorted. The figures for the cation-anion distances for tremolite (Papike, Ross, and Clark, 1969) are shown below the sites. M(4) is shown as an irregular eight-sided site.

In the lower half of Fig. 1-1 the double chain is shown as an approximate hexagon. Warren (1929) described this as a regular hexagon but recent structure determinations (Papike and Clark, 1968; Papike, Ross, and Clark, 1969; Colville and Gibbs, 1965) have shown these chains to be 'kinked' to varying degrees in different amphiboles. Two similar alkali amphiboles, magnesioriebeckite (crocidolite) and riebeckite are shown in Fig. 1-3 and the main difference in chemistry is that magnesioriebeckite has magnesium in M(1) and M(3) sites.

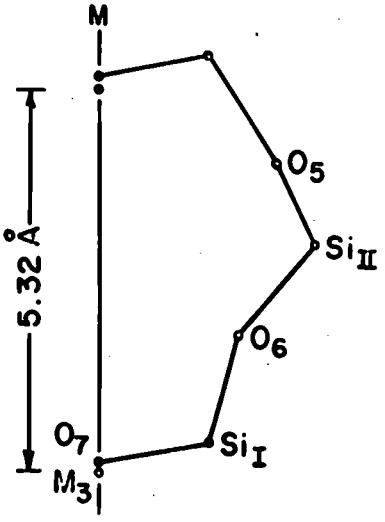

crocidolite (Whittaker 1949)

	b	c
Si_I	1.58	.43
Si_{II}	3.05	3.11
O_5	2.51	4.27
O_6	1.98	1.87
O_7	0.	.13
M_3	0.	0.

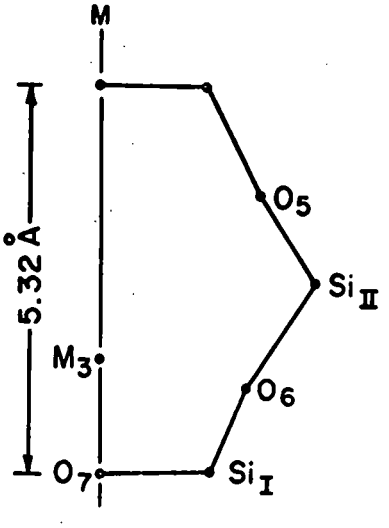

riebeckite (Colville and Gibbs 1965)

	b	c
Si_I	1.55	-1.53
Si_{II}	3.06	1.06
O_5	2.31	2.27
O_6	2.13	-.38
O_7	0.	-1.57
M_3	0.	0.

Fig.1-3 Half chain widths of riebeckite and magnesio-riebeckite to show 'kinking' of the chains.(after Ernst 1968.)

Warren (1929) in his original structure determination took rotation photographs about the 'c' axes of five monoclinic amphiboles, namely; tremolite, actinolite, hornblende, kupferrite, and grunerite. All the photographs were similar therefore it was assumed that the other amphiboles had essentially the same structure as tremolite.

From oscillation photographs about the 'b' axis the only reflections present were for h + k + l = even. Warren designated the lattice as body-centred and he used the superscript 'I'. The alternative is to use the face-centred or 'C' cell. Zussman (1959) shows the relationship between these two cells. The 'C' cell is now used exclusively to prevent confusion in presenting X-ray data.

Tremolite belongs to the monoclinic holohedral class and using the 'C' face-centred cell only $C2/_m$ and $C2/_c$ groups are possible. The oscillation photographs showed that there were some (h0l) reflections with both h and l odd therefore the space group must be $C2/_m$.

Brown (1966) described an amphibole intergrown with tremolite with the space group $P2_1/_m$, subsequently Papike, Ross, and Clark (1969) have determined the crystal structure of amphiboles with this space group. Reflections with this space group have the indices h0l, hkl, and 0k0 when k = 2n.

More recent X-ray structure determinations have been done by the following people:-

Whittaker (1949) - magnesioriebeckite.

Zussman (1955) - actinolite, (1959) tremolite.

Heritsch et al. (1957 and 1960) - hornblendes.

Ghose and Hellner (1959), Finger and Zoltai (1967), and Finger (1969) - grunerite.

Ghose (1961), Fischer (1966) - cummingtonite.

Kawahara (1963) - arfvedsonite.

Prewitt (1964) - two synthetic amphiboles.

Gibbs (1965 and 1969) - synthetic proto-amphibole.

Colville and Gibbs (1965) - riebeckite.

Papike and Clark (1968) - glaucophane.

Papike, Ross and Clark (1969) - various clinoamphiboles.

Finger (1969) - anthophyllite.

Mitchell, Bloss, and Gibbs (1971) - actinolite.

Papike and Ross (1969) - gedrites.

Robinson, Gibbs, and Ribbe (1969) - pargasite.

Whittaker (1969) - holmquistite.

The recent structural refinements have increased the knowledge on the three basic amphibole structures with the space groups $C2/m$, $P2_1/m$, and Pnma. They have discovered the relative positions of the tetrahedra in various amphibole compositions and that aluminium is enriched in T(1) compared to T(2). Papike, Ross, and Clark (1969) conclude that M(4)-O co-ordination polyhedra are responsible for the miscibility gaps between magnesium rich clinoamphiboles (cummingtonites) and Na, Ca rich amphiboles at low temperatures.

Work still remains to be done on amphiboles from igneous environments with compositions such as mboziite and amphiboles with high titanium and partial 'A' site occupancy in order to resolve further crystal chemical problems.

1-4. Site occupancy.

The formula for an amphibole is $A_{0-1}X_2Y_5Z_8O_{22}(OH)_2$ which represents one-half of the unit cell of a clinoamphibole. 'A' represents the twelvefold co-ordinated cations occupying the structural 'A' site; X the eightfold co-ordinated cations at M(4); Y indicates the octahedrally co-ordinated

cations at M(1), M(2), and M(3); Z represents the tetrahedrally coordinated cations at T(1) and T(2).

Ghose (1965) drew up a scheme of cation distribution in the amphibole group based upon crystal chemical considerations and the crystal structures available at the time (Table 1-1). This table is not exhaustive but it shows the general cation distribution in the monoclinic and orthorhombic amphiboles. The author disagrees with Ghose's (1965) suggestion on the position of lithium in the arfvedsonite-eckermannite series. This cation probably goes into the M(1) and M(3) sites, with subsequent charge balance, because of its size (Phillips, 1963). This opinion is substantiated by studies of the infra-red spectra of the fundamental hydroxyl stretching frequency of lithium-containing alkali amphiboles (Addison and White, 1968). Lithium in holmquistite is in the M(4) sites (Whittaker, 1969). The author has not noted any shift in OH^- stretching frequency of a holmquistite from Rwanda which would be expected if lithium were in the M(1), M(3) sites.

When hydroxyl is replaced by oxygen in the O(3) sites ferric iron should enter the M(3) sites to balance the charges (Phillips, 1963).

Recently much work has centred on the problem of site occupancy in the amphiboles. Single crystal X-ray, Mössbauer spectroscopic and infra-red spectroscopic techniques have been used to determine site occupancy.

In anthophyllite ferrous iron site preference is as follows: M(4) > M(1), M(3) > M(2) and this is similar to results for the cummingtonite-grunerite series (Bancroft, Maddock, Burns, and Strens, 1966). There is a strong preference for M(4) by ferrous iron and discrimination against the M(2) site. The magnesium ions tend to cluster more in the M(1) and M(3) sites.

TABLE 1-1

Cation distribution in the amphiboles (after Ghose, 1965)

Name	M(4)	M(2)	M(1) + M(3)	A	Si(I)	Si(II)
Glaucophane	Na	Fe^{3+}, Al	Mg, Fe^{2+}	-	Si	Si
Riebeckite	Na	Fe^{3+}	Mg, Fe^{2+}	-	Si	Si
Katophorite	$Na^{\frac{1}{2}}$ $Ca^{\frac{1}{2}}$	$(Fe^{3+} + Al)^{\frac{1}{2}}$ $(Fe^{2+} > Mg)^{\frac{1}{2}}$	$Mg > Fe^{2+}$	Na	$Al^{\frac{1}{4}}Si^{\frac{3}{4}}$	Si
Arfvedsonite Eckermannite	$(Na + Li)^{\frac{3}{4}}$ x $Ca^{\frac{1}{4}}$	$(Fe^{3+} + Al)^{\frac{3}{4}}$ $(Fe^{2+} > Mg)^{\frac{1}{4}}$	$Mg > Fe$	Na,K	$Al^{\frac{1}{4}}Si^{\frac{3}{4}}$	Si
Richterite	$Na^{\frac{1}{2}}$ $Ca^{\frac{1}{2}}$	Fe^{3+} + Mg +Al	$Mg > Fe^{2+}$	Na	Si	Si
Cummingtonite	Fe^{2+}	Mg^{2+}	$Mg > Fe^{2+}$	-	Si	Si
Actinolite	Ca	$Fe^{2+} > Mg$	$Mg > Fe^{2+}$	-	Si	Si
Hornblende	Ca	$Fe^{2+} > Mg$	$Mg > Fe^{2+}$ (Al , Fe^{3+})	Na,K	$Al^{\frac{1}{2}}Si^{\frac{1}{2}}$	Si
Edenite	Ca	$Fe^{2+} > Mg$	$Mg > Fe^{2+}$	Na	$Al^{\frac{1}{4}}Si^{\frac{3}{4}}$	Si
Pargasite-Ferrohastingsite	Ca	$Fe^{2+} > Mg$	$(Mg > Fe^{2+})$ (Al, Fe^{3+})	Na,K	$Al^{\frac{1}{2}}Si^{\frac{1}{2}}$	Si
Anthophyllite	Fe^{2+}	Mg	$Mg > Fe^{2+}$	-	Si	Si

x Position of Lithium

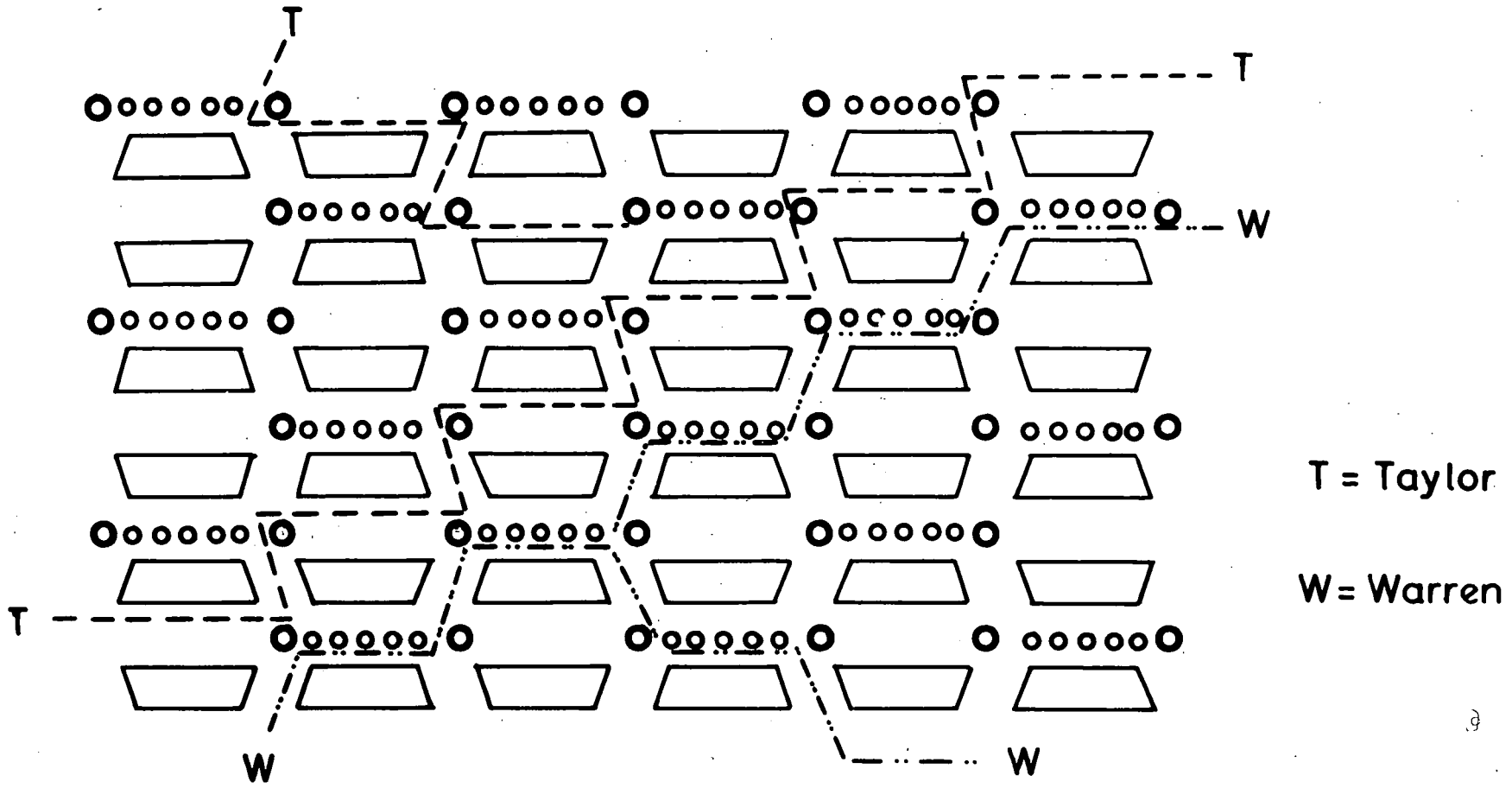

Fig. 1-4 Diagrammitic representation of possible cleavage planes in amphiboles.

The results from studies on actinolite (Burns and Strens, 1966), where M(4) is occupied by calcium, indicate that the $Fe/_{Fe + Mg}$ ratio in the M(2) position is about twice that in the M(1) and M(3) sites.

Strens (1967, 1968) and Burns and Prentice (1968a and b) have evaluated the site occupancy in fibrous riebeckite and magnesioriebeckite (crocidolites). Ferric iron predominates at the M(2) sites and ferrous iron is concentrated in the M(1) and M(3) sites with a preference for M(1). Cations in pegmatitic riebeckites and magnesioriebeckites are more randomly distributed than in the fibrous varieties, therefore site populations appear to be strongly temperature dependant.

In glaucophane ferric iron and aluminium are at M(2) and ferrous iron and magnesium at M(1) and M(3) with a slight preference for ferrous iron in M(3) (Papike and Clark, 1968; Strens, 1966).

Much of the work, to date, has been on amphiboles from low temperature and metamorphic environments and a great deal needs doing on the igneous amphiboles.

1-5. Amphibole cleavage.

The amphiboles possess two cleavage planes at 124° to each other, whereas in the pyroxenes they are at 90°. The cleavage directions are shown schematically in 1-4. The silicon-oxygen tetrahedra are back to back and the cations are distributed as shown. Warren (1929) concluded that the amphibole would cleave more readily at the edges of the chains, i.e. between the M(4) and M(2) sites because the M-O distances would be longer and hence weaker. His scheme for the amphibole cleavage passed between the metal ions and the apical oxygens of the silicon-oxygen tetrahedra then between adjacent chains and between M(2) and M(4) of the lower chain. This scheme is labelled (W). Taylor (1965) proposed an alternative to Warren's scheme.

This again passes between M(2) and M(4), between adjacent chains and then along the backs of the chains. Both hypotheses give the same cleavage angle but Taylor's has the advantage that it breaks fewer M-O bonds.

1-6. Nomenclature.

The amphiboles can be subdivided according to the following scheme, modified from Phillips and Layton (1964):-

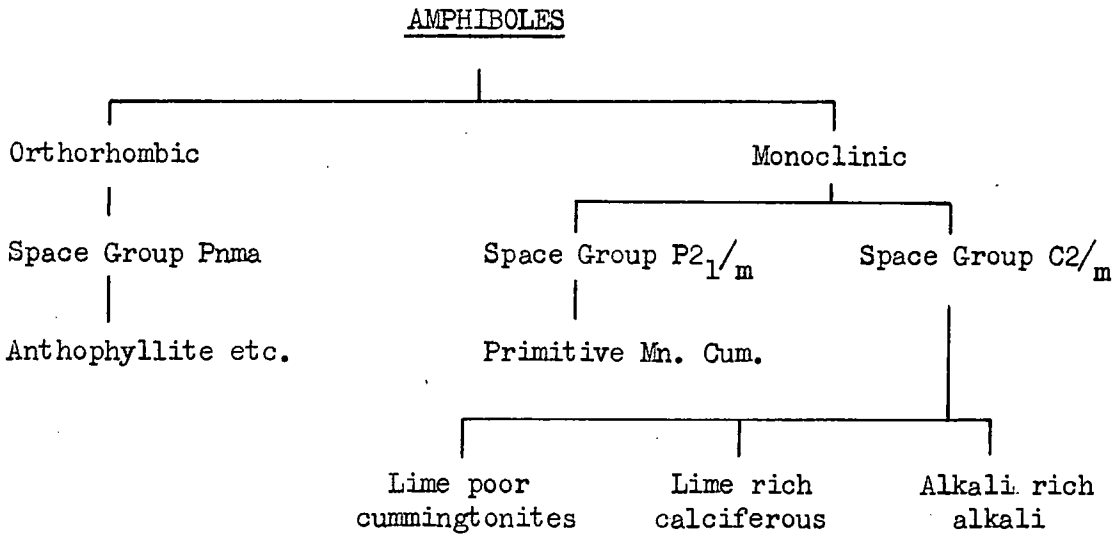

A profuse nemenclature has arisen within the amphibole group of minerals, but since the author is primarily concerned with alkali amphiboles this sub-group alone will be discussed. Alkali amphiboles are defined as having more than 1.00 atoms of sodium in X in the basic formula (Phillips, 1966).

Phillips and Layton (1964) define five alkali amphiboles of the following compositions:-

$\square Na_2Mg_3Al_2Si_8O_{22}(OH)_2$ - Glaucophane - K

$NaCaNaMg_5Si_8O_{22}(OH)_2$ - Richterite - K

$NaNa_2Mg_4AlSi_8O_{22}(OH)_2$ - Eckermannite - K

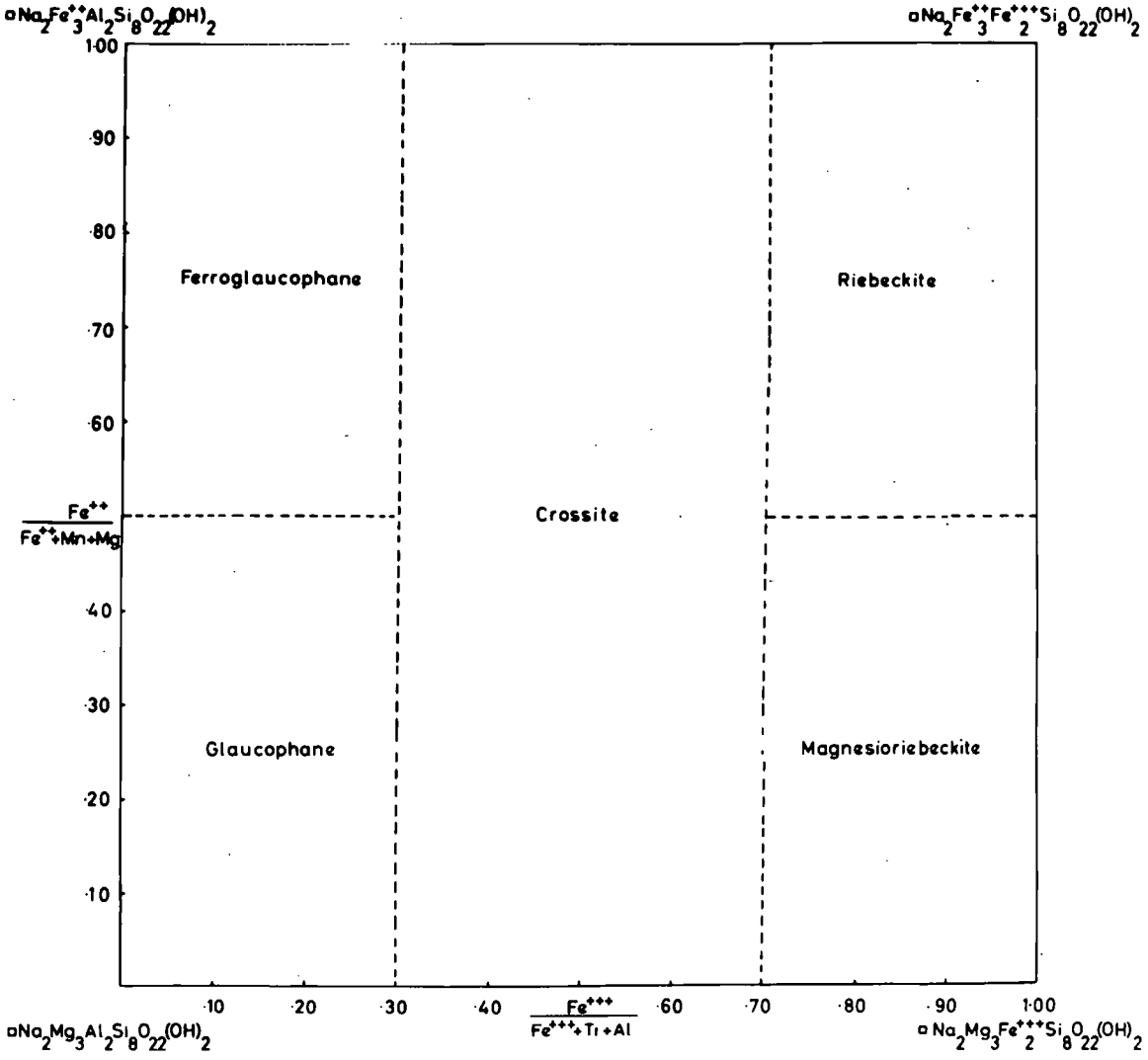

Fig.1-5 Nomenclature of the Glaucophane-Riebeckite series.

$NaNa_2Mg_3Al_2Si_7AlO_{22}(OH)_2$ - Miyashiroite - K

$NaCaNaMg_3Al_2Si_6Al_2O_{22}(OH)_2$ - Sundiusite - K

These are the magnesium end-members and the suffix - K^x (KAPPA) indicates a pure end-member composition (Phillips and Layton, 1964). The above formula for glaucophane followed by - K indicates the pure chemical compound and □ indicates a vacant lattice site. Minerals called glaucophane come within 10% of the pure compound.

The name glaucophane was first used by Hausmann (1845) and comes from the Greek "glaucos" and "phanos" meaning to appear bluish green.

Gastaldite was a name used for a mineral similar to glaucophane but more aluminous (Struver, 1875) but on re-analysis (Zambonini, 1906) it was shown to be glaucophane. The relationship between the various minerals in this compositional range is shown in Fig. 1-5. Phillips and Layton (1964) proposed the use of 'ferro' to denote the full substitution of ferrous iron for magnesium and 'ferri' for the full substitution of ferric iron for aluminium. Unfortunately the names of the minerals within this compositional range and the eckermannite-arfvedsonite compositions are entrenched in the literature.

Riebeckite, the ferrous ferric iron analogue of the glaucophane series, was originally described by Sauer (1888) and named after a Dr. Riebeck and came from the Island of Socotra in the Indian Ocean. This riebeckite is not a true riebeckite but a member of the riebeckite-arfvedsonite series.

Sub-glaucophane was a term used by Sundius (1946), Miyashiro (1957), and Winchell (1951) for minerals of intermediate composition between glaucophane and riebeckite but crossite, proposed by Palache (1894) in honour of J. W. Cross, is preferred bacause minerals of this composition have distinctive optical properties (Borg, 1967).

^{x} Greek Καθαρος= pure

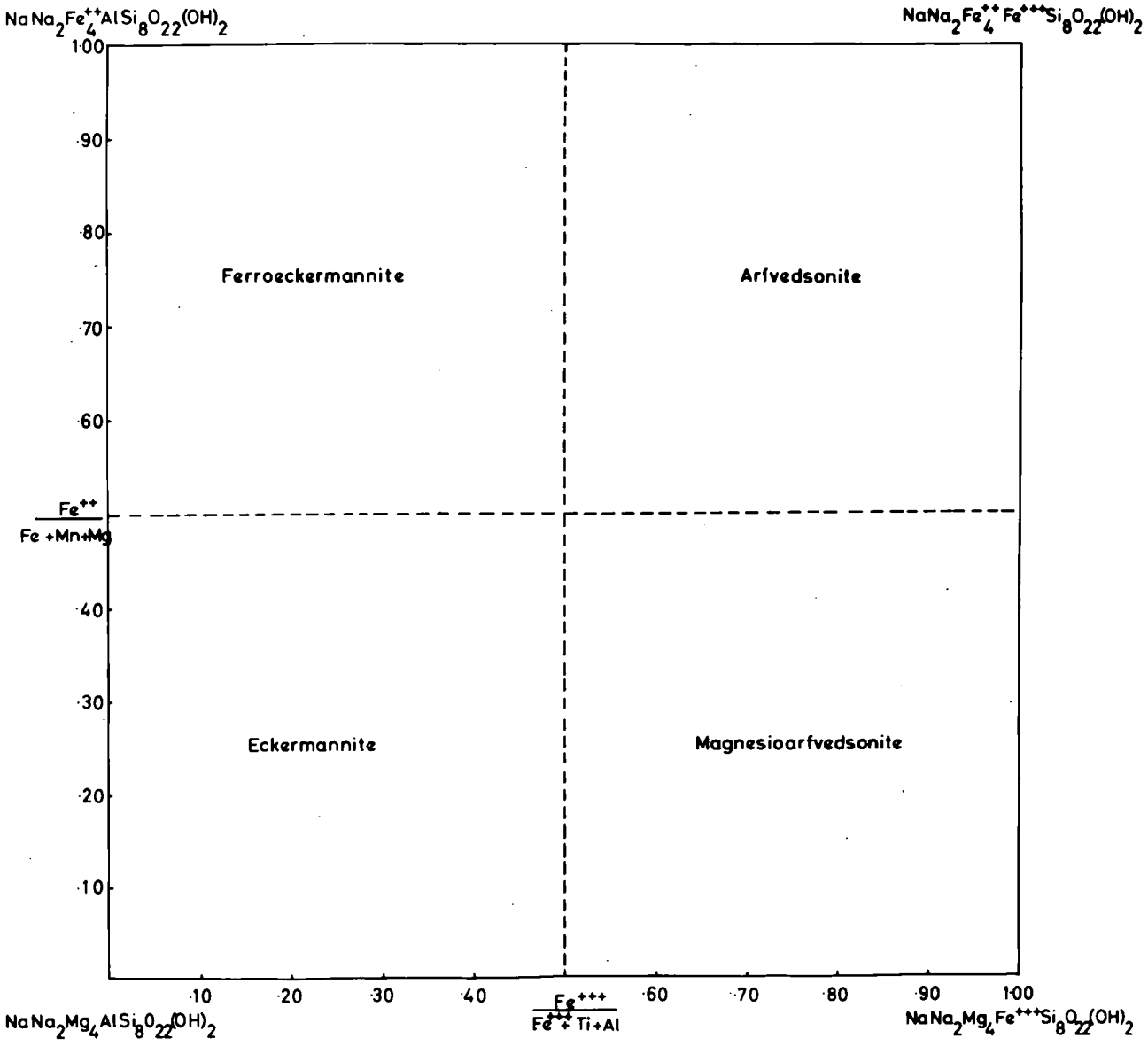

Fig.1-6 Nomenclature of the Eckermannite-Arfvedsonite series.

The term magnesioriebeckite (Ernst, 1957; Miyashiro, 1957) for the magnesium ferric iron end-member could be called ferriglaucophane according to the Phillips and Layton (op. cit.) scheme. The closest approximation to the ferroglaucophane composition is glaucophane 23 ferroglaucophane 77 (Black, 1970).

Crocidolite was first described by Stromeyer and Hausmann (1831) and means "woolly-stone". The term "crocidolite" has since been used to describe all forms of fibrous riebeckite and magnesioriebeckite. For the mineral the adjective, fibrous, should be attached followed by the specific mineral name. The name rhodusite has been introduced by the Russians for a fibrous magnesioriebeckite which has formed in authigenic environments.

The following list of mineral names can be adequately described by the present terminology (after Hey, 1954):

Osannite (Hiawatsch, 1906) - riebeckite.

Chernyshevite (Duparc and Pearce, 1907) - riebeckite.

Lanéite (Murgoci, 1906) - riebeckite.

Ternovskite (Polovinkina, 1924) - magnesioriebeckite.

Bababudanite (Smeeth, 1911) - magnesioriebeckite.

Naurodite (von Knebel, 1903) - glaucophane.

Ferriglaucophane (Rao, 1939) - glaucophane.

Fig. 1-6 shows the relationships in the eckermannite-arfvedsonite series. Both Figs. 1-5 and 1-6 should be used only to show relationships within the mineral composition range and not to show the systematic position of the composition within the amphibole group (Phillips, 1966).

Arfvedsonite was named by Brooke (1823) after the Swedish chemist J.A. Arfvedson and came from Kangerdlugsuak in southern Greenland. Eckermannite was named by Adamson (1942) after Professor H. von Eckermann

and came from Norra Kärr in southern Sweden. Szechenyiite (Krenner, 1900) analyses plot in both the eckermannite and richterite fields.

The following amphiboles are intermediate in composition between riebeckite and arfvedsonite and the author has determined that there is no chemical break between these minerals:

1. Heikolite (Kinosaki, 1935) from quartz syenite, Fukushin-zan, Korea.
2. Torendrikite (Lacroix, 1920), Ambatofinandrahana, Malagasy.
3. Taramite and fluor-taramite (Morozewicz, 1925, 1930) from Mariupol, Ukrainian S.S.R. One of these minerals plots in the Mboziite field.
4. Svidneite (Mincheva-Stefanova, 1951 and Grozdanov, 1964) from potash rich quartz syenites in the Western Balkans.

Juddite (Fermor, 1909) comes from the manganese deposits in India and typically contains manganese and ferric iron to the exclusion of ferrous iron. It was named after Professor J.W. Judd. The minerals of this composition should be called manganoan magnesioarfvedsonite. The adjective preceding the name is from the scheme proposed by Schaller (1930). Magnesioarfvedsonite (Andreev, 1957) was first described from a metasomatic environment in the Urals, U.S.S.R.

The Katophorite group ($NaCaNa(Fe^{++},Mg)_4(Fe^{+++},Al)Si_7AlO_{22}(OH)_2$) was named by Brögger (in Deer, Howie, and Zussman, 1963) for an amphibole characterised by a deep reddish brown colour and fairly large extinction angle. The name, Katophora, comes from the Greek meaning "a carrying down", referring to its volcanic origin. Miyashiro (1957) coined the name magnesiokatophorite for the magnesium-ferric iron end-member. No amphibole approximating the magnesium-aluminium end-member has yet been found in nature. Freudenberg (1910) proposed the name anophorite for a magnesio-katophorite from a nepheline syenite at Katzenbuckel, Odenwald, Germany.

The richterite-ferrorichterite group have the composition

$NaCaNa(MgFe^{++})_5Si_8O_{22}(OH)_2$. Breithaupt (1865) first described richterite from the manganese-iron deposits of Långban, Sweden and named it after Professor J.L. Richter. As this mineral was considered to be manganese-rich Larsen and Berman (1931) introduced the term soda-tremolite but reference to the analyses of the Långban richterites shows some of them to have normal (0.1 - 0.3 atoms) manganese contents. The name richterite is preferred by the author because it has no allusion to another mineral species.

There is a profusion of mineral names with the composition of richterite. Among these are szechenyiite (Krenner, 1900); imerinite (Lacroix, 1921) from a contact metamorphosed limestone at Imerina, Malagasy; tirodite (Dunn and Roy, 1939) from Tirodi, India (see present study); winchite (Fermor, 1906) from Central Provinces, India; chiklite (Bilgrami, 1955) from Chikla, India; magnophorite (Prider, 1939) and finally Isabellite (Chester, in Hey, 1954). Magnophorite is a potassium rich variety of richterite.

Phillips and Layton (op. cit.) named two amphiboles which were not known in the natural state, namely sunduisite-K ($NaCaNaMg_3Al_2Si_6Al_2O_{22}(OH)_2$) and miyashiroite-K ($NaNa_2Mg_3Al_2Si_7AlO_{22}(OH)_2$). Since publication of this work the iron analogue of sunduisite-K has been found in nature and was described by Brock et al. (1964) and called mboziite. More recently a more magnesium rich mboziite has been described by Linthout and Kieft (1970). No amphibole approximating miyashiroite has yet been found in nature.

1-7. Classification (Review).

A historical review of the various classifications that have been proposed for the amphibole group of minerals is given here. The classification thought to be most useful will be dealt with in detail in the chapter on the chemistry of the alkali amphiboles.

Larsen and Berman (1931) were the first to attempt systematically to classify the amphiboles and their subdivisions can be noted from the table:-

1. Tremolite $Ca_2Mg_5Si_8O_{22}(OH)_2$.
2. Soda Tremolite $CaNa_2Mg_5Si_8O_{22}(OH)_2$.
3. Arfvedsonite $Na_3Mg_4AlSi_8O_{22}(OH)_2$.
4. Hastingsite $Ca_2NaMg_4AlSi_6Al_2O_{22}(OH)_2$.
5. Glaucophane $Na_2Mg_3Al_2Si_8O_{22}(OH)_2$.

The above authors treated hornblende, actinolite and riebeckite as the iron analogues of hastingsite, tremolite and glaucophane respectively.

Berman (1937) took this classification one stage further and sub-divided the amphiboles from the following generalised formula $(W,X,Y)_{7-8}(Z_4O_{11})_2(O,OH,F)_2$. From this formula he generated the following sub-divisions:-

Anthophyllite series $X_7(Z_4O_{11})_2(OH)_2$ and subdivided it further into anthophyllites $(MgFe)_7Si_8O_{22}(OH)_2$ and gedrites $(MgFeAl)_7(SiAl)_8O_{22}(OH)_2$.

Cummingtonite series $X_7(Z_4O_{11})(OH)_2$ where X = (Mg,Fe,Mn).

Tremolite-actinolite series $W_2X_5Z_8O_{22}(OH)_2$, W = Ca, X = (Mg,Fe).

Hornblende series $2\left\{W_3(X,Y)_5(Z_4O_{11})_2(OH)_2\right\}$

where W = (Ca,Na), (X,Y) = (Mg,Fe^{++},Fe^{+++},Al), Z = (Si,Al).

He also divided the hornblende series into groups which are still recognized e.g. edenite, pargasite, hornblende, glaucophane etc.

Hallimond (1943) graphically represented 143 analyses of hornblendes and tremolites with two variables (a) the number of silicon atoms, (b) number of atoms allotted to the vacant space. A third variable was eliminated, i.e. the degree of replacement of sodium for calcium by selecting analyses with approximately two atoms of calcium. The main disadvantages of this system are that he disregarded substitutions in

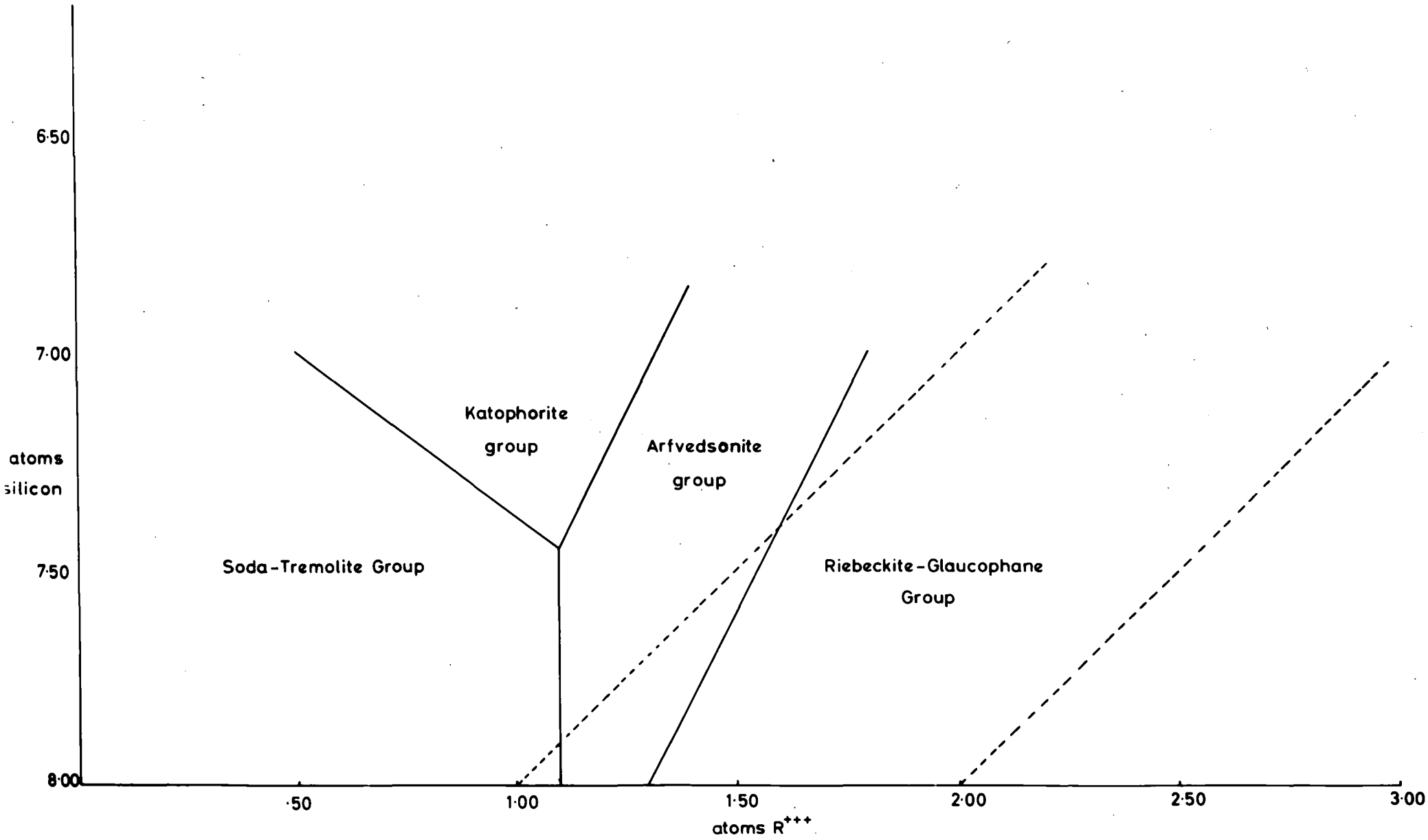

Fig.1-7 Classication of the amphiboles – Miyashiro 1957.

the mineral which do not affect the parameters he uses, and secondly he totally ignores substitutions in M(4).

Sundius (1946) classified what he called the hornblendes and studied the solid solution relations within the amphibole group. His proposed scheme of classification is shown below:-

Tremolite-Actinolite
$Ca_2(MgFe)_5Si_8O_{22}(OH)_2$

Richterite-ferrorichterite
$Na_2Ca(MgFe)_5Si_8O_{22}(OH)_2$

Eckermannite-Arfvedsonite
$Na_3(MgFe^{++})_4(Fe^{+++}Al)Si_8O_{22}(OH)_2$

Glaucophane-Riebeckite
$Na_2(MgFe^{++})_3(Fe^{+++}Al)_2Si_8O_{22}(OH)_2$

Edenite-ferroedenite
$NaCa_2(MgFe^{++})_5Si_7AlO_{22}(OH)_2$

Pargasite-Hastingsite
$NaCa_2(MgFe^{++})_4(AlFe^{+++})Si_6Al_2O_{22}(OH)_2$

Tschermakite-ferrotschermakite
$Ca_2(MgFe^{++})_3(AlFe^{+++})_2Si_6Al_2O_{22}(OH)_2$

Where calcium is exchanged for sodium then he uses the term alkali hornblende and he classes richterite as one of these.

Winchell (1951) split the hornblendes up into four end-members namely tremolite, edenite, pargasite and tschermakite with the same compositions as those proposed by Sundius.

Miyashiro (1957) attempted a classification of the alkali amphiboles. He divided the group into four sub-groups:- riebeckite-glaucophane, arfvedsonite, katophorite, and soda tremolite. He represented his classification diagrammatically as shown in Fig. 1-7 and plotted the number of silicon atoms against the trivalent atoms in Y. The boundaries between these groups are straight lines passing through two points:-

Between the fields riebeckite-glaucophane and arfvedsonite: (R^{+++} = 1.30, Si = 8.00) and (R^{+++} = 1.80 and Si = 7.00).

Between the fields of arfvedsonite and katophorite: (R^{+++} = 1.10, Si = 7.45) and (R^{+++} = 1.40 and Si = 6.85).

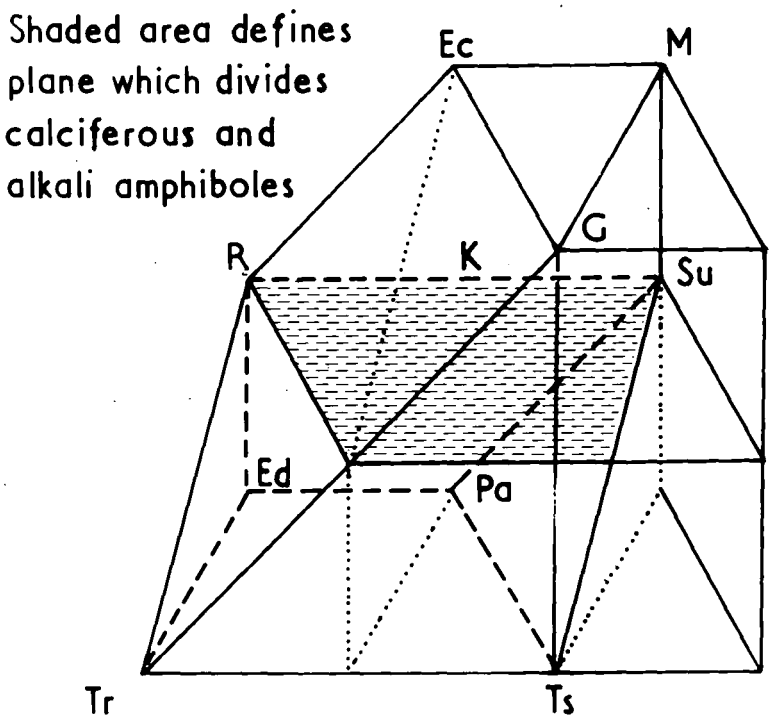

Modification of Smith's classification to include sundiusite and miyashiroite.

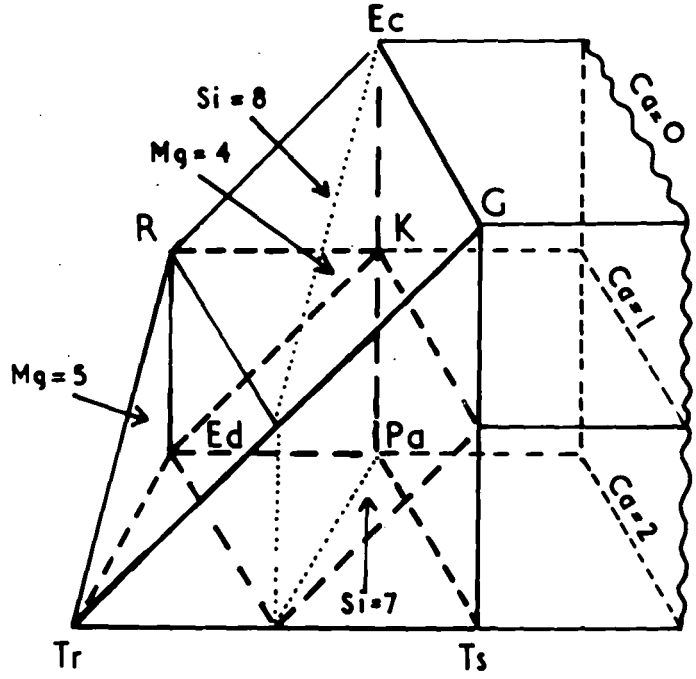

Fig.1-8 Classification of the amphiboles, J.V. Smith, 1959.

Between the fields of katophorite and soda tremolite: (R^{+++} = 1.10 Si = 7.45) and (R^{+++} = 0.50 and Si = 7.00).

Between the fields of arfvedsonite and soda tremolite: (R^{+++} = 1.10 and Si = 7.45) and (R^{+++} = 1.10 and Si = 8.00).

One useful facet of this classification is that the mode of occurrence can be shown to correlate roughly with composition. The minerals from igneous bodies are in the upper central portion of Fig. 1-7, the volcanic minerals to the upper left, crystalline schists to the lower right and the hydrothermal or contact metamorphic minerals to the lower left of the centre line.

Miyashiro further uses the calcium content of the minerals to arrive at an idealized formulae:

Riebeckite-glaucophane	$Na_2R^{++}_3R^{+++}_2Si_8O_{22}(OH)_2$
Arfvedsonite	$Na_2Ca_{0.5}R^{++}_{3.5}R^{+++}_{1.5}Si_{7.5}Al_{0.5}O_{22}(OH)_2$
Katophorite	$Na_2CaR^{++}_4R^{+++}Si_7AlO_{22}(OH)_2$

and compositional variation between the groups involves the substitution $R^{+++}Si \leftrightarrow CaR^{++}Al$.

The above formula for arfvedsonites has been accepted by Deer et al. (1963) but minerals approaching the arfvedsonite end-member formula $Na_3Fe^{++}_4Fe^{+++}Si_8O_{22}(OH)_2$ occur in some soda granites. This classification has the disadvantage of using only two substitutions in the alkali amphiboles.

J.V. Smith (1959) made the first serious attempt at classifying the calciferous and alkali amphiboles by means of a three dimensional plot (Fig. 1-8). In this diagram a vertical ordinate is used to express the variation $CaAl \leftrightarrow NaSi$. When all the calcium has been exchanged for sodium in the M(4) sites pargasite (Pa) and tschermakite (Ts) become eckermannite (Ec) and glaucophane (G) respectively. When only one calcium

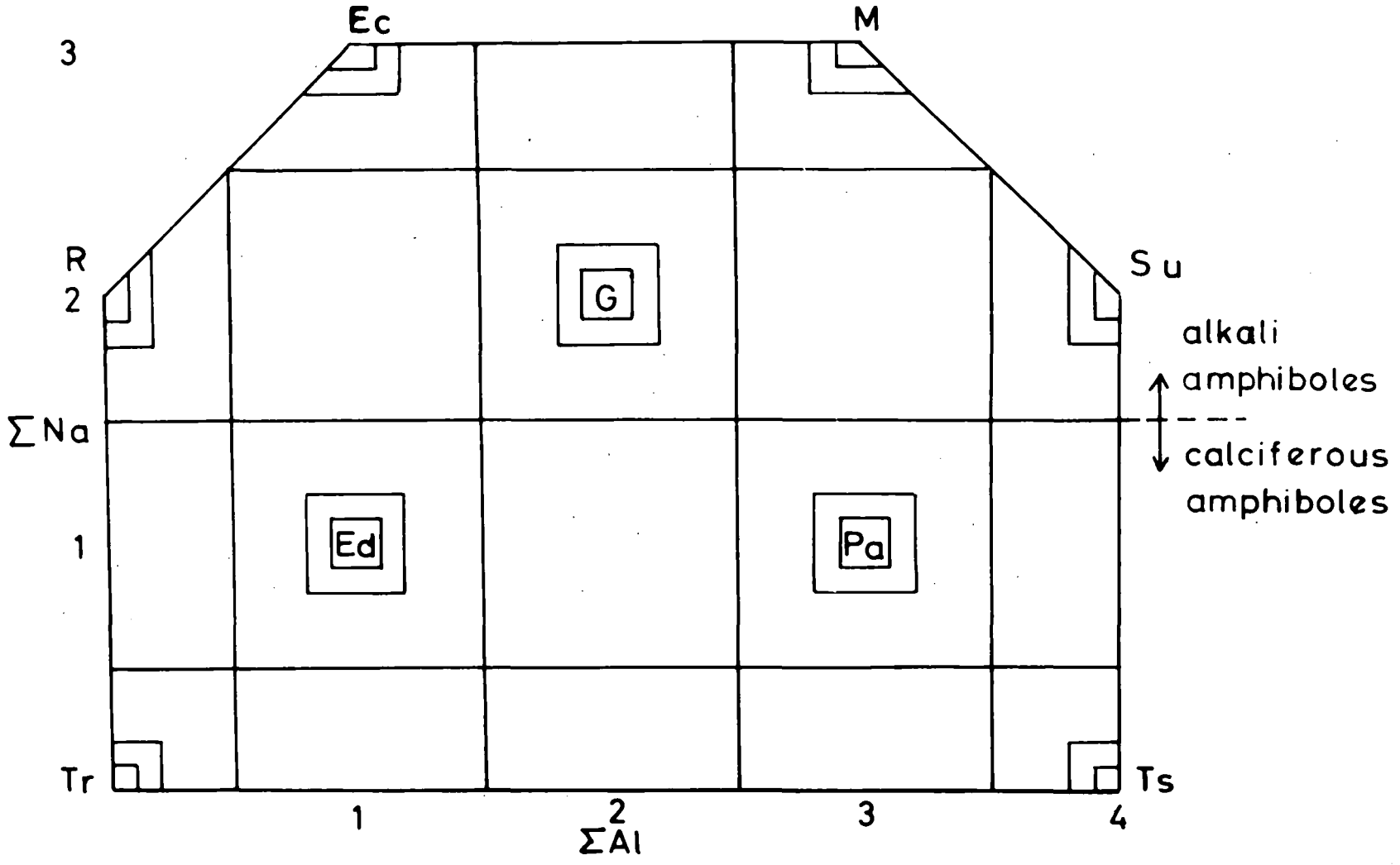

Fig. 1-9 Classification of the amphiboles — Phillips and Layton 1964.

atom has been exchanged edenite (Ed) becomes richterite (R). The upper limit of the diagram is fixed by the requirement that calcium should not fall below zero and the lower limit by the fact that calcium atoms never exceed two. The number of silicon atoms can never be greater than eight and a plane representing this passes through eckermannite, glaucophane, richterite and tremolite. Calcium plus sodium (or potassium) can never exceed three and never fall below two. The back plane is defined by R, Ed, Pa, and Ec and front plane by Tr, Gl, and Ts. There are only five magnesium sites available in these amphiboles therefore any analyses are forbidden beyond the plane Tr-Ed-R. It is to be noted that the substitution $Mg \leftrightarrow Fe^{++}$ is ignored. There is a lack of symmetry in this graphical representation and this is the main disadvantage.

Phillips and Layton (1964) took the tremolite composition as a starting point and bearing in mind the requirements of electrical neutrality, avaliable lattice sites, co-ordination number and evidence from a large number of chemical analyses worked out the limits of substitution for the calciferous and alkali amphiboles. Sodium and aluminium were taken as typical of the various elements which can substitute in the A, X and Y, Z positions in the general formula $AX_2Y_5Z_8O_{22}(OH)_2$. Substitutions involving cations of the same charge and similar ionic radii e.g. $Mg \rightleftharpoons Fe^{++}$, were regarded as trivial for the purpose of establishing the general classification. The following substitutions were considered to be possible:-

$$2Na \rightleftharpoons \square Ca,\ NaAl^{VI} \rightleftharpoons CaMg, \square Al^{vi} \rightleftharpoons NaMg,$$

$$Al^{VI}Al^{IV} \rightleftharpoons MgSi,\ CaAl^{IV} \rightleftharpoons NaSi,\ NaAl^{IV} \rightleftharpoons \square Si,\ Na^{A}Ca2Al \rightleftharpoons \square Na^{X}2Si$$

These substitutions give nine end-members namely Tr, Ed, Pa, Ts, Gl, R, Ec, M, Su of which the five alkali amphiboles were mentioned in the section on nomenclature and the calciferous amphibole names are generally accepted.

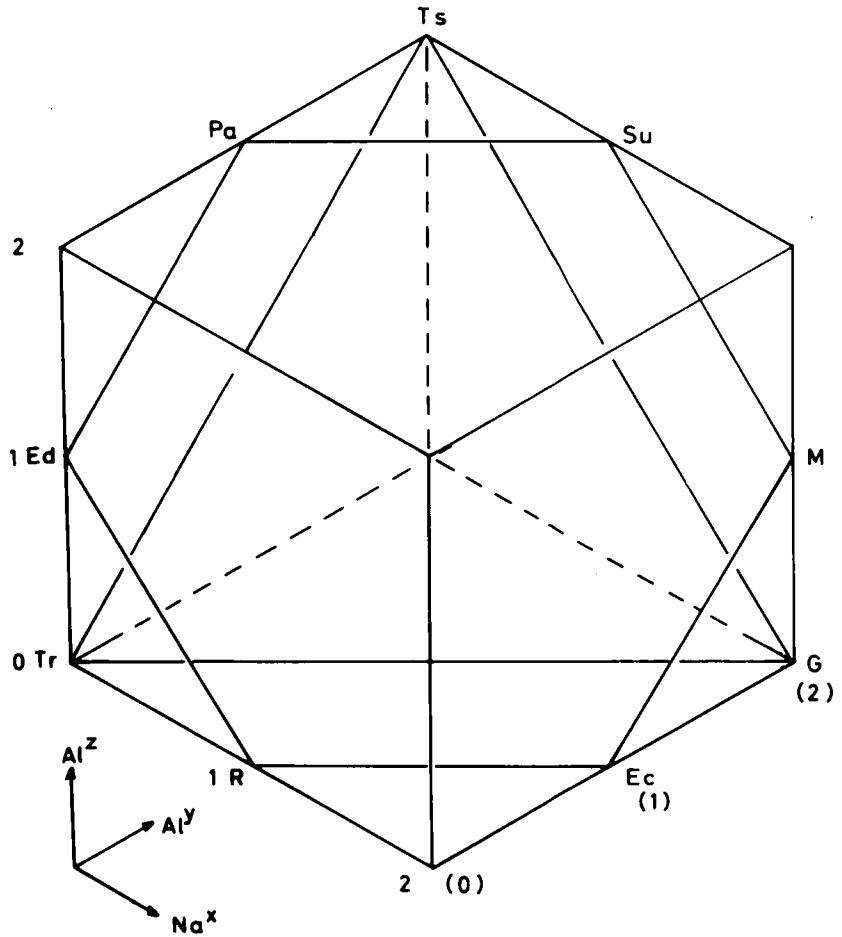

Units - atoms per lattice position.

Fig. 1-10 Amphibole compositional space (Phillips 1966).

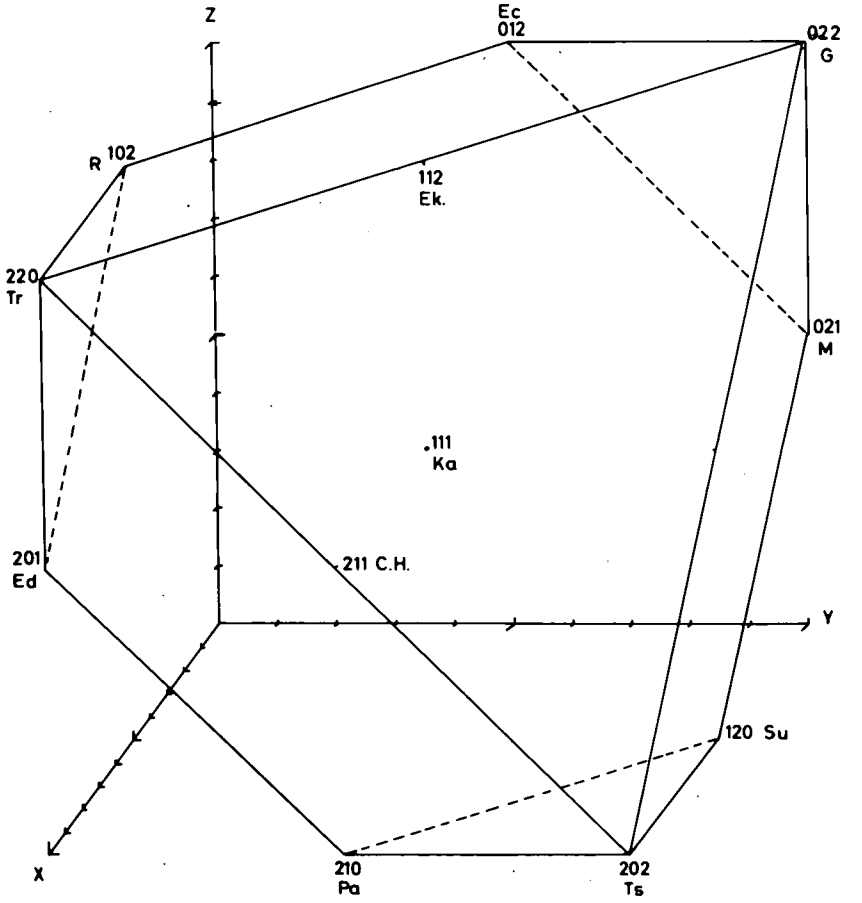

Fig.1-11 Whittaker's (1968) Charge-distribution space for the amphiboles.

Phillips and Layton proposed a simple two axis plot of the sum of sodium atoms against the sum of aluminium atoms (Fig. 1.9). This diagram indicates that there is no break between the calciferous and alkali amphiboles and they arbitrarily divided them at 1.5 atoms of sodium. The smaller square around the name represents 10% solid solution with other end-members, the next largest square 20% solid solution and to these minerals the suffix - sensu lato was applied. The largest square they referred to as - sensu extenso and represented a 50% solid solution between end-members.

Phillips and Layton (op. cit.) also introduced the concept of the basic formula which is calculated from the usual atomic formula. It is derived by converting the cations other than silicon into equivalent sodium, magnesium and aluminium depending upon their function and position in the lattice (Phillips, 1963).

Phillips (1966) takes these ideas one step forward and uses a method of representation that will distinguish between Na^A and Na^X and also between Al^Y and Al^Z. In the basic formula $Na^A + Al^Y = Na^X + Al^Z$ must hold. Knowing any three of these the fourth is determined by the need for balanced substitution.

Phillips constructed a diagram (Fig. 1.10) relative to the X, Y, Z, orthogonal axes in a conventional orientation, representing the number of atoms Na^X, Al^Y, Al^Z in the basic formula. The compositional space is an oblique slice through a cube bounded by faces equivalent to $\{100\}$ and $\{111\}$ planes. The limits are set by the number of X positions in the lattice and by assumptions (Phillips, 1963) about the limits of substitution in Y and Z positions. The calciferous amphiboles are separated from the alkali amphiboles by a boundary representing one atom of sodium in the X sites.

The relationship between this diagram and that proposed by Smith (1959)

may not be readily apparent but by extending Smith's diagram to include miyashiroite and sundiusite (Fig. 1.8b) the similarities can be seen. The six-sided figure containing Ed, R, Ec, M, Su, Pa and triangle containing Tr, Ts, Gl are in a different orientation but use the same concept. The disadvantage of this plot is its lack of symmetry which Phillips classification does possess.

Whittaker (1968) queried the desirability of trying to express the composition of amphiboles quantitatively in terms of end-members which was a feature of Phillips (op. cit.) classification. Whittaker uses orthogonal axes to derive the three dimensional diagram which classifies amphiboles in terms of the cationic charge distribution in the chains (Fig. 1.11a). The system works as follows:

The number of doubly charged atoms at X was taken to be the number of calcium atoms plus any excess of Y-type cations above 5.

x = number of doubly charged ions at X - number of vacancies at X.

y = number of triply charged ions at Y + 2x number of quadruply charged at Y(Ti) - number of singly charged ions at Y(Li) - 2x number of vacancies at Y.

z = number of silicon atoms at Z + number of vacancies at Z (assumed filled by H_4).

Then the amphiboles fall at the following co-ordinates:-

202	tremolite-actinolite
220	tschermakite, basaltic hornblende and kaersutite
022	glaucophane group
102	richterite
012	eckermannite group
210	pargasite, hastingsite
201	edenite
211	common hornblende
111	katophorite
120	taramite (mboziite)

CHAPTER TWO

Hydrothermal Synthesis

2-1. Introduction.

Phillips and Layton (1964), in attempting to systemise the nomenclature of the calciferous and alkali amphiboles, have considered for simplicity the possible range of substitution of sodium and aluminium in the tremolite structure. These two elements were chosen as typical of the various elements that may substitute in the A,X and Y,Z positions, taking the general formula as $AX_2Y_5Z_8O_{22}(OH)_2$. Substitutions involving cations of similar charge and ionic radium - as for example Fe^{++} for Mg - were regarded as being trivial for the purposes of fundamental classification.

It was found that nine end-member compositions were theoretically possible, two of which miyashiroite and sundiusite had not previously been described.

Phillips (1966) has shown how the relationships of these nine end-members may be represented on a simple diagram (Fig. 1.10) and has defined the alkali amphiboles as having at least 1.00 atoms of sodium in the X position of the above general formula. Five of the nine end-members are therefore classified as alkali amphiboles namely R, Ec, G, M, and Su (using abbreviations suggested by Phillips and Layton, 1964). The next logical step was to see if these compositions could exist as stable amphiboles and if possible to determine the stability range with varying temperature and pressure.

2-2. Previous Work.

Glaucophane-K ($\square Na_2Mg_3Al_2Si_8O_{22}(OH)_2$) has been prepared by Ernst (1959 and 1961) and the same author has shown that it has a pressure dependant polymorphism (1963). Charges of the bulk composition $Na_2O.3MgO.Al_2O_3.8SiO_2$ + excess water never completely crystallized to

amphibole. Additional phases to the glaucophane were forsterite, albite, enstatite, and a sodic montmorillonite. The present author performed several experiments (G.R. 4,5,6,7, and 113) with this composition and the phases encountered were the same as Ernst's even after seven days, but without the glaucophane. Ernst's experiments were up to six months in length and amphibole became more abundant with time. The high temperature stability is $864^{\circ} \pm 5^{\circ}C$ at 1000 bars pressure. Equilibrium was demonstrated by recrystallizing high temperature products within the glaucophane stability field (Fyfe, 1958). Glaucophane was also synthesized from the bulk composition $Na_2.3MgO.Al_2O_3.10SiO_2$. Glaucophane exhibits polymorphism which has been shown by a study of the X-ray cell parameters. The mineral which was synthesized below 2000 bars has larger cell dimensions than that synthesized above this pressure. Ernst has designated these two polymorphs I and II. Papike and Clark (1966) have elucidated the cation distribution in the crystal structure of glaucophane II and there is greater disordering than in the natural equivalents.

Ernst also synthesized magnesioriebeckite (1960), riebeckite and riebeckite-arfvedsonite (1962).

Michel-Lèvy (1957) hydrothermally synthesized an amphibole approximating to the chemical formula of richterite, with a composition said to be $Na_{1.5}Ca_{0.7}Mg_{5.4}Si_8O_{22}(OH)_{3.8}$. The mineral was synthesized from a mixture of $MgCO_3$, $CaCO_3$, Na_2CO_3 and SiO_2 at approximately $450^{\circ}C$. At $580^{\circ}C$ he also noted the appearance of pyroxene. The synthesis of various fibrous alkali amphiboles under hydrothermal conditions has been reported by Makarova, Korytkova, and Fedoseev (1967). The synthesis was carried out using autoclaves of platinum or silver at $350\text{-}600^{\circ}C$ at pressures between 300 and 2000 bars. Oxide mixes were starting materials and the mineral compositions had Na or Ca in X and Mg, Fe^{++}, Co or Ni in Y.

Schreyer and Seifert (1966) have synthesized amphiboles in the system Na_2O-MgO-SiO_2-H_2O. $Na_2Mg_6Si_8O_{22}(OH)_2$ represents one end-member and the other end-member is $Na_4Mg_4\ Si_8O_{20}(OH)_2\ (OH)_2$. The former breaks down to forsterite and an osumilite phase at 965 $\pm$ 20°C and 1000 bars and the latter at 770 $\pm$ 10 C. This work has two possible conclusions which can be seen from the equation:-

$$Na^+ + OH^- \rightleftharpoons Mg^{++} + O^=$$

(1) Amphiboles can accommodate more than three large cations.

(2) Some $O^=$ is replaced by OH^- in the main Si-O tetrahedra and could explain excess water in the analyses of certain amphiboles.

2-3. Experimental Details.

2-3-1. Starting Materials.

A total of 21 compositions were made up in stoichiometric proportions using a modification (D.L. Hamilton, personal communication) of the "organic silica-nitrate method" (Roy, 1956).

The following materials were used:

Na_2O: Sodium carbonate of "Analar" grade.

CaO: Calcium carbonate of "Analar" grade.

Al_2O_3: Finely divided aluminium powder supplied by British Aluminium Co. Ltd.

MgO: Pure magnesium metal supplied by Magnesium Elektron Ltd.

SiO_2: Tetraethylorthosilicate (T.E.O.S.) supplied by Monsanto Chemicals Ltd.

The following method is designed to produce 5 grams of a gel of known composition. All chemical powders should be kept in an oven at 110°C when not in use.

Weigh out in turn the calculated amounts of the powdered starting materials, wash these from the watch-glass with distilled water into a

P.T.F.E. beaker.

Holding a watch-glass firmly on top of the P.T.F.E. beaker introduce 1:1 nitric acid carefully at the spout of the beaker using a plastic wash bottle. Keep adding acid until the effervescence ceases, and then carefully wash splashes on the underside of the watch-glass into the beaker. If aluminium metal is present the solution should be heated on a water bath overnight. The watch-glass is then removed and the contents of the beaker allowed to evaporate until the solution begins to crystallize. Allow to cool and add about 25% of ethyl alcohol. A precipitate appears but the solution will clear on standing and stirring. Care must be observed when adding the ethyl alcohol because if there is any excess nitric acid it will oxidise the alcohol and in turn be reduced to nitrogen oxides and water.

T.E.O.S. is volatile and is weighed out in a weighing bottle with either a burette or hypodermic syringe and slight adjustments made using a 0.25 cc syringe. The bottle is sealed with a piece of "parafilm" which is a wax sheet, because T.E.O.S. is volatile. Wash the T.E.O.S. into the beaker using ethyl alcohol, stir thoroughly and while stirring add ammonia solution (0.88) until gelling is complete.

Leave this overnight to ensure complete gelling, dry out on a water bath and later in an oven at 110°C. Remove all the dried cake from the beaker and grind in a mortar under acetone. Place the powder in a noble metal container and decompose the nitrates by heating to dull red in a fume cupboard. Fire overnight at 700-850°C in a muffle furnace to ensure complete decomposition of the nitrates. The powder should be ground again to ensure complete homogeneity. These gels have been tested for homogeneity by C.M.B. Henderson (private communication) and have been found to be so.

The sealed tube method of Goranson (1931) was used in the experiment.

The gels were loaded, together with 5-10% water by weight, into gold or platinum capsules, depending upon the temperature and pressure of the experiments. The gold capsules were not used above 950°C.

2-3-2. Apparatus.

The experiments were carried out in three types of hydrothermal apparatus:- (1) "Cold-Seal" apparatus designed by Tuttle (1949); (2) a molybdenum - 0.5% titanium vessel described by Williams (1966); (3) an internally heated hydrothermal vessel which is a modification of that described by Yoder (1950).

The "cold-seal" vessels were made of a stellite alloy and used for experiments up to 900°C at 1000 bars pressure. The temperature of the vessel was measured by chromel-alumel thermocouples and continuously recorded on a Honeywell-Brown recording potentiometer. The temperature of the furnace was measured by a platinum-platinum 13% rhodium thermocouple and controlled by a temperature controller. The pressure in the vessel was measured by a Bourdon tube gauge and the fluctuations were not more than $\pm$ 10 bars. The vessels were cooled very quickly by an air blast and as the temperature dropped reaction was minimised.

The molybdenum-0.5% titanium vessel was used for experiments from 885° to 1250°C at 1 kilobar thus extending the range of the "cold-seal bomb" by 350°C. The "bomb" was protected from oxidation by an atmosphere of argon which is inside a "nimonic" sheath. A pressure of half a pound per square inch above atmospheric pressure was maintained inside the gas jacket throughout a run and this was monitored by a manometer. Argon gas was used as the pressure medium and raised from cylinder pressure to that required by a simple hand pump.

The third type of apparatus used was an internally heated vessel (Yoder, 1950; Burnham, 1962). The pressure medium was argon and was raised by two gas

intensifiers and the temperature of the experiment to the required pressure. This apparatus was used for experiments at 5 kilobars pressure and temperatures from 700 - 1000°C and also where large numbers of compositions were being investigated.

The condensed products were examined under a Zeiss petrographic microscope using white light and refractive index oils 1.590 - 1.650 depending upon the composition of the material.

All the samples were diffracted using a Philips diffractometer with CuKα radiation. The specimens were smear mounts with quartz as an internal standard. The mounts were scanned from 5° - 50° 2θ at 1° per minute for routine identification.

2-4. Results.

2-4-1. Richterite-K ($NaCaNaMg_5Si_8O_{22}(OH)_2$)

Fifteen experimental runs in which gels of composition $Na_2O.CaO.5MgO.8SiO_2$ were treated with excess water for 18-192 hours at 750 - 1075°C and 1 and 5 kilobars gave a product which was identified as richterite-K (Appendix 2). The mineral nucleated very quickly even at the lower temperatures investigated and appears to be formed stably over the whole range of temperatures and pressures indicated above. One run made at 1100°C and 1000 bars pressure gives condensed products which were identified as forsterite, diopside and a glass. The glass will presumably contain the sodium and therefore a sodium silicate glass. Equation:-

$$NaCaNaMg_5Si_8O_{22}(OH)_2 \rightleftharpoons \underset{Fo}{2Mg_2SiO_4} + \underset{Dp}{CaMgSi_2O_6} + (\text{sodium silicate glass}) + SiO_2$$

The author therefore tentatively puts the upper stability limit of richterite-K at 1087°C ± 12°C at 1000 bars pressure until equilibrium can be demonstrated by reversing the reaction. Equilibrium is thought

to be obtained because the end product is always 100% amphibole and there are no indications of metastability.

The richterite-K was holocrystalline. The crystals varied in size from 50 x 20μ to 200 x 70μ; they had a prismatic habit and were occasionally twinned. All had identical optical properties. Because of preferred orientation due to a prismatic cleavage, only two of the refractive indices could be obtained:-

$$\alpha' = 1.602 \pm .003$$
$$\gamma' = 1.624 \pm .003$$
$$\gamma' \wedge c = 15 \pm 2^{\circ}, \text{ optically negative.}$$

The refractive indices agree well with those of fluor-richterite (Kohn and Comeforo, 1955) which had $\alpha = 1.603$, $\beta = 1.614$, $\gamma = 1.622$, and those of natural richterite from Långban, Sweden (Sundius, 1946) which had $\alpha = 1.605$ and $\gamma = 1.627$.

The richterite-K has similar optical properties to tremolite-K. The distinguishing properties are 2V and extinction angle. The effect of sodium in minerals is to lower the refractive indices and hence change the values of the other optical properties. If we assume a β refractive index of 1.614 (that of fluor-richterite, op. cit.) the 2V should be 70°, whereas tremolite has 2V of 86°. The extinction angle ($\gamma \wedge c$) of tremolite-K is 21° and that of richterite-K 15°.

The X-ray pattern of the synthetic richterite was compared with those of natural richterite from Långban, Sweden and richterite from the Wichita meteorite (Olsen, 1967) and these are shown in Table 2-1. The small difference in pattern may be a result of the manganese content of the natural mineral which may be as high as 9%.

The cell parameters of richterite-K are shown below compared with synthetic tremolite-K (Colville et al., 1966) using the space group

TABLE 2-1

X-RAY POWDER DATA FOR SYNTHETIC RICHTERITE COMPARED WITH NATURAL RICHTERITE (LÅNGBAN, SWEDEN) AND METEORITIC RICHTERITE

hkl	Synthetic Richterite d	I/I_o	Richterite Långban d	I/I_o	Richterite Meteorite d	I/I_o
020	8.984	10	-	-	8.605	70
110	8.485	65	8.51	100	8.393	70
$\bar{1}11$	4.861	10	-	-	4.864	30
200	4.802	15	4.804	20	-	-
040	4.496	44	4.500	40	4.493	50
	-	-	-	-	4.160	70
111	-	-	-	-	4.004	30
$\bar{1}31$	3.865	28	3.858	20	3.850	50
131, 041	3.388	85	3.388	70	3.376	100
240	3.282	90	3.281	60	3.267	80
310	3.148	100	3.146	70	3.125	100
$\bar{2}41$	3.027	40	-	-	-	-
221	2.959	65	2.962	60	2.944	80
330	2.823	45	2.823	40	2.800	40
$\bar{3}31$	2.734	45	-	-	-	-
151	2.707	100	2.707	80	2.709	100
061	2.585	55	2.587	40	2.581	70
$\bar{2}02$	2.527	30	2.532	60	2.522	90
420	2.391	20	-	-	2.382	20
$\bar{3}51$	2.334	70	2.337	50	2.320	50
071	2.288	30	2.278	50	2.286	50
171	2.202	10	-	-	2.203	20
261	2.167	60	2.167	60	2.160	70
280	2.055	10	-	-	2.048	40

notation $C2/_m$.

Richterite-K	Tremolite-K
$a_o = 9.892\text{Å} \pm .005$	$a_o = 9.833 \pm .005\text{Å}$
$b_o = 17.958\text{Å} \pm .007$	$b_o = 18.054 \pm .009\text{Å}$
$c_o = 5.263\text{Å} \pm .002$	$c_o = 5.268 \pm 004\text{Å}$
$\beta = 104.28^o \pm .03$	$\beta = 104.52 \pm 07^o$
$a_o \sin\beta = 9.586\text{Å}$	$a_o \sin\beta = 9.52\text{Å}$
cell vol. $= 906.0\text{Å}^3 \pm 1.0$	cell vol. $= 905.3\text{Å}^3 \pm 1.0$
ρ (calc.) $= 2.994$ gm/cm^3	ρ (calc.) $= 2.980$ gm/cm^3

The significance of these cell parameters and of other synthetic monoclinic amphiboles will be discussed in the chapter on X-ray diffraction techniques.

2-4-2. Eckermannite-K ($NaNa_2Mg_4AlSi_8O_{22}(OH)_2$).

Thirteen experiments in which gels of composition $3Na_2O.8MgO.Al_2O_3.16SiO_2$ were treated with excess water for 18-92 hours at 770-1100°C and 1 and 5 kilobars gave mixtures of an amphibole with a talc-like mineral. The crystals of the amphibole were extremely small and of a fibrous habit. Their maximum size was 20 x 3μ and their average length was 10μ. None of the optical properties could be determined with any accuracy from such small crystals. The amphibole was considered to be synthetic eckermannite-K. In Appendix 2 the experimental conditions are shown for the various temperatures and pressures. In Table 2-2 synthetic eckermannite-K X-ray diffraction pattern is compared with those of natural eckermannite from Norra Kärr in Sweden and synthetic glaucophane I-K (Ernst, 1961). There is a close similarity between the patterns of glaucophane I-K and eckermannite-K at high 'd' values.

The cell parameters for the synthetic eckermannite-K are compared below with those of glaucophane I and II (Ernst, 1961 and 1963).

TABLE 2-2

X-RAY POWDER DATA FOR (1) NATURAL ECKERMANNITE, NORRA KÄRR, SWEDEN; (2) SYNTHETIC GLAUCOPHANE-K (ERNST, 1961); (3) SYNTHETIC ECKERMANNITE-K.

hkl	Natural Eckermannite		Synthetic Glaucophane		Synthetic Eckermannite	
	d	I/I_o	d	I/I_o	d	I/I_o
020	8.93	10	9.00	9	-	-
110	8.38	82	8.38	32	8.36	40
130	5.032	11	-	-	-	-
$\bar{1}11$	4.878	4	4.818	12	4.822	12
200	4.743	6	-	-	-	-
040	4.445	29	4.481	36	4.479	40
111, $\bar{2}01$	4.005	6	4.049	19	4.040	14
$\bar{1}31$	-	-	3.885	35	3.835	38
$\bar{2}21$	3.646	6	-	-		
131, 041	3.375	31	3.412	72	3.405	70
240	3.244	36	3.257	65	3.246	70
310	3.108	100	3.120	91	3.097	100
$\bar{3}11$	3.047	6	-	-	-	-
221	2.947	10	2.980	50	2.965	50
151	2.908	6	2.913	34	2.910	25
330	2.782	32	2.794	24	2.781	35
151	2.694	37	2.714	100	2.708	80
061	2.566	10	2.581	32	2.571	35
$\bar{2}02$	2.525	12	2.502	81	2.500	60
350	2.360	6	-	-	-	-
$\bar{4}21$, $\bar{3}51$	2.306	8	2.301	13	2.294	20
331	2.267	7	2.265	25	2.276	20
261	2.150	9	2.173	50	2.164	50
202	2.055	4	2.081	15	-	-
351	2.010	4	2.031	9	2.019	10

Eckermannite-K	Glaucophane I-K	Glaucophane II-K
$a_o = 9.762 \pm .006$Å	9.75Å	9.64Å
$b_o = 17.892 \pm .011$Å	17.91Å	17.73Å
$c_o = 5.284 \pm .006$Å	5.27Å	5.28Å
$\beta = 103.17^\circ$	102.8°	103.6°
$a_o \sin\beta = 9.505$Å	9.50Å	9.37Å
cell vol. $= 898.6 \pm 0.8$Å^3	897Å^3	877Å^3

The cell parameters show a close similarity which would be expected from the compositions.

The 'talc' type substance had optical and X-ray properties very similar to those of talc. The exact composition of the eckermannite is therefore uncertain. It must be close to or even at the end of the eckermannite-glaucophane join (see Figure 3 of Phillips, 1966) because the mineral is still stable at 1100°C at 1000 bars pressure. Glaucophane breaks down to forsterite, enstatite, albite and vapour at 835°C and 1000 bars pressure (Ernst, 1961). Another piece of evidence supporting the facts is the synthesis of 75 eckermannite - 25 richterite from the bulk composition $8Na_2O.CaO.17MgO.1.5Al_2O_3.16SiO_2$ with excess water.

2-4-3. Miyashiroite-K.

Alkali amphiboles were not among the products of runs using gels of miyashiroite-K composition ($3Na_2O.6MgO3Al_2O_3.14SiO_2$). The only phase to condense was a phase which has been identified as a "sodic-montmorillonite". The basal spacing (001) of this phase ranges from 11.89 - 12.2Å. Ernst (1961) noted the occurrence of this phase in runs of glaucophane composition together with glaucophane-K , forsterite, enstatite and albite. When left overnight saturated with ethylene glycol it does not expand, i.e. the basal spacing remains the same which is peculiar for a member of the montmorillonites.

The gels will react very quickly and presumably at low temperatures one would expect a clay mineral to crystallize if the composition were appropriate at these temperatures and pressures. Also it is possible that as the experiment is quenched montmorillonite forms as a quench product and evidence is supplied by G.R.183 where one crystal is completely armoured by other crystals which may be quench phases or the smaller crystal has acted as a nucleus.

The clay phase if of normal montmorillonite composition would become unstable as the temperature rises but the introduction of sodium into the lattice will raise the thermal stability level. The persistence of this phase outside its stability field leads to it being called a metastable phase. Fyfe (personal communication) has obtained nickel montmorillonites metastable to 900°C at 1000 bars.

Ames and Sand (1958) explain that the controlling factors which result in montmorillonites having the highest hydrothermal stability are:-

(a) all cation positions must be filled.

(b) there must be optimum substitution in either octahedral or tetrahedral positions to provide the excess charge for maximum base exchange capacity.

(c) there must be present exchangeable ions other than H^+ to satisfy the interlayer charge.

In the mineral at present under study aluminium will be available to substitute for silicon in tetrahedral co-ordination and sodium is available to become the exchangeable ion.

To discover what this phase was, natural montmorillonite from Montmorillon was utilised in several experiments. The first experiment was to X-ray the specimen in its natural state and also saturated with ethylene glycol. On glycolating the sample the basal spacing moved from 15 to 17Å.

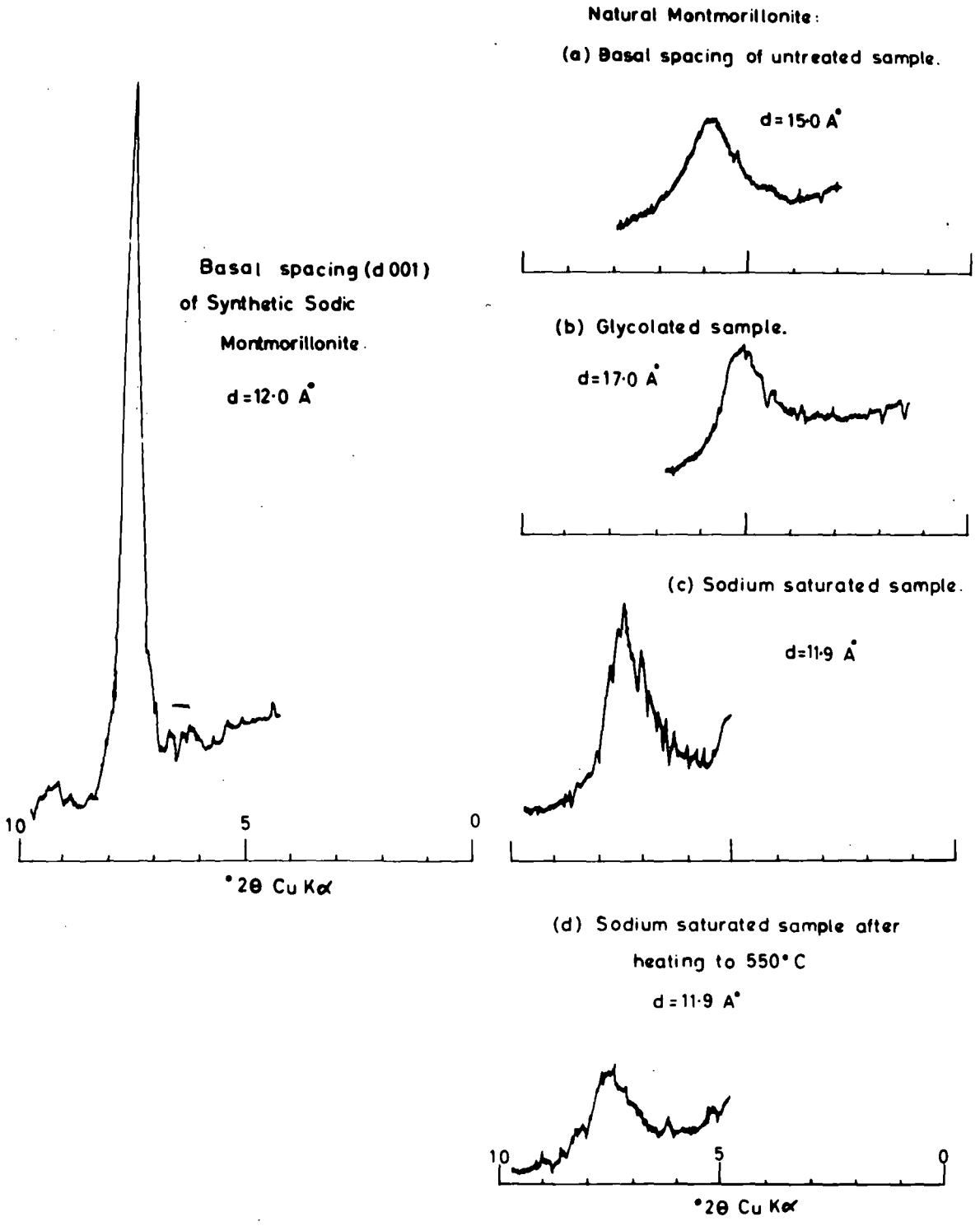

Fig. 2-1 Diffractograms of synthetic montmorillonite compared to natural montmorillonite, Poitiers, France.

The second experiment was to saturate the natural specimen with sodium ions. This was done by making up a solution of 2N sodium chloride and immersing the specimen in this solution. The specimen was then washed to free the sample of excess sodium chloride. This sample when diffracted gave a basal spacing of 11.9Å which is in accord with Ames and Sand's conclusion that sodium saturated montmorillonites have an (001) spacing between 11.00 and 12.50Å.

Hofmann and Endell (1939) stated that sodium montmorillonites lose the power to re-expand after heating to 390-490°C before dehydration becomes irreversible. The sodium sample was then heated to 550°C overnight and again X-rayed. The basal spacing was not affected by heating. The effect of quenching these experiments from very high temperature may create this situation too. The ethylene glycol does not affect the basal spacing of this specimen.

Greene-Kelly (1952) states that above 550°C there is total elimination of OH^- groups and that exchangeable cations giving easy collapse are surrounded by strongly absorbing cations, i.e. lithium and calcium, while those that don't give easy collapse are easily dehydrated such as sodium or potassium.

Hofmann and Klemen (1950) suggested that "place exchange" was responsible for the observed facts which depend upon the size of each cation only. Thus when sodium montmorillonite went above 540°C Na^+ (0.97Å) migrated into the vacant octahedral sites and the mineral is assumed to have a pyrophyllite structure and loss of expanding properties. An alternative view is that on heating the sample water is lost from the interlayer position and sodium ions bind the mineral.

The sequence of changes are shown as diffractograms in Fig. 2-1. These changes are compared with synthetic sodium montmorillonite.

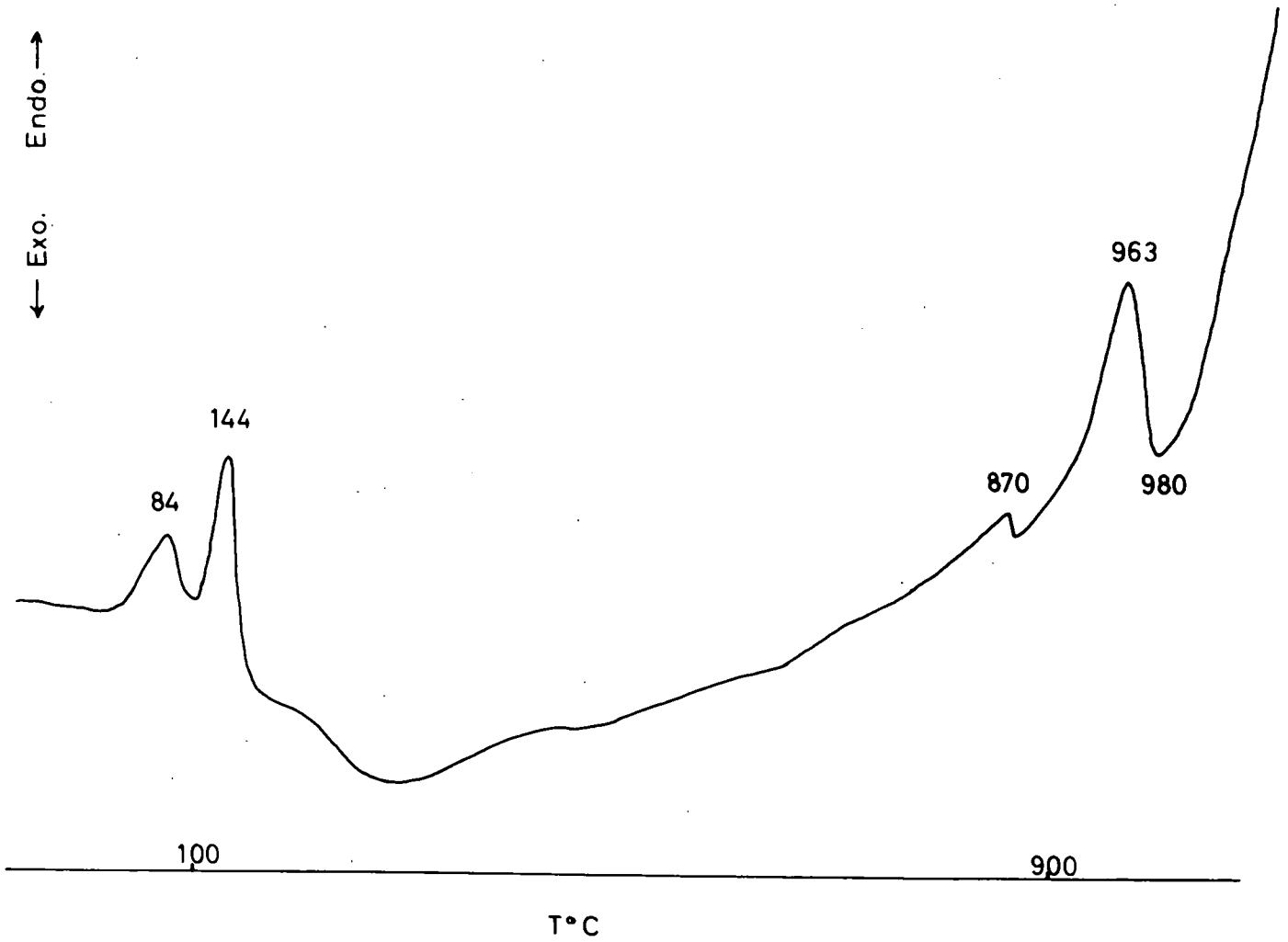

Fig. 2-2 Differential Thermal Analysis curve for synthetic sodic montmorillonite.

The experimental conditions for these runs are set down in Appendix 2 and from these it can be noted that we obtain sodium montmorillonite from all the runs of composition $3Na_2O.6MgO.3Al_2O_3.14SiO_2$. Seeding the gel of this composition has been attempted by using synthetic richterite but the richterite was absorbed by the rest of the gel and gave the same product as above. Attempts have been made to make the fluor-equivalent of miyashiroite-K and the results are set forward in a later section.

Miyashiroite belongs to the system Na_2O-MgO-Al_2O_3-SiO_2-H_2O which has been worked on in part by Iiyama and Roy (1963). The typical saponite which forms in their experiments breaks down as the temperature rises to anthophyllite and a smectite, therefore compared to the earlier saponite the smectite is richer in sodium and aluminium and poorer in magnesium and silicon.

$$Na_{\alpha}(Mg_{3-x}Al_x)(Si_{4-y})O_{10}(OH)_2.2H_2O, \quad \alpha = x + y$$

The smectite they obtained had a refractive index of between 1.52 - 1.48 for β whereas the sodium montmorillonite of these experiments was between 1.52 and 1.53 for β. The smectite had a basal spacing of 12.0 - 12.6Å, talc 9.3Å, and anthophyllite. The smectite field became smaller as the temperature rose and was tiny at 850°C.

A sample of this sodic montmorillonite was used for a differential thermal analysis investigation to see if it compared with natural montmorillonites. On the D.T.A. chart (Fig. 2-2) there are two low temperature endothermic peaks, one at 84°C and the other at 144°C. These two peaks denote the loss of adsorbed water; one peak may be the result of intergranular water the other may be capillary water. The rest of the pattern is closest in similarity to montmorillonite than any of the other clay minerals (Kerr et al., 1949) but the typical endotherm at 700°C

which marks dehydroxylation is at a higher temperature (870°C) and is quite small. The position of this peak depends upon the elements bonded to the hydroxyl and if these bonds are strong, dehydroxylation takes place at higher temperatures. The final breakdown of the sodic montmorillonite takes place at 963°C which is only slightly higher than for the natural minerals of similar composition. This is followed by a sharp exotherm and large endotherm which marks the progressive fusion of the mineral.

The material was removed after the final exotherm, examined by X-ray diffraction and gives the reaction:-

$$(NaNa_2Mg_3Al_2Si_7AlO_{22}) \rightleftharpoons \underset{\text{Nepheline}}{3NaAlSiO_4} + \underset{\text{Enstatite}}{3MgSiO_3} + \underset{\text{Cristobalite}}{SiO_2}$$

The breakdown products of this phase may be useful in attempting to synthesize the amphibole instead of starting with the gel.

2-4-4. Sundiusite-K.

Twenty four experiments of composition Na_2O-CaO-3MgO-$2Al_2O_3$-$6SiO_2$ were treated with excess water for 24-188 hours at temperatures from 800°C to 1000°C at one and five kilobars pressure (Appendix 2) resulted in three products at the lower temperatures 800-900°C and two at higher temperatures (900 - 1000°C). These products were identified as synthetic sundiusite, talc, and sodium-calcium montmorillonite. At higher temperatures the talc phase disappears and the montmorillonite shifts its basal spacing to higher 'd' values.

The synthetic sundiusite-K was at first confused with anthophyllite-K but the X-ray patterns do not agree and it would also mean that anthophyllite-K would be metastable above the stability range for the mineral (745°C at 1000 bars pressure, Greenwood, 1963). The remarks which applied to sodic montmorillonite also apply to this clay mineral which appeared in all experiments of this composition.

Three experiments were performed holding the temperature at 1200-1250°C for half an hour to melt the charge and then dropping the temperature to 900-975°C for forty eight hours. The clay phase persisted but the talc disappeared. From these observations the clay mineral is a quench phase and it implies that the amphibole grows relatively sluggishly which Ernst (1968) also concludes in his experiments with amphiboles.

The amphibole crystals are prismatic ranging in size from 40 x 5 μ to 10 x 2 μ, the larger crystals appear in runs of longer duration and at higher temperatures and pressures. They are occasionally twinned and of uniform birefringence.

Optical Properties:-	Sundiusite	Pargasite
α'	= 1.612 ± .003	1.624
γ'	= 1.634 ± .003	1.645
$\gamma' \wedge c$	= 10°	26°

The γ' refractive index is lower than that of pargasite because the latter mineral has much more calcium in the structure but higher than richterite where there is no Al for Si replacement in the tetrahedral sites. Unfortunately there are no values calculated for the optical properties of this composition.

The X-ray pattern of sundiusite-K is shown in Table 2-3 along with several other amphiboles also synthesized during this investigation. The cell parameters for this mineral are as follows:-

Sundiusite-K

a_o = 9.914 ± .014Å
b_o = 17.919 ± .024Å
c_o = 5.305 ± .008Å
β = 105.35 ± 0.12°
$a \sin\beta$ = 9.560Å
vol. = 908.8Å^3

TABLE 2-3

X-RAY DIFFRACTION PATTERNS OF SYNTHETIC AMPHIBOLES

hkl	Tschermakite	Sundiusite	Tremolite	Ed50R50	R75Tr25	R25Tr75	75R25Ec	25R75Ec
020	8.94	8.92	8.97	9.01	9.01	9.03	8.98	-
110	8.36	8.40	8.43	8.47	8.47	8.44	8.47	8.47
130	5.053	4.955	5.085	5.096	5.088	5.091	-	-
$\bar{1}11$	4.888	-	4.869	4.874	4.866	4.869	4.869	4.848
200	-	-	4.786	4.796	4.798	4.760	4.786	4.783
040	4.470	4.479	4.491	4.502	4.500	4.509	4.500	4.493
111	-	4.17.	-	-	-	-	-	-
$\bar{2}01$	-	4.029	4.006	3.994	-	3.995	4.010	-
$\bar{1}31$	3.880	3.877	3.872	3.873	3.865	3.868	3.861	3.863
131	3.354	3.364	3.389	3.381	3.390	3.384	3.391	3.401
240	3.246	3.260	3.277	3.282	3.280	3.270	3.277	3.269
310	3.101	3.127	3.142	3.147	3.147	3.125	3.143	3.130
$\bar{2}41$	-	-	2.989	2.988	2.992	2.991	-	-
221	2.967	2.960	2.956	2.950	2.953	2.944	2.961	2.956
$\bar{1}51$	2.914	2.921	-	-	2.896	2.894	-	-
330	2.783	2.803	2.818	2.819	2.822	2.805	2.817	2.808
$\bar{3}31$	2.728	2.744	2.766	2.739	2.734	2.724	2.729	2.719
151	2.683	2.686	2.706	2.704	2.707	2.706	2.707	2.707
112	-	2.958	-	-	-	-	-	-
061	2.572	2.573	2.584	2.584	2.585	2.590	2.585	2.583
$\bar{2}02$	2.539	2.545	2.517	-	2.520	2.527	2.525	2.448
350 400	-	2.410	-	2.389	-	2.381	2.387	2.385
$\bar{3}51, \bar{4}21$	2.327	2.340	2.328	2.337	2.334	2.331	2.329	-
$\bar{1}71$	-	-	2.285	-	2.287	2.294	-	-
$\bar{3}12$	-	-	2.269	-	-	2.269	2.268	
171 261	-	-	2.165	2.164	2.165	2.163	2.164	2.168

The a_o, b_o, and $a_o \sin\beta$ parameters are close to what would be expected for the composition of this mineral but the β angle is larger than expected ($\sim 104.70^\circ$).

2-4-5. Tschermakite-K. □ $Ca_2Mg_3Al_2Si_6Al_2O_{22}(OH)_2$.

This mineral was synthesized by D.L. Hamilton during an investigation of the anorthite-forsterite join of the system CaO-MgO-Al_2O_3-SiO_2-H_2O at 15 kb pressure and identified by the author. Metastable kaolinite, montmorillonite and minor pyrope were additional phases. The tschermakite is stable between 900-1100°C at 15 kb. The synthesis of this phase has recently been reported by M.C. Gilbert (1969) but no physical data were presented in the report.

The tschermakite crystals are prismatic and vary greatly in size from 50 x 10μ to 200 x 40μ.

Refractive Indices:-	Author (observed)	Winchell (calculated)
α'	1.626 ± .003	1.626
γ'	1.643 ± .003	1.646
$\gamma' \wedge c$	30°	14°

The X-ray diffraction pattern is shown in Table 2-3. The diffraction patterns of sundiusite-K and tschermakite-K are very similar and the (151) reflection for these two minerals and pargasite-K (Boyd, 1959) lies at a similar 2θ value, quite a distance from the (151) reflection of tremolite-K (Boyd, 1959) and richterite-K (present author), denoting a difference in the 'b' parameter for the aluminous and non-aluminous amphiboles.

	Tremolite	Richterite	Pargasite	Tschermakite	Sundiusite
151 ($2\theta CuK\bar{\alpha}$)	33.05	33.09	33.38	33.40	33.36

The cell parameters for tschermakite-K are:-

$a_o = 9.823\text{Å}$
$b_o = 17.921\text{Å}$
$c_o = 5.272\text{Å}$
$\beta = 105.51^\circ$
$a\sin\beta = 9.456\text{Å}$
vol. $= 894.27\text{Å}^3$

2-4-6. Intermediate composition amphiboles.

The following compositions were successfully synthesized:-

Composition	Abbreviation
$NaCa_{1.5}Na_{0.5}Mg_5Si_{7.5}Al_{0.5}O_{22}(OH)_2$	50Ed - 50R
$Na_{0.75}Ca_{1.25}Na_{0.75}Mg_5Si_8O_{22}(OH)_2$	75R - 25Tr
$Na_{0.25}Ca_{1.75}Na_{0.25}Mg_5Si_8O_{22}(OH)_2$	25R - 75Tr
$NaCa_{0.75}Na_{1.25}Mg_{4.75}Al_{0.25}Si_8O_{22}(OH)_2$	75R - 25Ec
$NaCa_{0.25}Na_{1.75}Mg_{4.25}Al_{0.75}Si_8O_{22}(OH)_2$	25R - 75Ec

All these compositions were synthesized at 900°C and 5 kb pressure. They were synthesized for three reasons: (1) no intermediate compositions had previously been attempted, (2) to observe changes in cell parameters with changes in chemical composition, (3) to observe the infra-red spectra of intermediate compositions.

2-5. Discussion.

TABLE 2-4 Thermal ranges of synthetic hydroxy-amphibole end-members.

Species	Composition	High Temperature Stability Limit, °C		
		500 bars	1000 bars	2000 bars
Anthophyllite	$Mg_7Si_8O_{22}(OH)_2$	-	745	765
Pargasite	$NaCa_2Mg_4AlSi_6Al_2O_{22}(OH)_2$	955	1045	-
Ferropargasite	$NaCa_2Fe^{++}_4AlSi_6Al_2O_{22}(OH)_2$	682	800	850
Tremolite	$Ca_2Mg_5Si_8O_{22}(OH)_2$	800	830	870
Ferrotremolite	$Ca_2Fe^{++}_5Si_8O_{22}(OH)_2$	437	465	506
Magnesioriebeckite	$Na_2Mg_3Fe^{+++}_2Si_8O_{22}(OH)_2$	921	928	935
Riebeckite	$Na_2Fe^{++}_3Fe^{+++}_2Si_8O_{22}(OH)_2$	481	496	515
Glaucophane I	$Na_2Mg_3Al_2Si_8O_{22}$	859	864	868
Richterite	$NaCaNaMg_5Si_8O_{22}(OH)_2$	-	1087	-
Eckermannite	$NaNa_2Mg_4AlSi_8O_{22}(OH)_2$	-	1100	-

Various cationic substitutions affect the thermal stability range of amphiboles differently. The lowest stability limit for the magnesium end-members is that of anthophyllite-K . When the magnesium in M(4) is replaced by calcium, as in tremolite, the thermal stability is raised to 830°C at 1000 bars. Substitution of sodium into one of the M(4) sites and addition of sodium in the previously vacant 'A' position raises the stability much further, to 1087°C. One can therefore state that the introduction of an alkali into the previously vacant 'A' site will increase the lattice energy of the crystal because it adds 12 M-O bonds of strength 1/6 to the lattice energy therefore it has a large effect upon the thermal stability.

Pargasite-K is stable to 1045°C at one kilobar pressure and also contains sodium in the 'A' site but in addition two silicon atoms have been replaced by aluminium in the tetrahedral sites and also one aluminium for magnesium in the octahedral sites. Slaughter (1966) studied the phyllosilicates and concluded that when aluminium substitutes for silicon it reduces the co-ordination effects thereby raising the thermal range of stability. Presumably the same criterion can be applied to the amphiboles. Harry (1950) stated that more aluminium appears to enter tetrahedral sites in the higher temperature hornblendes.

Comparison of the data for tremolite and glaucophane reveals that the coupled substitution $CaMg \rightleftharpoons NaAl$ influences the amphibole stability only slightly or may affect the stability in different directions. Eckermannite-K which has sodium in the 'A' sites and M(4) sites and only one aluminium atom in M(2) is quite refractory and is stable beyond 1100 C. It is therefore possible that sodic amphiboles of sundiusite-K and miyashiroite-K compositions are as stable or more stable than eckermannite. Sodium in M(4) may also raise thermal stability.

Ketelaar (1953) states that for many ionic substances the thermal stability range increases with decreasing valency and increasing radius of the non-complex ion. He demonstrates his conclusion by studying the heats of formation of the carbonates of Group 1 elements and these are more stable than Group 2 carbonates when thermal energy is applied to them. This simple picture has its attractions in discussing qualitatively the effects of substitutions in the amphiboles but we are not dealing with simple ionic salts.

Ferric iron substituted for aluminium as in magnesioriebeckite (Ernst, 1960) raises the thermal stability level compared to glaucophane but the ferrous iron end-members such as ferrotremolite and ferropargasite are much less stable than their magnesium equivalents.

Summarising the data for the amphiboles shown in Table 2-4

Effects which raise thermal stability:-

(1) Sodium for calcium in M(4).

(2) Sodium in 'A' sites.

(3) Aluminium for silicon in tetrahedral sites.

Effects which decrease thermal stability:-

(1) Vacant 'A' site.

(2) Aluminium for magnesium in M(2) sites.

(3) Ferrous iron for magnesium in M(1), M(2) and M(3) sites.

(4) Magnesium for calcium in M(4) sites.

The last condition also involves a difference in structure. From this very qualitative statement the amphiboles with highest stabilities will be either per-alkaline or per-aluminous.

CHAPTER THREE

Synthesis of Fluor-amphiboles

3-1. Previous investigations.

The first attempt to synthesize fluorine containing minerals was made by Bowen and Schairer (1935) who mixed orthopyroxene and sodium fluoride to produce fluor-amphiboles. The amphibole rimmed the pyroxene crystals. Grigoriev and Iskull (1937) fused powdered amphiboles with calcium fluoride to produce fluor-hornblendes.

Kohn and Comeforo (1955 and 1957) published work on fluor-tremolite ($Ca_2Mg_5Si_8O_{22}F_2$), fluor-richterite ($NaCaNaMg_5Si_8O_{22}F_2$), fluor-edenite ($NaCa_2Mg_5Si_7AlO_{22}F_2$) and fluor-boron-edenite ($NaCa_2Mg_5BSi_7O_{22}F_2$). The amphiboles produced were of an acicular habit.

Gibbs, Bloss and Shell (1960) synthesized a new poly-type by substituting lithium for sodium and magnesium. This amphibole they called protoamphibole ($Li_{.64}Na_{0.5}, Li_{0.48}Mg_{1.52}, Mg_5Si_{7.93}O_{21.91}F_{2.09}$). They noted that if calcium were present a monoclinic phase was formed. Gibbs (1969) has determined the crystal structure of this mineral.

Saito and Ogasawara (1959), Saito (1963), Shell, Comeforo, and Eitel (1958), and Grigorjeva, Chigarova and Fedoseev (1967) have produced amphiboles of varying compositions and the amphibole composition producing synthetic asbestos is the richterite composition.

3-2. Experimental details.

In the first experiments the Bowen and Schairer (1935) method was used. Powdered hypersthene was mixed with sodium fluoride and the mixture fused and subsequently cooled down. Small but detectable amounts of amphibole were produced.

The starting materials in most experiments were oxide gels made up to the stoichiometric proportions of the amphibole compositions by the

addition of sodium or magnesium fluorides. This method eliminates most of the volatile material such as carbon dioxide if carbonates are used.

The gel plus fluoride mixes were packed to hard tightness in 30 c.c. open graphite crucibles, placed in an open tube furnace, and heated to the required temperature. The mixes were heated to either 1100, 1200, 1300, or 1350°C and held at these temperatures for between 1 and 2 hours and cooled down to 1100°C at 35°/hour or 10°/hour.

3-3. Results.

All the magnesium end-member compositions were made up and reacted at various temperatures. Fluor-tremolite,-edenite, and-richterite were produced but phyllosilicates were the products of the compositions containing large amounts of aluminium.

Fluor-richterite was the most successful composition and the acicular crystals were up to $\frac{1}{2}$ cm. long and they had a vitreous lustre.

The cell parameters of the fluor-richterite is compared below to those determined by Kohn and Comeforo (1955):

fluor-richterite (this study)	fluor-richterite (Kohn and Comeforo)
$a_o = 9.817 \pm .002$Å	$a_o = 9.823$Å
$b_o = 17.956 \pm .004$Å	$b_o = 17.957$Å
$c_o = 5.263 \pm .002$Å	$c_o = 5.268$Å
$\beta = 104.36 \pm .02°$	$\beta = 104.33°$
$a\sin\beta = 9.510$Å	$a\sin\beta = 9.517$Å
vol. = 898.8Å^3	vol. = 900.31Å^3

The crystal size of the fluor-richterite increased as the temperature was slowly reduced to induce orientation of the crystals by establishing a thermal gradient through the melt.

CHAPTER 4

Chemistry of the Alkali Amphiboles

4-1. General Statement

The chemistry of the alkali amphiboles has been the subject of several studies (Sundius, 1945; Miyashiro, 1957; Borg, 1967; Kovalenko, 1968). These previous studies have only dealt with a portion of the alkali amphibole mineral group. The present study has involved a collation of all the available alkali amphibole analyses, a recalculation of these analyses and then these are plotted on to the compositional space devised by Phillips (1966). Various coupled substitutions in the alkali amphiboles have been discussed and the general chemistry of certain elements in alkali amphiboles.

4-2. Recalculation of the alkali amphibole analyses

The analyses were recalculated to both 24 and 23 oxygens following Phillips' (1963) procedures:-

1. The hydroxyl positions are made up to two with oxygen if necessary, and for this substitution ferric ions equal to the number of oxygen atoms are required in the Y sites to balance this substitution. If ferric iron is not available and cation numbers are high then a negative error in the water content is indicated. If hydroxyl exceeds two atoms the excess hydrogen goes into the 'A' site. Excess hydrogen with low cation numbers indicates a positive error for water.
2. The Z sites are made up to 8.00 atoms with tetrahedral aluminium, insufficient of this element and a low total indicates an error.
3. The X sites are made up to 2.00 with calcium and sodium; and possibly made up with excess manganese, ferrous iron, or

magnesium from Y sites. The excess sodium goes with the potassium and excess hydrogen into the 'A' sites. If 'A' is greater than one an error is indicated.

The sum of the valencies in A should balance the substitution of sodium for calcium in X or the balance completed by triply charged ions in Y.

4. The atoms in the Y site should lie between 4.95-5.10 and the following substitutions take place within the Y sites:-

(1) $2Mg \rightleftharpoons Li\ Al$

(2) $2Mg \rightleftharpoons Ti^{4+} + \square$

(3) $3R^{2+} \rightleftharpoons 2R^{3+} + \square$

The latter not being common.

For superior analyses Phillips' suggestions were accepted for recalculation:-

1. Si and Al^{IV} are the only occupants of Z sites and must total between 7.92 and 8.08 atoms.
2. The sum of the Y group must be between 4.95 and 5.05 atoms.
3. The sum of the X group must be between 1.98 and 3.03 atoms.
4. The silicon total must not be below 5.94 atoms.
5. Ferric iron must equal or exceed the amount of oxygen replacing the hydroxyl.

Of all Phillips' suggestions for an amphibole superior analysis the most suspect is that ferric iron substitutes for a divalent ion in M_1 and M_3 sites when oxygen replaces hydroxyl or fluorine in O_3. Leake (1968) demonstrated that for the calciferous amphiboles there is a positive correlation between ferric iron and (OH, F, and Cl). This is supported by the author's data on riebeckite-arfvedsonites (Fig. 4-1).

Although there is no close correlation between low hydroxyl contents

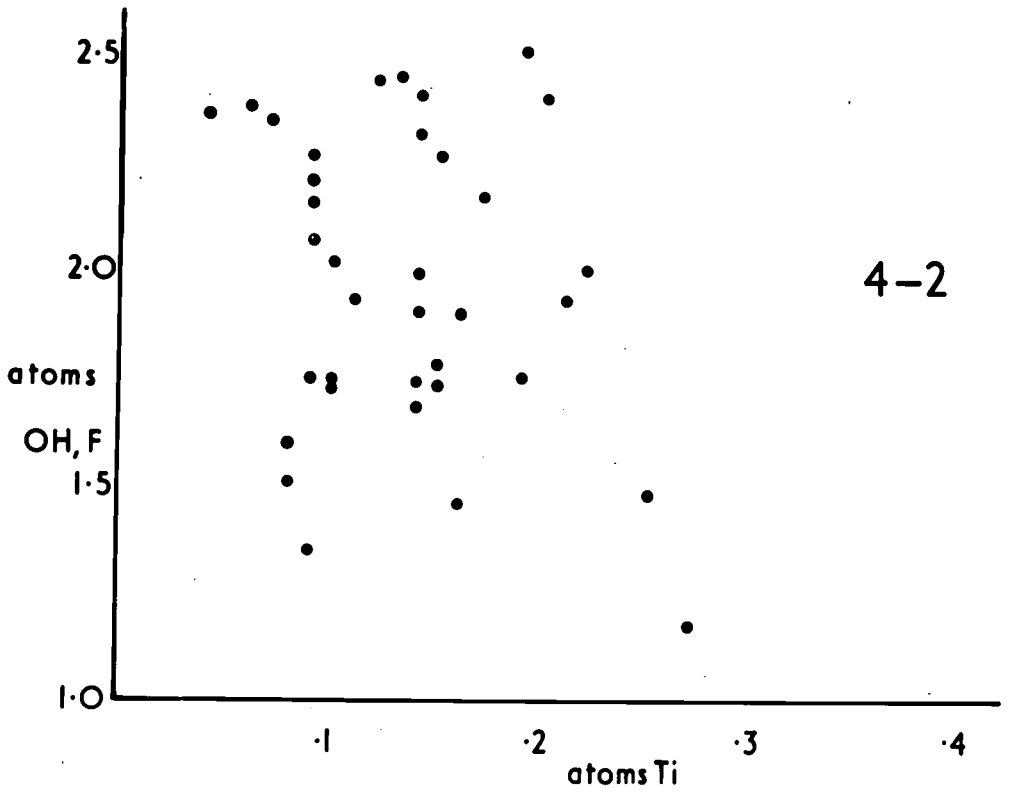

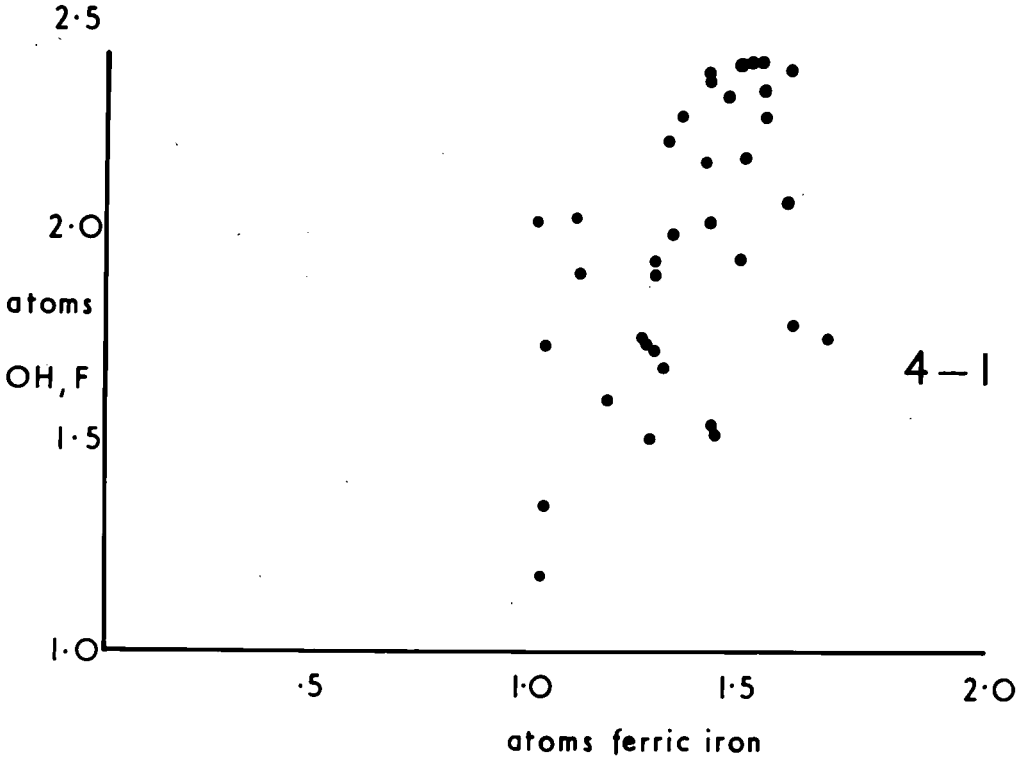

Fig. 4–1 } Correlation of OH^- and F^- with Fe^{+++} and Ti^{++} contents.
4–2 }

and oxysubstitution this does not negate the possibility that it takes place in high temperature oxyhornblendes.

In figure 4-1 the riebeckite-arfvedsonites of Borley (1963) and the author are plotted and show a very slight positive correlation; if ferric iron were making up the deficiency in the O_3 sites it should show negative correlation. The values for titanium (Fig. 4-2) show a negative correlation, but the points are too scattered for the results to be significant.

Excess hydroxyl up to three atoms are common in crocidolites (riebeckite). Hodgson et. al (1965) have shown that the values for combined water (H_2O^+) should be taken at a temperature above 570°C for crocidolites, and when this is applied good results occur.

There is no evidence presented to date supporting the idea that hydrogen enters the 'A' sites, nor that the hydronium ion (H_3O^+) is present. The latter would have possibly been detected by infra-red spectroscopy. The 'A' site in the alkali amphiboles is often full or nearly so without need for hydrogen to fill the sites therefore a more plausible answer is that hydroxyl in excess of 2.00 atoms indicates analytical error.

Leake (1968) observes that the Phillips' suggestions for superior analysis are unrealistically stringent because each oxide must be determined to within 1% and Leake advances several criteria himself to be used to adjudge whether an analysis is superior. The analyses are divided into superior, moderate and inferior by Leake.

The differences in suggestion by Leake from those of Phillips are:-

1. That the sum of calcium + sodium + potassium atoms should lie between 1.75 and 3.05 atoms, and that calcium in excess of 2.00 is present in Y or A.
2. The number of Y atoms should total between 4.75 and 5.25 atoms, i.e. $\pm$ 5%.

3. That the O_3 occupants ($OH^- + F^- + Cl^-$) should total between 1.00 - 2.99 atoms, i.e. an error of +50% — -100%.

Due to poor results in water determinations workers now tend to recalculate amphiboles to an anhydrous basis, i.e. 23(0). Borg (1967) concludes that the apparent superiority of the recalculation to 23(0) is by virtue of compensating errors of opposite sign. The 23(0) recalculation approaches to closer theoretical values of X, Y, and Z when (OH^-, F^-) are greater than $\pm$ .30 units from 2.00. When there is little error in the amount of hydroxyl both the 24(0) and 23(0) recalculations approach ideal. Table 4-1 shows two of the author's analyses, one superior (10941 from a naujaite, Ilímaussaq) and one inferior (12837, naujaite pegmatite) water and fluorine determination.

TABLE 4-1 Recalculated alkali amphibole analyses of two arfvedsonites.

	D.U. 12837		D.U. 10941	
	Cations/ 23 Oxygens	Cations/ 24 Oxygens	Cations/ 23 Oxygens	Cations/ 24 Oxygens
SiO_2	7.508	7.612	7.306	7.295
Al_2O_3	0.526	0.533	0.664	0.663
Fe_2O_3	1.031	1.046	1.022	1.020
FeO	3.560	3.609	3.580	3.575
MnO	0.078	0.079	0.087	0.087
MgO	0.024	0.024	0.031	0.031
ZnO	0.007	0.007	0.008	0.008
TiO_2	0.093	0.095	0.219	0.219
CaO	0.461	0.467	0.458	0.457
Na_2O	2.281	2.313	2.153	2.149
K_2O	0.373	0.378	0.349	0.348
H_2O^+	1.187	1.204	1.892	1.889
F	0.153	0.155	0.179	0.179

Recalculation of these analyses and subsequent plotting of the results on to Phillips diagram was performed using a computer program (MINDATA) written by R. Phillips in PL.1. for use on the IBM 360/67 N.U.M.A.C. Computer. The results were plotted on to the diagram using isometric graph paper.

Using Phillips method the various substitutions are converted as follows:-

In Z : all the substitutions are reduced to equivalent aluminium.

In Y : all the substitutions are reduced to equivalent aluminium or equivalent magnesium.

In A and X : all the substitutions are reduced to equivalent sodium.

In the basic formula (Phillips, 1966) the equation

$$Na^{A} + Al^{Y} = Na^{X} + Al^{Z}$$

must hold and knowing three of these values the fourth is completely determined.

Whittaker (1968) devised an alternative scheme to Phillips and is related to the latter as follows:-

$$X\ (W) \equiv 2 - X\ (R.P.)$$

$$Y\ (W) \equiv Y \quad (R.P.)$$

$$Z\ (W) \equiv 8 - Z\ (R.P.)$$

The major difference between the two methods is the use of vacancies which occur after recalculation. Phillips ignores vacancies in Z and X but Whittaker makes these sites up to whole numbers. In X, Whittaker removes the vacancies as though they were alkalis.

Whittaker's diagram is shown in figure 1-11. Superior alkali amphibole analyses will plot on complementary points in both Phillips and

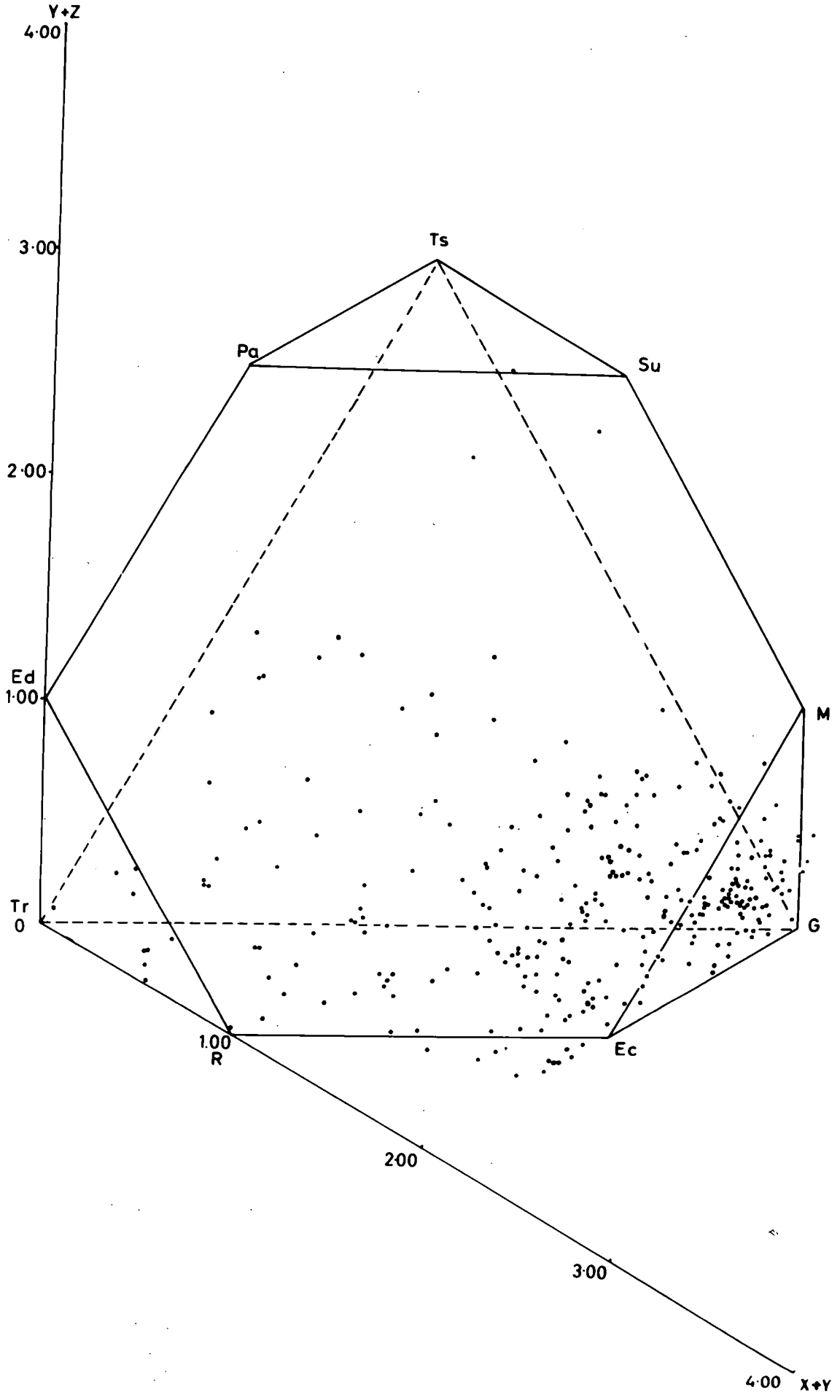

Fig.4-3 Distribution of alkali amphibole analyses in Phillips' compositional space

Whittaker's diagrams. Both figures have the advantage that they can be easily plotted and will fall into a cell which already has some name.

4-3. Assignment of Alkali Amphibole analyses to Compositional Cells.

A total of 310 analyses of alkali amphiboles, including the present author's, were recalculated to the basis of 24 oxygens and plotted on to the Phillips' compositional space (op. cit.) (Fig. 4-3). Of these analyses, 26 (8%) plot within the calciferous amphibole compositional field, i.e. less than 1 atom of sodium at X in the basic formula. Twenty of these plot in the tremolite sensu extenso (s.e.) field, 2 in the calciferous sundiusite, 3 in the pargasite and 1 in the tschermakite fields. The pargasites and one sundiusite plot close to the katophorite composition (Brögger in Deer, Howie and Zussman, 1963). Phillips makes no allowance for the katophorite composition, treating it as a mixture of $R_{50}Su_{50}$, or $Ec_{50}Pa_{50}$, or $Ed_{50}M_{50}$ (abbreviations as in Chapter 1).

The remaining 284 analyses plot either in the alkali amphibole field or outside the compositional space (O.S.). Table 4-2 shows the distribution of alkali amphibole analyses within the compositional space.

TABLE 4-2 Distribution of alkali amphibole analyses within Phillips compositional space.

Alkali Amphibole described as:-	Plots in the field of:-
Katophorite	Ec(3), Su(1), Pa(3), Tr(1).
Sundiusite (Mboziite)	Su(3).
Eckermannite	Ec(5), R(1), Gl(1).
Magnesioarfvedsonite	Ec(13), Gl(4), R(1), Su(1), Tr(1).
Arfvedsonite	Ec(58), M(5), Gl(14), R(9), Tr(3), O.S.(7).
Riebeckite	Gl(34), R(3), M(2), Ec(1), Tr(2), O.S.(12).
Magnesioriebeckite	Gl(7), R(1), Ec(1), O.S.(1).
Glaucophane	Gl(48), Ec(9), M(3), Ts(1), R(2), O.S.(9).
Richterite	R(19), Tr(14), Ec(4), Gl(3), O.S.(6).

Although these results show that most of the basic formulae calculated from the analyses can be given an amphibole basic formula name (89%), and plot inside or close to the compositional space, there are a great number which are unsatisfactory; a total of 105 analyses (33%). Many of these poor results are obtained by virtue of the water contents of the amphiboles being in error. Serious errors are obtained when there is a critical lack or excess of water.

When positive errors occur in Y sites, they are put into X sites, which increases the number of divalent cations at X i.e. the analysis lies closer to the calciferous field in the compositional space.

The correct assignment of analyses to particular cells by authors were tested using Phillips' (1963) suggestions for recalculation:-

Assigned to the Glaucophane cell $\frac{89}{136}$ or 65%

Assigned to the Eckermannite cell $\frac{76}{123}$ or 62%

Assigned to the Richterite cell $\frac{19}{46}$ or 41%

These results do not allow for isomorphous substitution between groups e.g. riebeckite - arfvedsonite, eckermannite - richterite and richterite - tremolite.

The low percentage of correct assignments in the glaucophane cell are due to the extremely poor water results for "crocidolites" and the excess of trivalent cations in Y for these minerals. If minerals of glaucophane composition were used solely for the Glaucophane cell, almost 100% of these plot in the cell. The eckermannite series also contain minerals which are deficient in hydroxyl.

4-4. Quality of Alkali Amphibole Analyses.

4-4-1. O(3) sites.

In the alkali amphibole analyses water determinations appear to

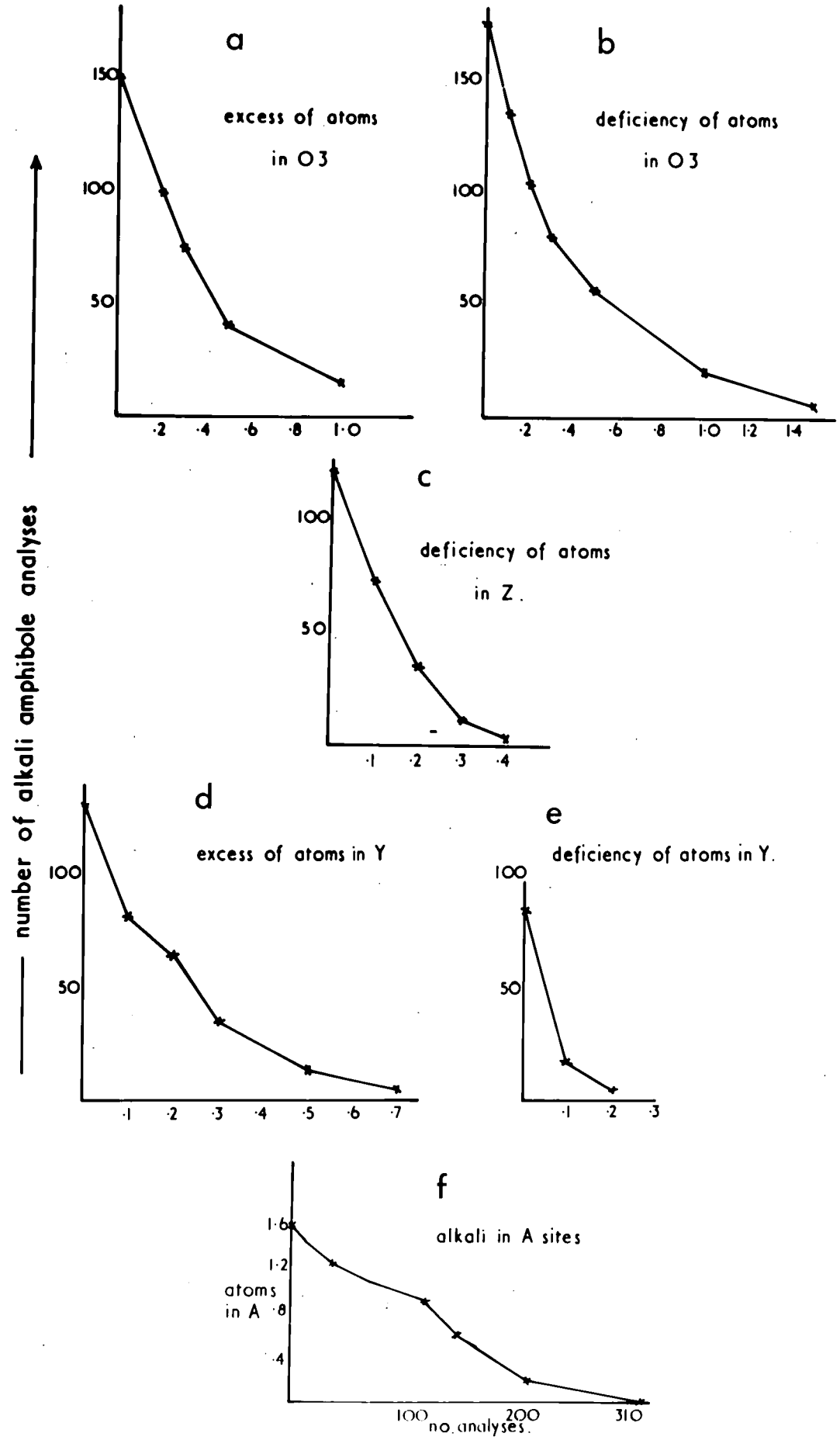

Fig. 4–4 Deviation from ideal occupancy of the O3, Z, Y and A sites.

show the greatest errors. There are 173 alkali amphiboles with a water deficiency, 150 with water excess and 1 with exactly 2.00 atoms of water. The errors are so large that placing a $\pm$ 5% error as a superior analysis is unreasonable for amphiboles.

If $\pm$ 0.30 atoms (15%) is taken to be the limit for a superior analysis then 170 alkali amphiboles are superior. This assumes that oxy-amphibole substitution is negligible.

The two curves for excess and deficient water are shown in figure 4-4 (a) and (b). Leake accepts an error of $\pm$ 50% on the water determinations for them to be superior, if this were accepted all but 35 analyses of alkali amphiboles would be considered as superior.

4-4-2. Z sites.

In the Z group only silicon and aluminium are considered to occupy the tetrahedral sites. Only 7 analyses have greater than 8.10 atoms in Z but 120 alkali amphiboles are deficient in Z (Fig. 4-4(c)) and of these 71 contain less than 7.90 atoms in Z. It therefore appears reasonable to propose that superior analyses should have 8.00 $\pm$ .1 atoms in the tetrahedral sites.

4-4-3. Y sites.

In the Y sites it appears to be more common to have excess values rather than deficiencies (Fig. 4-4(d) and (e)). Leake (1968) also found this to be so for the calciferous amphiboles. Using Phillips' (op. cit.) system of recalculation the excess in Y is placed in X in the order 1) Mn, 2) Fe^{++}, 3) Mg.

If the water determinations are low, these tend to create excesses in the Y group determinations. Low values for Z sites also raises the value for the Y sites. Deficiencies in the Y site totals may arise because

of high water determinations or non-determination of certain elements e.g. Li, Zn, Zr, Nb etc., which are present in igneous alkali amphiboles.

A limit of ± 0.1 atoms from the theoretical value (5.0 atoms) is suggested for an analysis to be superior. There are a total of 214 alkali amphiboles with errors in the Y group and if the above suggestion is accepted then this total drops to 97 or 30%.

4-4-4. X sites.

The X sites are only deficient in 52 alkali amphiboles, these are mainly metamorphic riebeckites (crocidolites) and glaucophanes. A reasonable lower limit for this site is 1.95 atoms.

4-4-5. A sites.

If the system of recalculation of alkali amphiboles proposed by Phillips (1963) is adopted, then errors tend to be concentrated in the 'A' site. Atoms in excess of 2.00 from the X sites are situated in 'A' together with excess hydrogen from the O(3) sites.

In figure 4-4(f) a curve is drawn of the number of amphiboles against atoms in 'A' when the hydrogen has been removed from the 'A' site values. An upper limit of 1.10 atoms in 'A' would place 50 alkali amphiboles outside this limit i.e. 15% of the total, but as these amphiboles are restricted to arfvedsonites, eckermannites, and richterites, then this represents 27% of this total.

4-5. Chemical variations within the Alkali Amphiboles.

4-5-1. Chemical variation in the glaucophane - riebeckite - magnesioriebeckite - ferroglaucophane group.

In figure 4-5 the ratio $Fe^{++}/_{TotR^{++}} \times \frac{100}{1}$ is plotted on the ordinate and $Fe^{+++}/_{TotR^{+++}} \times \frac{100}{1}$ on the abscissa. Miyashiro (1957) and Borg (1967)

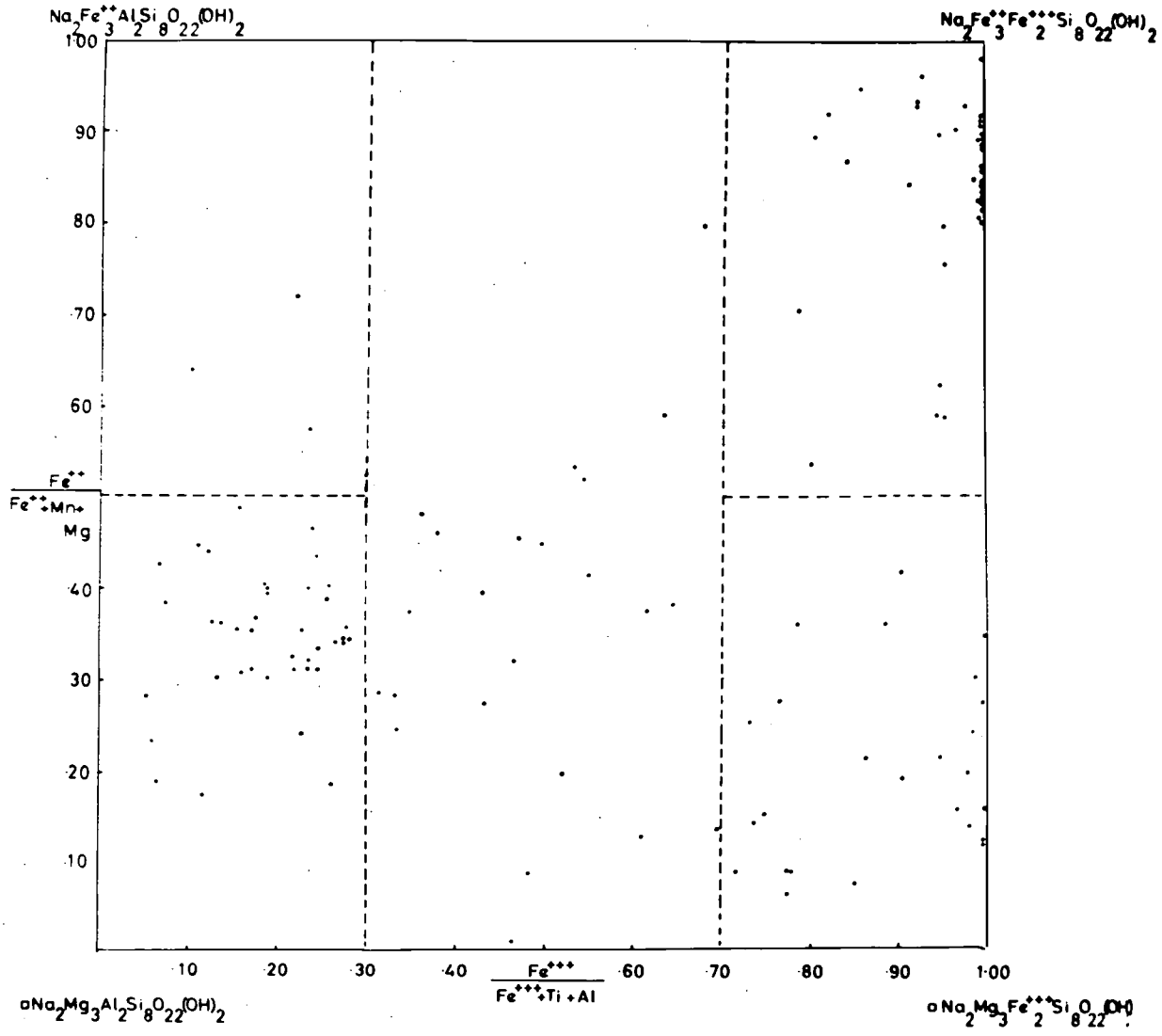

Fig 4-5 Distribution of compositions in the glaucophane–riebeckite series.

used this diagram to plot on the analyses of this group. There are a total of 140 amphiboles of this composition plotted on the diagram. In addition to the diagram showing iron (III) substituting for aluminium (and titanium) and iron (II) substituting for magnesium; the diagonals across the field show the coupled substitutions:-

$$MgAl \rightleftharpoons Fe^{++}Fe^{+++}$$

$$MgFe^{+++} \rightleftharpoons Fe^{++}Al$$

Borg pointed out that the distribution of compositions attests the above coupled substitutions. The riebeckites plotted are not riebeckite-arfvedsonites; these minerals have been plotted with the arfvedsonites as most of them are closer in composition to the latter.

The analyses plot into the following fields:-

Glaucophane	40
Ferroglaucophane	3
Crossite	23
Magnesioriebeckite	25
Riebeckite	49

The solid solution series between glaucophane and riebeckite appears to be almost complete apart from the gap between Glaucophane 85 and Riebeckite 15 and the glaucophane end-member. This has been substantiated by Miyashiro (1957), Deer, Howie and Zussman (1962), Borg (1967), and Coleman and Papike (1968).

The substitution $MgFe^{+++} \rightleftharpoons Fe^{++}Fe^{+++}$ is also complete except for the magnesioriebeckite end-member. Many of these analyses are from crystalline schists and meta-iron formations and commonly called crocidolite. The range of compositions of "crocidolite" emphasize that the name should not be used to indicate a specific composition.

Twelve of these analyses are glaucophanes from the Isle de Groix,

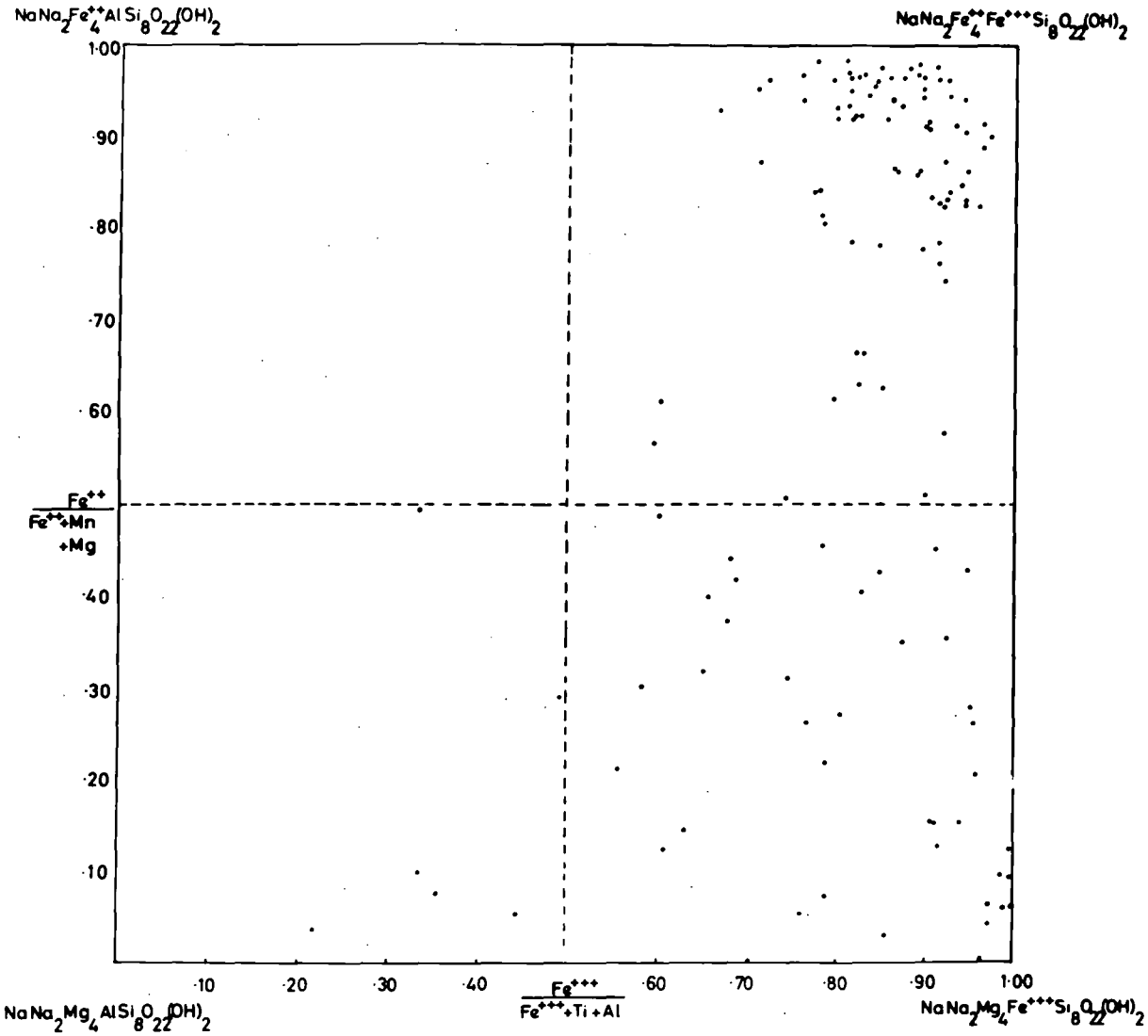

Fig.4-6 Distribution of compositions in the Eckermannite–Arfvedsonite series.

Brittany, analysed by Manyiukuola and Howie (Howie, personal communication). One of these amphiboles plots in the ferroglaucophane field and until recently was the only alkali amphibole of this composition. Recently, Black (1970) has described two amphiboles of ferroglaucophane composition from siliceous metasediments in New Caledonia. These analyses extend the substitution $Fe^{++}Al \rightleftharpoons MgAl$ to 72% ferroglaucophane and the substitution $MgFe^{+++} \rightleftharpoons Fe^{++}Al$ to 77 ferroglaucophane-23 magnesioriebeckite.

4-5-2. Chemical variation in the eckermannite - ferroeckermannite - arfvedsonite - magnesioarfvedsonite group.

The dividing planes between the various compositions in this group (Fig. 4-6) have been taken at 50% of each end-member. This has been adopted until definite chemical and optical criteria have been shown for this not to be so.

There are 129 analyses of amphiboles of this composition and they are divided into the following fields:-

Eckermannite	6
Magnesioarfvedsonite	41
Arfvedsonite	82
Ferroeckermannite	0

The isomorphous substitutions are the same in this group as for the glaucophane group.

The $MgAl \rightleftharpoons MgFe^{+++}$ appears to be almost complete i.e. within 20% of the eckermannite end-member. The isomorphous substitution between arfvedsonite and magnesioarfvedsonite is complete but there is not complete replacement of ferric iron for (Ti + Al) as in the riebeckite-magnesioriebeckite series.

The coupled substitutions $MgFe^{+++} \rightleftharpoons Fe^{++}Al$, and $MgAl \rightleftharpoons Fe^{++}Fe^{+++}$ do not appear to be as important in the glaucophane group as the results

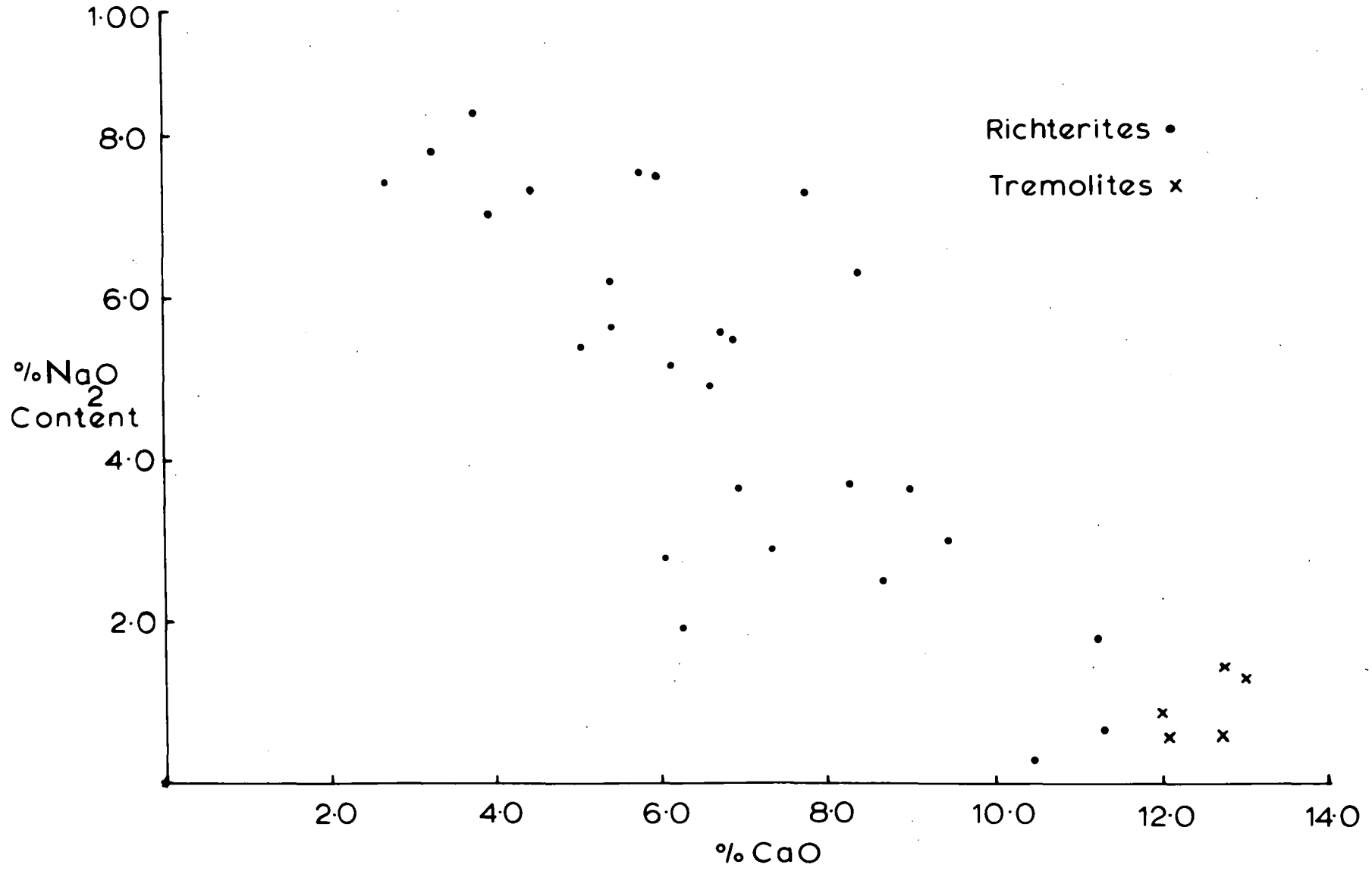

Fig.4–7a Sodium plotted against calcium in the Richterite series.

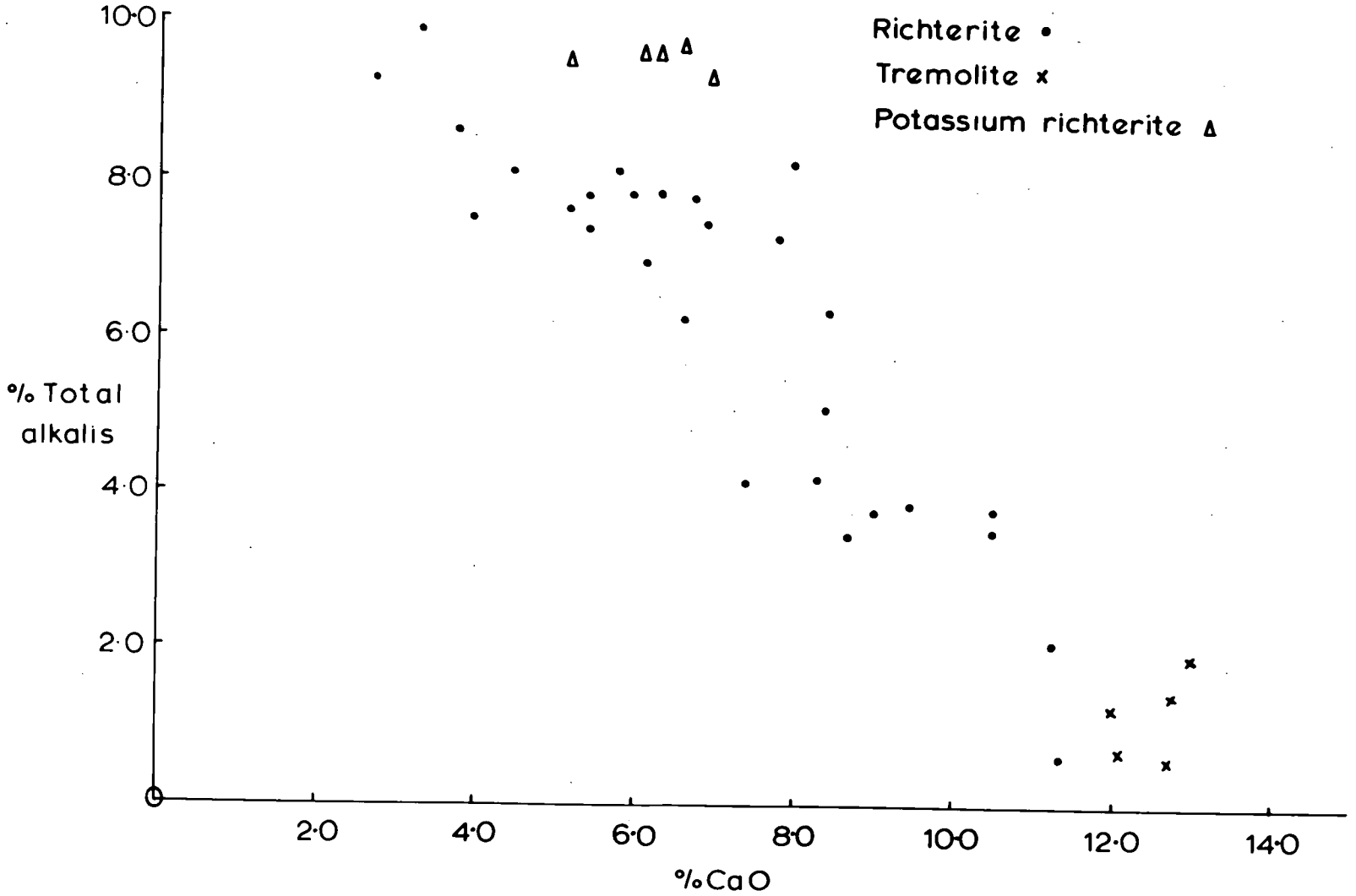

Fig.4–7b Total alkalis plotted against calcium in the Richterites

are more scattered.

4-5-3. Chemical variations in the richterite group.

All the analyses which fall into the richterite field plot into what may be termed the "ferririchterite" field. Richterites contain only small amounts of trivalent cations and ferric iron is the most important of these. There is one example of a "ferri-richterite", chiklite (Bilgrami, 1955), which has 2.03 atoms of Fe^{+++}. This specimen yields a pyroxene diffraction pattern when X-rayed and indeed the analysis recalculates to $Di_{31}Ac_{54}Jo_{15}$ i.e. a member of the blandfordite group of pyroxenes.

Richterites have been described from alkaline igneous rocks Prider, 1939; Carmichael, 1968), metasomatic rocks (Larsen, 1942; Puustinen, 1970), pegmatites closely related to manganese mineralisation (Sundius, 1945; Roy, 1964; Ridge, 1959), meteorites (Olsen, 1967; Douglas, personal communication) and have recently been described in Apollo XI lunar samples (Gay et. al., 1970).

The substitutions $CaR^{++} \rightleftharpoons NaR^{+++}$ and $MgAl \rightleftharpoons Fe^{++}Fe^{+++}$ are not important in the richterite group, but the substitution $Ca \rightleftharpoons Na(K)Na$ (Figs. 4-7(a) and (b)) is of paramount importance. This substitution indicates that there is a complete solid solution series between richterite and tremolite. Sodium and potassium are completely interchangeable in the 'A' sites of richterites, the highest concentration of potassium being in potassium richterites (magnophorites).

4-5-4. Chemical variations in intermediate compositions of the alkali amphiboles.

1. Intermediate members of the riebeckite - arfvedsonite series.

A useful way of plotting amphiboles of intermediate composition is to use the substitutions in Y which are balanced by substitutions in Z

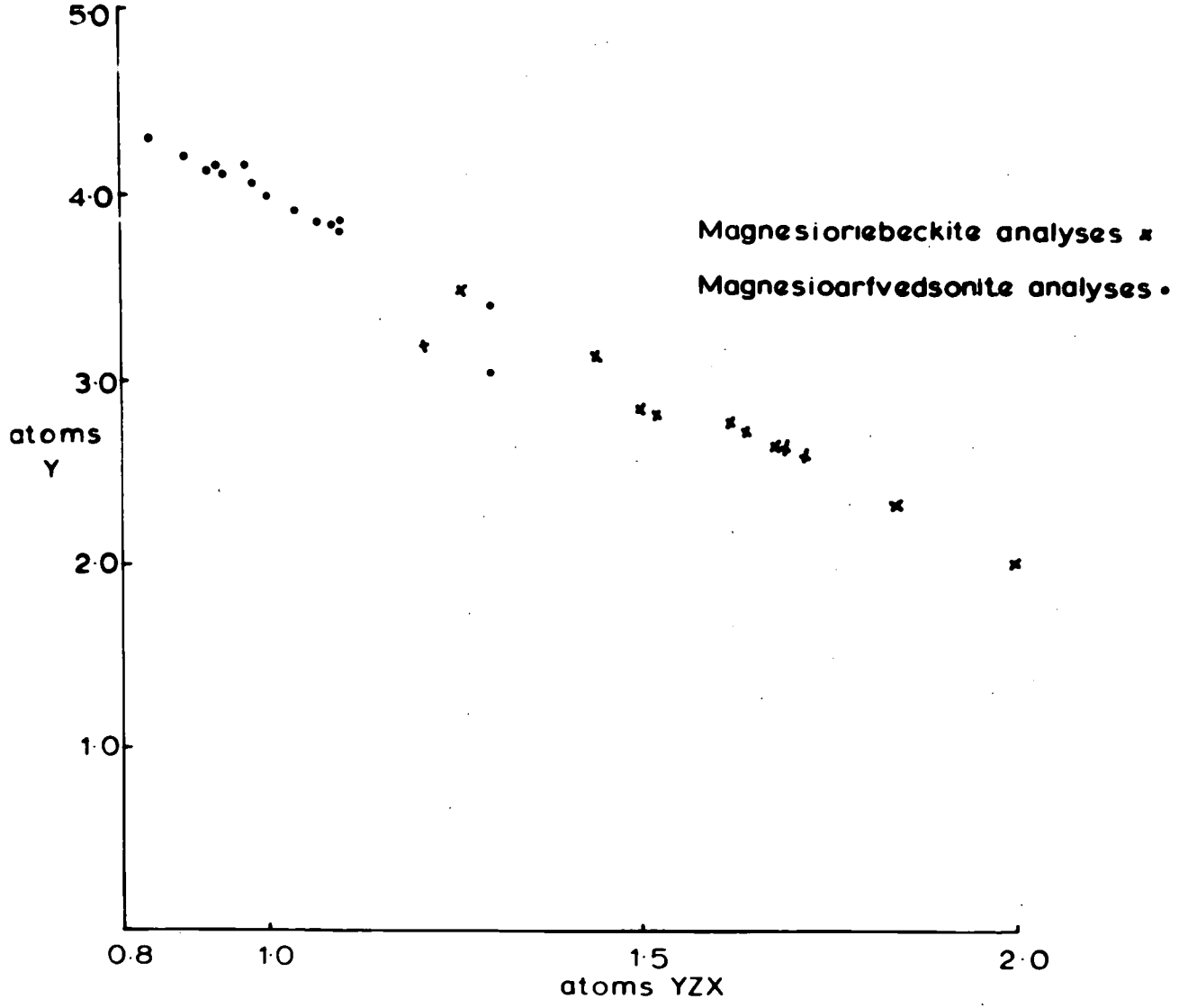

Fig.4-9 Intermediate compositions between Magnesioriebeckite and Magnesioarfvedsonite.

and X, these substitutions are designated YZX substitutions. The YZX substitutions are plotted against Y in figure 4-8. For the alkali amphiboles, YZX will be 0 for richterite, 1.00 for eckermannite and 2.00 for riebeckite.

In figure 4-8 both the author's arfvedsonites, Borley's riebeckite-arfvedsonites and metamorphic riebeckites are plotted. There is a complete isomorphous replacement between riebeckite and arfvedsonite and beyond the latter towards the richterite composition. The metamorphic riebeckites extend to 1.60 atoms YZX and igneous arfvedsonites to 0.80 atoms YZX and this latter value is beyond the end-member composition of arfvedsonite, namely, $NaNa_2R_4^{++}R^{+++}Si_8O_{22}(OH)_2$.

Although this series is continuous a suggested nomenclature for this group could be: Riebeckite 2.00 - 1.60 YZX; riebeckite - arfvedsonite 1.60 - 1.20 YZX; arfvedsonite 1.20 - 0.80 YZX.

Kovalenko (1968) devised a subdivision of this group based upon atoms within the AX sites: Riebeckite 1.5 - 2.4 atoms in X; riebeckite - arfvedsonite 2.4 - 2.8 atoms; arfvedsonite 2.8 - 3.3 atoms. Both the upper limit for arfvedsonite and lower limit for riebeckite are outside the bounds set by the author for superior analyses. Otherwise, both the author's and Kovalenko's divisions agree.

2. Intermediate members of the magnesioriebeckite - magnesioarfvedsonite series.

The recalculated analyses both from the literature and those determined by the author have been plotted on figure 4-9. Again, as for the previous group, there appears to be no miscibility gap in the compositions between magnesioriebeckite and magnesioarfvedsonite. The compositions extend to 0.80 YZX and 4.20 Y which lies between magnesioarfvedsonite and richterite. Members which lie close to

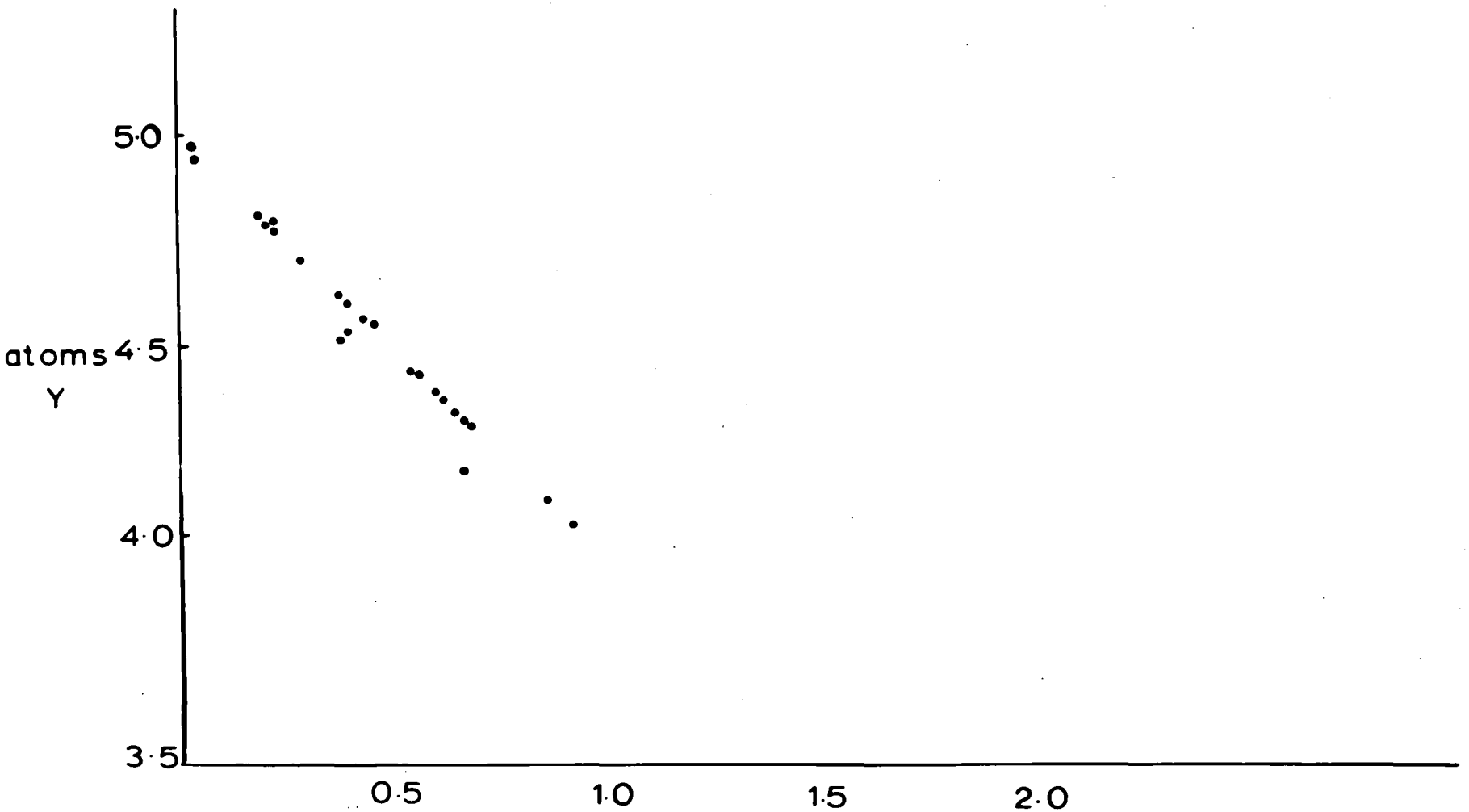

Fig. 4-10 Intermediate compositions between Richterite and Eckermannite.

magnesioriebeckite are typically from crystalline schists and meta-iron formations (asbestiform variety). Analyses close to magnesioarfvedsonite come from igneous bodies and metasomatic rocks.

The suggested division of this group is that magnesioriebeckite is the name to be applied to minerals with the compositions between 2.00 YZX and 1.4 YZX and magnesioarfvedsonite between 1.4 YZX and 0.80 YZX. This division is based upon the range of compositions of amphiboles from crystalline schists.

3. Intermediate members of the richterite-eckermannite series.

Analyses of richterites have been plotted in figure 4-10. The range of compositions is from 0.93 YZX, 4.07 Y in a richterite from Iron Hill, Colorado (Larsen, 1942) to a composition OYZX, 5.00 for a richterite from Långban, Sweden (Sundius, 1945). This corresponds to end-member richterite. The potassium richterite compositions are scattered and two examples of meteoritic richterite (Olsen, 1967 and Douglas, personal communication) plot close to the end-member.

4-6. Additional substitutions in the alkali amphiboles.

1 (a). The substitution Ca Mg $\rightleftharpoons$ Na Al.

This substitution is represented by the base of the triangle Ts-Tr-Gl in Phillips' compositional space. The end-members involved in this substitution are tremolite and glaucophane and amphiboles of these compositions co-exist in the glaucophane schist facies (Chapter 6 for electron probe microanalysis of these amphiboles).

The occurrence of calcium in the M4 sites of alkali amphiboles of the glaucophane group and sodium in actinolites indicates that there is miscibility between the two groups. Amphiboles from the blue-schist facies (glaucophane schist) are plotted in figure 4-11. Iwasaki (1963)

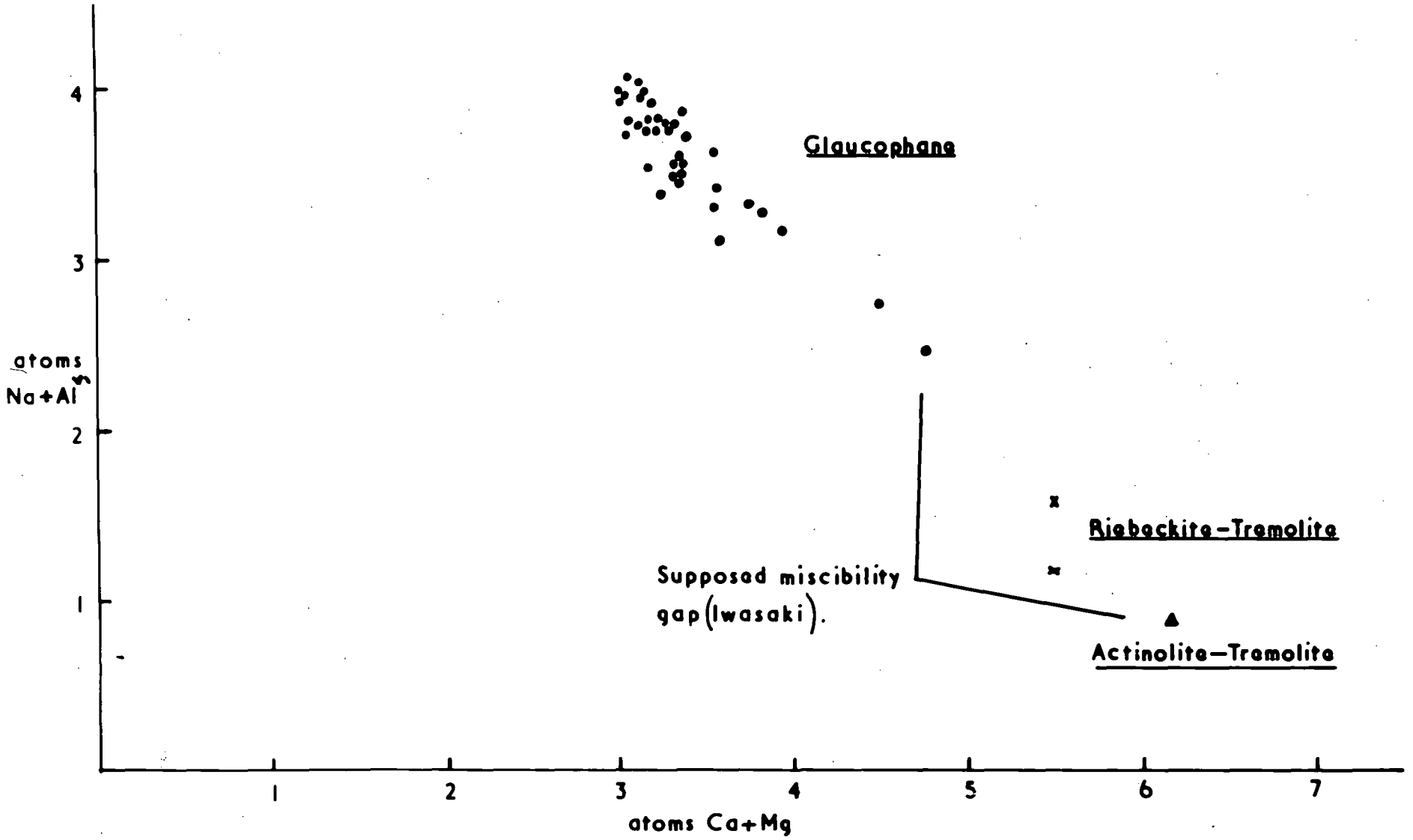

Fig. 4–11. Limits of substitution $(NaAl^{VI} \rightleftharpoons CaMg)$ between glaucophane and tremolite.

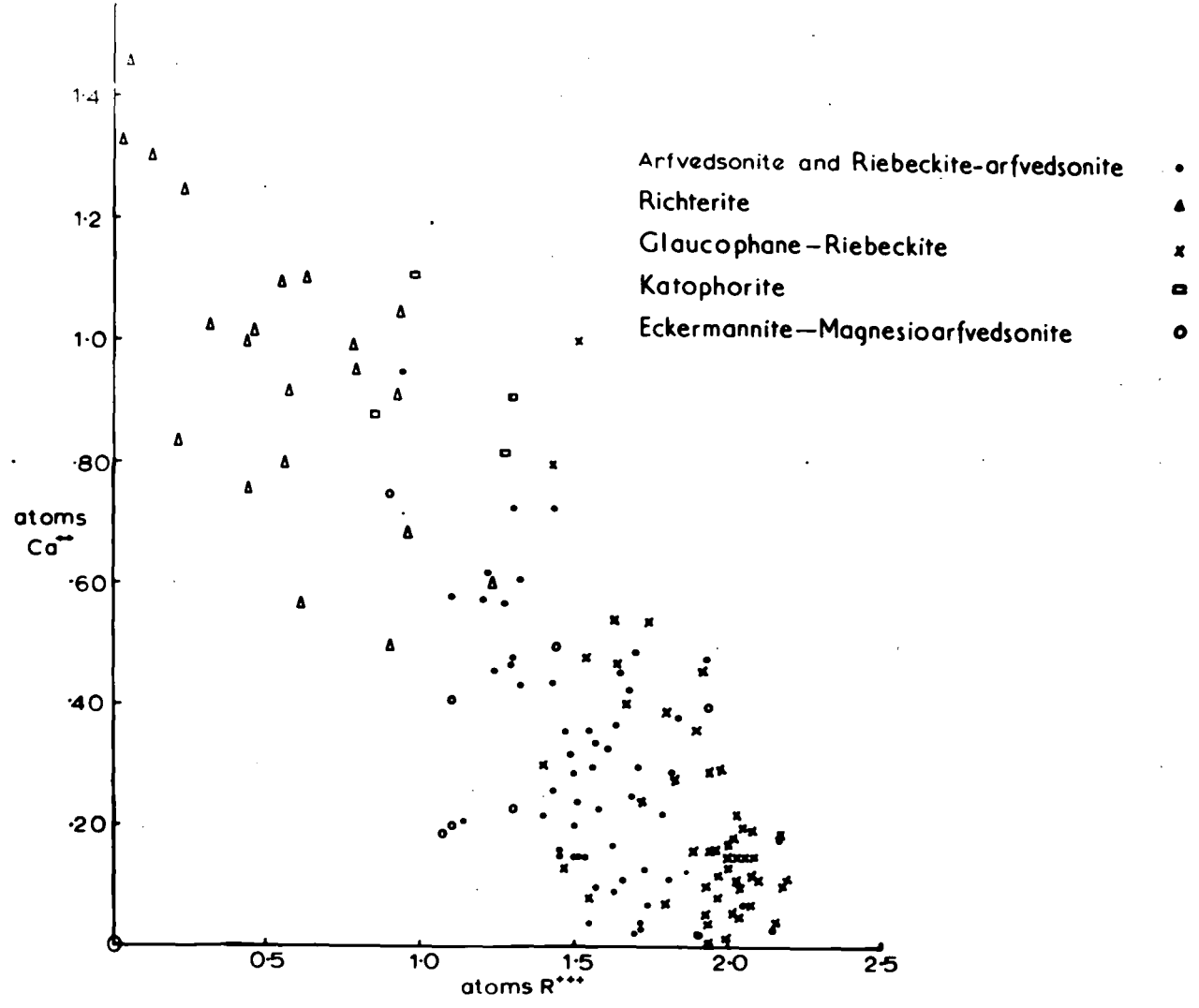

Fig 4-12 The Ca^{++} content of the alkali amphiboles plotted against total R^{+++}.

claimed that there was a miscibility gap between Gl_{20} Ac(actinolite)80 and Gl_{50} Ac_{50} but since his work was published Klein (1966) has described two amphiboles from the Wabush Iron Formation, Labrador which he calls riebeckite-tremolites. These two amphiboles are indicated on figure 4-11 and they plot in the miscibility gap proposed by Iwasaki (ibid.). These amphiboles come from the staurolite-kyanite zone of metamorphism and indicate that there is no miscibility gap between the amphiboles, glaucophane and tremolite at higher temperatures and pressures.

1 (b). The general substitution Ca $R^{++} \rightleftharpoons$ Na R^{+++}.

Miyashiro (op. cit.) showed that the calcium content of alkali amphiboles increases as the amount of trivalent cations decrease. This holds throughout the alkali amphiboles despite Miyashiro's reluctance to consider richterite with the other alkali amphiboles. The sole exception is the mboziite composition.

The glaucophane - riebeckite groups have the lowest calcium contents (Fig. 4-12). The amount of calcium in the structure appears to be linked with the temperature of origin in the riebeckite - arfvedsonite - katophorite series. The maximum amount of calcium in any alkali amphibole is 1.50 atoms in a richterite.

2. The substitutions $(NaK)R^{++} \rightleftharpoons \square\, R^{+++}$ and $(NaK)Al \rightleftharpoons \square\, Si$.

Miyashiro (ibid) used these substitutions to divide up the alkali amphiboles. Silicon and trivalent cations are plotted against each other in figure 4-13 for the alkali amphiboles. The compositional limits for the alkali amphiboles are 7.00 atoms of silicon and 2.50 atoms of trivalent cations, this latter figure could be error in analysis. The full range of alkali amphibole compositions cannot be represented on this diagram e.g. mboziite and sundiusite, and the compositional fields are not

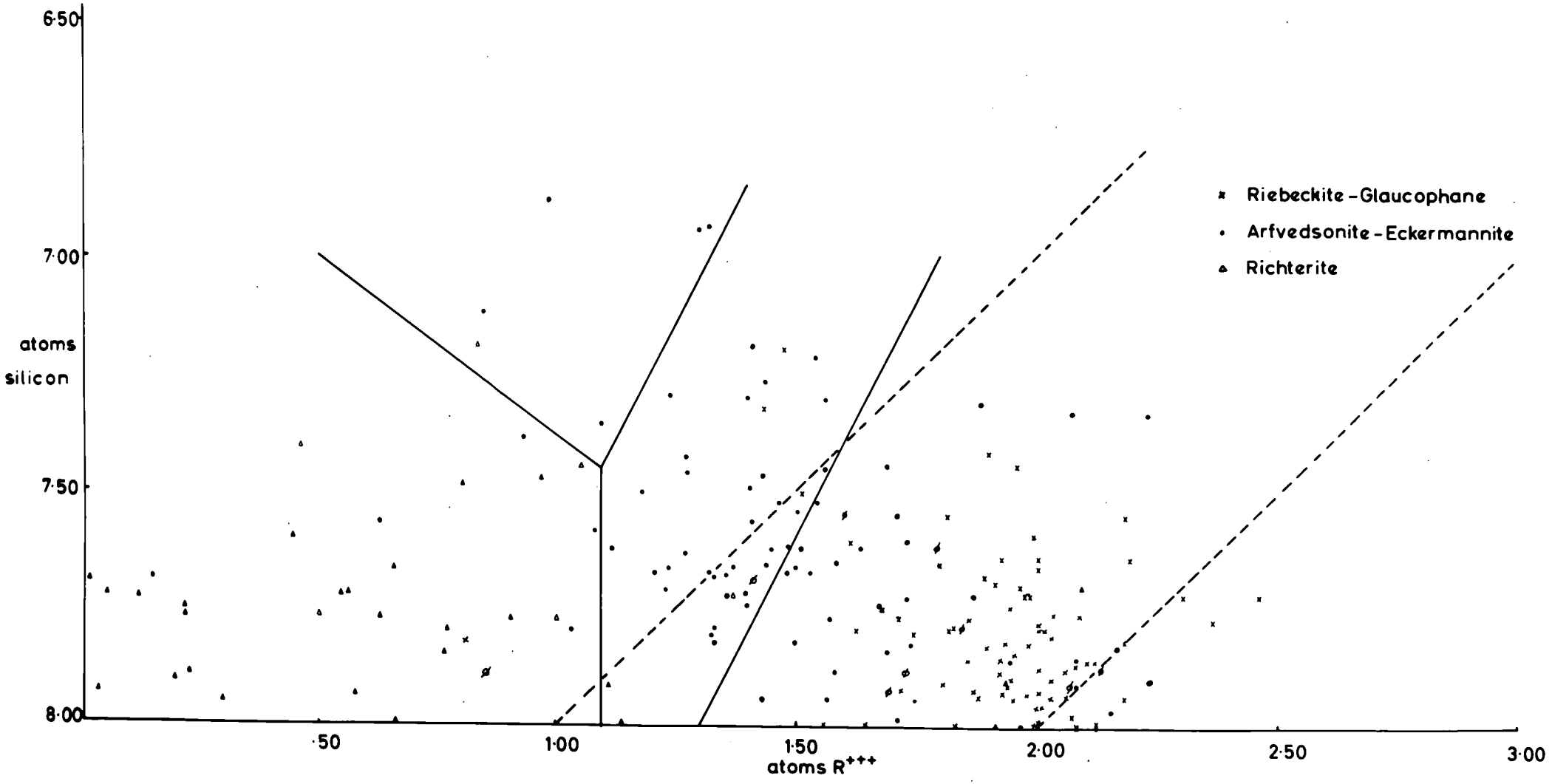

Fig. 4-13 Distribution of alkali amphibole compositions in Miyashiro's diagram and the substitutions $(Na,K)R^{++} \rightleftharpoons \square R^{+++}$ and $(Na,K)Al \rightleftharpoons \square Si$.

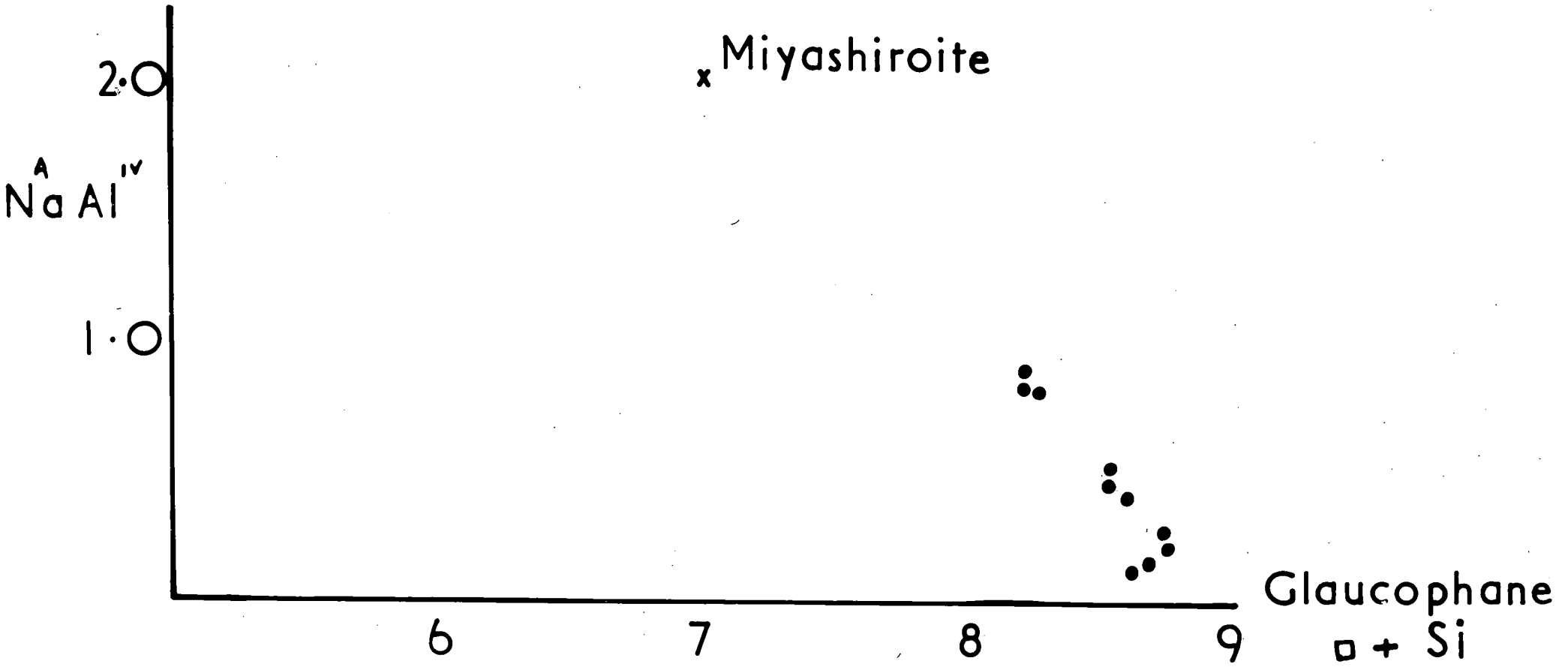

Fig. 4—14. Extent of solid solution between glaucophane and miyashiroite.

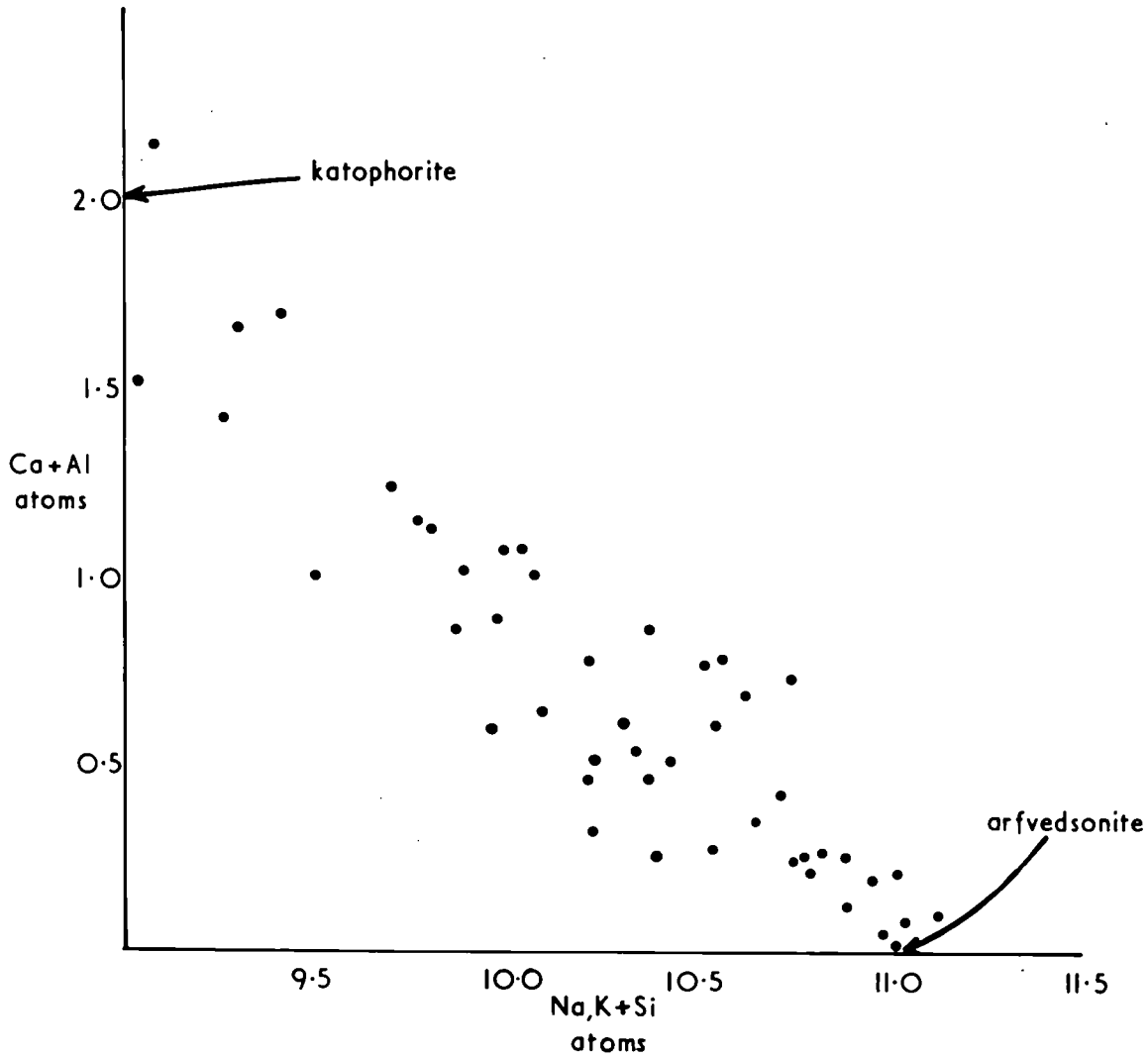

Fig. 4–15 The coupled substitution $CaAl \rightleftharpoons Na(K)Si$ in riebeckite–arfvedsonites from Greenland and Lovozero, U.S.S.R.

symmetrical. The analyses show that these substitutions are important especially in the riebeckite - arfvedsonite intermediate compositions.

3. The substitution Ca Al $\rightleftharpoons$ Na^{X} Si.

The substitution Ca Al^{IV} $\rightleftharpoons$ Na Si is important in the katophorite - arfvedsonite series. In figure 4-15 all the analyses of katophorite and arfvedsonite show there is a complete isomorphous series between these two alkali amphiboles.

In figure 4-15 all the author's analyses of riebeckite - arfvedsonite and arfvedsonites from S.W. Greenland, and Jebel Sileitat, Sudan fall on or close to the line between katophorite and arfvedsonite. The amount of Ca Al^{IV} decreases with increasing differentiation of the S.W. Greenland intrusions (Chapter 5). The maximum amount of this substitution in the author's analyses is 9.7 atoms (Na Si) and 1.26 atoms (Ca Al).

4. The substitution Na^{A} Al^{IV} $\rightleftharpoons$ $\square$Si.

The replacement of tetrahedral aluminium for silicon and balanced by the introduction of alkali ions in the 'A' site was suggested by Phillips and Layton (1964) to be an isomorphous substitution between glaucophane and an amphibole they called miyashiroite. Ten analyses plot in the miyashiroite field but few of these are superior analyses. Reference to figure 4-14 shows that no available analysis plots closer to miyashiroite than Gl_{60} M_{40} which may indicate a gap in amphibole compositions.

4-7. General Chemistry.

Certain elements which occur in the alkali amphiboles have not been dealt with in sufficient detail in the preceding section.

4-7-1. Aluminium.

The amount of aluminium in alkali amphiboles varies from less than

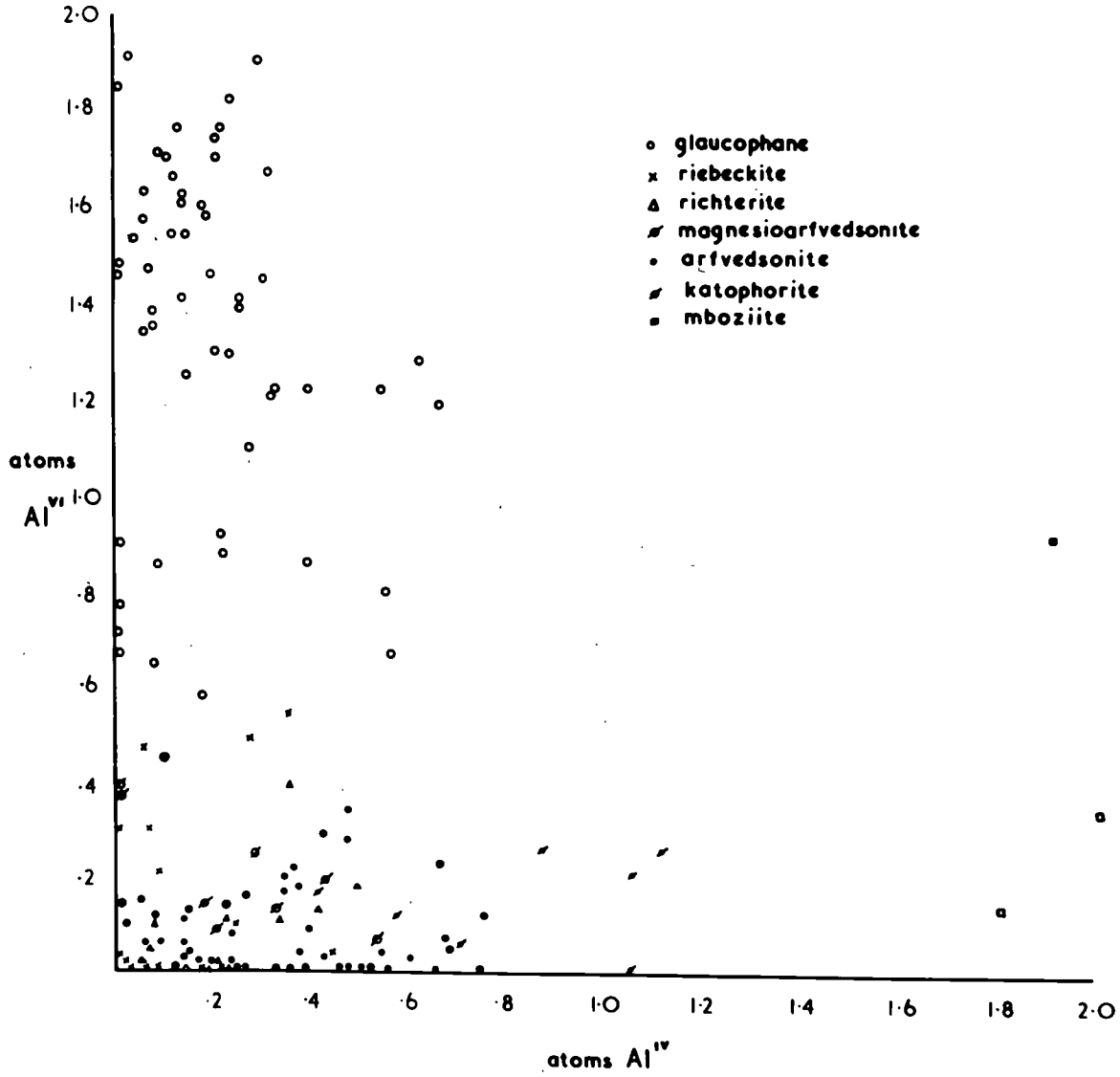

Fig. 4–16 The amounts of Al in 4- and 6-fold co-ordination in members of the alkali amphiboles

0.1 atoms in riebeckites and richterites to more than 2.00 atoms. Howie and Manjukuola (personal communication) recorded 2.20 atoms of aluminium in a glaucophane from the Isle de Groix and a mboziite from Darkainle (Brock et. al., 1964) contains 2.35 atoms. More recently Linthout and Kieft (1970) have reported a mboziite from Sierra de los Filabres (S.E. Spain) with 2.83 atoms of aluminium (Fig. 4-16).

Aluminium occupies two sites in the alkali amphiboles, the M_2 and T sites. Wickman (1943), Harry (1950), Thompson (1957), Leake (1962), and Boyd and England (1962) claimed that aluminium in tetrahedral co-ordination can be correlated with high temperature and octahedral aluminium tends to form at high pressures.

This claim can be supported by observation of the alkali amphiboles. The highest concentrations of octahedral aluminium are in the members of the glaucophane series which formed at between 7 - 8 kb (Coleman and Taylor, 1968). The largest amounts of Al^{VI} (1.90 atoms) are in two glaucophanes, one published by Borg (1967) the other Manjukuola and Howie (personal communication). The author's analyses yield values of 1.46 atoms (302-143 T.W.B.1) and 1.63 atoms (302-143 T.W.B.2) and both specimens come from Valley Ford, California.

Glaucophanes range from 1.90 - 0.50 atoms of Al^{VI} and up to 0.65 atoms of tetrahedral aluminium. The increase in tetrahedral aluminium correlates with an increase of crossite content of the amphibole.

The highest content of tetrahedral aluminium occurs in three analysed samples of mboziite (1.82, 1.90, and 2.02 atoms). The mboziite of Linthout and Kieft (op. cit.) also contains 0.93 atoms of octahedral aluminium. Katophorite analyses contain up to 1.15 atoms of Al^{IV} and 0.26 atoms of Al^{VI}. Most of the riebeckites, arfvedsonites and eckermannites lie between the boundaries 0.50 Al^{VI} and 0.80 Al^{IV}. The richterite group have very low concentrations of aluminium.

4-7-2. Zinc.

Zinc has been analysed for in relatively few alkali amphiboles and substitutes for ferrous iron in silicates (Wedepohl, 1953; Taylor, 1966). Many authors believe that the zinc occurs as submicroscopic sphalerite. This phase was not detected by single crystal X-ray methods (Frost in Borley, 1963). Zinc has been detected in the author's alkali amphiboles by use of the electron microprobe and does not apparently occur as small inclusions but throughout the amphibole crystals. The zinc species which is stable at the same oxygen pressure as the formation of the amphiboles is $ZnSO_4$ which is soluble (Holland, 1959, 1965).

Zn^{++} has the same ionic radius as Fe^{++} but, as the Zn-O bond is more covalent than the Fe-O bond, then the Zn^{++}/Fe^{++} ratio will increase during fractionation (Taylor, 1966). Zinc increases in the late stage alkali amphiboles of the Ilímaussaq intrusion (up to 0.18%) and in the riebeckite-arfvedsonites from the Nigerian granites (up to 0.78%) (Borley, 1963; Butler and Thompson, 1966).

Zinc is concentrated in the later amphiboles of the Ilímaussaq intrusion. Zinc is also concentrated into the amphibole rather than the pyroxene (Butler and Thompson op. cit.), and hence the high concentration of zinc in the arfvedsonite from the hyjavrite.

4-7-3. Manganese.

The manganese content of alkali amphiboles varies from 0-8.56% MnO. The low concentrations are confined to amphiboles which have formed in low temperature environments (glaucophane and riebeckite). In the igneous alkali amphiboles the concentration varies between 0.5% and 2.9% MnO. The latter value is for a katophorite from Sao Miguel (analyst Osann, in Miyashiro, 1957). Most of these amphiboles have ~1.00% MnO.

Certain members of the magnesioarfvedsonite group (Juddites) have

variable amounts of manganese, up to 5.04% MnO have been recorded by the author. A tirodite (Appendix 3), analysed by the author contains 8.38% MnO and this is close to the maximum recorded for alkali amphiboles. Recalculation of this analysis requires that manganese should be in both M4 and M(1,3) sites and this conclusion is supported by the infra-red data. Richterites have very variable manganese contents.

4-7-4. Magnesium.

The magnesium contents of alkali amphiboles are extremely variable from zero concentration up to 5.00 atoms in a meteoritic richterite (Douglas, personal communication). In the glaucophane-riebeckite and eckermannite-arfvedsonite groups there is a complete replacement of magnesium by ferrous iron.

4-7-5. Titanium.

The variation in titanium content in the alkali amphiboles is between 0.0 atoms in members of the glaucophane-riebeckite group to 0.66 atoms in a potassium richterite from the Leucite Hills (Carmichael, 1967). Intermediate concentrations are present in arfvedsonites and katophorites. The titanium content of amphiboles increases with an increase in temperature of formation and degree of silica undersaturation (Verhoogen, 1962). Verhoogen concludes that the solubility of titanium in silicates increases with the amount of aluminium that can substitute for silicon in Z sites. This conclusion is true for kaersutites (Aoki, 1961; Wilkinson, 1961), katophorites and arfvedsonites (Deer, Howie, and Zussman, 1962). This conclusion breaks down in the titanium-rich potassium richterites, where there is a molecular excess of alkalis over alumina (Carmichael, 1967). There is a total lack of iron titanium oxides in the Ilímaussaq intrusion and in the leucite volcanic rocks of

Western Australia, Wyoming, and Spain. The excess alkalis react with silica, titania and zirconia to form minerals such as aenigmatite, eudialyte, priderite and wadeite and in addition titanium is incorporated into the normal ferromagnesian minerals.

In the alkali amphiboles the oxidation state of titanium is probably Ti^{4+} but in the presence of iron it is not possible to determine the oxidation state of both elements (Verhoogen, op. cit.). Verhoogen also demonstrated the reluctance of titanium to enter tetrahedral sites using thermodynamic methods. He utilised the reaction:-

$$CaMgSi_2O_6 + m\ CaMgTi_2O_6 \rightleftharpoons CaMgSi_{2-2m}Ti_{2m}O_6$$

$$G = +\ 14.4\ \text{k.cal.}$$

The free energy of reaction is positive and large showing the reluctance of titanium to substitute for silicon.

Titanium therefore substitutes for Mg or Fe in octahedral sites and two probable coupled substitutions are:-

$$(1)\quad Mg + 2Si \rightleftharpoons Ti + 2Al$$

$$(2)\quad MgMg \rightleftharpoons Ti + \square$$

The first substitution is operative in katophorite, kaesutite and arfvedsonite and the second in potassium richterites and other alkali amphiboles from peralkaline rocks.

4-7-6. Fluorine.

The fluorine content of alkali amphiboles varies with the mineral paragenesis. The lowest concentration is in the metamorphic alkali amphiboles and highest (3.31% in riebeckite-arfvedsonite from Nigeria (Borley), 3.75% riebeckite-arfvedsonite, Tugtutôq (Macdonald, 1968) in late stage alkali amphiboles and in fenitic amphiboles.

Fluorine replaces hydroxyl in the amphiboles and when more than one of the two hydroxyl ions have been replaced by fluorine the mineral should have the prefix fluor-, as suggested by Schaller (1930).

Fig. 5-1

GRØNLANDS GEOLOGISKE UNDERSØGELSE
THE GEOLOGICAL SURVEY OF GREENLAND

(after Emeleus and Harry 1970)

MEDDR GRØNLAND BD. 186 NR. 3 (C. H. EMELEUS AND W. T. HARRY)

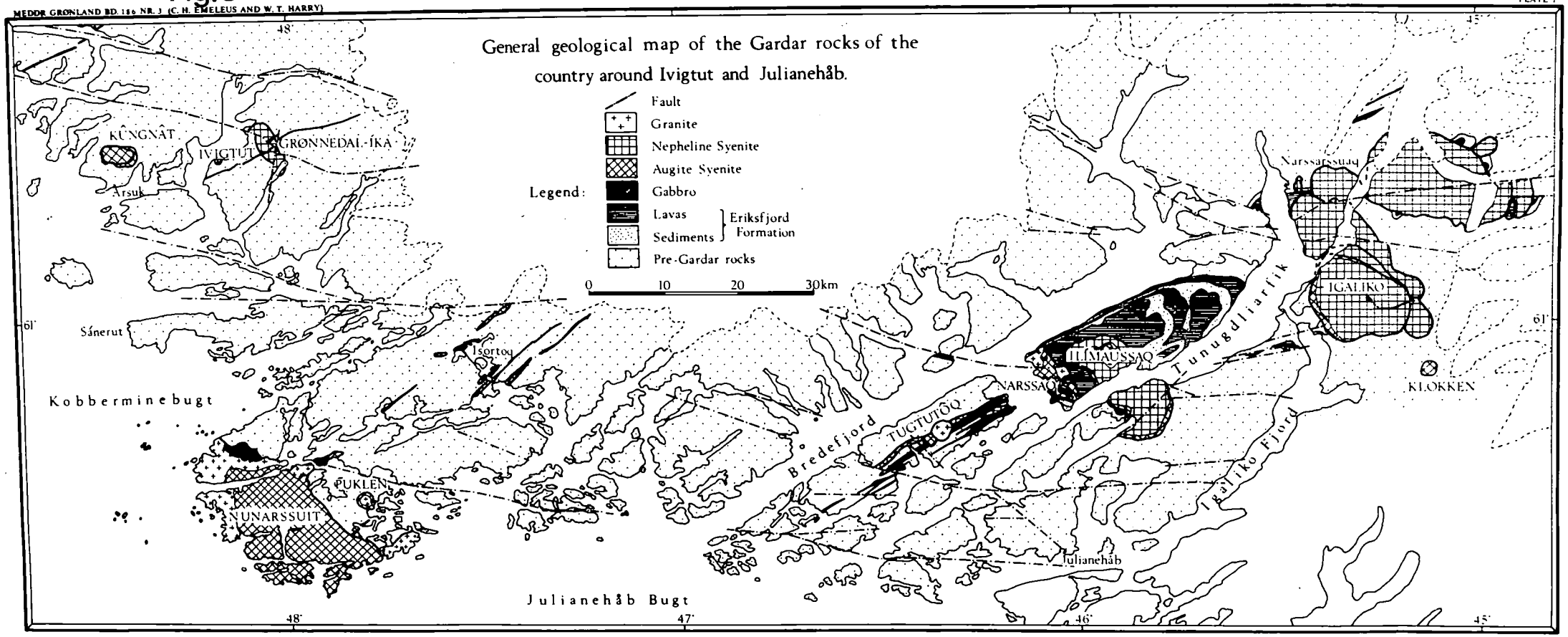

CHAPTER FIVE

Alkali Amphiboles from the Ilímaussaq Intrusion, S.W. Greenland

5-1. Regional Setting.

The Ilímaussaq igneous intrusion forms part of the Gardar alkaline province of south-west Greenland. The Gardar period is the latest of the Pre-cambrian events in the area (Berthelsen, 1962; Pulvertaft, 1968):-

3. Gardar (1300 - 1000 m.y.)
2. Ketilidian (1760 - 1500 m.y.)
1. pre-Ketilidian (> 1760 m.y.)

The basement complex in S.W. Greenland in the Narssaq area (Fig. 5-1 after Emeleus and Harry, 1970) consists of supracrustal rocks, the Julianahaab Granite (~1600 m.y.) and gneisses of the Ketilidian mobile belt. The Gardar formation lies above the Julianahaab Granite unconformably and the earliest members are continental sandstones and extrusive volcanic rocks.

The Gardar formation can be divided into three divisions, namely, early-, mid-, and late-Gardar (Bridgewater, 1965).

The late-Gardar is characterised by the emplacement of alkaline plutonic bodies, which include from west to east (Fig. 5-1), Kûngnât (Upton, 1960), Nunarssuit (Harry and Pulvertaft, 1963; Greenwood, in preparation), Tugtutôq (Upton, 1962 and 1964; Macdonald, 1968), Ilímaussaq (Ussing, 1912; Wegmann, 1938; Sørenson, 1962 and 1964; Ferguson, 1964 and 1967; and Hamilton, 1964) and Igaliko (Ussing, 1912; and Emeleus and Harry, 1970).

The Ilímaussaq intrusion is the youngest of these alkaline centres with an age of 1020 ± 24 m.y. (Bridgewater, 1965; Moorbath et. al., 1960).

The Gardar era is characterised by intense faulting, which probably caused and controlled magmatic activity (Berthelsen and Noe-Nygard, 1965).

The main faults are sinistral tear faults with a WNW-ESE trend (Fig. 5-1). The Gardar alkaline plutonic complexes are often intruded where E.N.E.-trending dyke swarms are crossed by these faults.

5-2. Rock types in the Ilímaussaq Intrusion.

The names of these rocks were given by Ussing (1912).

1. Augite Syenite:- consists of alkali feldspars, augite, olivine, biotite, Kaersutite (titaniferous pargasite), acmitic pyroxene and magnetite. The pyroxenes are often zoned from augite cores to aegirine-augite rims.
2. Heterogeneous Syenite (Ferguson, 1969):- the mineralogy differs markedly from the augite syenite although the chemistry is similar. The minerals are alkali feldspars, alkali pyroxenes, alkali amphiboles and occasionally olivine and nepheline.
3. Alkali Granite:- apart from some metasomatic acid rocks this is the only acid rock in the intrusion with a mineralogy consisting of alkali feldspars, quartz, arfvedsonite, and occasionally aenigmatite and alkali pyroxenes.
4. Quartz Syenite:- Mineralogically contains the same as the alkali granite but the percentage of quartz is lower and the pyroxene content is higher.
5. Pulaskite:- consists of alkali feldspars, nepheline, alkali pyroxenes and amphiboles, and aenigmatite.
6. Sodalite Foyaite:- contains the same minerals as the pulaskite but in addition the phases eudialyte and sodalite appear.
7. Naujaite:- the same mineralogy as the sodalite foyaite but the individual minerals are pegmatoid in appearance with the exception of the euhedral sodalite crystals. The minerals crystallized around the sodalite crystals giving a poikolitic texture to the rock.

8. Kakortokite:- the kakortokite suite of rocks are rhythmically layered into arfvedsonite rich (black), eudialyte rich (red), and feldspar rich (white) with transitional rock types developed between these. Common additional phases are alkali pyroxenes and nepheline.

9. Lujavrite:- these are finer grained rocks than the others and possess a marked fissility and preferred orientation of pyroxene (aegirine) and arfvedsonite. The lujavrites are both green (pyroxene rich) and black (arfvedsonite rich). The mineralogy is similar to the kakortokites, but with many more rare minerals, plus U, Th mineralisation (Sørenson, 1969).

5-3. Origin of the Ilímaussaq Intrusion.

The most satisfactory interpretation of the sequence of events in the intrusion is by Ferguson (1964, 1967). Ussing (1912) and Sørenson (1958, 1962) also provide useful but inadequate interpretations of the available data.

All the students of geology working in south-west Greenland agree that the earliest magma of these plutonic complexes had an augite syenite composition (Upton, 1960, 1962, 1964; Ferguson, 1964, 1967; Sørenson, 1958, 1962).

The intrusion of the main mass of rocks appears to have been in two stages. The first stage involved the intrusion of the augite syenite following cauldron subsidence and is now represented as a discontinuous shell. It is thought that this magma then underwent differentiation along an under-saturated trend. The sodic pyroxenes within the augite syenite appear to be zoned from augite cores → hedenbergite → sodic hedenbergite → aegirine augite (preliminary electron probe microanalysis, author) which indicates aubstantial differentiation of the augite syenite, in situ.

5-4. Chemistry of the alkali amphiboles in the Ilímaussaq Intrusion.

5-4-1. Formulae of the alkali amphiboles.

The analyses of the alkali amphiboles were recalculated to 24 oxygens using the scheme outlined by Phillips (1963). The formulae of riebeckite ($Na_2Fe_3^{2+}Fe_2^{3+}Si_8O_{22}(OH)_2$) and arfvedsonite ($NaNa_2Fe_4^{2+}Fe^{3+}Si_8O_{22}(OH)_2$), both after Sundius (1945), have been used as a basis for discussing the variations in these alkali amphiboles.

5-4-2. General remarks.

The alkali amphiboles of the Ilímaussaq intrusion (Appendix 3) all belong to the riebeckite-arfvedsonite-katophorite series and the main features of their chemistry are:-

1. High Fe^{++}/Fe^{+++} contents.
2. Very low magnesium contents (0-0.20%).
3. Low titanium (0.08 - 0.25 atoms).
4. Moderate to low calcium and low aluminium.
5. Uniform potassium (0.27 - 0.41) except in the lujavrites where it rises to 0.57 - 0.65 atoms.
6. Higher hydroxyl than fluorine.
7. High sodium (2.00 - 2.70 atoms).
8. Uniform manganese (0.12 atoms) except in the lujavrites.

Many of the amphiboles from Ilímaussaq were seen to possess slightly different pleochroic schemes. These differences could be attributed to (a) different optic orientation or (b) different chemical composition. An analysed amphibole from a kakortokite (D.U. 10936) was re-analysed using the electron microprobe. Six results from this investigation (Table 5-1) reveal that differences in pleochroic scheme could be due to chemical differences. Analyses 2, 3, and 6 (dark blue-blue pleochroism)

have lower aluminium and higher potassium than analyses 1, 4, and 5 (green-brown pleochroism).

TABLE 5-1 Partial Analyses of Irregularly Zoned Arfvedsonite, D.U. 10936, Ilímaussaq.

Analysis	Al_2O_3	CaO	Na_2O	K_2O
1	2.38	1.19	6.31	1.71
2	1.96	1.21	5.99	2.05
3	1.71	1.26	5.60	2.81
4	2.58	1.73	6.18	1.52
5	2.43	1.59	6.23	1.54
6	1.93	1.28	6.22	1.98

Preliminary investigations of the distribution of elements between pyroxene and alkali amphibole (D.U. 10921) in the nepheline syenites of Ilímaussaq show that K, Na, Mn, and Al are more abundant in the amphibole and calcium in the pyroxene.

Small blue, fibrous amphiboles accompany the primary amphibole occasionally and these crystals are pure secondary riebeckite. The analyses of these alkali amphiboles and their recalculations are shown in the appendix.

5-4-3. Hydroxyl group.

Fluorine substitutes for hydroxyl in the O(3) sites. The highest values for fluorine were obtained for amphiboles from the arfvedsonite granite (D.U. 10919, D.U. 10927) with a concentration up to 0.78 atoms. In the agpaitic rocks there is variation within each rock type but in general the lowest concentrations occur in amphiboles from the lujavrites (0.15 - 0.35 atoms), followed by the kakortokites (0.20 - 0.59 atoms), naujaites (0.18 - 0.74 atoms), sodalite foyaite (0.46 atoms) and pulaskite

(0.42 atoms). Where the fluorine content is low the hydroxyl content is high but often there is a deficiency in the O(3) sites, which is probably due to poor water determinations. It could also be partly due to oxy-amphibole substitution balanced by Fe^{3+} or Ti^{4+}.

5-4-4. The Z group.

This group includes silicon (r = 0.42Å) and aluminium (0.51Å). In contrast to Borley's (1963) analyses there are no deficiencies in the Z sites and only the above two elements are needed to fill these sites except in two samples (10941, 10957) both naujaites. In these two, only 0.07 and 0.08 atoms are needed to fill the sites.

The lowest number of silicon atoms is 7.27 for an arfvedsonite from a naujaite (10941) and the highest (7.99 atoms) for an amphibole from the lujavrites (10951). The alkali granite amphibole has 7.93 atoms of silicon.

5-4-5. The Y group.

The Y group includes ferrous iron (0.74Å), lithium (0.68Å), manganese (0.80Å), Magnesium (0.66Å), zinc (0.74Å), ferric iron (0.64Å), titanium (0.68Å) and aluminium (0.51Å).

There may be relatively large trace amounts of elements such as zirconium (0.79Å), niobium (0.69Å) and yttrium (0.92Å) concentrated into these sites because of their abundance in these undersaturated rocks. Zirconium values go up to 1% in the agpaitic rocks but is concentrated in the complex sodium zirconium titanium silicates such as eudialyte and aenigmatite. Niobium reaches 1400 p.p.m. in arfvedsonite lujavrites. Unfortunately, these elements have only been determined qualitatively, to detect their presence.

Ferrous iron is the dominant cation in the Y group followed by ferric iron. The ferrous/ferric iron ratio ranges from 1.779 in an arfvedsonite

in the lujavrites to 3.504 in an amphibole in a naujaite, which is more extreme than Borley's amphiboles from late stage soda granites (1.36 - 3.12).

It is noteworthy that in these amphiboles the magnesium concentration is very low varying from 0 to 0.20 atoms, lithium varies from 0.12 to 0.25 atoms and manganese from 0.07 to 0.18 atoms.

Also substituting for ferrous iron in this group is zinc which has the same ionic radius as ferrous iron (0.74Å) but only achieves a maximum concentration of 0.02 atoms in the pulaskite.

All the above elements would occupy the M(1) and M(3) sites in a well ordered structure and ferric iron, titanium and aluminium would occupy the M(2) sites. The maximum amount of octahedral aluminium is 0.31 atoms in an arfvedsonite from the lujavrites (10930) but otherwise is extremely low. Titanium is generally low and constant 0.08 - 0.21 atoms in the agpaites, whereas in the alkali granite it is slightly higher (0.26 atoms).

5-4-6. The X group.

The cations in the X sites (M(4)) are sodium (0.97Å), calcium (0.99Å), ferrous iron and manganese. These latter two elements only enter the M(4) sites to a minor extent, i.e. up to 0.12 atoms (in 10927, 10941, 12837). The most important cation is sodium which varies from 1.33 atoms in an amphibole from a naujaite pegmatite to 1.98 atoms in an arfvedsonite from a lujavrite. The calcium varies from 0.02 to 0.90 atoms.

5-4-7. The A group.

Sodium and potassium are the only cations which occupy these sites and the amount of potassium in 'A' is quite constant within most of the samples viz. 0.27 - 0.41 atoms, except in the lujavrites where the potassium content rises to 0.57 - 0.65 atoms. The 'A' sites are largely filled and occasionally excess hydrogen atoms enter the 'A' site (Phillips, 1963; Nicholls and Zussman, 1955) which results from high water values.

5-5. Comparison of Petrochemistry and the chemical composition of the alkali amphiboles in Ilímaussaq.

5-5-1. General remarks.

Recently Gerasimovskii and Kuznetsova (1968) have published more recent chemical analyses of the rocks in the Ilímaussaq intrusion and their conclusions, which are pertinent to the present discussion, are:-

1. Elements vary considerably even within one rock type especially aluminium, calcium, and ferrous iron.
2. Not only does the total iron vary but also the Fe^{+++}/Fe^{++}, which varies from 0.46 to 1.01 and is greatest in the aegirine lujavrites (4.7 - 10.1) and least in the arfvedsonite lujavrite (0.54 - 0.97). The ferric iron, of course, is concentrated into the aegirine and ferrous iron into the arfvedsonite.
3. The agpaitic ratio:-

$$(= \frac{Na + K}{Al})$$

varies from 1.20 to 2.33 and if this value is greater than one, the nepheline syenite is called an agpaite, if less than one, a miaskite.

The agpaites of the Ilímaussaq intrusion are characterised by:-

1. A very high content of alkali metals with Na_2O (12.95%) being greater than K_2O (3.40%).
2. The agpaitic ratio average is 1.39.
3. Fe^{+++}/Fe^{++} average is 1.40.
4. Low concentrations of calcium (1.09%) and magnesium (0.35%).
5. Low titanium (0.35%) and high zirconium (0.75%).
6. Very high chlorine (1.11%).
7. A considerable amount of water (2.27%).
8. Relatively low fluorine content (0.19%).

Ramberg (1952) has pointed out that the ions with a higher electronegativity are favoured by structures with low polymerisation. In nepheline syenites where pyroxenes and amphiboles are the main ferromagnesian minerals the cations with higher electronegativities (sodium and calcium in X sites and ferric iron in Y sites) are preferentially incorporated into the single chain pyroxene structure and those with the lower electronegativities (potassium in 'A' sites and ferrous iron in Y sites) will be concentrated in the double chain amphibole structure. Therefore the elements which are incorporated into the amphiboles and pyroxenes will monitor the petrochemistry of those elements.

The above statement can be concluded from a comparison of the mineral data with that of the petrochemistry.

Several elements display interesting phenomena in the amphiboles and their related minerals.

5-5-2. Potassium (r = 1.33Å).

Potassium varies from 0.27 to 0.41 atoms in the alkali amphiboles from the agpaites, with the exception of those from the lujavrites where the content is 0.57 - 0.65 atoms. The potassium is concentrated into the 'A' sites of the amphiboles. When comparing the petrochemistry to the mineral chemistry one observes that the potassium values are fairly constant in the rocks.

The percentage of potassium in the green (aegirine) and black (arfvedsonite) lujavrites is as follows:-

	1	2	3	4	5	6	7	8
Green	2.17	3.42	5.00	3.02	2.80	3.71	3.46	-
Black	2.60	3.50	3.20	3.08	3.97	5.58	3.50	3.02

1-4 Ferguson (1967).

5-8 Gerasimovskii and Kuznetzova (1968).

This demonstrates that the overall concentration is of the same order for both the green and the black lujavrites.

The petrography of the two rock types differs only in the modal content of aegirine and arfvedsonite. Pyroxenes cannot incorporate potassium into their structure to any large extent. The maximum percentage for aegirines (Deer, Howie and Zussman, 1963) is 0.40% and alkali pyroxenes from the Nunassuit alkaline intrusion, S.W. Greenland, analysed by means of the electron microprobe by P.B. Greenwood (personal communication) show very little if any potassium in the alkali pyroxenes.

Potassium is therefore largely concentrated in the two alkali feldspars, nepheline, and arfvedsonite in these lujavrites. Ferguson (op. cit.) has determined the chemistry of the microcline and albite by optical methods and they indicate no difference in chemical composition of the minerals between the two rock types i.e. > 90% Or in the microcline laths coexisting with pure albite (Ab_{100}).

Ferguson has determined the kalsilite contents of the nephelines in the two rock types:

aegirine lujavrite $Ks_{27.6}$

arfvedsonite lujavrite $Ks_{15.4}$

Therefore potassium is apportioned between nepheline and alkali amphibole in these late stage rocks. The kalsilite value is always high (Ks_{25}) when alkali pyroxene is the dominant ferromagnesian mineral and low when alkali amphibole is the sole ferromagnesian mineral.

Hamilton (1961) has suggested that at subsolidus temperatures chemical exchange takes place between nepheline and alkali feldspar and may only involve larger cations such as sodium and potassium. In nepheline the potassium occurs in two sites which are ninefold co-ordinated (Buerger et. al., 1954; Hahn and Buerger, 1955), and the sodium in octahedral sites.

Hamilton goes on to conclude that the framework cation ratio Al:Si remains constant based upon the absence of exsolved feldspars in nepheline. The lujavrites of the Ilímaussaq intrusion contain separate phases of microcline and albite and no indication of exsolution is detected in these nor in the nephelines.

In the lujavrites there is obviously no base exchange phenomena between the alkali feldspars and nepheline but there is between nepheline and alkali amphiboles.

Alkalis appear to be readily exchanged in silicates which have sites which are relatively large e.g. feldspars, nephelines, amphiboles and micas. Experiments have been performed in NaCl and NCl melts to exchange the alkali cations in nephelines (Debron, 1965); in feldspars (Orville, 1967; Wright and Stewart, 1968); and recently amphiboles (Huebner and Papike, personal communication). The amphibole in these experiments was richterite.

The 'A' site of the amphiboles appears to be a site where alkali exchange can take place quite readily and will be of importance in rocks where amphiboles are crystallizing with minerals which possess this same property.

The same phenomenon can be seen in the hornblende lujavrites of the Lovozero alkaline massif, Kola, U.S.S.R.

5-5-3. Lithium (r = 0.68Å).

The following figures show the concentration of lithium in the agpaitic rocks of the Ilímaussaq intrusion:-

Black Lujavrite		200 p.p.m. (Li)
Sodalite Foyaite		127 "
Naujaite		130 "
Kakortokite	white	142 "
	red	117 "
	black	114 "

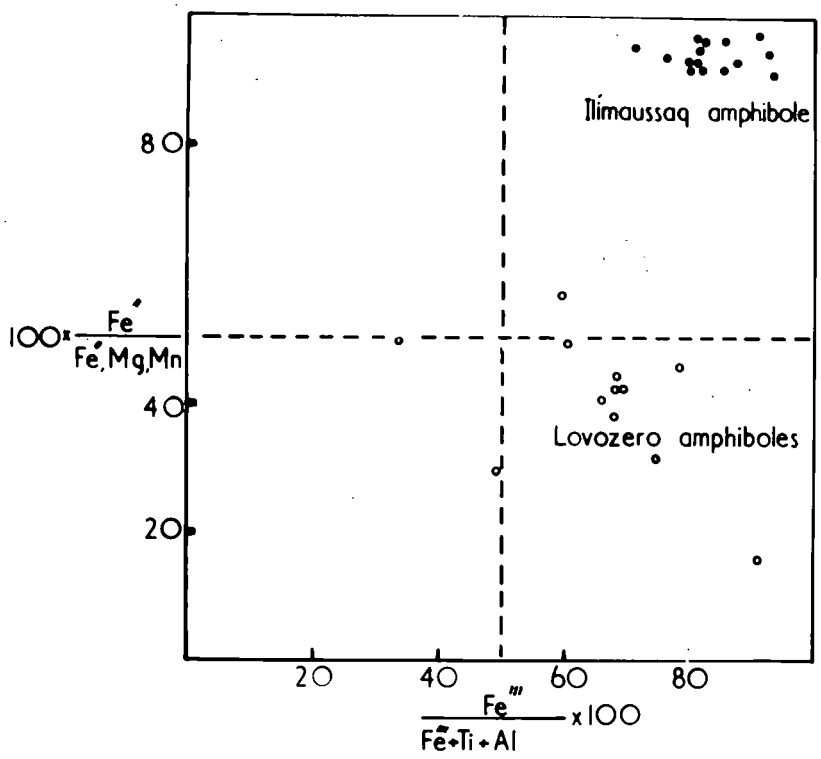

Fig.5-4 Comparative compositions of Lovozero & Ilímaussaq alkali amphiboles.

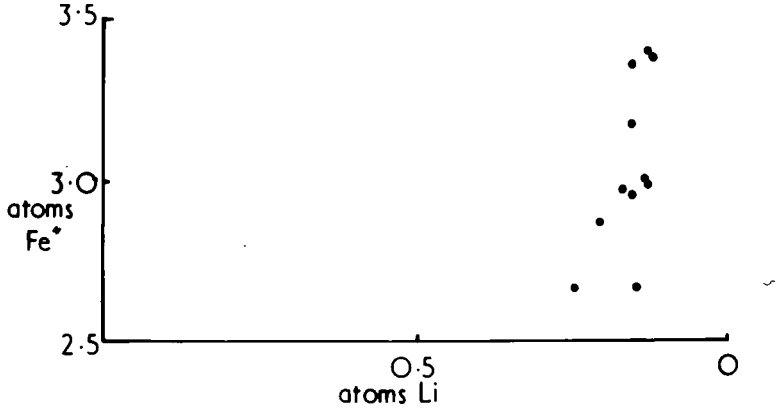

Fig.5-2 Correlation of lithium & ferrous iron in Ilímaussaq amphiboles

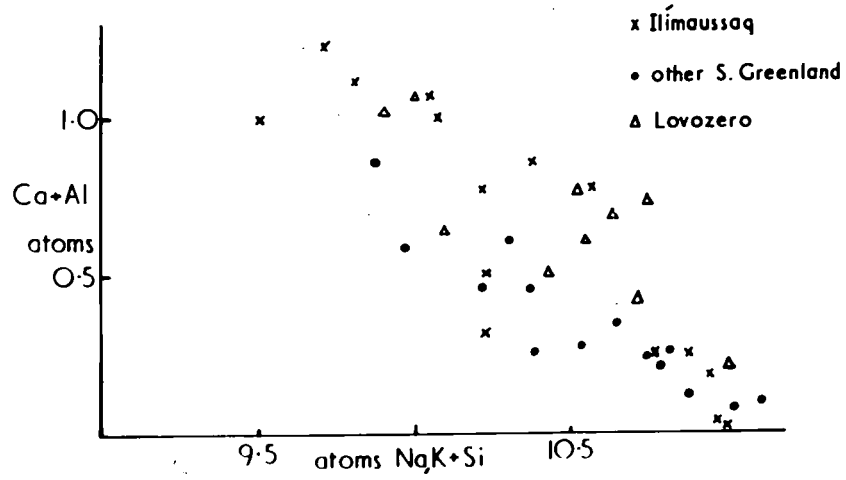

Fig.5-3 Coupled substitution Ca Al ⇌ Na(K)Si in amphiboles from Lovozero & S.Greenland.

Hybrids	128 p.p.m. (Li)
Green Lujavrite	78 "

The two extreme concentrations are the two varieties of lujavrite with the other agpaitic rocks displaying constant values. The minerals also emphasize this feature. Lithium is concentrated in the alkali amphibole from the black lujavrites (.33 - .39% Li_2O).

Ferguson (op. cit.) is of the opinion that lithium is concentrated in lithium minerals e.g. polylithionite and lepidolite, which because of sporadic occurrence may explain the erratic distribution of lithium. This erratic distribution is not so apparent when considering the distribution of ferromagnesian minerals and these may be the hosts for lithium, and are also much more abundant in the rocks.

Ahrens (1965), Taylor (1966), Vlasov (1959, 1966) consider that lithium substitutes for magnesium and ferrous iron in ferromagnesian minerals. Lithium substitutes for magnesium in octahedral sites (M(1) and M(3)) in amphiboles (Phillips, 1963). The Li-O bond is more ionic than Mg-O and is admitted into the lattice and concentrated in late stage fractions (Taylor, 1966).

The substitution considered to be likely in the amphiboles is:-

$$Li(Al,Fe^{3+}) \rightleftharpoons 2(MgFe^{2+})$$

Lithium being monovalent when substituting in M(1), M(3) sites will require a trivalent cation to accompany it to balance the charge. Borley (1963) plots the amount of lithium against ferrous iron content and shows a correlation between them. Fig. 5-2 also demonstrates this substitution of lithium for ferrous iron for the Ilímaussaq amphiboles. The correlation is not so good as Borley's, probably because the concentration of lithium is lower.

In the black lujavrites the concentration is 200 p.p.m. (Li) and the amphiboles contain most of this. The low value for lithium in the

green lujavrites (78 p.p.m. Li) supports the thesis that lithium substitutes for ferrous iron and not ferric iron.

5-5-4. Titanium (0.68Å).

The amount of titanium in the alkali amphiboles varies from between 0.08 atoms in the lujavrites to 0.21 atoms in a naujaite amphibole, generally the value lies between 0.08 - 0.15 atoms. This can be correlated with the relatively constant percentage obtained for the agpaitic rocks (~0.50%) by Gerasimovskii and Kuznetzova (op. cit.).

The titanium concentration increases to 0.26 atoms in an arfvedsonite from the alkali granites but this increase is not reflected in the concentration in the rock. In the agpaites titanium is partitioned between amphibole, eudialyte, and aenigmatite whereas in the alkali granite the arfvedsonite is the dominant and often only ferromagnesian mineral.

5-5-5. Manganese (r = 0.80Å).

The manganese contents of the alkali amphiboles in the differentiated rocks vary from 0.07 - 0.18 atoms and in the alkali granites 0.13 atoms. In the kakortokites, sodalite foyaites, and naujaites the value lies between 0.07 - 0.12 atoms and the lujavrites 0.18 atoms.

A study of the rock analyses shows that the manganese concentration increases with the amount of ferrous iron, which is highest in the black lujavrite. In the green lujavrite manganese varies from 0.17 - 0.26% whereas in the black varieties from 0.38 - 1.04%. The ferrous iron contents of the green lujavrites are 0.80 - 1.72% and in the arfvedsonite rich rocks 5.80 - 10.04%. This indicates that divalent manganese is following ferrous iron into lattice sites and will therefore be concentrated in the alkali amphiboles.

5-5-6. Calcium (r = 0.99Å).

Calcium is an element which is partitioned between alkali pyroxene; alkali amphibole and eudialyte in these nepheline syenites and the content in the amphiboles varies from 0.02 - 0.62 atoms. Unfortunately analyses for the pyroxenes and eudialytes are not available therefore any comparison is invalid.

The calcium is preferentially incorporated into the earlier formed amphiboles, where the concentration in the rocks is higher too. The increase in $Ca + Al^{IV}$ in alkali amphiboles has been correlated with higher temperatures of formation (Miyashiro, 1957). In Fig. 5-3 $Ca + Al^{IV}$ is plotted against Na(K)Si to show the change from katophoritic to arfvedsonitic composition with differentiation.

5-5-7. Fluorine and hydroxyl anions.

Fluorine occurs not only in ferromagnesian minerals in the Ilímaussaq intrusion but also in fluorine minerals such as fluorite and villiaumite (NaF). Again we must regard the main hosts of fluorine as the alkali amphiboles because of their relative abundance. The table below shows the general pattern of fluorine and water distribution in the agpaitic rocks:-

Naujaites	↑ increasing	
Sodalite Foyaite		
	fluorine	increasing
Kakortokites		
	↓	water
Black Lujavrites		↓

Fluorine does not build up to the last stages of differentiation as in acid peralkaline magmas and miaskitic magmas because it is removed from the magma by the crystallizing amphiboles and fluorine minerals which occur throughout the rocks. The water content of these rocks, however, does increase, therefore it appears that fluorine

enters the amphiboles preferentially under these conditions.

The amphiboles again monitor the petrochemistry. The highest fluorine concentrations in the amphiboles are in the early formed naujaites and lowest in the late stage lujavrites (see Appendix 3). The water content of the amphiboles is the reverse of the fluorine.

Chlorine although it does not enter the amphibole lattice to any great degree is concentrated in the early stages of differentiation where it is concentrated in the sodalite minerals.

5-6. Comparison of alkali amphiboles from the Ilímaussaq intrusion and Lovozero (Kola, U.S.S.R.) intrusions.

The Lovozero massif on the Kola peninsula in the Soviet Union is very similar in petrology, petrochemistry and mineralogy to the Ilímaussaq intrusion. These two bodies are the classic examples of differentiated nepheline syenites of the agpaitic type (Vlasov et. al., 1968).

The main differences between the two in petrochemistry are that in the Lovozero massif the nepheline syenites contain more manganese, magnesium, phosphorous and titanium and the Fe^{+++}/Fe^{++} ratio is 4.4 compared to 1.4 in the Ilímaussaq intrusion. The latter contains more water, chlorine, and sodium.

Some of these differences in petrochemistry are emphasized by the alkali amphiboles developed in them. The main difference is the magnesium concentration relative to the ferrous iron. In Fig. 5-4 the $\frac{Fe^{++}}{Li, Mg, Mn, Fe^{++}}$ is plotted against $\frac{Fe^{+++}}{Fe^{+++}, Ti, Al}$ i.e. $\frac{Fe^{++}}{\text{Total } R^{++}}$ and $\frac{Fe^{+++}}{\text{Total } R^{+++}}$.

All the Ilímaussaq amphiboles plot close to the arfvedsonite composition i.e. $> 90\% \frac{Fe^{++}}{\text{Total } R^{++}}$ and $> 75\% \frac{Fe^{+++}}{\text{Total } R^{+++}}$. The minerals from Lovozero are not strictly arfvedsonites but magnesioarfvedsonites.

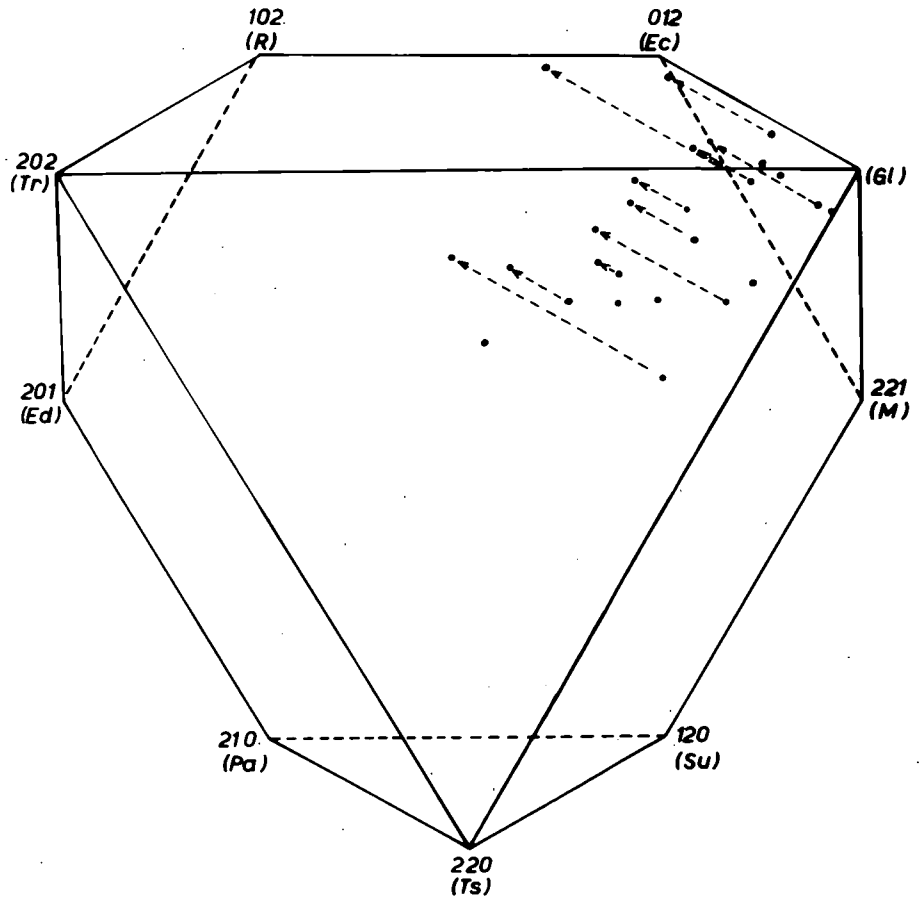

Fig.5-5 Alkali Amphibole compositions Ilímaussaq, S.W. Greenland.
(Whittaker's Compositional Space.)

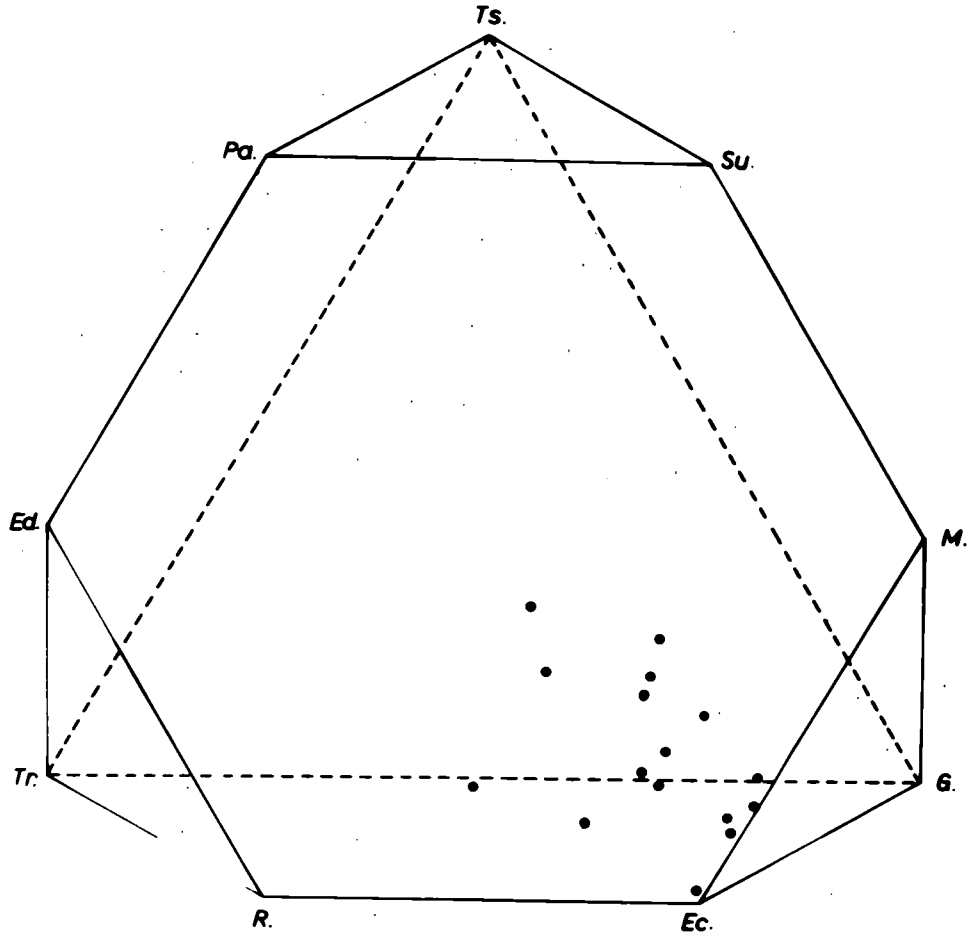

Alkali Amphibole compositions, Ilímaussaq, S.W. Greenland.
(Phillips' Compositional Space.)

The composition of the Lovozero amphiboles are widely scattered, two compositions occuring in the eckermannite field. This may indicate poor analytical results rather than variable petrochemistry.

The amphiboles from Lovozero contain more fluorine, magnesium, manganese, aluminium, and titanium than the arfvedsonites from the agpaites of Ilímaussaq. With the exception of the magnesium content the arfvedsonite from the alkali granite resembles the Lovozero minerals.

One of the main coupled substitutions in these amphiboles is:-

$$CaAl^{IV} \rightleftharpoons Na(K)Si$$

shown in Fig. 5-5. The amount of this substitution does not appear to be so extreme for the Lovozero minerals as for the Ilímaussaq ones. These latter amphiboles vary from almost the arfvedsonite end-member ($NaNa\ Fe_4^{++}Fe^{+++}Si_8O_{27}(OH,F)_2$, after Sundius op. cit.) to 9.27 Na(K)Si and 1.42 $CaAl^{IV}$. On the other hand the values obtained for the Lovozero alkali amphiboles lie between these values.

Fig. 5-5 shows the distribution of compositions for the alkali amphiboles (Phillips, 1966). The Ilímaussaq amphiboles all plot within the arfvedsonite field and trend from compositions close to that for katophorite ($NaCaNaFe_4FeSi_7AlO_{22}(OH)_2$) to that close to the end-member arfvedsonite composition. Therefore a line from the amphiboles which crystallized in the naujaite to those which occur in lujavrites show a descent in the crystallization sequence of the Ilímaussaq intrusion.

The two major substitutions involved are:-

(1) $CaAl^{IV} \rightleftharpoons NaSi$

(2) $NaFe^{++} \rightleftharpoons \square Fe^{+++}$

together with minor substitutions:-

(3) $Li(AlFe^{+++}) \rightleftharpoons 2(Fe^{++},Mg)$

(4) $Fe^{++} \rightleftharpoons Mg$

The Lovozero alkali amphiboles show no obvious distribution pattern. The cause of this may be bad documentation of rock types from which the minerals were extracted. Several amphiboles from this massif plot in the "miyashiroite" field. These may be poor analyses or the effect may be due to the large ferric iron content of these minerals. No trend can be discovered for the Lovozero alkali amphiboles because the minerals from known rock types plot fairly close together.

CHAPTER SIX

Electron Microprobe Investigations of Alkali Amphiboles

6-1. General Statement.

The technique of electron probe microanalysis used in the Geology Department in the University of Durham is in the appendix. The electron probe was used to investigate the following problems:-

6-2 Continuously Zoned Amphiboles

6-3 Discontinuously Zoned Amphiboles

6-4 Co-existing Amphiboles

6-5 Amphibole Compositions from the Tugtutôq dykes

6-6 Study of Alkali Amphiboles from late-stage differentiated rocks

6-7 Manganese content of Juddites (magnesioarfvedsonites) from India

6-2. Continuously Zoned Amphiboles.

6-2-1. Amphibole from the Arfvedsonite Granite (D.U. 12833, D.U. 10919) Ilímaussaq, S.W. Greenland.

Plate 1 shows a zoned amphibole from the Arfvedsonite Granite in the Ilímaussaq intrusion. Occasionally, acmite replaces the amphibole along the cleavage traces and around the rim. This amphibole has an extinction angle ($\gamma \wedge c$) of 19°.

Two traverses (Fig. 6-1) were made across the mineral to determine which elements varied and by how much. Magnesium, sodium, calcium, potassium, aluminium and titanium all show variation. The sodium analyses were erratic in Traverse B. Iron did not seem to vary systematically possibly because of changes in valence state across the crystal.

Apart from the ocassional spurious result, the chemistry of the amphibole changes smoothly across the crystal. Titanium decreases from 1.25% in the core to less than 0.50% on the rim and similar decreases

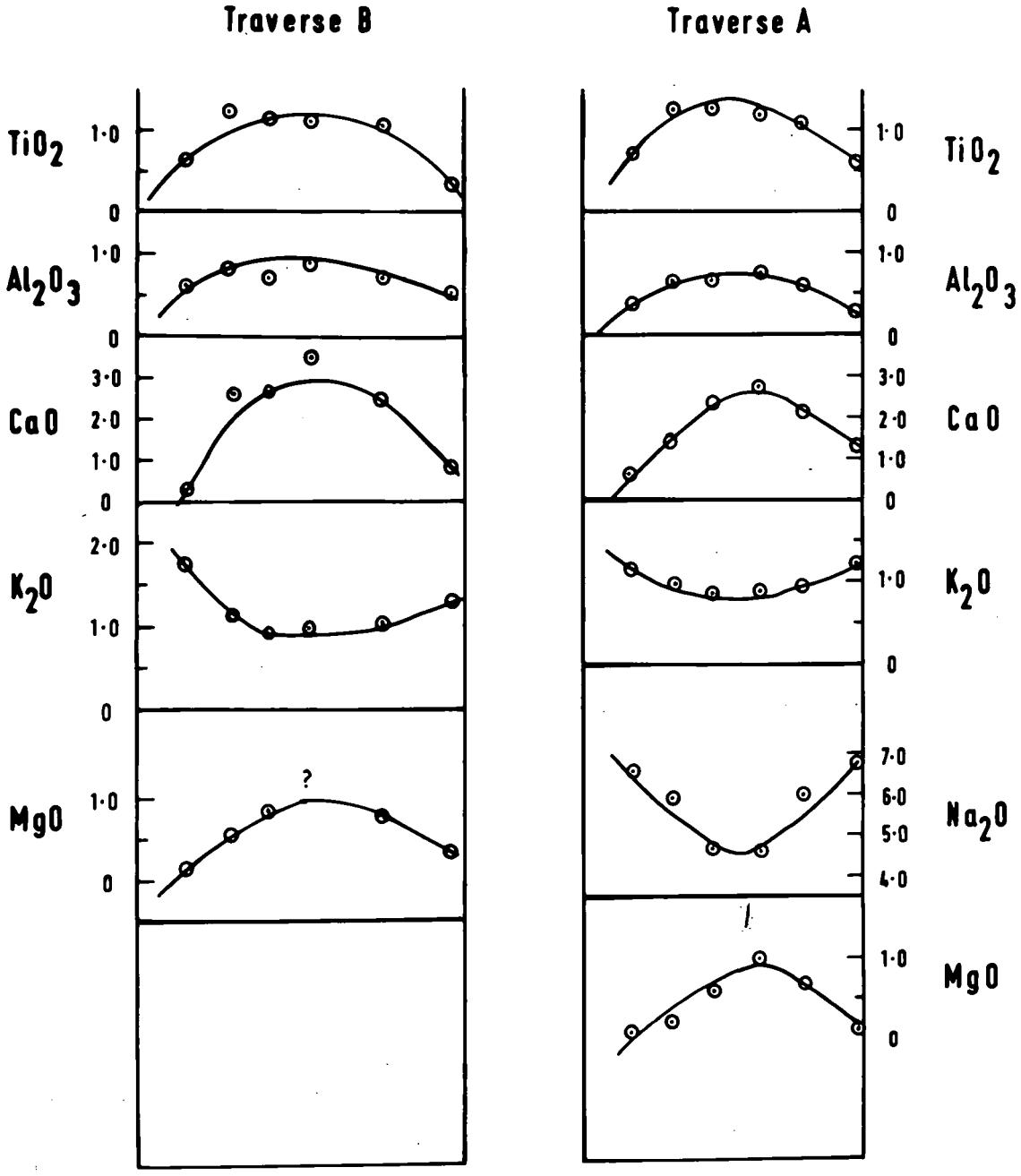

Fig.6-1 Continuous zoning in Arfvedsonite (D.U.12833,10919), Alkali Granite, Ilímaussaq S.W.Greenland.

PLATE 1

Continuously zoned amphibole (dark grey) from arfvedsonite granite (D.U. 12833, 10919) Ilímaussaq, Greenland. Additional phases present are alkali feldspar and quartz (clear areas). (x 35)

PLATE 2

Continuously and discontinuously zoned amphibole from the Assorutit syenite, Tugtutôq, S.W. Greenland (D.U. 10987). The riebeckite-arfvedsonite is light grey, other amphiboles dark grey. Quartz and alkali feldspar additional phases. (x 50)

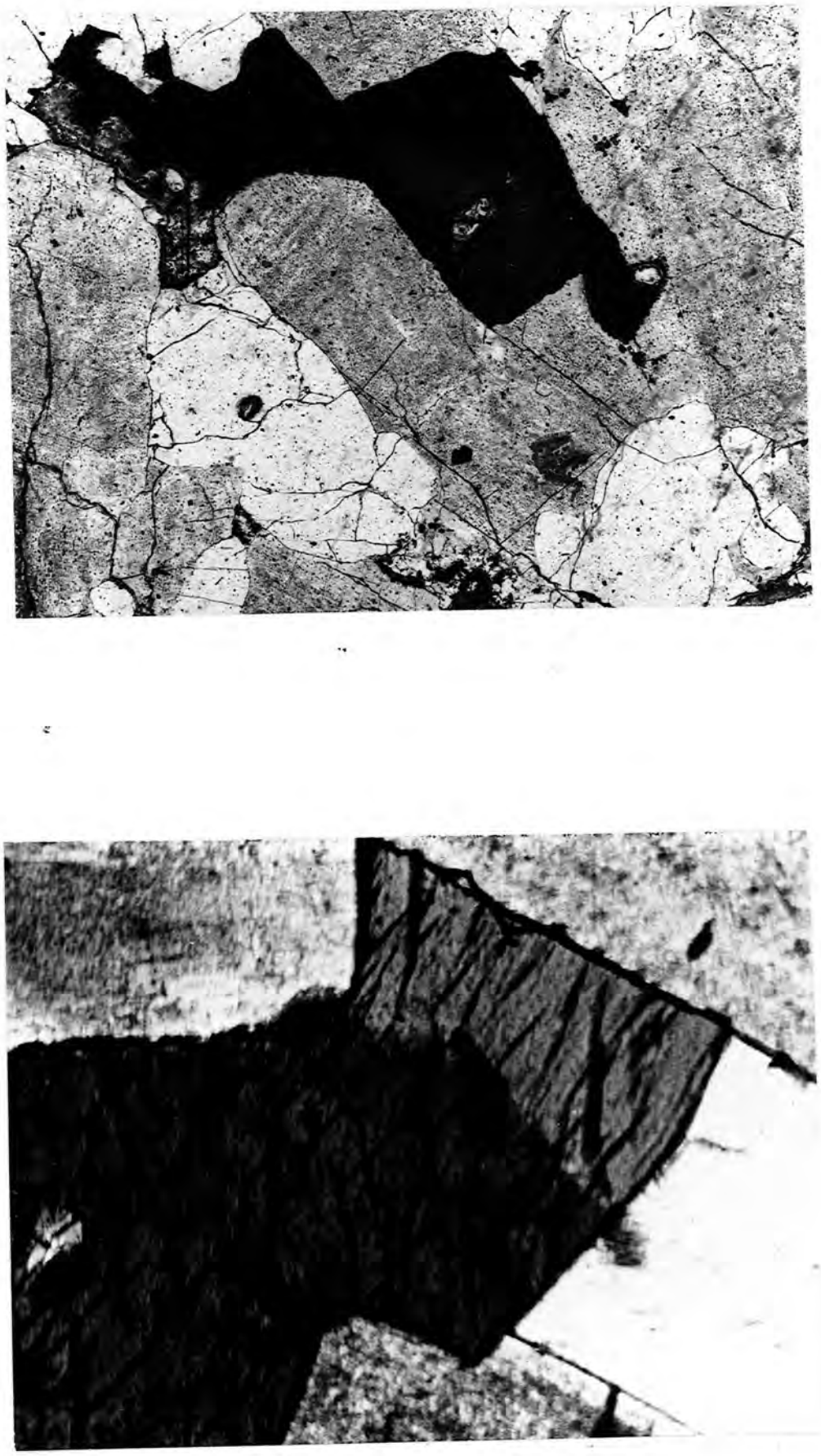

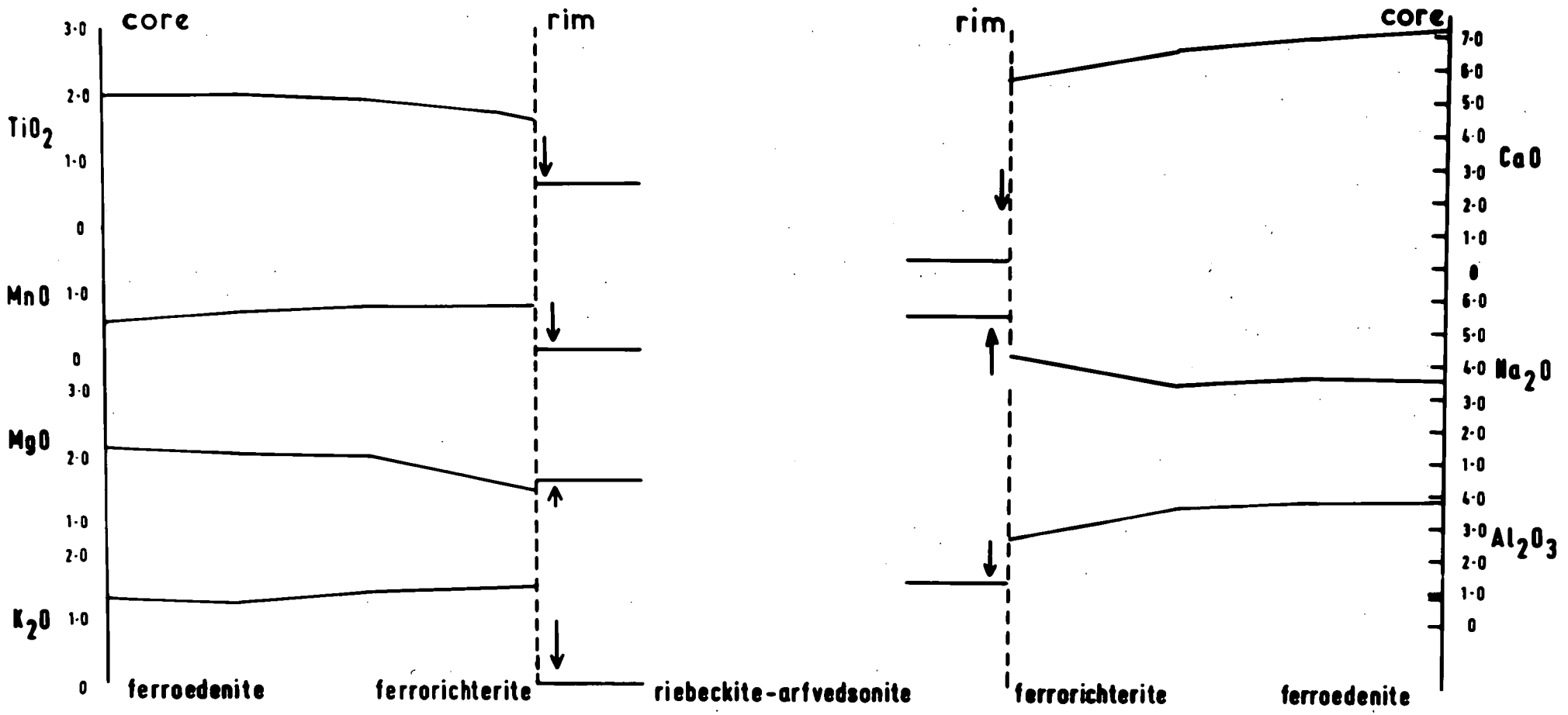

Fig.6-2 Continuous and discontinuous zoning in amphiboles from the Assorutit Syenite, Tûgtutôq S.W.Greenland.

occur in magnesium (1.00 - 0.10%), calcium (3.00 - 0.30%), and aluminium (1.00 - 0.30%). Sodium and potassium both increase from core to rim (4.60 - 6.80% and 0.80 - 1.75% respectively).

The amphibole changes from a more calcium rich arfvedsonite to almost a pure arfvedsonite during its crystallization.

6-3. Discontinuously Zoned Amphiboles.

6-3-1. Amphiboles from the Assorutit Syenite (D.U. 10987,) Tugtutôq, S.W. Greenland.

The amphiboles of the Assorutit Syenite crystallised subsequent to the olivines and pyroxenes and they exhibit examples of both continuous and discontinuous reaction. The minerals which have been analysed show a continuous colour change from brown through blue-green to green varieties followed by a sharp transition to blue-black riebeckite-arfvedsonite.

Optics of the amphiboles:-

"Hornblende" A
α = light cinnamon brown
β = brown
γ = deep brown
$\gamma \wedge c = 28^\circ$

"Hornblende" B
α = olive green
β = deep blue-green
$\gamma \wedge c = 36^\circ$

Riebeckite - Arfvedsonite
α = deep blue-black
γ = dull bluish green
$c \wedge \alpha = 5^\circ$

Plate 2 shows one of the crystals which has been traversed. The changes in chemistry across amphibole B are shown in figure 6-2. These brown, blue-green, and green amphiboles have been designated ferrohastingsites by Upton (1962), but the overall amounts of calcium and aluminium are insufficient in all the analyses for them to be

called ferrohastingsites. Recalculations of the analyses to 23 oxygens and plotting them on to Whittaker's (1968) compositional diagram places them between edenite and richterite but outside the body of the compositional space. This situation arises because of the lack of control on Fe^{++}/Fe^{+++} in the minerals. The brown varieties plot close to ferroedenite (201 in Whittaker's compositional space) whereas the green minerals plot close to ferrorichterite (102).

One large phenocryst of amphibole shows the changes in chemistry across the grain (Fig. 6-2). There is a gradual decrease in calcium, aluminium, titanium and magnesium, and increase in sodium, potassium and manganese as the traverse proceeds from the brown through blue-green to green varieties. The dark-blue amphibole (riebeckite-arfvedsonite) is in razor-sharp contact with the green mineral (ferrorichterite). The riebeckite-arfvedsonite shows an abrupt decrease in calcium, aluminium, titanium, manganese, and surprisingly potassium. There is an increase in sodium and magnesium.

In the Assorutit Syenite there is little approach to equilibrium in the ferromagnesian minerals, with continuous reaction in the earlier phases of amphibole development followed by an abrupt change to riebeckite-arfvedsonite. This change is probably due to changes in partial pressure of oxygen i.e. a slowly evolving increase in the $pp O_2$ and when the pressure has exceeded a certain value other ferromagnesian minerals crystallize and finally when the value is much higher riebeckite-arfvedsonite becomes stable and uses the previous amphibole as a nucleus.

6-3-2. Eckermannite from a nepheline syenite, Norra Kärr, Sweden.

This type of alkali amphibole has been analysed by Bygden (Sundius, 1945), Howie (personal communication) and by the author using a combination of wet chemical and X.R.F. methods. Dr. Howie separated two

PLATE 3

Zoned eckermannite, Norra Kärr, Sweden. Eckermannite medium grey, alkali feldspar clear and ore minerals black. (x 100)

PLATE 4

Discontinuously zoned magnesioarfvedsonite (G.G.U. 27281) Grønnedal-Íka, S.W. Greenland. The iron rich magnesioarfvedsonite forms around the rims of the magnesian rich magnesioarfvedsonite and along the cleavage traces, aegirine forms rhombic shaped crystals with very high relief. Phlogopite is an additional phase. (x 50)

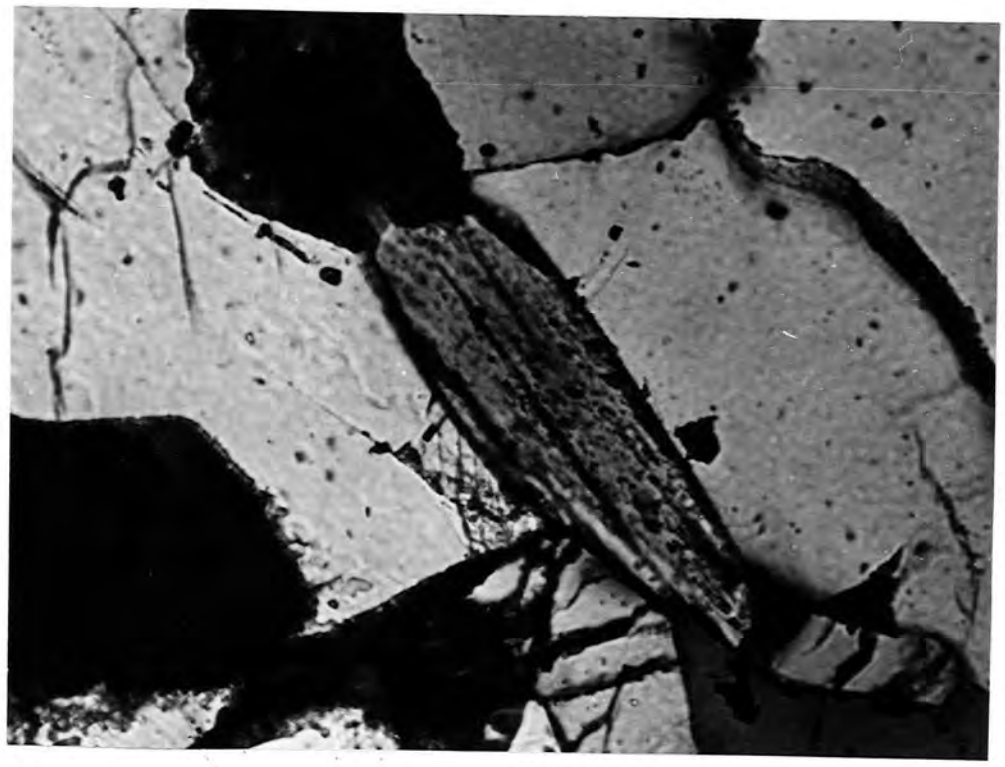

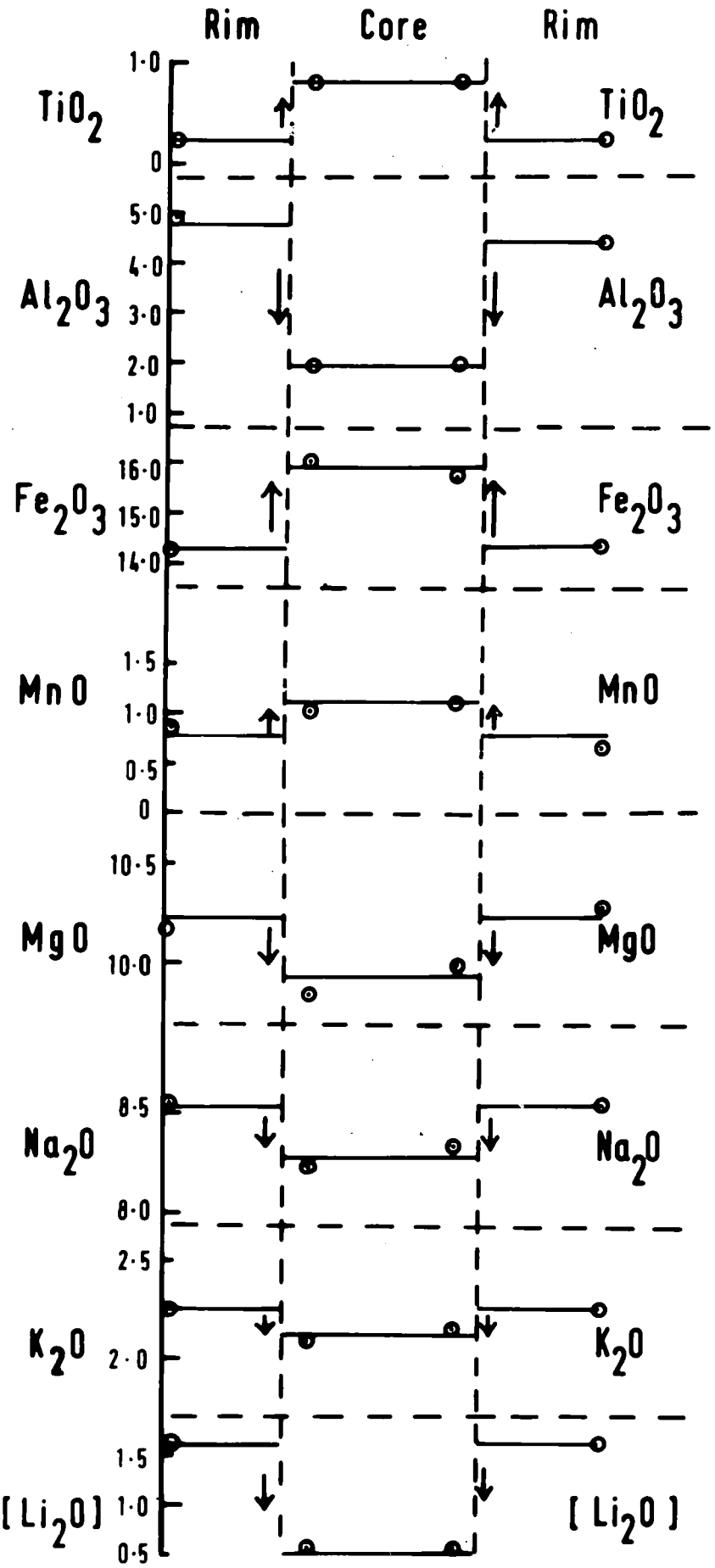

Fig.6-3 Schematic representation of discontinuous zoning in Eckermannite, Norra Kärr, Sweden.

phases from the bulk amphibole into two analyses and he considers that one phase is exsolved from the other. The author's electron probe and chemical analyses together with Howie's for comparison are in Table 6-1 (Tables of electron probe analyses at the end of chapter). The optics of this mineral are extremely variable and the extinction angle $\alpha:\mathfrak{z}$ varies from 35° in the core to 25° on the rim (Plate 3).

The chemical variations in the eckermannite are shown schematically in figure 6-3. Traverses across the individual crystal show no gradation but a sharp change in composition from core to rim. Titanium, total iron, and manganese are higher in the core and potassium, sodium, magnesium, and aluminium at the rim. Lithium has been added to the diagram using values obtained chemically by Howie; the wet chemical value for the author's sample is 0.84%.

The electron probe analyses show that type eckermannite is zoned and probably represents two waves of metasomatism. It is interesting to note that all the analyses including electron probe results of type eckermannite plot outside the compositional space of Phillips.

The two waves of metasomatism probably involved:- (1) K, Na, and Fe metasomatism and (2) K, Na, Mg, Li metasomatism with a concomitant increase in Fe^{+++}/Fe^{++} ratio.

Likely substitutions involved in the changing chemistry of the eckermannite are:-

core		rim
Fe^{++} Mn	$\rightleftharpoons$	Al Fe^{+++}
Fe^{++} (Mg, Mn)	$\rightleftharpoons$	Li (Al Fe^{+++})
Ti^{4+} + □	$\rightleftharpoons$	2(Mg, Fe^{++})

Substitutions involving calcium are not applicable because both the E.P.M. and chemical analyses reveal little calcium in either core

or rim. The larger amount of manganese in the core probably reflects a higher concentration of ferrous iron there.

6-3-3. Zoned magnesioarfvedsonite (GGU27281) from fenitised amphibolite, Grønnedal-Íka complex, S.W. Greenland.

The Grønnedal-Íka complex (Emeleus, 1964) consists of foyaitic nepheline syenites and carbonatite intruded into a basement consisting of gneisses, metasediments, and metaigneous rocks. Large slices of the basement within the complex have been metasomatised by both the syenite and the carbonatite (Emeleus, personal communication) and the present account describes the metasomatism of an amphibolitized basic dyke within a basic slice.

The unmetasomatised basic dyke (G.G.U. 126720) consists of hornblende (65%), biotite (15%) and severely altered plagioclase feldspar. One characteristic feature of the fenitised dyke rocks is the total lack of feldspar.

The fenitisation appears to occur in two zones and the earlier phase involves the presence of zoned alkali amphibole, aegirine, phlogopite, and calcite (G.G.U. 27281).

The alkali pyroxene occurs as euhedral crystals which are rarely zoned. The alkali amphibole is discontinuously zoned from a colourless core to a blue rim and grows as anhedra. The core has an extinction angle of $\alpha : 3$ of 18° whereas the rim has $\alpha : 3$ of 29°. Occasionally the amphibole is seen developing at the expense of aegirine laths. Plate 4 shows the relationship between amphibole and pyroxene. The phlogopite is concentrated within certain areas of the rock and in many crystals there are patches where the mica exhibits a reversed pleochroic scheme:-

i.e. α = deep orange brown

β = pale yellow

γ = colourless - pale yellow

absorption $\alpha > \beta > \gamma$

whereas the normal phlogopite has the absorption scheme:-

$$\gamma = \beta > \alpha$$

Rims of this mineral have been noted by Walton (1955), Puustinen (1970) and Rimskaya-Korsakova and Sokolova (1964) have described manganophyllites, biotites and phlogopites with this reversed pleochroism. This is correlated with ferric iron replacing aluminium in tetrahedral sites. This phlogopite was called "tetraferriphlogopite" by Rimskaya-Korsakova and Sokolova (ibid), and it is characteristically developed in aluminium-poor environments i.e. pyroxenites, kimberlites and carbonatites associated with carbonate minerals.

In the present phlogopite the species tetraferriphlogopite is concentrated along cleavage traces and as rims to the parent phlogopite.

The later phase of fenitisation consists of larger amounts of alkali amphibole with the iron-rich amphibole dominant over small amounts of aegirine, phlogopite and calcite.

The pleochroic scheme of the blue amphibole is:-

α = blue green

β = lilac

γ = pale yellow

absorption $\alpha > \beta > \gamma$

extinction angle $\alpha \wedge c = 29^{\circ}$

X-ray cell parameters (whole grains)

$a_o = 9.843\text{Å}$

$b_o = 17.915\text{Å}$

$c_o = 5.289\text{Å}$ cleavage angle $(110 : 1\bar{1}0) = 56°8'$

$\beta = 103.88°$

$a\sin\beta = 9.556\text{Å}$

Vol. $= 905.41\text{Å}^3$

Chemistry of the phases

In Table 6-2 the chemistry of the amphibole (core and rim), pyroxene, and phlogopite are compared.

The calcium is concentrated in the core of the amphibole with very little entering the other phases. Sodium reaches a maximum value in the aegirine (12.09%), where it is the sole M2 site occupant, it is also present in the alkali amphibole both core and rim at an identical concentration (8.17%). Potassium prefers the mica structure (8.54%) and builds up from 0.47% in the core of the amphibole to 1.39% in the rim. Iron is in the trivalent state in aegirine because there is no calcium present to balance the charge if ferrous iron were present. The concentration of iron is low in the core of the amphibole (7.07%) and much higher in the rim (15.30%).

TABLE 6-2 Comparison of chemistry in ferromagnesian minerals in fenitised dyke.

	$Ca/_{Ca+Na} \times 100$	$Mg/_{Mg+Fe} \times 100$	$Ca/_{Ca+Na+K} \times 100$
Amphibole core	25.6	77.9	24.5
Amphibole rim	4.1	53.4	3.2
Aegirine	0.9	0	0
Phlogopite	⁂ (13.6)	65.1	0.3

⁂ very small amounts of Ca and Na

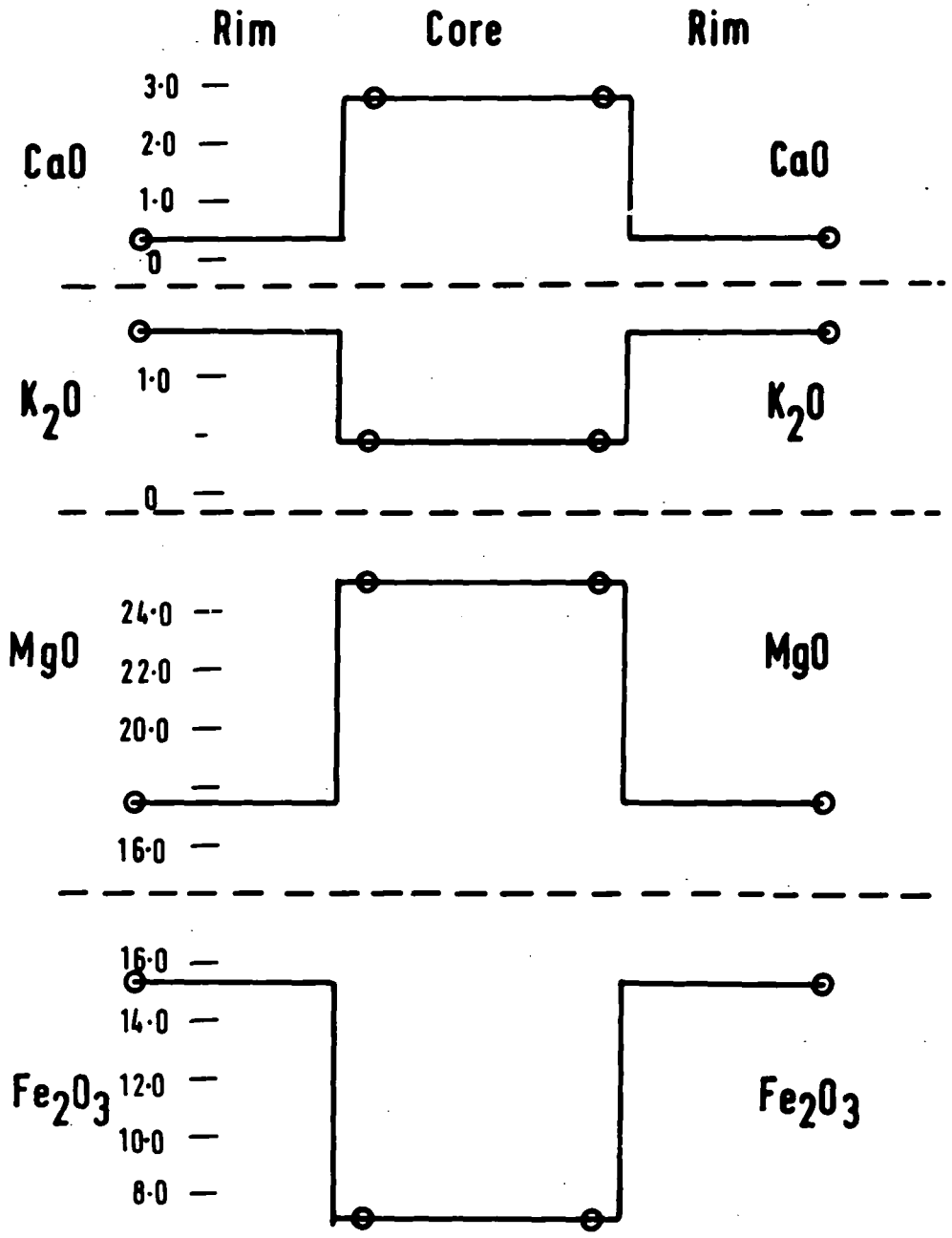

Fig.6-4 Schematic representation of discontinuous zoning in metasomatic Magnesioarfvedsonite, Grønnedal Íka.

As the valence state of iron increases from two to three from core to rim so the potassium increases and a probable substitution involved is:-

$$K^{A}\,Fe^{+++Y} \rightleftharpoons Ca^{X}\,Mg\,(Fe^{++})^{Y}$$

Evidence for this substitution is shown schematically in figure 6-4. The zoning in the alkali amphibole is discontinuous, there being no gradient from core to rim but the zones are not as abrupt as in the Assorutit Syenite (Fig. 6-2). The overall chemistry of the mineral together with other analyses are shown in Table 6-3.

Discussion

J.B. Thompson (1959) states that during metasomatism there is a tendency to reduce the number of phases present in a rock. In the present study three phases are reduced to one (amphibole) with minor calcite present. If this situation is truly metasomatic there is the possibility that one or other or both of Korzhinski's (1948) classes of metasomatism: (1) Diffusion metasomatism (2) infiltration metasomatism are operating. In Diffusion metasomatism the boundaries between zones are not abrupt as they are in infiltration metasomatism and solid solution in minerals takes place uniformly; therefore infiltration appears to be dominant in the present study.

The Grønnedal-Íka example of fenitisation appears to involve the addition of sodium, potassium, ferric iron and fluorine to the system.

The first zone of fenitisation involves the formation of pyroxene, colourless amphibole, and phlogopite by the addition of alkali metals and oxidation of the ferrous to ferric iron. The next zone develops deeply coloured amphibole and tetraferriphlogopite by the continuation

of the supply of the fenitising solutions. The stable development of the amphibole may be due to the high volatile content, particularly fluorine, and the presence of magnesium in the original rock. This situation is summarised in Table 6-4 and the likely mineralogical changes in Table 6-5.

TABLE 6-4

Original Magma	Zone 1A	Zone 1B	Zone 2
Syenite Carbonatite mobile elements Na^+, K^+, OH^-, F^-, $CO_2^=$	aegirine, Mg - magnesio-arfvedsonite, phlogopite.	tetraferriphlogopite, Fe - magnesio-arfvedsonite.	Fe - magnesio-arfvedsonite.

TABLE 6-5

Likely mineralogical changes in the fenitic zones.

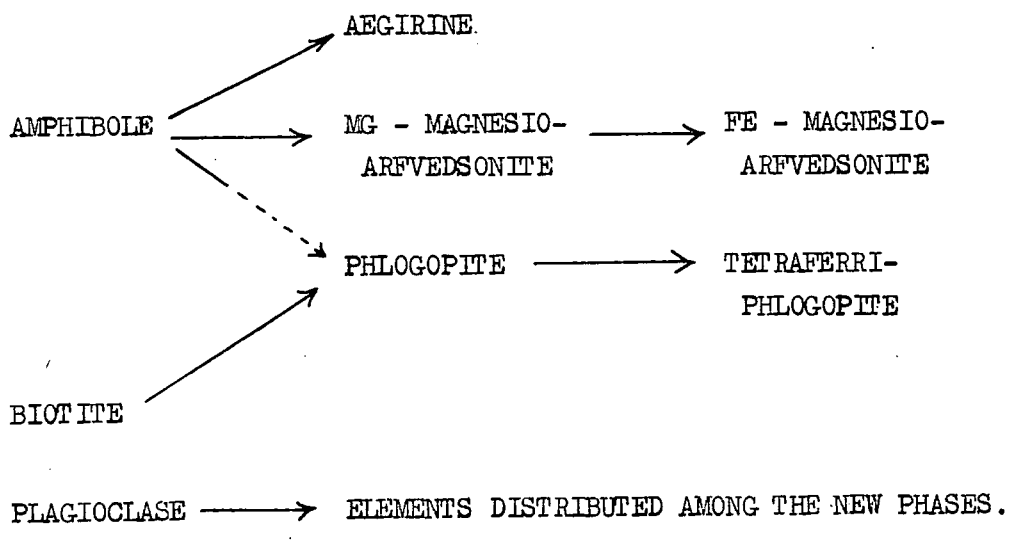

PLATE 5

Co-existing glaucophane and hornblende from modified eclogite lens, Phouria, N. Syros (X1172). Glaucophane forms rims to the hornblende cores. Light areas are chlorite. (x 35)

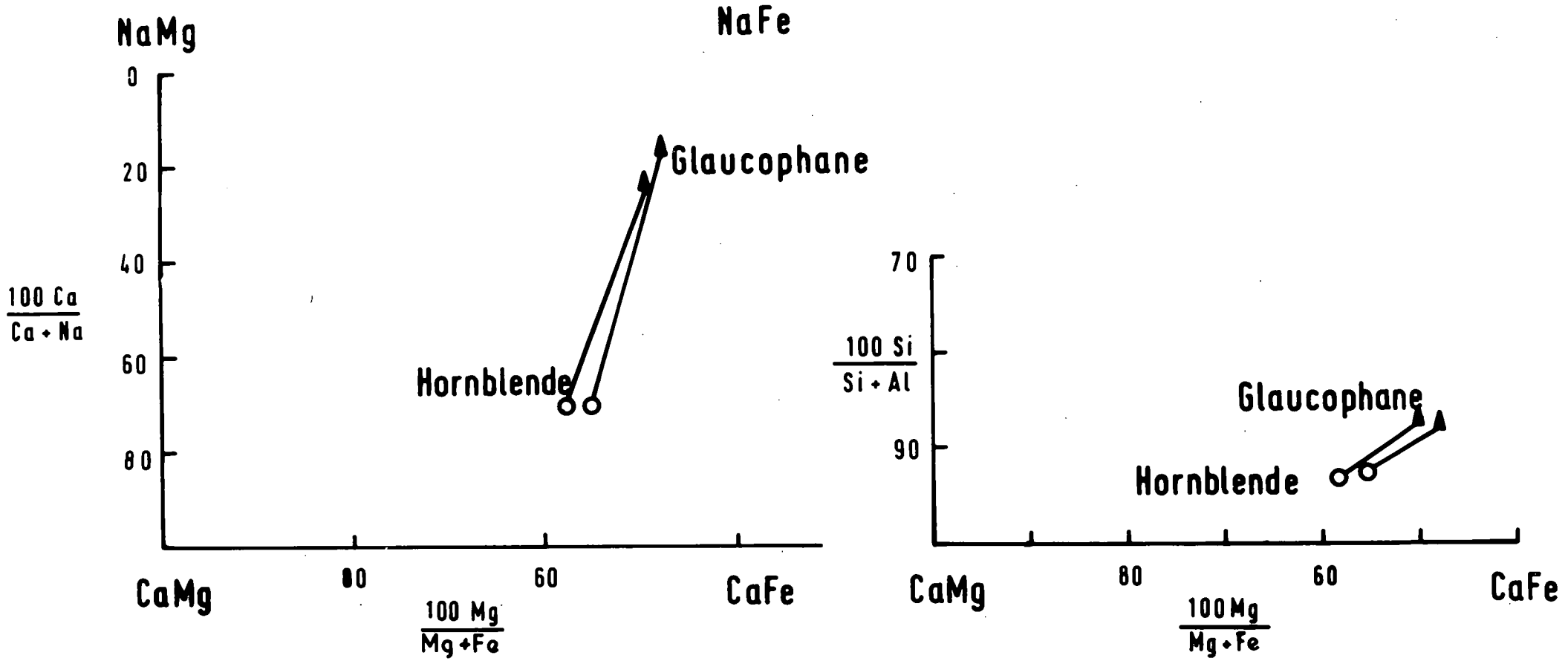

Fig.6-5 Compositions of co-existing amphiboles from modified eclogite lens, Phouria, Syros.

later growth on an already formed amphibole nucleus.

Physical properties of the amphiboles

1. Glaucophane

Pleochroism

α colourless

β violet

γ blue

Extinction $\gamma \wedge c = 7^{\circ}$

cleavage angle $(110 \wedge 1\bar{1}0) = 55^{\circ}14'$

absorption $\beta = \gamma > \alpha$

cell parameters

$a_o = 9.588\text{Å}$

$b_o = 17.801\text{Å}$

$c_o = 5.299\text{Å}$

$\beta = 103.66^{\circ}$

$a \sin\beta = 9.317\text{Å}$

Vol. $= 878.83\text{A}^{03}$

composition from Borg's (1967) curves
Glaucophane 68
Riebeckite 32

2. Calciferous amphibole

Pleochroism

α green

β olive green

γ colourless

absorption $\beta > \gamma > \alpha$

Extinction $\gamma \wedge c = 18^{\circ}$

Chemistry of the amphiboles

The calciferous amphibole has been called hornblende because of the larger content of sodium (3.30%) and aluminium (4.90%) than actinolite (Table 6-6).

In figure 6-5 a tieline distribution is shown for the two amphiboles. The $Mg/Mg+Fe$ is higher in the hornblende than the glaucophane and the

$\frac{Ca}{Ca+Na}$ gap is from .25 to .70 (hornblende), a closer parallel to Klein's (1968) data for co-existing hornblende and glaucophane than for glaucophane - actinolite (.10 - .85). The $\frac{Si}{Si+Al}$ ratio is lower for hornblende than glaucophane (Fig. 6-5b) but much of the aluminium in glaucophane is in six-fold co-ordination.

Discussion

Klein (1968) and Himmelberg and Papike (1969) have determined the chemistry of discrete co-existing amphiboles from Glaucophane schist facies rocks and conclude that the amphiboles which form are co-existing pairs and are in equilibrium and that the compositions represent points across a miscibility gap. They found textures such as in the present study much more difficult to interpret.

Lee et. al. (1966) suggest that gross chemical adjustment in calcium and sodium are needed if one amphibole replaces the other. In the present study petrographic evidence shows that rutile, typical of eclogites, is breaking down to sphene, more typical of glaucophane schists and therefore the original rock may have been an eclogite.

The glaucophane always rims the hornblende and therefore appears to be formed later (Plate 5). There are sharp optical and chemical discontinuities between the amphiboles but they never occur as discrete grains.

If the rock was originally an eclogite the glaucophane is replacing the hornblende and the calcium liberated is going to make up sphene which is developing from rutile. The garnet has been replaced by chlorite and the pyroxene by hornblende and glaucophane.

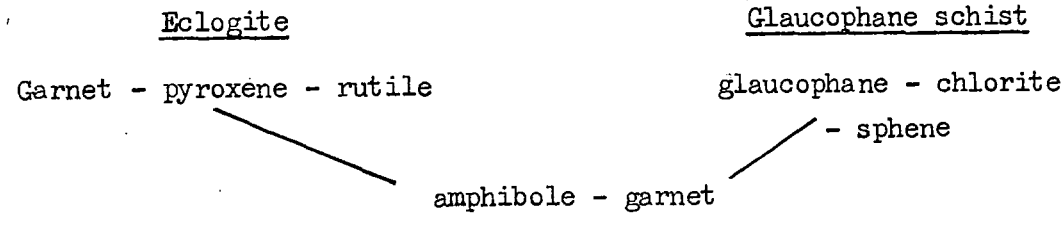

Some of the eclogites described by Coleman et. al. (1965) show features between the above mineralogy and eclogites.

6-4-2. Co-existing riebeckite - arfvedsonite and astrophyllite from Ekerite, Oslo Fjord, Norway.

Riebeckite-arfvedsonite and astrophyllite $(K,Na)_3(Fe,Mn)_7Ti_2Si_8(O,OH)_{31}$ occur together, often intergrown, in many late stage peralkaline environments. The two minerals are both intergrown and occur in discrete grains in the rock under study.

From Table 6-7 the chemistry of the two phases can be compared. The sodium, magnesium and aluminium are preferentially incorporated into the riebeckite structure whereas potassium, manganese, iron, and titanium are concentrated in the astrophyllite structure. The titanium is very low in the riebeckite-arfvedsonite (0.76%) and very high (10.81%) in astrophyllite. This is probably due to the special position of titanium (TiO_6 octahedra linking SiO_4 chains) in astrophyllite (Woodrow, 1967).

6-5. Amphiboles from peralkaline dykes, Tugtutôq, S.W. Greenland.

A suite of amphiboles from a differentiated set of peralkaline dykes has been analysed by the electron probe to reveal a new fractionation sequence in the calc/alkali and alkali amphiboles. These rocks from the island of Tugtutôq, S.W. Greenland, have been described by Upton (1962) and Macdonald (1966 and 1969).

Macdonald (1966) describes the sequence of rocks which vary from trachydolerite composition (slightly anorthite normative) through a set of syenites to microgranites (acmite normative). Nepheline also appears in the norms of the trachydolerites. The dyke swarm therefore possesses a peralkaline trend.

The trachydolerites contain fayalite and augite in the mode

whereas amphiboles are the sole ferromagnesian minerals in the microsyenites and earlier formed microgranites, aegirine is present in the latest differentiates.

Macdonald (1969) discussed the petrochemistry of these dykes in which the major fractionating phase is alkali feldspar. With increasing fractionation there is a decrease in MgO, CaO, TiO_2, P_2O_5; an overall decrease in FeO + Fe_2O_3 + MnO; Al_2O_3 falls steadily from a point where potassium feldspar first precipitates; SiO_2 increases from 49 - 76%. The Na_2O + K_2O increases from the dolerites to the microsyenites but decreases in the microgranites. Macdonald advances several causes for this.

The description of the separate rocks are assembled in order of crystallization:-

T.78. Microsyenite.

This microsyenite contains phenocrysts of alkali feldspars and in the groundmass alkali feldspar, amphibole and ore. The amphibole is often zoned and the two zones have the following pleochroic schemes:-

	γ	-	β
(1)	light blue green	-	light blue
(2)	olive green	-	mauvish brown

The optics of the zoned crystals can be correlated with the chemistry. The light blue-green zones are calcic ferrorichterites and the darker varieties between alkali ferrorichterite and arfvedsonite in composition.

The zoning in these early phase amphiboles is discontinuous, the blue-green variety containing up to 8.10% CaO and 5.80% MgO compared to the brown amphiboles 7.03% and 1.74% respectively. The calcium rich amphiboles have smaller amounts of alkali metals (1.96% Na_2O, 0.62% K_2O) than the ferrorichterite-arfvedsonites (3.28% Na_2O, 1.22% K_2O). The

overall amount of ferric iron must be low because of the low alkali values. The chemistry of three crystal pairs are shown in Table 6-8 and also in figure 6-6.

T.256. Microsyenite.

Alkali feldspar and ore are phenocryst phases in this microsyenite and in the groundmass small amounts of quartz are additionally present. The amphiboles in the rock possess darker hues than T.78 and have the following pleochroic scheme:-

α = yellow brown

β = brown $\qquad \gamma' \wedge c = 15°$

γ = olive green

Compared to the earlier amphiboles the amount of aluminium has increased (2.09% max.) and so too has the ratio of alkalis to calcium (Table 6-8). The crystals are very occasionally zoned to a pale green variety rich in calcium and iron and much lower alkalis.

The analyses indicate that the amphiboles lie between ferrorichterite and arfvedsonite.

T.306 and T.142. Quartz microsyenites.

Alkali feldspar phenocrysts and modal quartz are present in these dyke rocks. The amphiboles present are occasionally replaced by a brown micaceous mineral or contain blebs of ore. The pleochroic scheme of the amphibole is:-

α = yellow brown

β = brown

γ = olive green

The chemistry of the amphiboles in these two dyke rocks is similar, the major differences being in calcium and potassium. T.306 has smaller

amounts of these two elements (CaO = 4.40% and 0.78% K_2O) than T.142 (6.67% CaO, 1.31% K_2O). Fluorine and water have been determined on bulk amphibole for T.142 and are F 0.59% and H_2O^+ 1.06%. The minerals are early members of the arfvedsonite group.

T.202. Microgranite.

Both Quartz and alkali feldspar occur as phenocrysts and among the ferromagnesian minerals amphibole is dominant. Aegirine is present in the groundmass but there is a complete lack of ore.

The amphiboles are typical members of the riebeckite-arfvedsonites, variable amounts of calcium and sodium are present (Table 6-8) but they appear to be mutually exchangeable. Magnesium is low with a maximum value of 0.38%.

T.136. Microgranite.

This microgranite contains phenocrysts of quartz, alkali, feldspar, and riebeckite-arfvedsonite. The same minerals are present in the groundmass together with aegirine.

Chemical analysis of the phenocrysts of amphibole show them to be more highly evolved alkali amphiboles than the previous members. The chemistry of each phenocryst is fairly uniform but changes in composition occur from crystal to crystal. Three phenocrysts have been presented (Table 6-8) for comparison and elements which vary are sodium, calcium, and aluminium.

This mineral has been analysed by wet chemical methods for ferrous iron (21.75%), water (0.30%) and fluorine (2.75%).

Discussion

Both Macdonald (op. cit) and Upton (1962) have mistakenly called the amphiboles in the microsyenites "hastingsites" because of the

similarity in optics of the ferrorichterites to hastingsites. There is too little tetrahedral aluminium or calcium for these amphiboles to plot anywhere near hastingsites. Therefore the amphiboles in the early members of the microsyenites lie along the tie line ferrotremolite ($Ca_2Fe_5Si_8O_{22}(OH)_2$) —— ferrorichterite ($NaCaNaFe_5Si_8O_{22}(OH)_2$).

Recently Nicholls and Carmichael (1969) have described an analysed ferrorichterite from a Kenyan pantellerite with similar chemistry to the Tugtutôq dyke amphiboles.

There are several prominent substitutions in these amphiboles from peralkaline dykes:-

(1) $Ca\ Fe^{++} \rightleftharpoons Na\ Fe^{+++}$

(2) $Ca\ Al^{IV} \rightleftharpoons Na\ Si$

With little tetrahedral aluminium present in the early stages of differentiation (T.78, 256, 306, 142), the second coupled substitution appears to be minor.

A third substitution may be present in the earlier formed amphiboles and appears feasible from the chemical analyses:-

(3) $Ca \rightleftharpoons Na\ Na$

There is no direct experimental evidence to suggest whether ferrorichterite could co-exist with liquid. Indirect evidence may be supplied from a comparison of the data available for tremolite, ferrotremolite and richterite. Ferrotremolite (Ernst, 1966) is stable to 543°C at 3000 bars pressure using the Quartz - fayalite - magnetite buffer (QFM). Above this temperature it breaks down to fayalite, quartz, hedenbergite, and fluid. At higher oxygen fugacities the assemblage magnetite, hedenbergite and quartz is stable. Ferrorichterite would be thermally more stable than ferrotremolite; the magnesium equivalent richterite-K breaks down at 1075°C at 1000 bars

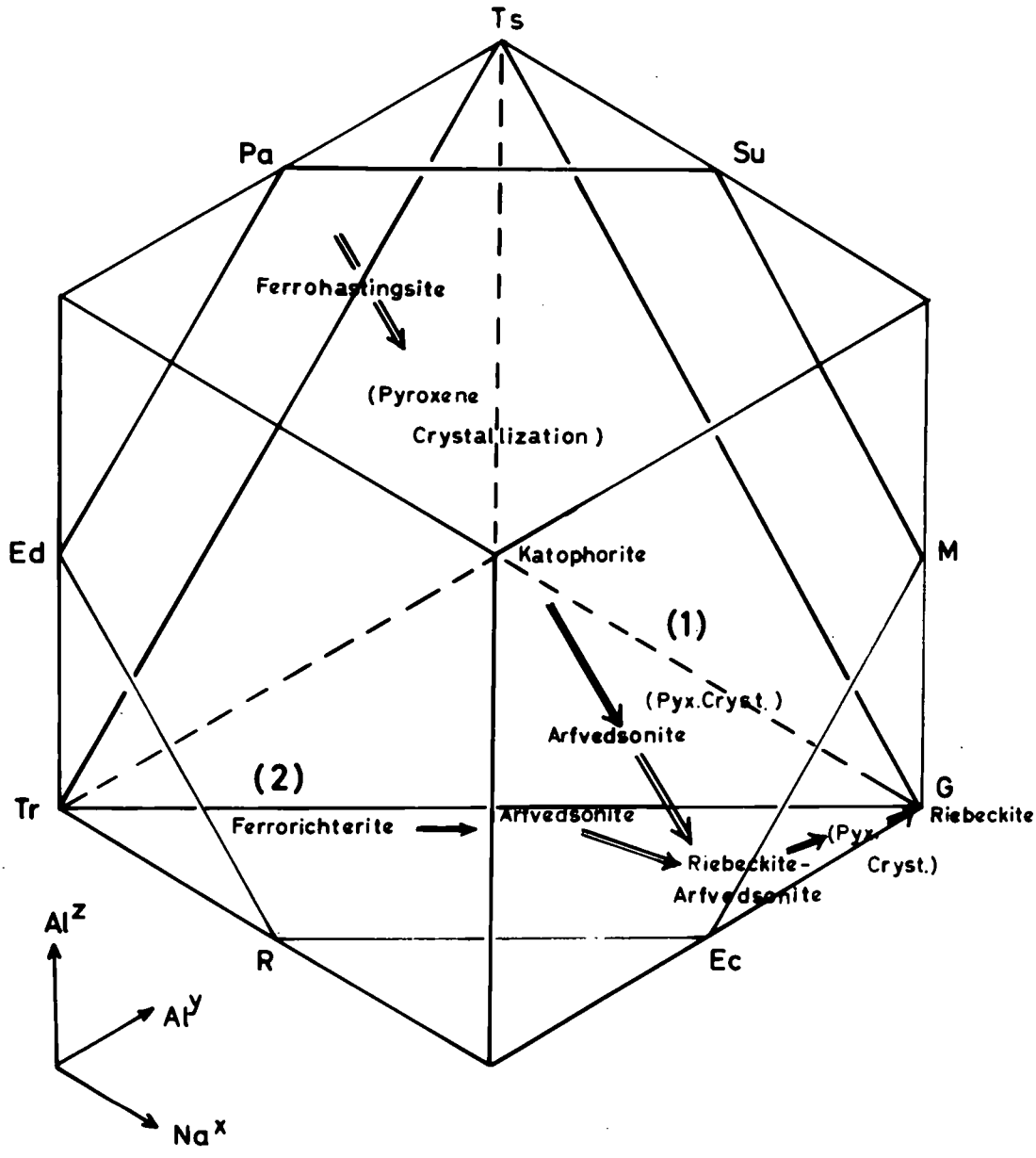

Fig.6-6 Trends in Amphibole crystallization in (1) Ilimaussaq and (2) Tugtutoq, S.W. Greenland.

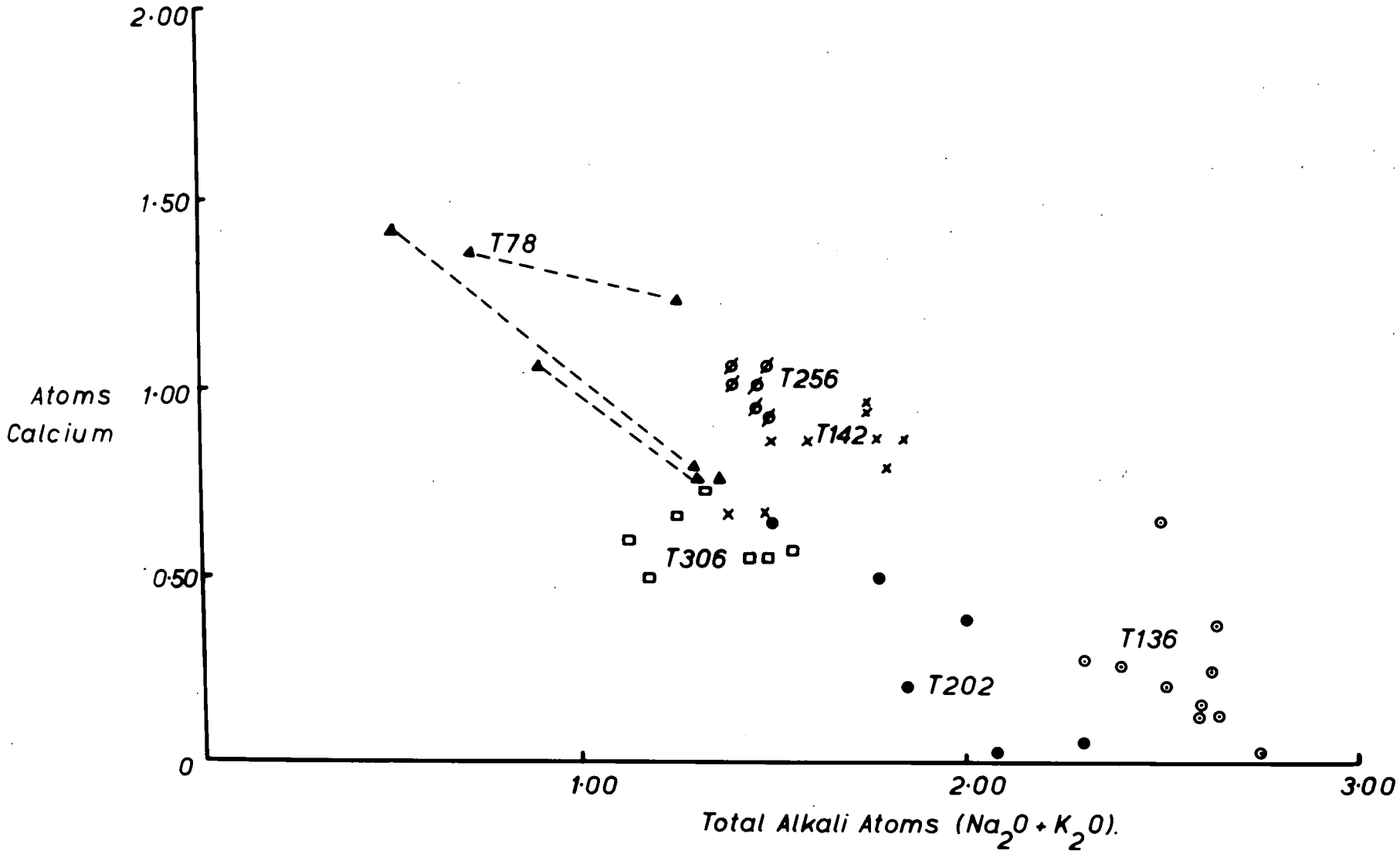

Fig6-7 *Alkali Amphibole compositions from Tugtutoq, S.W. Greenland.*

pressure (present study) compared to 835°C for tremolite (Boyd, 1959). Therefore ferrorichterite would be expected to be stable at magmatic temperatures > 750° C at 3000 bars probably defined by a maximum oxygen fugacity equivalent to the QFM buffer.

The trachydolerites appear to have a petrochemistry similar to the parent augite syenite of Ilímaussaq (Chapter 5). From this common parental magma two trends have been followed:- (1) an undersaturated trend (Ilímaussaq) and (2) a saturated trend (Tugtutôq).

The amphiboles from these two fractionation trends exhibit two patterns (Fig. 6-6):- (1) Ilímaussaq: kaersutite → katophorite → arfvedsonite → riebeckite - arfvedsonite. (2) Tugtutôq: ferrorichterite → arfvedsonite → riebeckite — arfvedsonite.

In figure 6-7 all the amphibole analyses from the Tugtutôq dykes are plotted showing the trend from ferrorichterite to riebeckite-arfvedsonite.

The concentration of water and fluorine appears to be complementary i.e. high water, low fluorine in the early members and high fluorine low water in the microgranite amphiboles. This concentration is opposite to the Ilímaussaq amphiboles where fluorine is fixed early in the differentiation.

6-6. Study of amphiboles occurring in late stage differentiated rocks.

6-6-1. Riebeckite-astrophyllite granite, White Mountain Magma Series, New Hampshire (D.U. 13170).

The amphibole in the granite is discontinuously zoned and the chemistry of the two zones is compared in Table 6-9. The core amphibole is more arfvedsonitic than the rim which is a riebeckite-arfvedsonite. The core has larger amounts of aluminium (1.20% max.),

titanium (0.64%), calcium (2.47%) and presumably ferrous iron than the rim (0.61%, 0.33%, 0.68% respectively). The rim contains more sodium, potassium, silicon and probably ferric iron; magnesium and manganese do not vary.

6-6-2. Riebeckite microgranite (G.G.U. 86163) and Grørudite (Grey) dyke (G.G.U. 86157), Kûngnât, S.W. Greenland.

These rocks are the last phases of intrusion in the Kûngnât syenites and the microgranites occur as sheets cut by the grey dykes (Upton, 1960). Alkali amphibole is the only ferromagnesian mineral in the earlier soda granites and microgranites and in the Grørudite dykes aegirine appears in the mode.

G.G.U. 86163

The riebeckite microgranite consists of quartz, microcline, and albite. Quartz is late and is replacing the alkali feldspars and the amphibole, which occurs as anhedral grains, is the only ferromagnesian mineral and has the following optics:-

α dark blue-black

β yellow-brown $\qquad C:\alpha = 5^{\circ}$

γ grey/blue

G.G.U. 86157

The grørudite dyke contains quartz, microcline and albite, with aegirine and amphibole as the dark minerals. The amphibole is anhedral whereas the aegirine occurs as subhedral needles. The optics of the pyroxene are:-

α green

γ pale yellow green $\qquad C:\alpha = 5^{\circ}$

and the amphibole has the same optics as in the microgranite.

Chemistry

The alkali amphiboles in these rocks have the optics of riebeckite but from their chemical analyses (Table 6-9) it is apparent that the values for the alkali metals are too high ~ 3.00 atoms to be riebeckites and in fact are riebeckite-arfvedsonites. The grorudite dykes are known to be later than the microgranites and this is borne out by the chemistry. Higher contents of calcium and aluminium are thought to be good indicators of temperature (Miyashiro, 1957) in amphiboles and they are lower in the dyke amphiboles (0.06 - 0.50% CaO, 0.12 - 0.46% Al_2O_3) than in the sheets (0.18 - 0.76% CaO, 0.67 - 0.88% Al_2O_3). Also the total alkalis ($Na_2O + K_2O$) are higher in 86157 at 9.50% than 86163 at 8.11%.

Discussion

In the New Hampshire riebeckite-arfvedsonite granite reaction is still proceeding in the amphiboles towards a calcium and aluminium free amphibole i.e.

$$Ca\ Al^{IV} \rightleftharpoons Na\ Si$$

Indeed this substitution appears to be the dominant one in addition to increasing ferric iron in late stage amphiboles. This sequence of events appears in all the examples quoted by the author throughout the text.

The appearance of aegirine in the mode indicates the highest degree of peralkalinity reached in the alkaline rocks and the amphibole "co-existing" with this phase is riebeckite-arfvedsonite with 2.5 atoms of Na_2O and up to 0.40 atoms of K_2O. Therefore the 'A' site in these amphiboles is either completely filled or nearly so, thus supporting the experimental evidence of Bailey (1969) and Ernst (1962) that pure riebeckite cannot co-exist with liquid but that it only occurs as a secondary or metamorphic mineral.

TABLE 6-1 Comparison of recent analyses of Eckermannite, Norra Kärr, Sweden

	1(Sundius)	2(Howie)	3a(Howie)	3b(Howie)	4(author)	E.P.M.(author) core	E.P.M.(author) rim
SiO_2	57.10	57.62	51.91	57.97	57.01	56.23	56.75
Al_2O_3	6.19	7.90	3.61	7.99	4.04	1.97	4.93
TiO_2	0.35	0.27	0.95	0.26	0.81	0.80	0.26
Fe_2O_3	8.01	6.36	9.88	7.05	12.49	15.99	14.24
FeO	2.69	2.65	6.15	2.00	2.63		
MnO	0.34	0.63	1.11	0.66	1.01	1.04	0.85
MgO	9.13	8.01	10.04	8.01	9.08	9.84	10.18
ZnO	0.59	0.45	0.02	0.50	n.d.	-	-
CaO	0.31	0.37	2.15	0.50	0.05	0.11	0.01
Na_2O	9.77	10.04	9.02	10.03	9.92	8.24	8.54
K_2O	2.38	2.56	2.80	2.62	2.67	2.09	2.24
Li_2O	1.15	1.64	0.54	1.64	0.84		
F	2.69	2.84	2.78	2.78	2.70	-	
H_2O^+	0.50	0.42	0.73	0.20	0.50	-	
H_2O^-	0.08	n.d.	n.d.	n.d.	n.d.		
	101.28	101.76	101.69	102.21	103.75		
	1.13	1.20	1.17	1.17	1.13		
	100.15	100.56	100.52	101.04	102.62		

Recalculation of analyses to the basis of 24(O)

Si	8.02	8.00	7.57	8.03	7.77	8.09	7.97
Al	1.03	1.29	0.43	1.31	0.23	0.33	0.81
Ti	0.04	0.03	0.10	0.03	0.08	0.09	0.03
Fe^{+++}	0.85	0.66	1.09	0.73	1.28		
Fe^{++}	0.32	0.31	0.75	0.23	0.30	1.72	1.50
Mn	0.04	0.07	0.14	0.08	0.12	0.13	0.10
Mg	1.91	1.66	2.18	1.65	1.84	2.12	2.14
Zn	0.06	0.05	0.00	0.05	-	-	-
Li	0.65	0.92	0.32	1.91	0.46	-	-
Ca	0.05	0.06	0.34	0.07	0.00	0.02	0.00
Na	2.66	2.71	2.55	2.69	2.62	2.29	2.32
K	0.43	0.45	0.52	0.46	0.47	0.38	0.49
F	1.19	1.25	1.28	1.22	1.16		
OH	0.47	0.39	0.71	0.18	0.45		
	4.90	4.99	4.77	4.99	4.50	4.39	4.55
	3.14	3.22	3.41	3.22	3.09	2.69	2.81
	1.66	1.64	1.99	1.40	1.61		

TABLE 6 - 3 CHEMISTRY OF THE FERROMAGNESIAN PHASES IN FENITISED AMPHIBOLITE, GRØNNEDAL IKA, S. W. GREENLAND.

	ELECTRON PROBE				X.R.F.+ CHEMICAL
	AEGIRINE	PHLOGOPITE	AMPHIBOLE		AMPHIBOLE
			CORE	RIM	
SiO_2	53·98	40·79	57·91	55·88	54·20
Al_2O_3	1·11	10·09	0·90	0·83	0·98
TiO_2	-	-	-	-	0·01
Fe_2O_3	36·08	13·00	6·75	14·47	11·39
FeO					4·24
MnO	0·03	0·17	0·26	0·14	0·26
MgO	Tr.	24·20	24·95	17·54	16·29
CaO	0·11	0·03	2·81	0·35	1·51
Na_2O	12·09	0·19	8·17	8·17	7·85
K_2O	Tr.	8·55	0·47	1·39	1·51
H_2O+					0·71
H_2O^-					0·10
F					2·35
TOTAL					101·40

TOTAL

TABLE 6-7 Partition of elements between riebeckite-arfvedsonite and astrophyllite in Ekerite, S. Norway.

	Rieb.	Ast.	Rieb.	Rieb.	Ast.
SiO_2	51.37	37.08	51.82	51.88	37.51
Al_2O_3	2.28	0.37	1.14	0.56	0.27
TiO_2	0.71	10.76	0.94	0.94	10.79
Fe_2O_3, FeO	27.71	35.02	28.09	29.21	34.53
MnO	2.05	4.77	1.95	1.67	4.75
MgO	5.09	1.06	4.09	4.73	0.90
CaO	1.15	0.99	0.97	0.77	1.07
Na_2O	6.83	1.99	6.87	6.93	1.99
K_2O	1.22	5.09	1.38	1.54	4.76

TABLE 6 - 8 ELECTRON MICROPROBE ANALYSES OF AMPHIBOLES FROM TUGTUTOQ PERALKALINE DYKES.

T78

SiO_2	51·01	48·78	51·83	50·84	50·20	50·10
Al_2O_3	0·58	1·34	0·73	0·62	0·60	0·79
Fe_2O_3	29·58	34·96	33·01	37·37	37·15	37·09
MnO	0·74	0·84	1·06	0·82	0·85	0·77
MgO	5·56	1·62	4·95	1·75	1·34	1·66
CaO	8·24	7·20	8·88	4·32	6·35	4·71
Na_2O	1·82	2·95	1·32	3·25	2·31	3·18
K_2O	0·63	1·24	0·47	1·06	0·46	1·10

T.256

	1	2	3	4	5	6	7
SiO_2	48·76	48·09	48·89	46·61	47·20	47·23	47·08
Al_2O_3	1·60	1·85	1·04	2·09	2·03	0·92	1·50
Fe_2O_3	38·17	37·33	38·79	35·51	36·81	38·40	39·80
MnO	0·70	0·73	1·02	0·61	0·64	0·90	0·78
Mgo	1·49	1·43	0·52	2·90	1·52	0·89	0·84
CaO	5·89	5·85	5·24	6·04	6·02	5·30	7·36
Na_2O	3·92	4·08	4·19	3·66	4·01	3·99	1·27
K_2O	1·02	0·97	0·93	1·12	1·12	0·85	0·35

T202

	1	2	3	4	5	6
SiO_2	49·99	50·36	50·94	51·67	50·58	49·14
Al_2O_3	0·77	0·56	0·51	0·90	0·52	1·10
Fe_2O_3	35·88	35·57	35·58	37·65	35·81	35·53
MnO	0·52	0·40	0·57	0·41	0·48	0·64
MgO	0·13	0·01	0·02	0·38	0·01	0·01
CaO	2·71	0·33	0·94	0·09	0·43	2·13
Na_2O	4·88	8·85	5·27	5·84	6·45	4·98
K_2O	1·05	1·15	0·75	1·62	1·33	1·10

TABLE 6-10 Electron microprobe analyses of manganoan magnesioarfvedsonites (Juddites) Central Provinces, India

	A	B	C	D	E	F	G	H
SiO_2	57.06	57.52	56.89	56.95	57.20	56.88	56.34	57.91
Al_2O_3	0.51	0.46	0.46	0.77	0.97	0.54	0.61	0.37
Fe_2O_3, FeO	8.29	11.67	5.82	5.88	9.53	8.55	10.24	12.82
MnO	4.26	2.71	5.04	1.76	3.43	4.41	0.63	2.02
MgO	16.56	17.37	19.23	19.55	16.65	16.19	17.23	16.98
CaO	1.53	1.18	0.63	2.22	1.26	0.89	0.73	1.64
Na_2O	8.46	7.25	8.03	7.88	6.85	8.23	6.48	7.32
K_2O	1.09	1.24	1.01	0.97	1.80	1.06	1.29	1.97
Li_2O	0.88							

Recalculation of analyses to the basis of 23(O)

Si	8.07	7.96 + 0.04 = 8.00	8.05	8.03	8.04	8.08	8.13	7.93 + 0.06 = 8.00
Al	0.08	0.03	0.08	0.12	0.16	0.09	0.10	
Fe^{+++}	0.87	1.21	0.62	0.62	1.01	0.91	1.11	1.32
Mn	0.47	0.32	0.60	0.21	0.41	0.53	0.07	0.23
Mg	3.48	3.58	4.05	4.10	3.48	3.43	3.70	3.46
	4.90	5.14	5.35	5.05	5.06	4.96	4.98	5.01
Ca	0.23	0.17	0.01	0.34	0.19	0.15	0.11	0.24
Na	2.30	1.94	2.19	2.15	1.86	2.26	1.81	1.94
K	0.20	0.22	0.11	0.17	0.32	0.19	0.24	0.35
	2.43	2.33	2.31	2.66	2.37	2.60	2.19	2.53

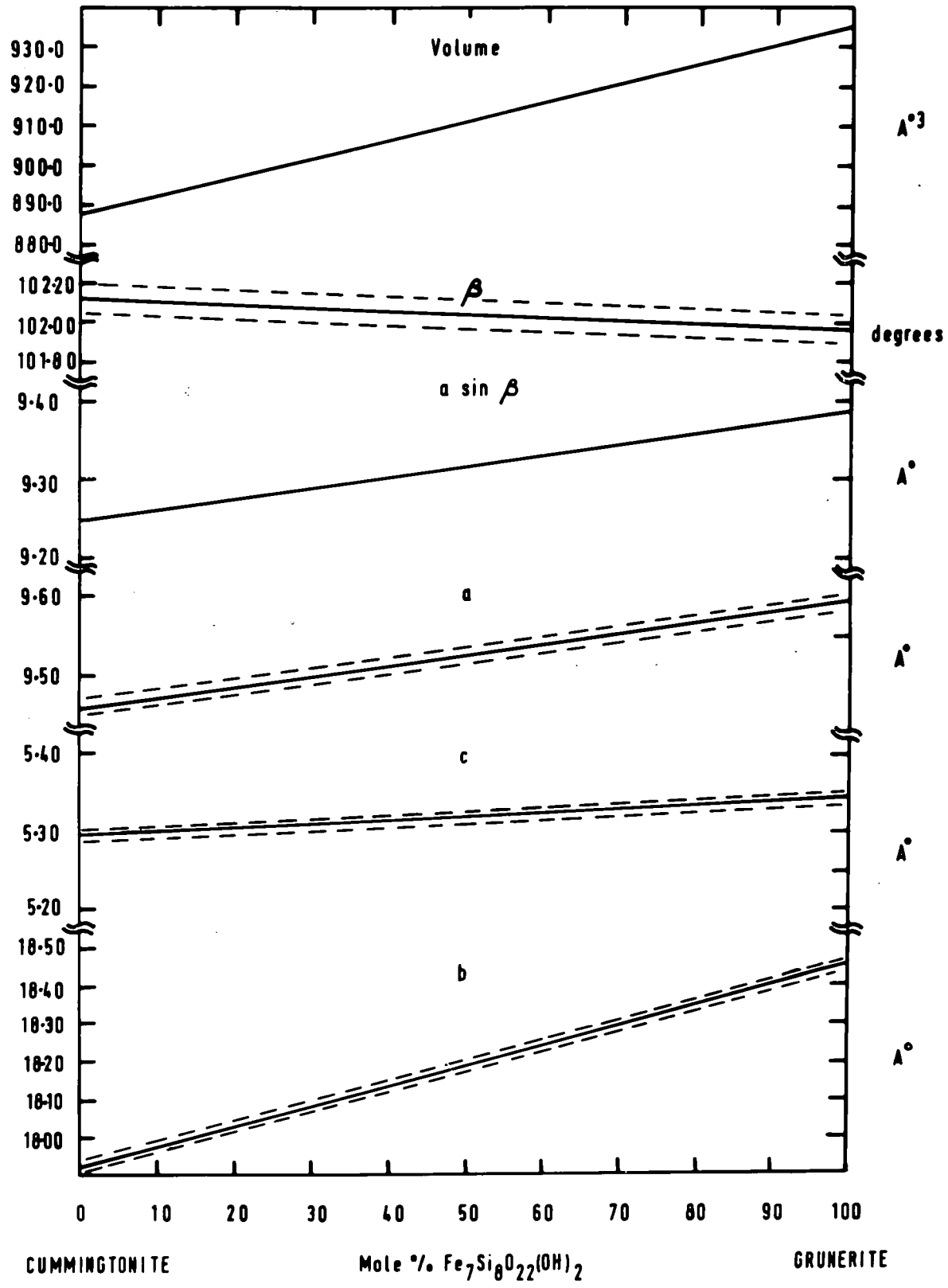

Fig. 7-1 Variations in cell dimensions of the Cummingtonite - Grunerite series. (Redrawn from Klein and Waldbaum, 1967.)

CHAPTER SEVEN

Cell Dimensions of the Alkali Amphiboles

7-1. General Statement.

The variation of the cell parameters of amphiboles depends upon the cations occupying the octahedral and tetrahedral sites. In general the larger the cations the greater will be the cell dimensions. The monoclinic (C2/m) amphiboles can be divided into three groups:-

i) Cummingtonite-grunerite series.

ii) Calciferous amphiboles.

iii) Alkali amphiboles.

These three series have distinct cell parameters and recently several workers have reported their findings: Frost (1963), Binns (1965), Viswanathan and Ghose (1965), Colville, Ernst and Gilbert (1966), Klein and Waldbaum (1967), Borg (1967), Coleman and Papike (1968), Ernst (1968), Colville and Gibbs in Ernst (ibid.) and Kempe (1969). A short summary of the conclusions to be obtained from a study of the cell dimensions is included at the end of the chapter.

7-2. Cummingtonite Series.

In the cummingtonite-grunerite series the M(4) and M(1), M(2), M(3) sites are occupied by ferrous iron and magnesium. Occasionally, manganese substitutes up to 4.00 atoms (Klein, 1966) for ferrous iron and magnesium. The variation of cell dimensions in this series is shown in figure 7-1 (after Klein and Waldbaum, 1967). The data extends from 37.5 molecular percentage $Fe_7Si_8O_{22}(OH)_2$ to 100%. The b_o parameter is shown to be the most sensitive to compositional variation. The β angle lies between 102.17° for a cummingtonite with 37.7% iron substitution

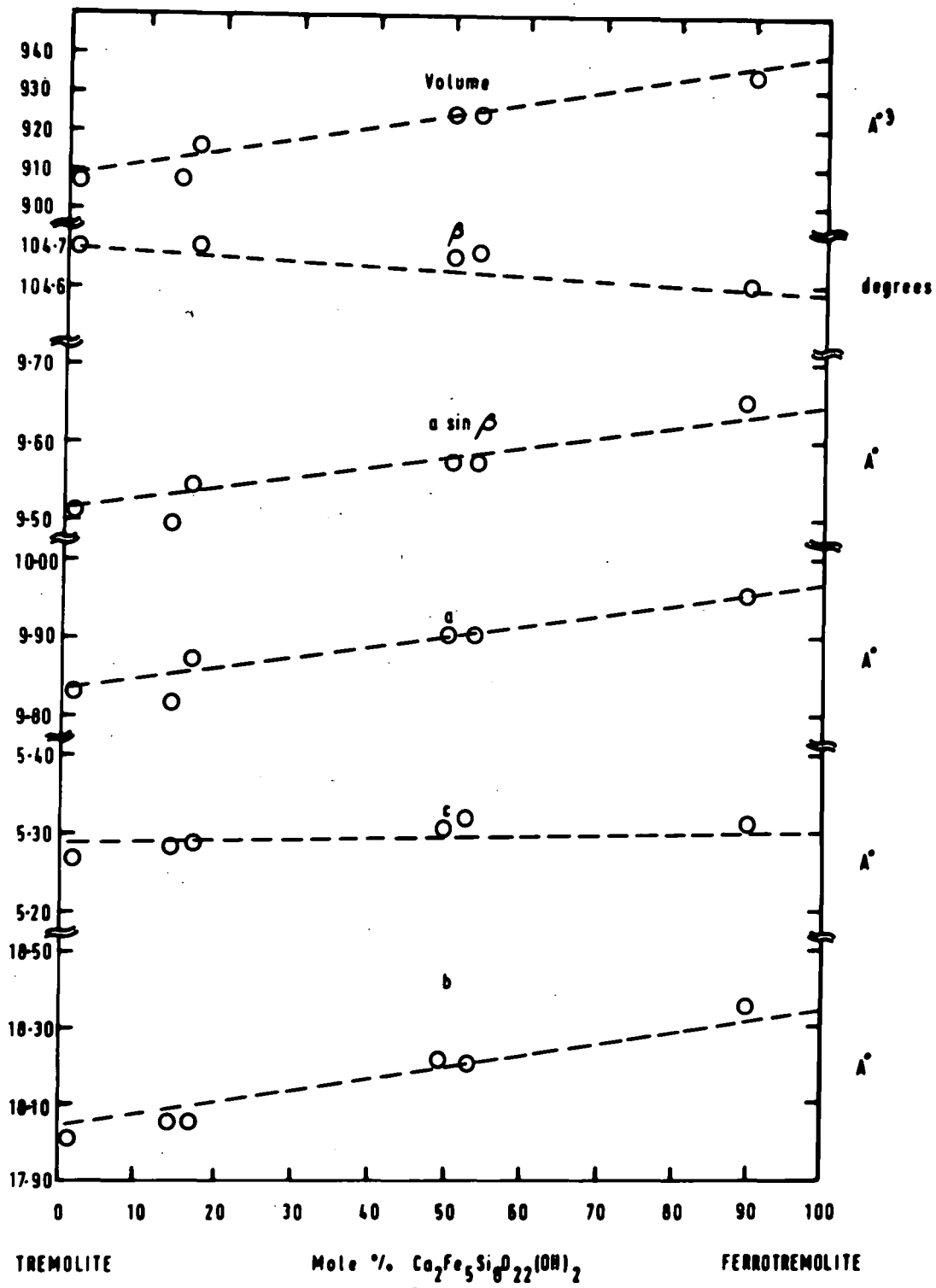

Fig.7-2 Variations in cell dimensions (tentative) of the Tremolite-Ferrotremolite series.

to 101.99 for a grunerite with 100% iron substitution. The c_o axis varies the least of the cell parameters.

7-3. Calciferous amphiboles.

(a) Tremolite-ferrotremolite.

The cell dimensions of six members of the tremolite-ferrotremolite series are plotted against composition in figure 7-2. This diagram is only tentative because certain of the errors on the parameters are not stated by all the authors. It will be noted that the b_o, c_o, a_o, $a_o \sin\beta$ and cell volume increase with the amount of ferrotremolite in the molecule. Again the b_o axis increases most and could possibly be used for a rough approximation of the Mg/Fe ratio in this series. The β angle tends to decrease from 104.7° to 104.6° as the iron increases.

(b) Common hornblendes and ferrohastingsites.

There are very few cell parameters for the large area of compositional space where most hornblendes (edenite, pargasite, and tschermakite) occur, no systematic work has been attempted for these compositions. Eighteen common hornblendes were analysed by Binns (1965) and their cell parameters determined. Frost (1963) published the cell dimensions of five analyzed ferrohastingsites.

It is difficult to demonstrate the variations of the cell dimensions within the hornblendes. In general the b_o axis repeat distance increases with an increase in ferrous iron content and the β angle increases with the calcium content.

Ferrohastingsites have much higher concentrations of ferrous iron and total iron than common hornblendes and have larger a_o, b_o, $a_o \sin\beta$ and β angle than hornblendes.

Barroistic hornblende (Binns, 1967) is a calciferous amphibole close to the compositional plane X=1 i.e. calciferous and alkali

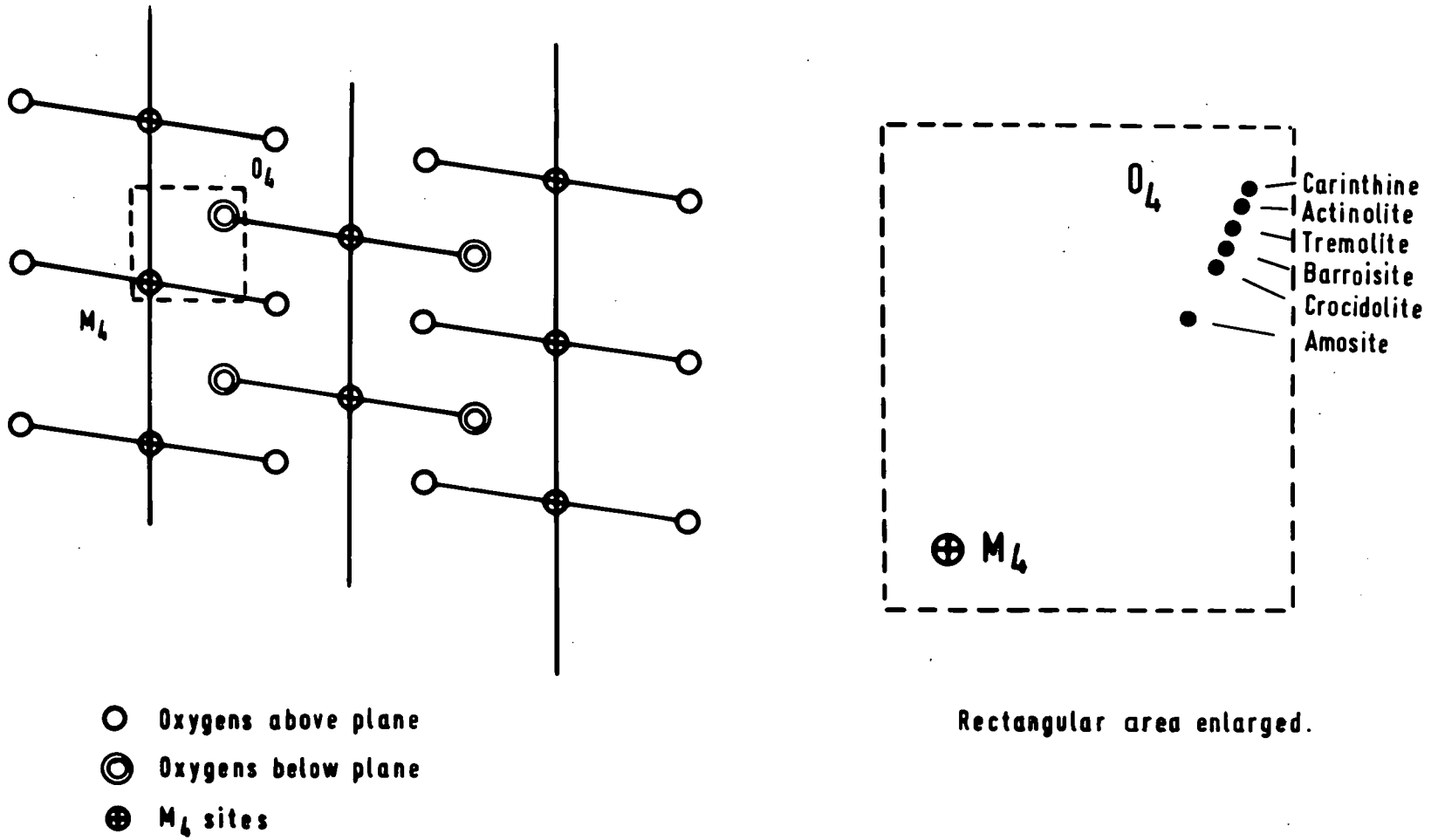

Fig.7-3 The relative positions of the O(4) and M(4) atoms in various amphiboles. (after Whittaker, 1960).

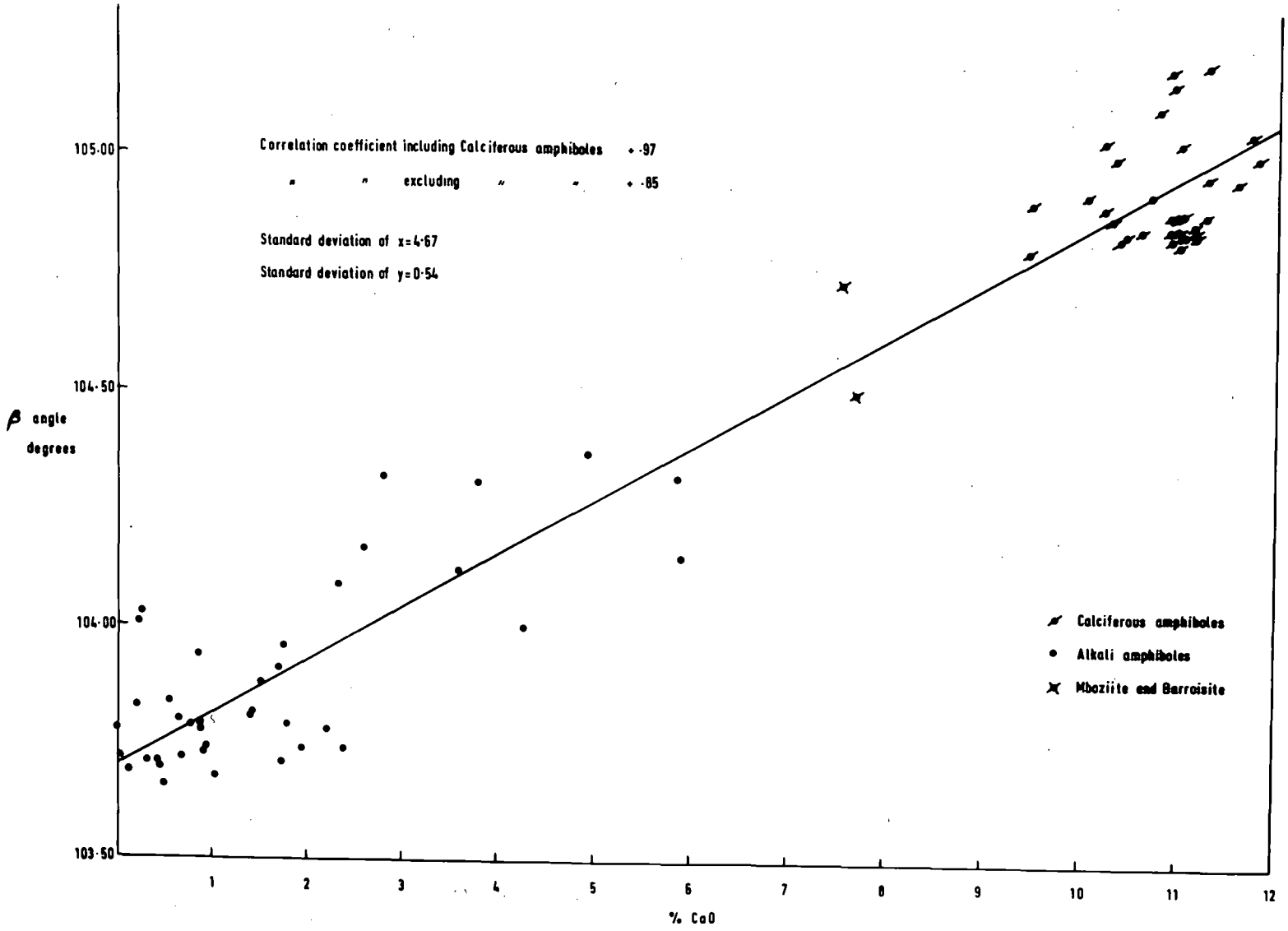

Fig.7-4 The variation of β angle with increasing calcium content in M(4) in the calciferous and alkali amphiboles.

amphibole dividing plane and has a β angle (104.50°) between hornblendes (104.85°) and alkali amphiboles (103.6°-104.28°).

7-4. β angle variation in the monoclinic amphiboles.

Whittaker (1960) discussed the relationship of the β angle in the monoclinic amphiboles to the radius of the cation occupying the M(4) site. He concluded that if β is controlled by inter-chain contacts they must be controlled by those that affect the relative translation of the chains parallel to the c_o axis and where the interlocking of the chains is considerable. The most favourable contact is the M(4) cation at the outside of the cation "strip" with O(4) of the chain. Figure 7-3 (after Whittaker) shows the relative positions of O(4) to M(4). The lines connecting atoms are not bonds but linking atoms of the same chain. As O(4) approaches M(4) (i.e. as the cation at M(4) becomes smaller) the β angle becomes smaller.

The β angle for the cummingtonite-grunerites is 101.99°-102.17° (Klein and Waldbaum, 1967), between 103.2° and 104.28° for the alkali amphiboles (present work) and between 104.50° and 106.0° for calciferous amphiboles (Colville and Gibbs, in Ernst, 1968).

To test Whittaker's conclusions all the β angles of analyzed calciferous and alkali amphiboles were plotted against calcium content (Fig. 7-4). The β angle shows a strong positive correlation (correlation coefficient 0.97) with calcium content. When the calciferous amphiboles are removed from the least squares calculation (Fig. 7-4) there is still a strong positive correlation (correlation coefficient = +0.85) between β angle and calcium content, but there are additional factors controlling β.

Borg (1968) and Klein and Waldbaum (1967) published cell parameters for the glaucophane-riebeckite series and cummingtonite-grunerite

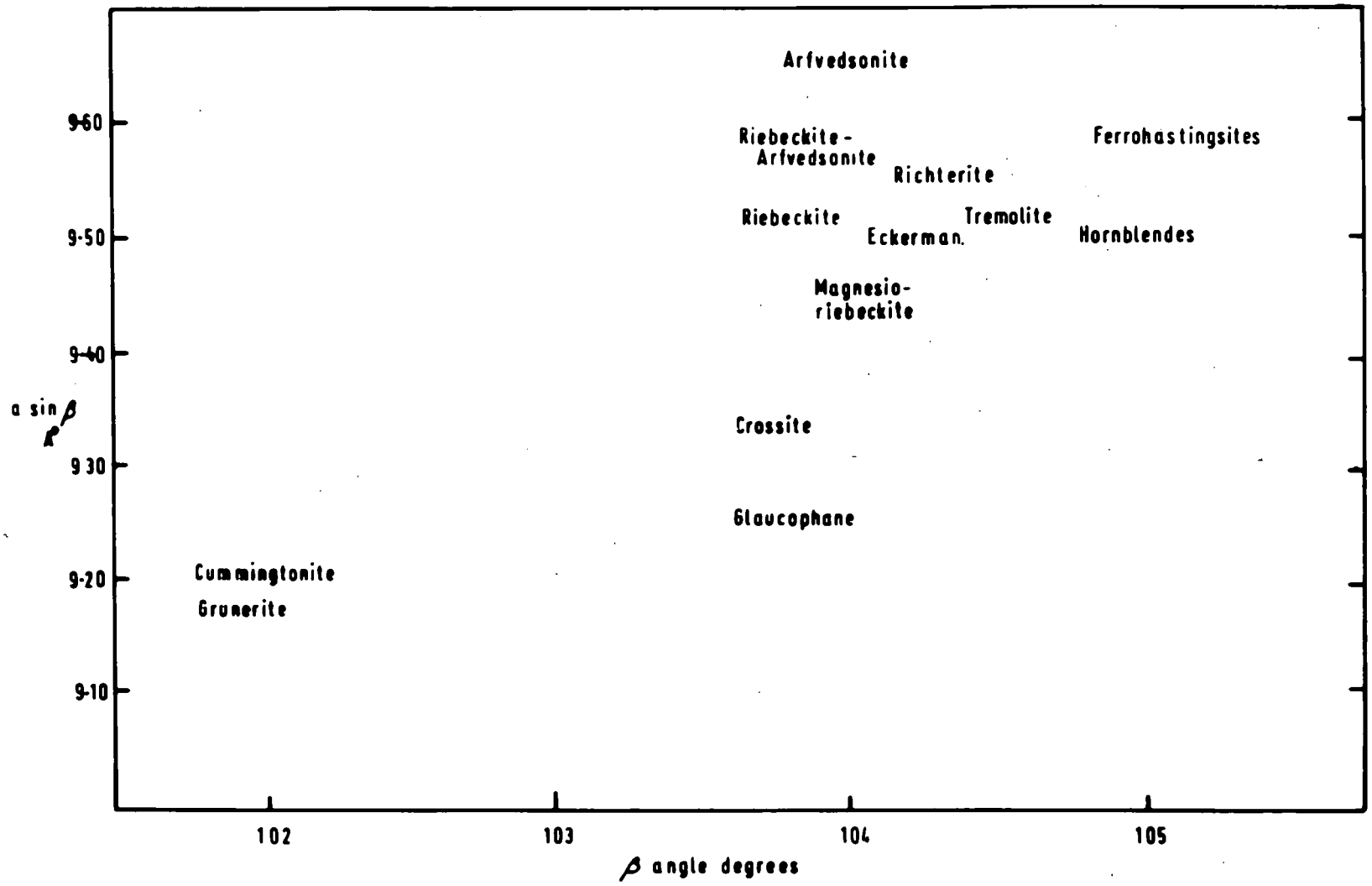

Fig.7-5 The plot of the a sin β parameter against the β angle for monoclinic amphiboles.

series respectively. Examination of their results (Figs. 7-1 and 7-7) shows that the β angle is greater for the magnesium end-member than the iron end-member.

Colville and Gibbs (1969) considered the structure of magnesium and iron rich alkali amphiboles and conclude that the double chains of the iron rich amphibole (riebeckite) approach a more regular six-sided figure than magnesium rich amphiboles (glaucophane) and consequently becomes smaller.

Colville and Gibbs (ibid.) also devised a scheme to separate the amphibole group into sub-groups. They plotted $a_o \sin\beta$ against the angle for the various amphibole compositional ranges. The $a_o \sin\beta$ parameter increases as the size of the cations in the octahedral strip increases thus splitting up the sub-groups (Fig. 7-5).

7-5. Cell Dimensions of synthetic calciferous and alkali amphiboles.

The cell parameters for many synthetic monoclinic amphiboles are set out in Table 7-1. Ernst (1961, 1962, and 1963) and Colville, Ernst and Gilbert (1966) have synthesized amphiboles whose bulk compositions were always such that the structural 'A' site should have been either completely full or empty. The author has succeeded in synthesizing amphiboles of intermediate composition where the 'A' site is only partially filled. The compositions of these two amphiboles are 75 richterite - 25 tremolite ($Na_{0.75}Ca_{1.25}Na_{0.75}Mg_5Si_8O_{22}(OH)_2$) and 25 richterite - 75 tremolite ($Na_{0.25}Ca_{1.75}Na_{0.25}Mg_5Si_8O_{22}(OH)_2$). In addition to amphiboles with different occupants of the 'A' and 'M' sites Colville et.al. (op.cit.) have synthesized amphiboles with (i) all silicon in the 'Z' sites i.e. tremolite, (ii) 12.5% aluminium replacing silicon i.e. edenite and (iii) 25% aluminium in fourfold co-ordination. The author has synthesized amphiboles in groups (i) and

TABLE 7-1 Cell Dimensions of Synthetic Monoclinic Amphiboles

Name	$a_o(A^o)$	$b_o(A^o)$	$c_o(A^o)$	(β^o)	$a_o \sin\beta(A^o)$	$vol(A^{o3})$
Tremolite (Boyd 1959, Colville et.al 1966)	9.833	18.054	5.268	104.52	9.52	905.3
Fluortremolite (Kohn and Comeforo 1954)	9.78	18.01	5.27	104.5	9.47	899
Ferrotremolite (Ernst 1966)	9.87	18.34	5.30	104.5	9.59	939
Pargasite (Boyd 1959, Colville et.al 1966)	9.906	17.986	5.265	105.30	9.51	904.7
Ferropargasite (Gilbert 1966)	9.95	18.14	5.33	105.3	9.60	928
Tschermakite (author)	9.823	17.921	5.272	105.51	9.466	894.3
Magnesiohastingsite (Colville et.al 1966)	9.925	17.982	5.289	105.61	9.56	909.1
Hastingsite (Colville et.al 1966)	9.979	18.152	5.325	105.20	9.58	930.8
Edenite (Colville et.al 1966)	9.853	18.005	5.236	104.40	9.51	899.8
Fluoredenite (Kohn and Comeforo 1955)	9.85	18.00	5.28	104.8	9.52	905
Ferroedenite (Colville et.al 1966)	9.999	18.217	5.314	105.50	9.59	932.8
Magnesioriebeckite (Ernst 1963a)	9.73	17.95	5.30	103.3	9.47	901
Riebeckite (Ernst 1962)	9.73	18.06	5.33	103.3	9.47	913
Riebeckite-Arfvedsonite (Ernst 1962)	9.85	18.15	5.32	103.2	9.59	926

TABLE 7-1 (Continued)

Name	a_o(A°)	b_o(A°)	c_o(A°)	(β°)	$a_o \sin\beta$(A°)	vol(A°)
Glaucophane I (Ernst 1963a)	9.75	17.91	5.27	102.8	9.50	897
Glaucophane II (Ernst 1963a)	9.64	17.73	5.28	103.6	9.37	877
Fluor-magnesiorichterite (Prewitt 1964)	9.677	17.914	5.274	102.95	9.429	890.8
Richterite (author)	9.892	17.958	5.263	104.28	9.586	906.0
Eckermannite (author)	9.762	17.892	5.284	103.17	9.505	898.6
75Richterite25Tremolite (author)	9.895	17.985	5.259	104.40	9.584	906.5
25Richterite75Tremolite (author)	9.812	18.010	5.237	104.69	9.517	900.3
Sundiusite (author)	9.921	17.921	5.305	105.39	9.565	909.4
75Eckermannite25 Richterite(author)	9.803	17.947	5.254	103.72	9.523	898.98
25 Eckermannite75 Richterite(author)	9.866	17.965	5.270	104.09	9.569	905.9
50Edenite50Richterite (author)	9.907	18.025	5.267	104.68	9.583	909.8
Fluor-richterite (author)	9.817	17.956	5.263	104.35	9.510	898.8

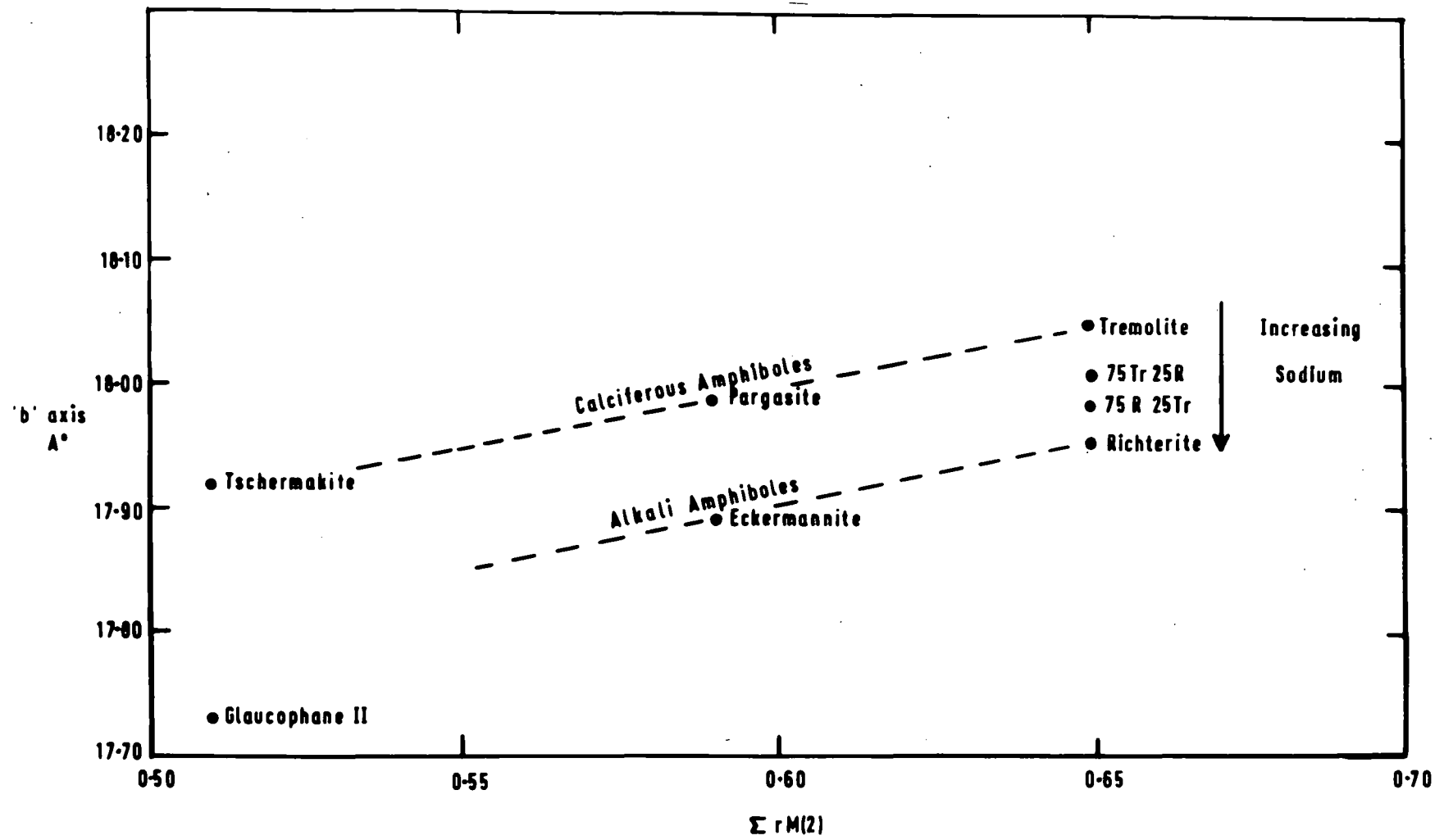

Fig.7-6 Variation in 'b' axis for synthetic clinoamphiboles as a function of the mean ionic radius (ΣrM2) of the cations occupying M(2), also denotes the effect of increasing sodium at M(4).

(iii) above i.e. richterite, eckermannite and the intermediate compositions in group one, and sundiusite and tschermakite in group three. In addition an amphibole with 6.25% aluminium in Z has been synthesized namely 50 edenite - 50 richterite ($NaCa_{1.5}Na_{0.5}Mg_5Si_{7.5}Al_{0.5}O_{22}(OH)_2$).

7-5-1. b_o axis variation.

Whittaker (1949) stated that the octahedrally-bound metal atoms comprise two distinct types (i) the smaller cations which prefer M(2) and (ii) the larger cations which prefer the M(1) and M(3) sites. These conclusions have been substantiated by recent structural refinements.

Colville et. al. (op. cit.) concluded that the b_o axis repeat of the amphiboles must be a function of the mean sizes of the lateral cations occupying the M(2) and M(4) sites and not the cations within the body of the chain, M(1) and M(3). In the amphiboles which they synthesized the M(4) site was occupied either by calcium or sodium and not mixed therefore the control on this parameter depends upon the occupancy of the M(2) site. Indeed, in several amphibole studies (Klein and Waldbaum, 1967; Borg, 1967; and Ernst, 1968) the b_o dimension has been shown to be the most sensitive to compositional change.

Colville et. al. have shown that the substitution of ferrous iron for magnesium increases the b_o axis 0.29A° from tremolite-K ($Ca_2Mg_5Si_8O_{22}(OH)_2$) to ferrotremolite ($\square Ca_2Fe_5Si_8O_{22}(OH)_2$). To correlate the b_o axis repeat with composition, Colville et. al. computed the mean ionic radius ($\bar{r}M(2)$) of the cations in M(2) by summing to 2 cations per 24 anions, in sequence, Al^{VI}, Ti, Fe^{3+}, Li, Mg, and Fe^{2+} as necessary, assuming complete preference for this site of the smallest cations. This assumption has recently been proved by structural refinements (Papike et. al., 1969; Papike and Clark, 1968). Theoretically, the b_o axis of ferrotremolite should be 0.32A° larger than tremolite. Colville et. al.

observe that in the synthetic amphiboles the replacement of magnesium or ferric iron by aluminium causes the b_o axis to decrease by 0.30A°.

The diagram (Fig. 7-6) of b_o axis variation against $\bar{r}M(2)$ is modified from Colville et. al. (op. cit.) and Ernst (1968). The author's synthetic amphiboles are plotted together with other synthetic amphiboles. Richterite-K with M(2) occupied by magnesium has the same b_o axis repeat as magnesioriebeckite where the M(2) sites are occupied by ferric iron which is marginally smaller (0.64A° compared to 0.66A°).

In figure 7-6 the calciferous amphiboles lie along one curve and the alkali amphiboles along another. These two curves support Colville et. al.'s conclusion that the b_o axis variation depends upon occupancy of the M(4) and M(2) sites. Introduction of sodium into the M(4) sites decreases the b_o axis as shown by the following four compositions:-

Tremolite-K	18.054A°	(Colville et. al., 1966)
75 Tremolite - 25 Richterite	18.010A°	(author)
25 Tremolite - 75 Richterite	17.985A°	(author)
Richterite-K	17.958A°	(author)

Forbes (1971) has stated that sodium entering the 'A' site decreases the b_o axis from tremolite to richterite and not the sodium-calcium substitution in M(4). Shannon and Prewitt (1969) have calculated that in eight-fold co-ordination sodium and calcium have similar radii and Forbes (ibid.) put this forward to explain that the 'A' site occupant affects the length of the b_o axis. Substitution of potassium for sodium in the 'A' site would also be expected to produce changes in b_o. This parameter increases by 0.009A° from sodium-richterite-K to potassium richterite, a value much too small if the sole criterion is ionic size.

Pargasite-K ($NaCa_2Mg_4AlSi_6Al_2O_{22}(OH)_2$) has a $\bar{r}M(2)$ of 0.59A°, the same as for eckermannite-K ($NaNa_2Mg_4AlSi_8O_{22}(OH)_2$) and the former has a b_o axis of 17.986 and the latter one of 17.892. Tschermakite-K ($\square Ca_2Mg_3Al_2Si_6Al_2O_{22}(OH)_2$) has the same $\bar{r}M(2)$ (0.51A°) as glaucophane -II-K ($Na_2Mg_3Al_2Si_8O_{22}(OH)_2$) and the b_o parameter of tschermakite-K is 17.921A° compared to 17.73A° for glaucophane-II-K.

Therefore the b_o axis length decreases as the $\bar{r}M(2)$ decreases for both the alkali and calciferous amphiboles but with sodium in M(4) in the former this too decreases the b_o axis. These observations are in agreement with those of Colville et. al. (op. cit.). The plot of $\bar{r}M(2)$ against b_o will separate the calciferous and alkali amphiboles where the former have a b_o dimension 0.10A° greater than the latter. The exceptions to this will be in adjacent compositions across the plane X = 1 (Phillips notation, 1966).

7-5-2. $A_o \sin\beta$ variation.

The $a_o \sin\beta$ dimension represents the unit repeat across facing double chains, these chains are cross linked to each other by strips of octahedrally co-ordinated cations. Colville et. al. (1966) conclude that the value of $a_o \sin\beta$ will be a function both of the sizes of the atoms in tetrahedral co-ordination and octahedral co-ordination between facing chains. In addition to the M sites in this $a_o \sin\beta$ -b_o plane there is also the 'A' site.

The $a_o \sin\beta$ dimension reaches a minimum of 9.30A° where silicon occupies all the tetrahedral sites and aluminium occupies both M(2) sites and magnesium in M(1) and M(3) sites as in glaucophane-II-K and a maximum of 9.60A° where ferrous iron occupies these sites as in ferrotremolite-K. The $a_o \sin\beta$ value for tremolite-K is 9.52A° which is

0.32A° greater than the value for glaucophane-K. The occupant of M(2) affects the $a_o \sin\beta$ more than changes in M(1) and M(3).

Richterite-K has an $a_o \sin\beta$ dimension of 9.586A° compared to that of tremolite-K (9.52A°) which indicates that sodium in the 'A' site increases $a_o \sin\beta$. Papike et. al. (1969) determined the cell parameters of a potassium richterite with 4.5 atoms of magnesium and only 0.28 atoms of ferrous iron. This mineral has an $a_o \sin\beta$ parameter of 9.721A° which is larger than richterite-K. Therefore alkali in the 'A' site expands the $a_o \sin\beta$ parameter. Huebner and Papike (1970) reported cell dimensions of synthetic potassium ferrorichterite with $a_o \sin\beta$ 10.03A° i.e. the highest reported value for a clinoamphibole.

7-5-3. β angle variation.

Whittaker (1960) plotted the mean size of the cations in M(4) against the β angle and found a linear relationship using ionic radii after Goldschmidt (Fig. 7-3). The minerals which have calcium in M(4) have the largest β angles (104.50° for tremolite-K to 105.60° for magnesiohastingsite-K), alkali amphiboles have intermediate values (103.2° for riebeckite-arfvedsonite and eckermannite to 104.28° for richterite-K) and the cummingtonite-grunerite series have the smallest values (Klein and Waldbaum, 1967), where magnesium and ferrous iron occupy the M(4) sites (101.8° to 102.7°). The β angle values for certain synthetic alkali amphiboles are lower than those for the equivalent natural alkali amphiboles (e.g. glaucophane) and this cannot yet be explained.

Support for Whittaker's conclusion is contained in the following amphiboles where calcium decreases from tremolite-K to richterite-K:-

richterite-K	104.28°
75 richterite - 25 tremolite	104.40°
25 tremolite - 75 richterite	104.68°
tremolite-K (Colville et. al. 1966)	104.52°
tremolite (Zussman, 1959)	104.70°

7-5-4. c_o axis variation.

The c_o axes for the author's synthetic amphiboles vary only very slightly and not systematically. The c_o axis increases about 0.05A° where Fe^{2+} replaces Mg in all the metal positions.

7-6. Cell Dimensions of natural Alkali Amphiboles.

The cell dimensions of a number of alkali amphiboles are tabulated in the appendix. These minerals have been subdivided into five groups, although limits of solid solution between these groups have yet to be delineated:-

(a) glaucophane - riebeckite series

(b) arfvedsonite - eckermannite series

(c) richterite series

(d) katophorite - magnesiokatophorite series

(e) mboziite - sundiusite series

7-6-1. Glaucophane-Riebeckite series.

This series has been the subject of two studies (1) Borg (1967) and (2) Coleman and Papike (1968). The low-temperature minerals have been shown to be well ordered (Papike and Clark, 1969; Burns and Strens, 1966; and Burns and Prentice, 1970). The smallest cell parameters are found when aluminium is the sole occupant of the M(2) sites; magnesium in M(1) and M(3) and sodium in M(4). The variations in the cell parameters are shown in the appendix.

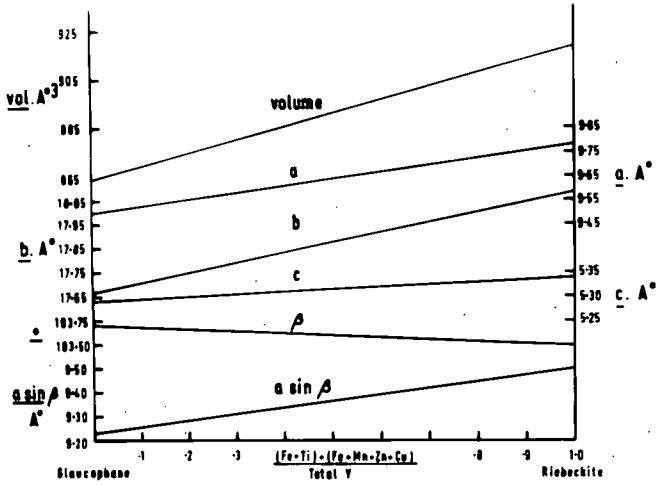

Variation in cell dimensions of the Glaucophane-Riebeckite series.

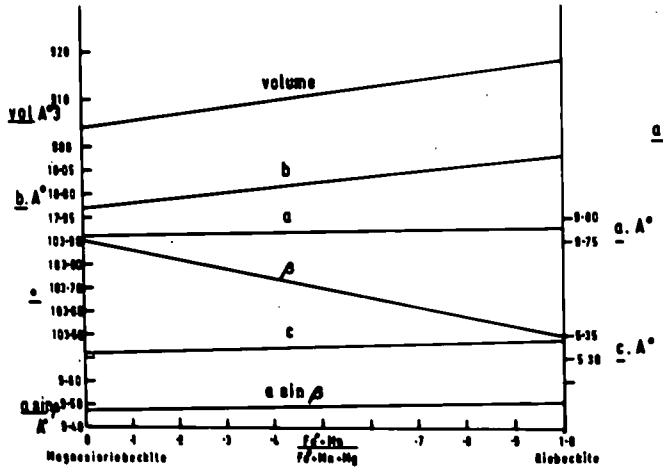

Variation in cell dimensions of the Magnesioriebeckite-Riebeckite series.

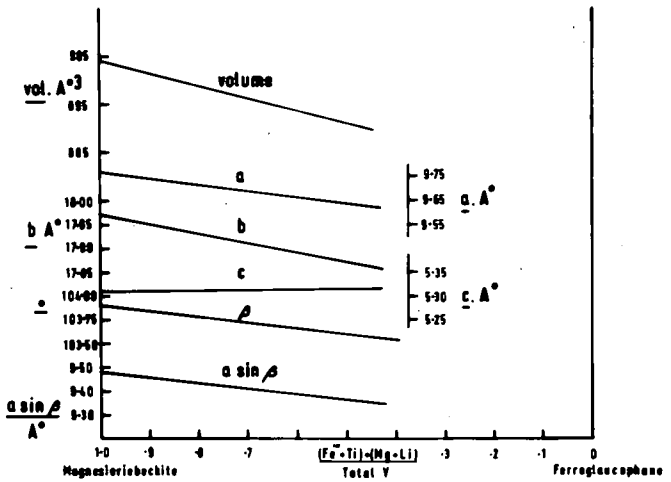

Variation in cell dimensions of the Magnesioriebeckite-Ferroglaucophane series.

(Redrawn from Borg, 1967).

Fig. Variation in cell dimensions within the Glaucophane compositional sub-group.

The dimensions of glaucophane are smaller than those of crossite and riebeckite with the exception of the β angle. The β angle has been shown to decrease as the ferrous iron content rises by Borg (ibid.) and by Klein and Waldbaum (1967) for the cummingtonite-grunerite series.

Figure 7-7 shows Borg's extrapolations of the cell parameters for this series. Coleman and Papike (op. cit.) have also generated a set of curves for this group of minerals and the two sets are similar. The main difference between these two sets of curves is the value for the b_o axis repeat for the glaucophane end-member composition. Borg takes a value of 17.67A°, whereas Coleman and Papike use the b_o axis of synthetic glaucophane II (Colville et. al., 1966) which is 17.73A°. A magnesium rich glaucophane (gastaldite, Val d'Aosta, Piemonte, Italy; B.M. 1924, 689) has a b_o axis repeat of 17.73A° the same value as Colville and Gibbs end-member composition. An infra-red spectrum of the hydroxyl stretching region of "gastaldite" indicates the presence of ferrous iron, therefore the author prefers to use Borg's values extrapolated from natural amphiboles.

From the two sets of curves evaluated by Borg the most useful parameters for the determination of composition are $a_o \sin\beta$, b_o, and cell volume. The c_o axis becomes larger as the larger cations (Fe^{2+}, Fe^{3+}) enter the lattice and as the chains begin to unkink (Ernst, 1968). The variation in the c_o axis is only a half that of the $a_o \sin\beta$ dimension and hence not so useful.

The β angle is larger for magnesioriebeckite than for riebeckite therefore the occupants of M(1) and M(3) must affect this parameter more than the neighbouring occupant of M(2). Klein and Waldbaum (op. cit.) also noted the decrease in β as the amount of ferrous iron in the cummingtonite-grunerite series increased.

In figure 7-7 the ferrous iron substitution for magnesium is shown to affect the b_o axis more than the a_o axis. This is revealed by reference to the magnitude of slope in the curves representing the substitutions $Mg_3Al_2 \rightleftharpoons Fe_3^{2+}Fe_2^{3+}$ and $Fe_3^{2+}Al_2 \rightleftharpoons Mg_3Fe_2^{3+}$ in the case of the b_o axis. In section 7-5-1 the occupants of the M(2) sites in synthetic alkali amphiboles were shown to have a large effect upon the b_o dimension.

The curves (Fig. 7-7) for the magnesioriebeckite-riebeckite series are derived from Borg's (1967) data. The four parameters a_o, b_o, c_o, and volume all increase from magnesioriebeckite to riebeckite but the β angle decreases.

The large β angle could be correlated with the magnesium content of the amphibole and to a lesser extent ferric iron. The change in β from glaucophane to magnesioriebeckite is 0.20° and corresponds to two atoms of ferric iron having replaced two aluminium atoms at M(2). The β angle decreases 0.40° from magnesioriebeckite to riebeckite where three ferrous iron atoms have replaced three magnesium atoms at M(1) and M(3). This is unexpected as the M(1) and M(3) sites are within the cation strips and not at the edges. The β angle has already been shown to increase in clinoamphiboles as the radius of the cation at M(4) increases (Whittaker, 1960 and present study). The M(4) sites in the glaucophane-riebeckite series are almost always completely filled with sodium.

The crystal structure determinations of magnesium and ferrous iron rich amphiboles (Ernst, 1968; Papike, Ross, and Clark, 1969; and Mitchell, Bloss and Gibbs, 1971) show that the T(1)-O(6)-T(2) angle is smaller in magnesium rich amphiboles than in ferrous iron rich amphiboles i.e. magnesium rich amphibole chains are more "kinked". Whittaker (1960),

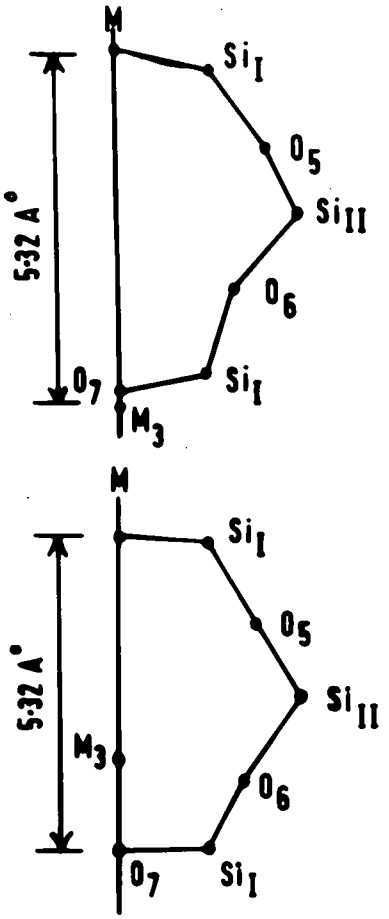

Magnesioriebeckite (Whittaker, 1949)

	b	c
Si_I	1·58	·43
Si_{II}	3·05	3·11
O_5	2·51	4·27
O_6	1·98	1·87
O_7	0	·13
M_3	0	0

Riebeckite (Colville and Gibbs, 1965)

	b	c
Si_I	1·55	-1·53
Si_{II}	3·06	1·06
O_5	2·31	2·27
O_6	2·13	- ·38
O_7	0	-1·57
M_3	0	0

Fig.7-8 Comparison of the projection of amphibole chains on (100) for riebeckite and magnesioriebeckite.

Zussman (1955, 1959), Papike et. al. (ibid.), and Mitchell et. al. (ibid.) have all demonstrated that amphibole chains are not as regular as in Warren(s (1928) original structural analysis of tremolite. The projection of the riebeckite and magnesioriebeckite chains on (100) (Fig. 7-8) shows that the magnesioriebeckite chain is less regular. Mitchell et. al. (ibid.) conclude that one of the causes of slight differences in structure of the amphiboles is the average electronegativity of non-tetrahedral cations. This factor may explain the larger β angles for magnesium rich clinoamphiboles.

7-6-2. Eckermannite - Magnesioarfvedsonite - Arfvedsonite Series.

a) Eckermannite - Magnesioarfvedsonite

In this series sodium completely fills the M(4) sites, the 'A' site is filled with sodium and potassium, magnesium occupies M(1), M(3) and one of the M(2) sites; the other M(2) site is occupied by either aluminium (eckermannite) or ferric iron (magnesioarfvedsonite). Many of the samples for which there is diffraction data (Appendix 4) have been called juddite (manganoan magnesioarfvedsonite).

One feature of the cell parameters of this group is the high value for the β angle (average 104°) despite the low calcium content. A possible reason for these values has been put forward in section 7-6-1.

The lengths of the b_o axes are shorter than those of richterites because of the $Mg \rightleftharpoons Al$ substitution at M(2) in addition to the substitution $Na \rightleftharpoons Ca$ at M(4). Magnesioarfvedsonite has ferric iron at one of the M(2) sites and ferric iron and magnesium have similar ionic radii. The b_o axes of magnesioarfvedsonites are smaller than those of richterites indicating that the substitution $2Na \rightleftharpoons Ca$ at M(4) decreases the length of the b_o axis.

The manganese content of the manganoan magnesioarfvedsonites only

reaches a value of 0.3 atoms which only marginally affects the cell parameters.

(b) Riebeckite - Arfvedsonite Series

In the riebeckite-arfvedsonite series the main substitution is:-

$$Fe_3^{2+}Fe_2^{3+} \rightleftharpoons Fe_4^{2+}Fe^{3+} + Na \text{ (in the 'A' site)}$$

Calcium also enters the arfvedsonite lattice and to a much smaller extent riebeckite. The cell parameters of this series (Appendix 4) are among the largest for clinoamphiboles.

In hydroxyl-rich arfvedsonites and riebeckite-arfvedsonites the cell parameters increase as the proportion of arfvedsonite in the amphibole increases. Where the substitution $OH^- \rightleftharpoons F^-$ has taken place the cell parameters a_o, b_o, and β are smaller. This affect was first noted by Borley and Frost (1963) and subsequently by Kempe (1969).

Data for synthetic fluor-richterite (Huebner and Papike, 1971 and the present study) compared to the hydroxy equivalent show that a_o decreases by 0.08-0.10A° and b_o and c_o by 0.01A°. In amphiboles of riebeckite-arfvedsonite compositions b_o appears to decrease more than a_o. Huebner and Papike (ibid.) ascribe this contraction to the absence of hydrogen between the 'A' site and O(3) allowing the alkali ion at this site to settle more deeply into the Si_6O_{18} ring and permitting the chains to approach more closely. This difference in behaviour between richterite and the riebeckite-arfvedsonites awaits further study.

The cell parameters for both fluor- and hydroxy riebeckite-arfvedsonites increase as the ferrous iron content increases but the values for the fluorine rich minerals are systematically lower.

The magnesium contents of these minerals are extremely low therefore the β angle is dependant upon the occupant of the M(4) sites. Arfvedsonites with substantial calcium at M(4) do indeed have larger

β angles but several arfvedsonites from the lujavrites of Ilímaussaq have high β angles (104°) but no calcium or magnesium in the structure. These amphiboles do however have high potassium concentrations (0.6 atoms). Huebner and Papike (op. cit.) have prepared synthetic potassium richterite which has a β angle of 104°48' compared to a value of 104°15' for their preparation of sodium richterite. Papike, Ross and Clark (1969) conclude that as potassium substitutes for sodium at the 'A' site the chains are moved apart and the site becomes more regular increasing the β angle.

7-6-3. Richterite Series.

Small amounts of ferric iron often substitute for magnesium in minerals of richterite composition. There is also limited solid solution between richterite and ferrorichterite (Carmichael, 1967 and present study) but there is no diffraction data for these compositions. The synthesis of intermediate members between tremolite and richterite (present study) and the distribution of natural amphiboles of these compositions indicate complete solid solution between tremolite and richterite. The lattice parameters (Appendix 4) of this series are affected by the presence of manganese which becomes an important constituent; ferrous iron, aluminium and titanium are very low.

The b_o axis is smaller for minerals of richterite composition than tremolite but is larger than the other magnesium rich alkali amphiboles. The β angle is also greater than other alkali amphiboles (values up to 104.50°). Fluorine rich richterites (Iron Hill, Colorado, I.H. 111, 121) have shorter a_o axes than than the hydroxyl rich richterites (Långban, Sweden, RLa 1, 2, 3). This observation supports shortening of the a_o axes in synthetic fluor-richterite.

Tirodite which occurs in the manganese metasediments of India is thought to have affinities with richterite (Dunn and Roy, 1939, Bilgrami, 1956, and Roy, 1964) and also to manganoan cummingtonite (Segeler, 1961). The lattice parameters for a manganoan cummingtonite (Klein, 1964) are compared to those of richterite-K and tirodite from W. Tirodi in table 7-2. The main chemical differences between Mn-cummingtonite and tirodite (analysis appendix 3) are the manganese, sodium and calcium concentrations. Manganese is much higher in the former (16.62% MnO) than the latter (8.56%), and sodium and calcium much lower in Mn-cummingtonite. From a study of the chemistry and cell dimensions tirodite is intermediate between the (Fe, Mg) clinoamphiboles and richterite/tremolite. These compositions plot in the supposed miscibility gap in clinoamphiboles.

7-6-4. Katophorite - magnesiokatophorite.

The cell dimensions of two amphiboles of katophorite composition (Kempe, 1969) have been determined but conclusions derived from results merely extend the observations outlined for arfvedsonite.

7-6-5. Mboziite - Sundiusite.

Two amphiboles close to the mboziite end-member compositions have cell parameters intermediate between ferrohastingsite and arfvedsonite (appendix). The a_o axes of mboziite are similar to these amphiboles but the b_o axis is shorter due to the presence of octahedral aluminium and larger ferric iron concentrations. The β angle (104.70) is higher than other alkali amphiboles due to the larger calcium contents in M(4).

TABLE 7-2 Lattice parameters and chemical analyses of manganoan cummingtonite (Klein, 1966), richterite-K, and tirodite.

	Mn cummingtonite	Richterite-K	Tirodite
$a_o(A^o)$	9.583	9.892	9.799
$b_o(A^o)$	18.091	17.958	17.993
$c_o(A^o)$	5.315	5.263	5.289
$\beta(^o)$	102.63	104.28	103.89
$a_o \sin\beta(A^o)$	9.351	9.586	9.512
$vol(A^{o3})$	899.1	906.0	905.3

Chemical analyses

	Mn cummingtonite	Tirodite
SiO_2	55.27	55.84
Al_2O_3	0.34	0.86
Fe_2O_3	nil	7.08
FeO	4.52	tr.
MnO	16.62	8.38
MgO	19.18	17.34
TiO_2	nil	0.71
CaO	1.19	2.78
Na_2O	0.26	3.92
K_2O	nil	1.00
F	0.30	n.d.
H_2O^+	2.16	1.98

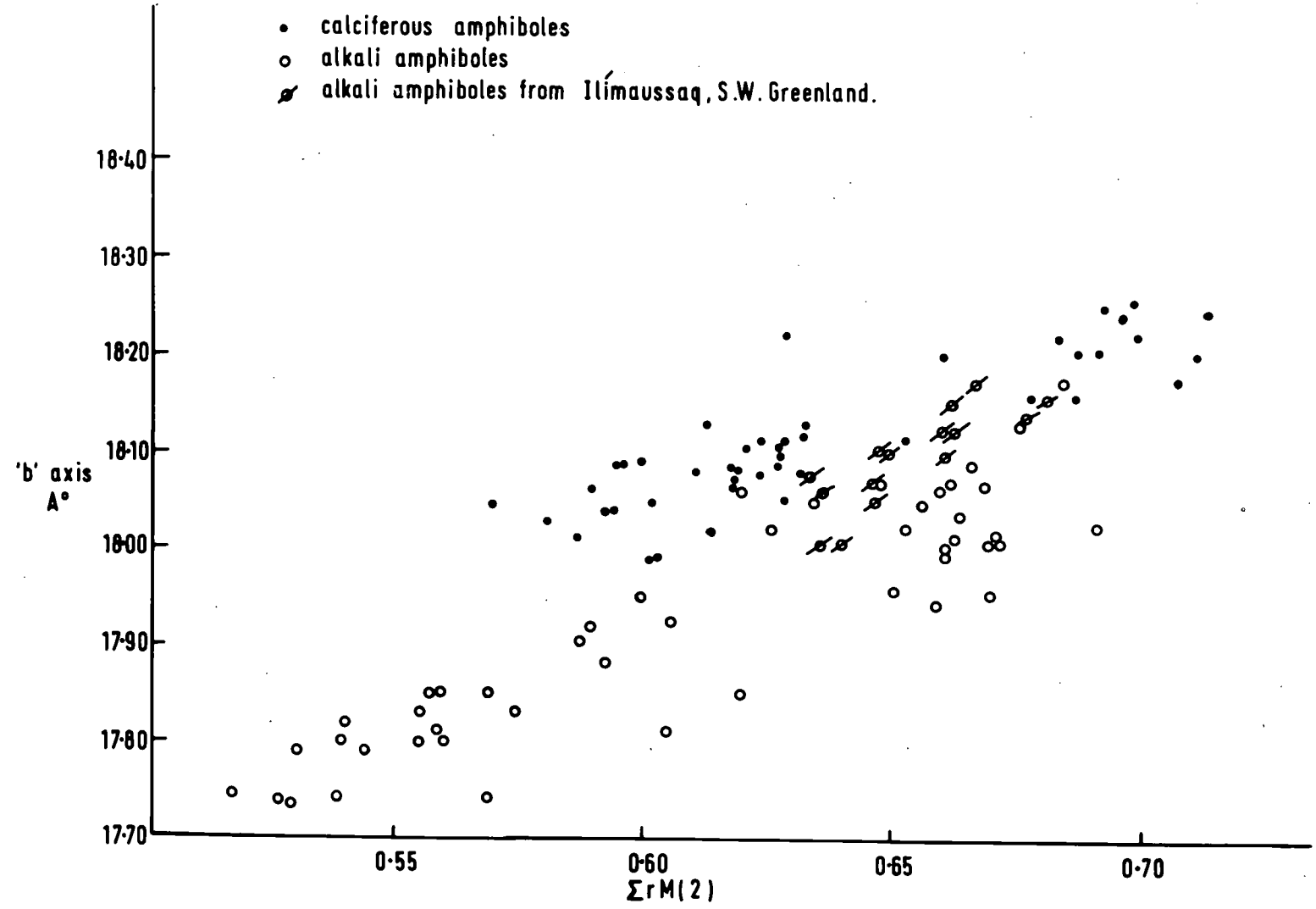

Fig.7–9 Variation in 'b' axis for natural clinoamphiboles as a function of the mean ionic radius of the cations occupying the M(2) site.

7-7. Parameters useful for the determination of alkali amphibole subgroups.

7-7-1. The effect of M(2) occupancy on the b_o axis in natural alkali and calciferous amphiboles.

Colville et. al. (1966) and Ernst (1968) have concluded that M(4) and M(2) occupancy affects the b_o axis. The present study substantiates the conclusion that M(4) occupancy in synthetic alkali amphiboles affects the length of the b_o axis. In figure 7-9 all the alkali and calciferous amphiboles for which there are X-ray and chemical data are plotted.

There is a linear relationship of b_o with $\bar{r}M(2)$ for compositions between the glaucophane and riebeckite end-members, which must indicate the substitution of Al^{3+} by Fe^{3+} in the M(2) sites.

The introduction of fluorine into the O(3) sites has been demonstrated to decrease the b_o axes of riebeckite-arfvedsonites (Borley and Frost, op. cit.). Alkali amphiboles of riebeckite-arfvedsonite composition with high fluorine contents have shorter b_o axes than the equivalent hydroxyl rich amphiboles. Minerals from the Ilímaussaq intrusion (high hydroxyl) follow the trend of increasing b_o axis with increasing average ionic size in M(2); minerals from Nunassuit and Nigeria (high fluorine) have consistently lower b_o axes.

The calciferous amphiboles (Fig. 7-9) have longer b_o axes ($0.10A^o$) than the alkali amphiboles for the same $\bar{r}M(2)$. Again there is an approximately linear relationship between hornblendes, actinolites, and ferrohastingsites. Both barroisite and mboziite, which plot close to the boundary between calciferous and alkali amphiboles ($Na^X = 1$, Phillips, 1966), have intermediate values between the two groups.

Riebeckite-arfvedsonites and arfvedsonites from Greenland have variable total iron contents. When these values are plotted against the b_o axes (Fig. 7-9) there is a scatter of the data points mainly due to

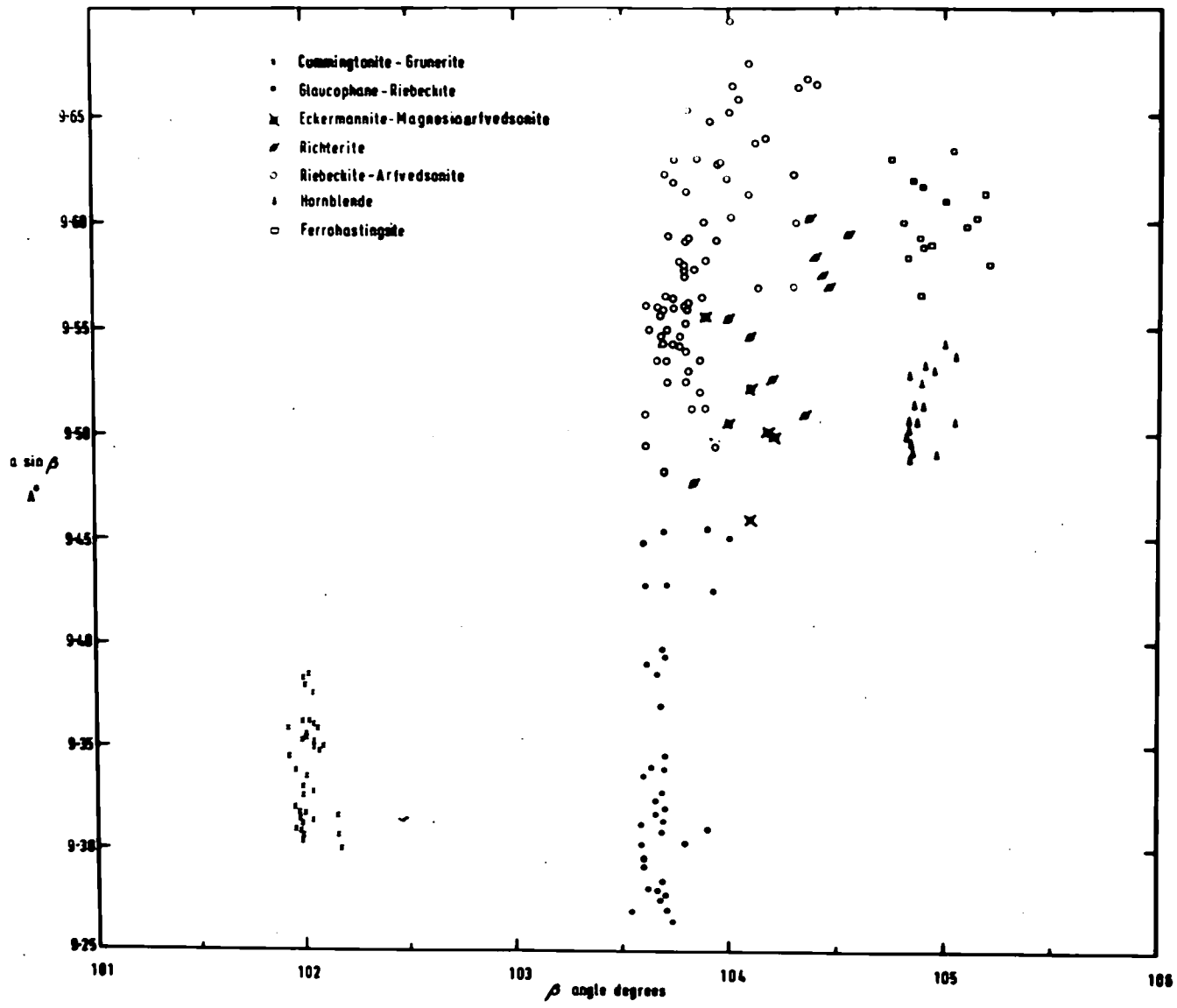

Fig.7-10 The plot of $a_o \sin\beta$ parameter against the β angle for the monoclinic amphiboles.

the variable fluorine content of these amphiboles.

7-7-2. The variation of $a_o \sin\beta$ and the β angle in alkali amphiboles.

Colville and Gibbs (in Ernst, 1968) have plotted the parameter $a_o \sin\beta$ against the β angle and have shown that the clinoamphiboles distribute themselves into their respective groups. Whittaker (1960) and Colville and Gibbs (1969) have demonstrated that in monoclinic amphiboles the β angle increases from 101.8°-102.1° for amphiboles with Fe^{2+} and Mg^{2+} at M(4) to 103.3°-104.0° for 2Na at M(4) and 104.5°-106.1° for calciferous amphiboles.

The range of angles for β in the alkali amphibole group ought to be revised in the light of date for natural arfvedsonites, eckermannites and richterites which all have values greater than 104°. A suggested new range of values for the angle of alkali amphiboles is 103.3°-104.40° to include the above minerals. The lower value (103.3°) has only been noted for synthetic alkali amphiboles and natural amphiboles occur in the range 103.5°- 104.4°, with rare exceptions such as mboziite (104.70°) and potassium richterite (104.98°).

The data for cummingtonite-grunerite series (Klein and Waldbaum, 1967) and the hornblendes are plotted on figure 7-10 for reference.

(a) Glaucophane-riebeckite series

End-member glaucophane has a calculated value of 9.23A° for $a_o \sin\beta$ and riebeckite 9.508 (Borg, 1967). Between these limits crossites and magnesioriebeckites have intermediate values. The β angle varies slightly but significantly; 103.7° for glaucophane, 103.5° for riebeckite and 103.90° for magnesioriebeckite. The results obtained by the author (Appendix 4) compare favourably with those computed by Ernst (1963, 1964), Borg (1967), and Coleman and Papike (1968). The $a_o \sin\beta$ parameter increases

with greater ferrous and ferric iron in the octahedral sites.

The glaucophane-riebeckite series can be subdivided by using these two parameters:-

	$a_o \sin\beta$ (A°)	β °
Glaucophane	9.23 - 9.34	103.7
Crossite	9.34 - 9.40	103.7 - 103.6
Riebeckite	9.40 - 9.56	103.5 - 103.8
Magnesioriebeckite	9.45 - 9.50	103.9

(b) Riebeckite-arfvedsonite series

The lattice parameters $a_o \sin\beta$ and β of riebeckite-arfvedsonite from Nigeria (Borley and Frost, op. cit.) are very similar to those from Nunassuit and Igaliko (S.W. Greenland) (Fig. 7-10). The β angle increases from 103.6° to 103.95° and $a_o \sin\beta$ from 9.525A° to 9.600A°. Increase in $a_o \sin\beta$ correlates with increasing ferrous iron. Borley and Frost conclude that $a_o \sin\beta$ increases with the amount of calcium, ferrous iron and fluorine but the data presented here indicates that fluorine and calcium decrease $a_o \sin\beta$.

The variation in these two parameters for arfvedsonites from Ilímaussaq are 9.600-9.675A° for $a_o \sin\beta$ and between 103.8° and 104.4° for the β angle. As the calcium content increases the β angle does so too. The β angle varies from 103.5°- 104.0° in alkali amphiboles with no calcium in M(4) and increases to a maximum value of 104.4° in arfvedsonites containing calcium.

(c) Richterite-tremolite series

In the richterite-tremolite series the β angle increases from 103.83° (Winchite, Netra, India - Appendix) to 105° (actinolite, Zussman, 1955). Minerals of richterite composition can be divided into alkaline

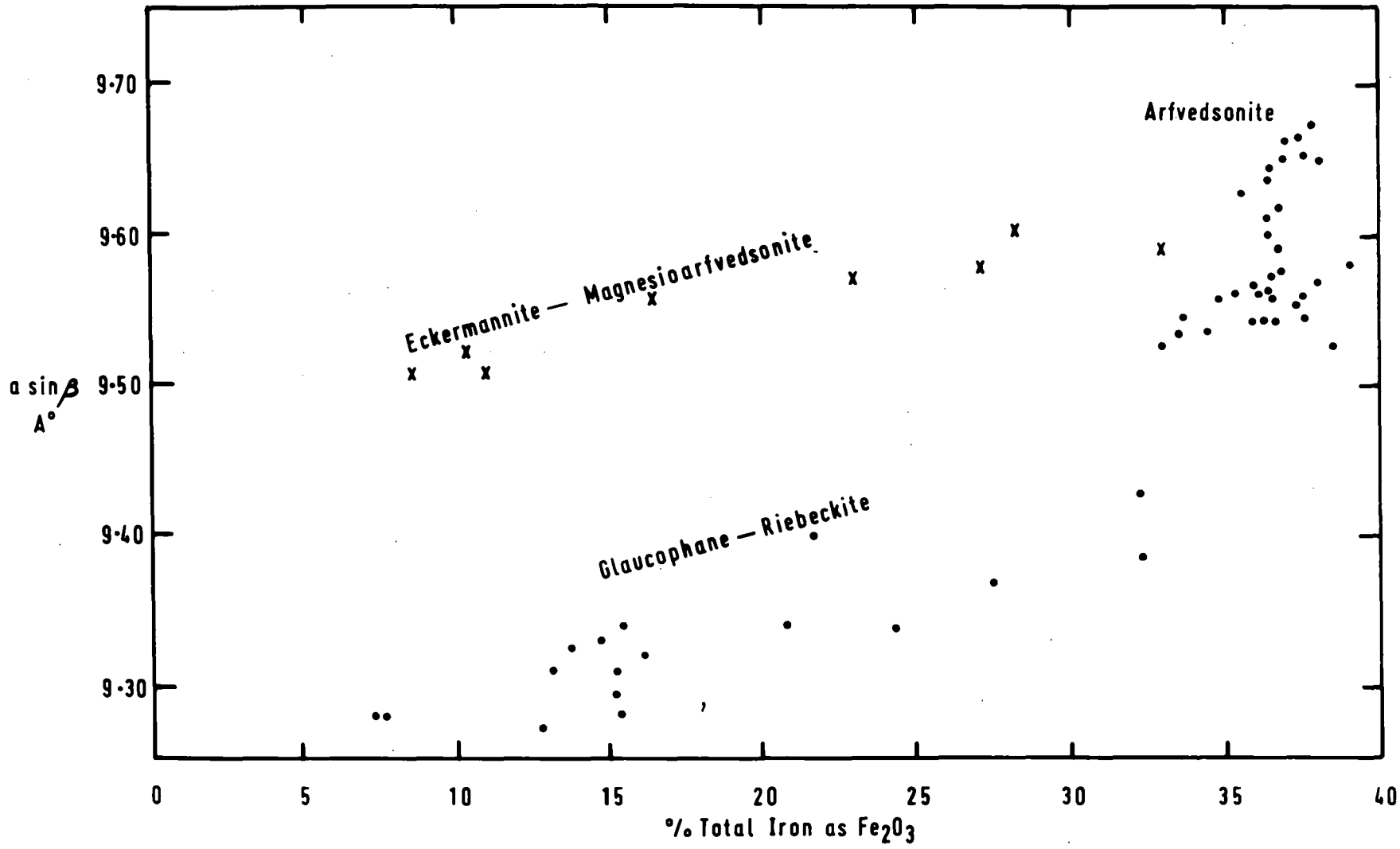

Fig.7-11 Variation in the a.sin β parameter with increasing total iron content in alkali amphiboles.

richterites (affinities with alkali amphibole i.e. Na^{X} 1) and calciferous richterites. In addition minerals of tremolite composition can be separated from the richterites. Richterite-K has a β angle of 104.28° therefore minerals with β angles less than this value could be called alkaline richterites, between 104.28° and 104.50° calciferous amphiboles and between 104.50° and 104.70° tremolite.

The $a_0 \sin\beta$ parameter varies from 9.47A° (tremolites) to 9.60A° (richterites).

(d) Eckermannite-magnesioarfvedsonite

In this series the $a_0 \sin\beta$ dimension varies from 9.45 - 9.55A° and the β angle from 103.9 - 104.2°. Minerals of eckermannite composition cluster around 9.50A° ($a_0 \sin\beta$) and magnesioarfvedsonite 9.55A°. The angle distinguishes between this group and richterite. The eckermannites are readily distinguished from the arfvedsonites and riebeckite-arfvedsonites by the lower $a_0 \sin\beta$ parameter and from glaucophane by a larger $a_0 \sin\beta$ and β angle. The β angle also distinguishes eckermannite from magnesioriebeckite.

7-7-3. The effect of total iron content on $a_0 \sin\beta$ and the cell volume of the alkali amphiboles.

Iron (both ferrous and ferric) is the dominant oxide in many alkali amphiboles and its variation is greater than other oxides. In iron free glaucophane there are two Al^{3+} ions in M(2), one in eckermannite and none in richterite, in addition alkali ions occupy the 'A' site in the latter two. Therefore $a_0 \sin\beta$ should be greatest for richterites and smallest for glaucophanes for the same amount of total iron. There are three separate curves for the separate groups of the alkali amphiboles (Fig. 7-11). The curve of the glaucophane-riebeckite series is joined to the curve of the eckermannite-magnesioarfvedsonites by the riebeckite-arfvedsonites.

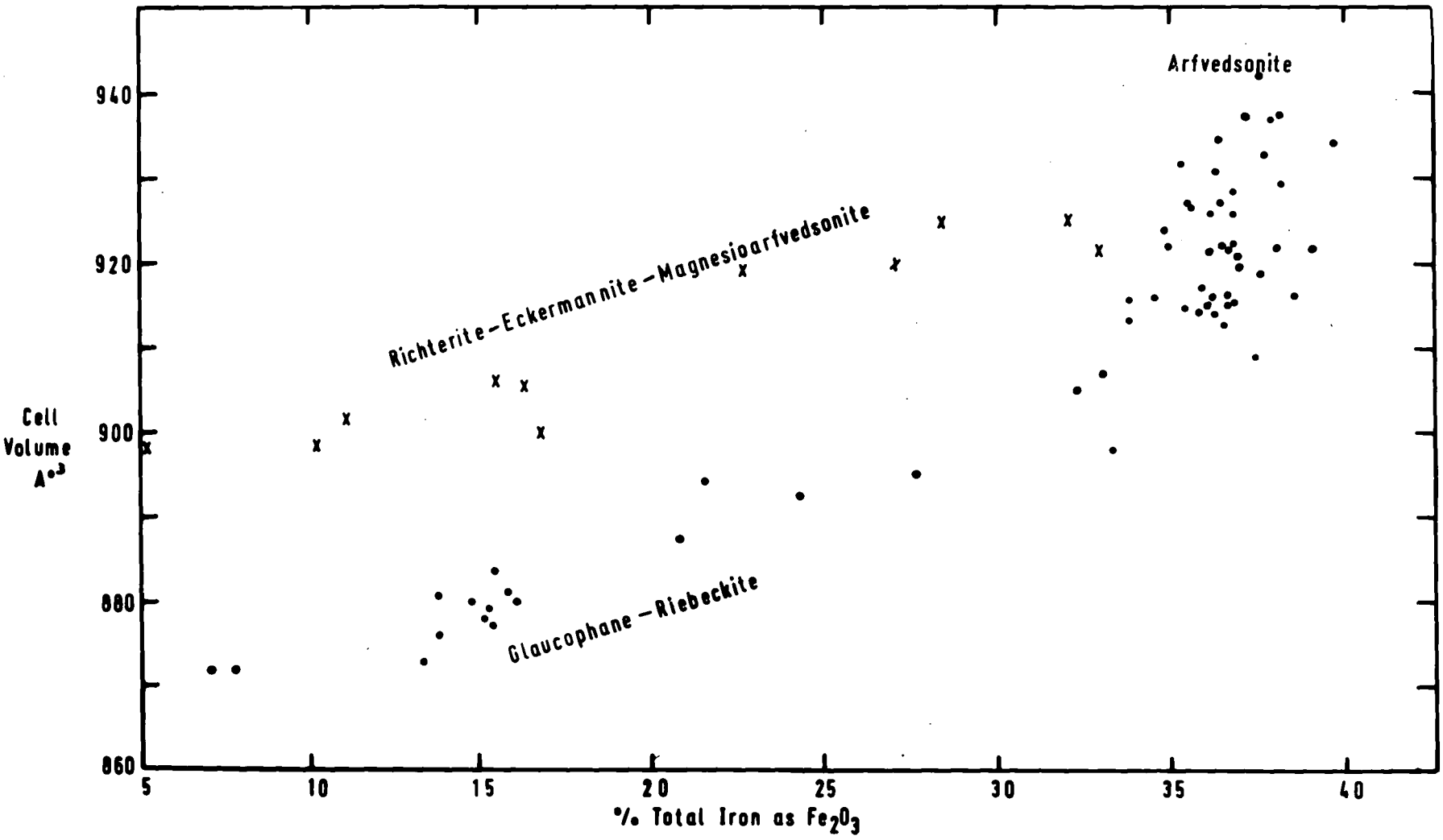

Fig.7-12 Cell volume plotted against total iron content of analysed alkali amphiboles.

The cell volume of the alkali amphiboles increases from 864A^{03} (glaucophane) to 942A^{03} (D.U. 10942 Ilímaussaq, arfvedsonite). The cell volume in common with the other parameters increases as the larger cations fill the metal sites. In figure 7-12 total iron is plotted against cell volume and there are three curves present for alkali amphiboles with total iron between 5-30%. In the riebeckite-arfvedsonite series there is little increase in total iron but a greater proportion of ferrous iron and alkalis in arfvedsonite which increases the cell volume.

Summary

To summarise the main conclusions which can be derived from this survey it is proposed that we must have a starting composition and as the cell parameters of tremolite are accurately known, this is a good starting position.

If we look at substitutions which take place in the alkali amphiboles we see the following effects. The substitution $\square Ca \rightleftharpoons NaNa$, i.e. tremolite to richterite the a_o parameter increases whilst b_o and β decrease. Variations in richterite compositions often involve $Na \rightleftharpoons K$ in the A site, $Mn \rightleftharpoons Mg$ in M(1) and M(3), and $OH \rightleftharpoons F$ at the O(3) site. Complete substitution of K for Na in A increases all the lattice parameters. Increase of Mn increases the b_o dimension mainly and F decreases the a_o parameter.

The substitution $CaMg \rightleftharpoons NaAl$, i.e. tremolite to glaucophane and richterite to eckermannite produces a decrease in all the lattice parameters. The compositional points of eckermannite and glaucophane have four end members involving the substitutions: 1) $Al \rightleftharpoons Fe^{+++}$ 2) $Mg \rightleftharpoons Fe^{++}$ 3) $MgAl \rightleftharpoons Fe^{++}Fe^{+++}$.

The first of these substitutions increases all the parameters the second increases a_o, b_o, and c_o and decreases β. The third also increases a_o, b_o, c_o and decreases β. The effect of $K \rightleftharpoons Na$ increases a_o and β in arfvedsonites. Fluorine replacing hydroxyl in O_3 decreases b_o axis mainly, in contradistinction to the a_o axis in richterites. The substitution $CaAl \rightleftharpoons NaSi$ which mainly affects members of the arfvedsonites increases b_o, c_o, and the β angle and only marginally affects a_o. The substitution $NaMg \rightleftharpoons \square Al$ (eckermannite to glaucophane) produces a decrease in all the parameters.

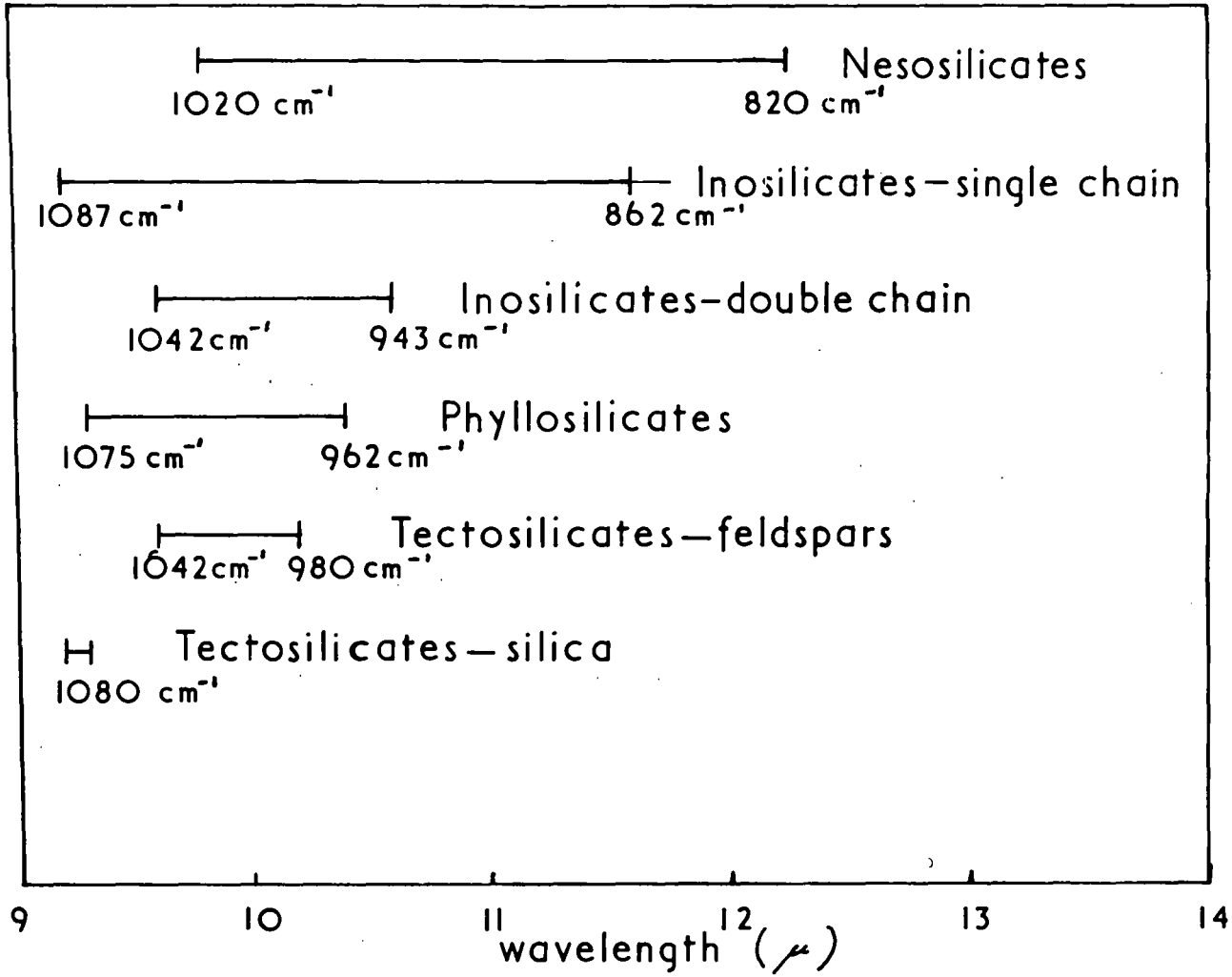

Fig. 8-1 Silicon oxygen stretching frequencies of silicates. (after Launer, 1952).

CHAPTER EIGHT

Infra-Red Spectroscopic Studies of Alkali Amphiboles

8-1. General statement.

Wave numbers are used, throughout the present study, to express frequency, and 1 micron (μ) equals 10,000 wavenumbers (cm^{-1})

The infra-red absorption spectra of silicates occur in the range 4000 cm^{-1} down to very low frequencies. All the silicates show a strong absorption near 1000 cm^{-1} associated with silicon-oxygen stretching vibrations. The position of this maximum absorption readily splits the silicates up into their various groups (Launer 1952, Fig. 8-1). The region of strongest absorption tends to shift towards shorter wavelengths and occupy a smaller range as the ratio of silicon to oxygen increases. The amphiboles absorb strongly from 1150 cm^{-1} to 850 cm^{-1} (Lyon 1962, and present study).

The silicon-oxygen bending vibrations occur at lower frequencies and vary more in their position in the various silicate groups than do the stretching vibrations (Farmer, 1964). These bending vibrations can vary within mineral groups (present study).

The metal-oxygen stretching vibrations occur at still lower frequencies 100-500 cm^{-1} (Lyon, 1967). These vibrations are very weak and are beyond the efficiency of normal infra-red spectrometers.

Bending and stretching vibrations of silicates may mix making an accurate assignment of absorption peaks to specific inter-atom motions almost impossible.

In hydrous silicates an additional motion can be observed, this is attributable to structurally bound water and may be termed the hydroxyl stretching frequency (Burns and Strens, 1966). This vibration

occurs between 3300-3750 cm^{-1} and in the amphiboles varies from 3615-3734 cm^{-1} depending upon the amphibole sub-group and type of cation bonded to the hydroxyl ion.

The peaks in this region are called the fundamental absorption bands and additional weak bands may arise as sums or differences of the fundamental bands (Farmer, 1964). The fundamental hydroxyl stretching band occurs at 3600 cm^{-1} and there is a weaker band at 7200 cm^{-1} called the overtone band (Burns and Strens, 1966). The sums or differences of these bands are called combination bands.

There is very little published work on the infra-red absorption spectra of silicates. The study of Launer (1952) was of a very general nature and not until 1962, when Lyon presented his data was there any attempt to systematise the various sub-groups of the amphiboles. In recent years emphasis has been placed upon the fundamental hydroxyl stretching frequency of amphiboles; Burns and Strens (1966), Strens (1966), Burns and Prentice (1968), Addison and White (1968), and Burns and Law (1970) have assigned the various peaks within the band to specific cation-hydroxyl bands.

The present investigation was initiated in an attempt to produce a method of fingerprinting the various alkali amphiboles by using infra-red spectroscopy. The second reason was to extend the work on the hydroxyl stretching frequency from the simpler ordered structures of glaucophane and riebeckite to other alkali amphiboles, notably those with 'A' site occupancy.

8-2. Silicon-oxygen stretching and bending frequencies in alkali amphiboles.

8-2-1 (a). richterite series both synthetic and natural.

8-2-1 (b). richterite-tremolite series.

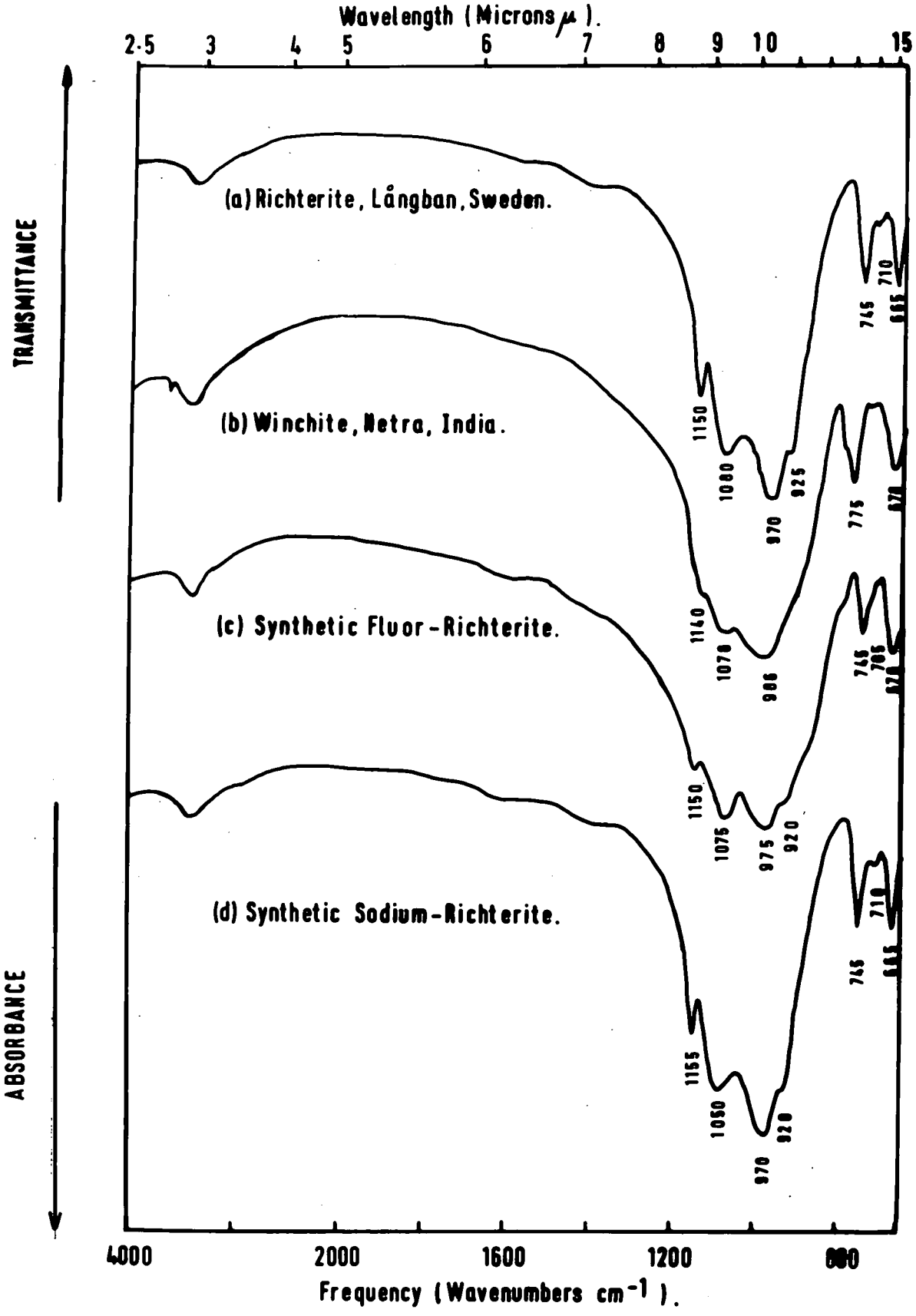

Fig 8-2 Infra-red spectra of richterite group minerals.

Fig.8-3 INFRA-RED SPECTRA OF SYNTHETIC RICHTERITES

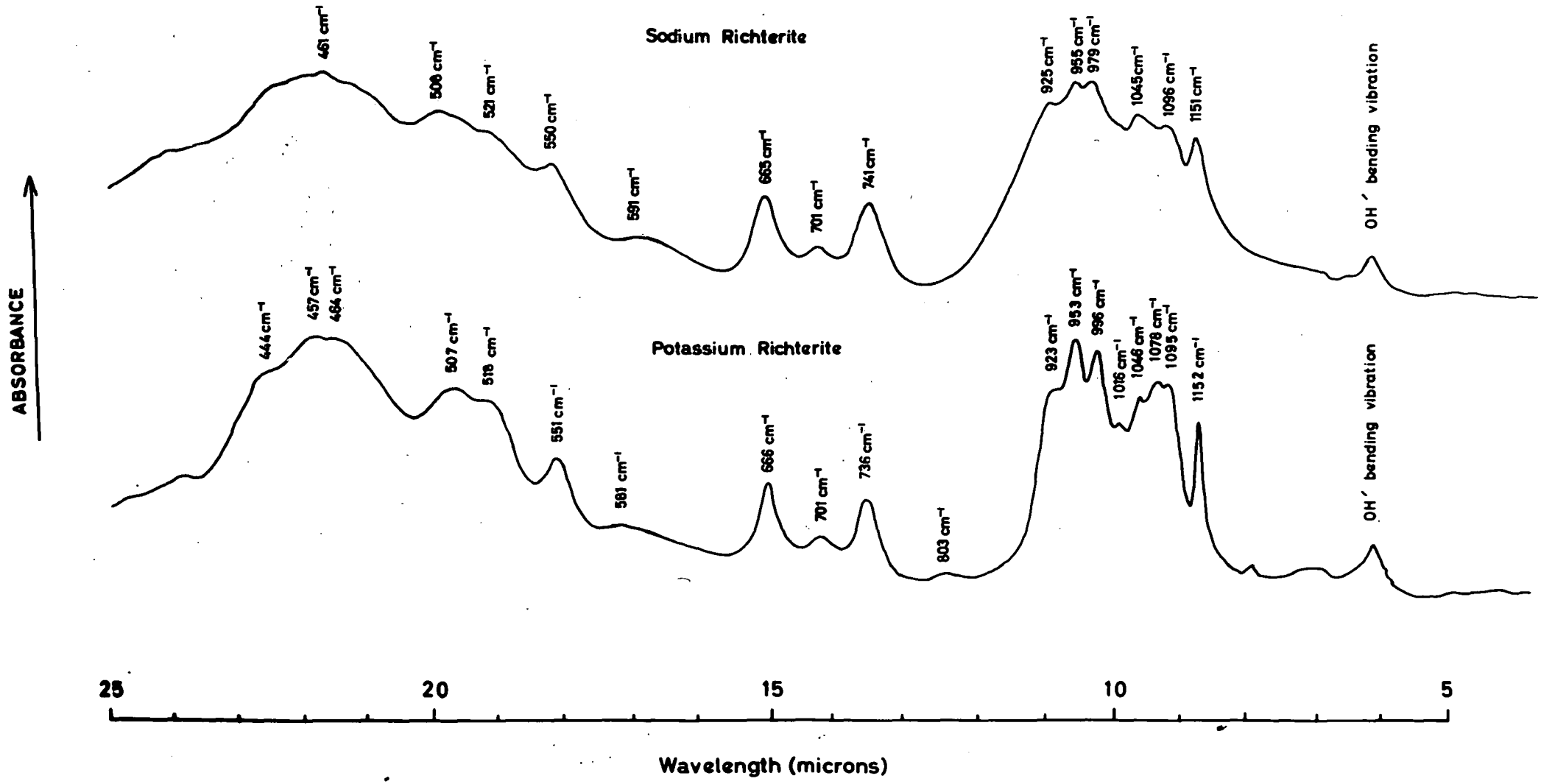

8-2-2. glaucophane-riebeckite series.

8-2-3. eckermannite-arfvedsonite series.

8-2-1. Richterite Series.

This is the first report of the infra-red spectrum of richterite and includes both synthetic and natural varieties.

(a) Natural Minerals

The infra-red spectra of two natural richterite minerals have been determined (Fig. 8-2). The specimens are from the type area of richterite (Långban, Sweden), and a richterite (winchite) from Netra, Madhya Pradesh, India.

Within the region of maximum absorption (1150-900 cm^{-1}) four peaks are shown. These peaks are the silicon-oxygen stretching frequencies; the silicon-oxygen bending frequencies occur between 775 and 660 cm^{-1}. The peaks at 745 cm^{-1} and 667 cm^{-1} are of equal intensity and this phenomenon is also shown in the synthetic varieties.

(b) Synthetic richterites

Synthetic sodium richterite is compared to fluor-richterite (Fig. 8-2) and potassium richterite (Fig. 8-3) and the resultant spectra are very similar. Fluorine, replacing hydroxyl, does not affect this region of the infra-red spectrum.

In the Si-O stretching region there are seven peaks in the sodium richterite spectrum with a maximum absorption at 970 cm^{-1}; the potassium variety has one additional peak at 1016 cm^{-1} which could be present in the sodium richterite if the spectrum were sharper. In the fluor-richterite the peaks are less well defined but are present in the same positions.

In the Si-O bending region there are many peaks developed down to 444 cm^{-1}.

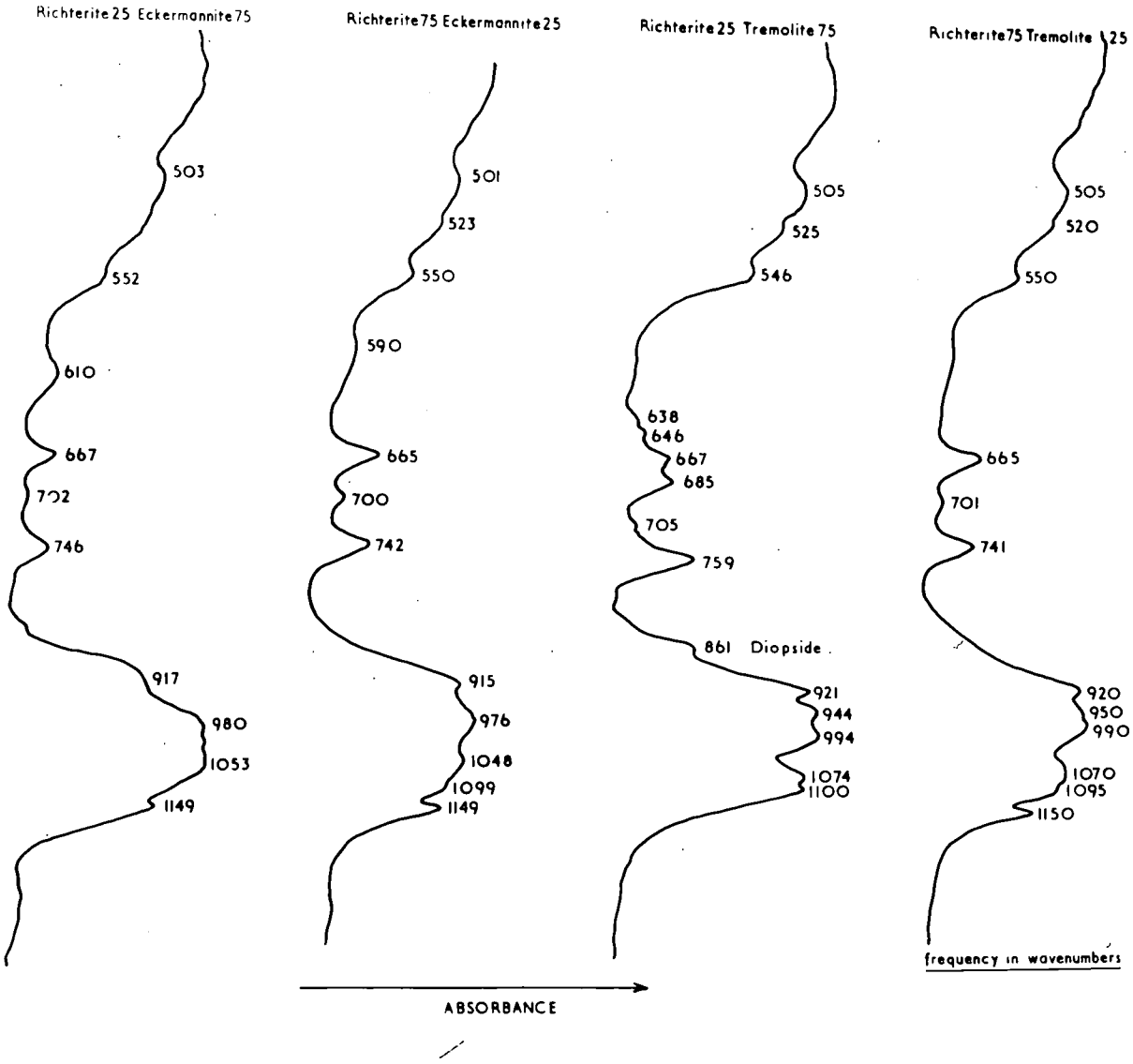

Fig. 8–4. Infra–red spectra of synthetic richterite–tremolites and richterite–eckermannites.

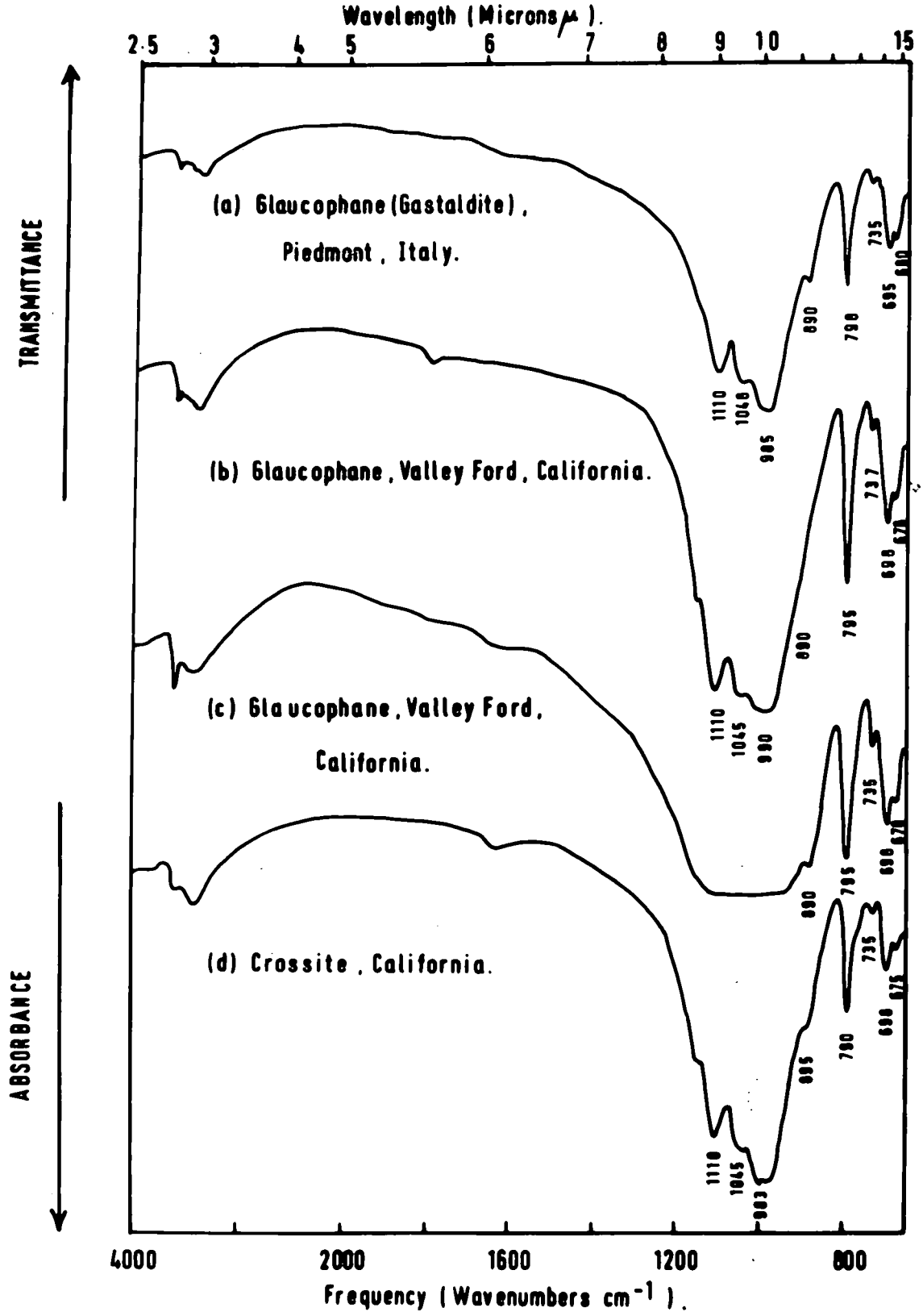

Fig 8-5a Infra-red spectra of glaucophane-crossite series.

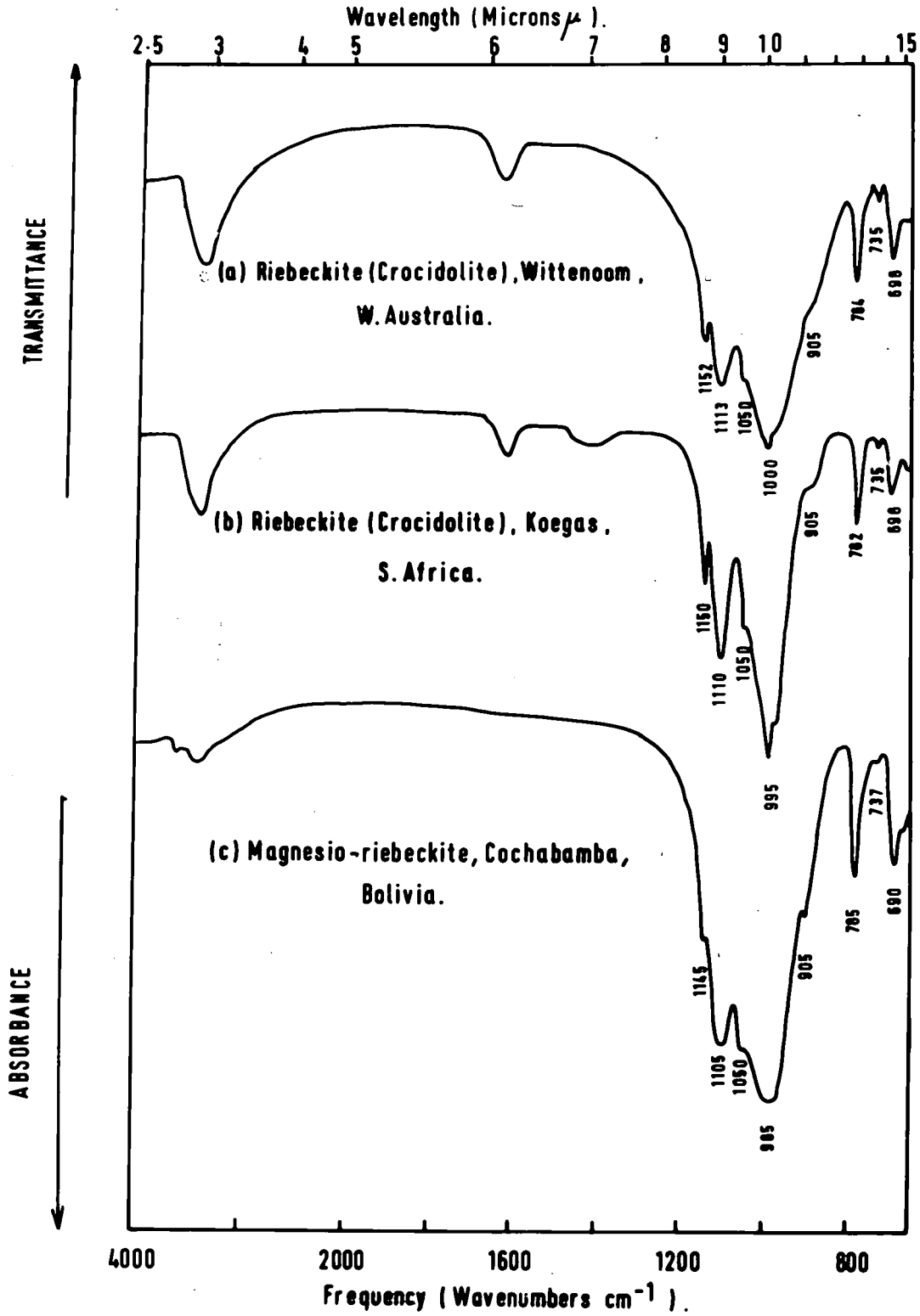

Fig 8-5 b Infra-red spectra of riebeckite & magnesioriebeckite.

8-2-1 (b). Richterite-Tremolite Series.

Intermediate compositions between the end-members richterite and tremolite were synthesized during the hydrothermal synthesis investigations (Chapter Two). The infra-red spectra for two of the intermediate compositions are shown in Fig. 8-4.

Richterite 75 - Tremolite 25 (R75-T25) has a spectrum extremely close to sodium richterite. Richterite 25 - Tremolite 75 (R25-T75) differs from the latter by lacking a peak at 1150 cm^{-1} and having an additional peak at 685 cm^{-1} which can be correlated with the data obtained by Lazarev and Tenisheva (1962) for tremolite. In addition to these peaks R25-T75 contains a non-amphibole peak which appears at 861 cm^{-1} and which can be correlated with diopside. This shows the high sensitivity of the infra-red method compared to X-ray and optical methods which did not detect this phase.

8-2-2. Glaucophane-Riebeckite Series.

The infra-red spectra of the glaucophane-riebeckite series have been the subject of various recent studies (Lyon 1962, 1968; Farmer in Hodgson et. al., 1965).

The Si-O stretching frequency region is the same for all the members of this series (Figs. 8-5a and b) and consists of five absorption peaks. The riebeckites all show extremely sharp spectra compared to members of the glaucophane group. In one sample of riebeckite (crocidolite from South Africa), in addition to the Si-O absorption peaks, there are two bands at 1430 cm^{-1} and 880 cm^{-1} which are caused by a small amount of carbonate impurity (possibly dolomite). The glaucophane-riebeckite series have, therefore, two fewer peaks in the Si-O stretching region than richterites.

The silicon-oxygen bending vibrations occur between 800 cm^{-1} and

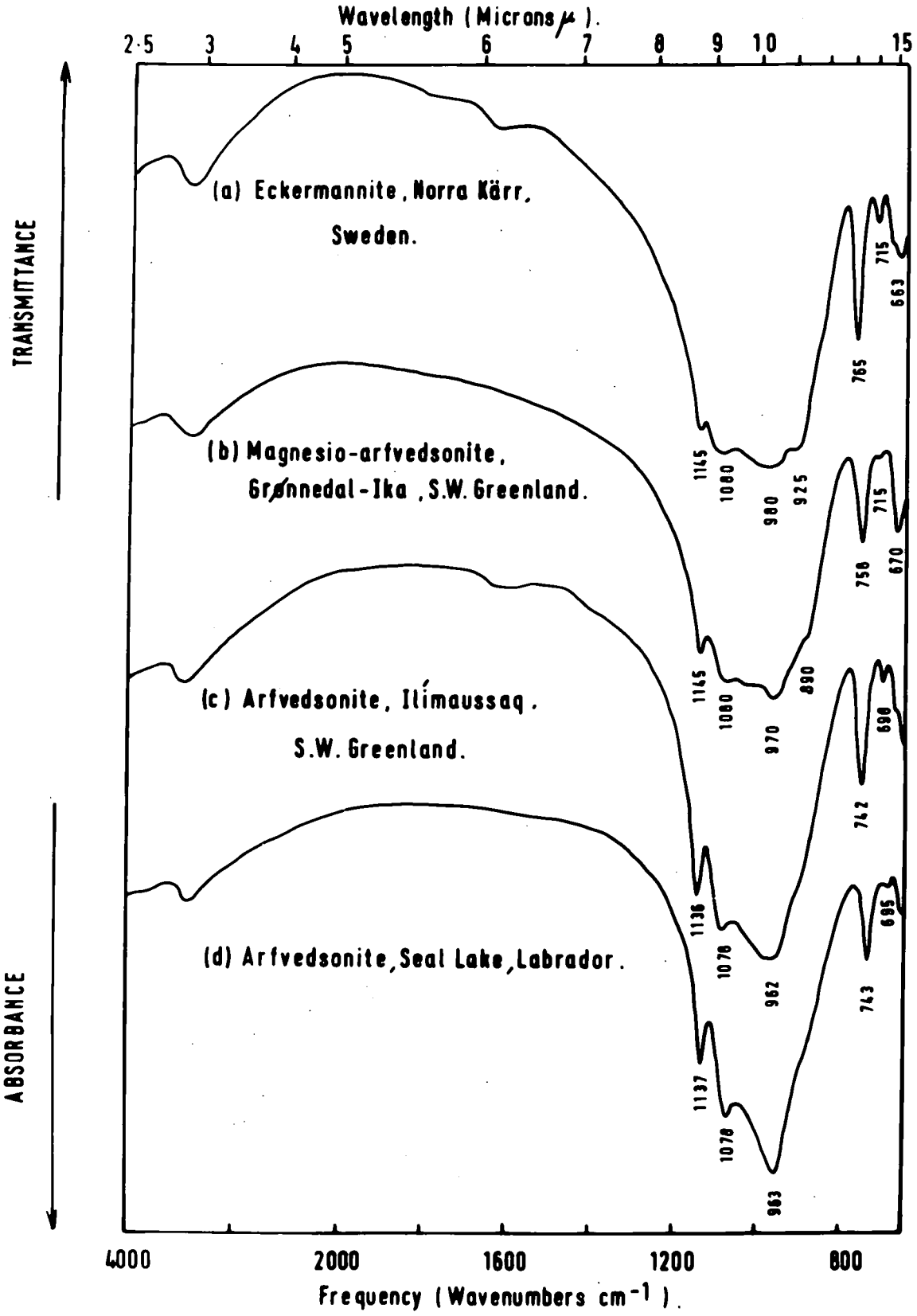

Fig 8-6 Infra-red spectra of the eckermannite–arfvedsonite series.

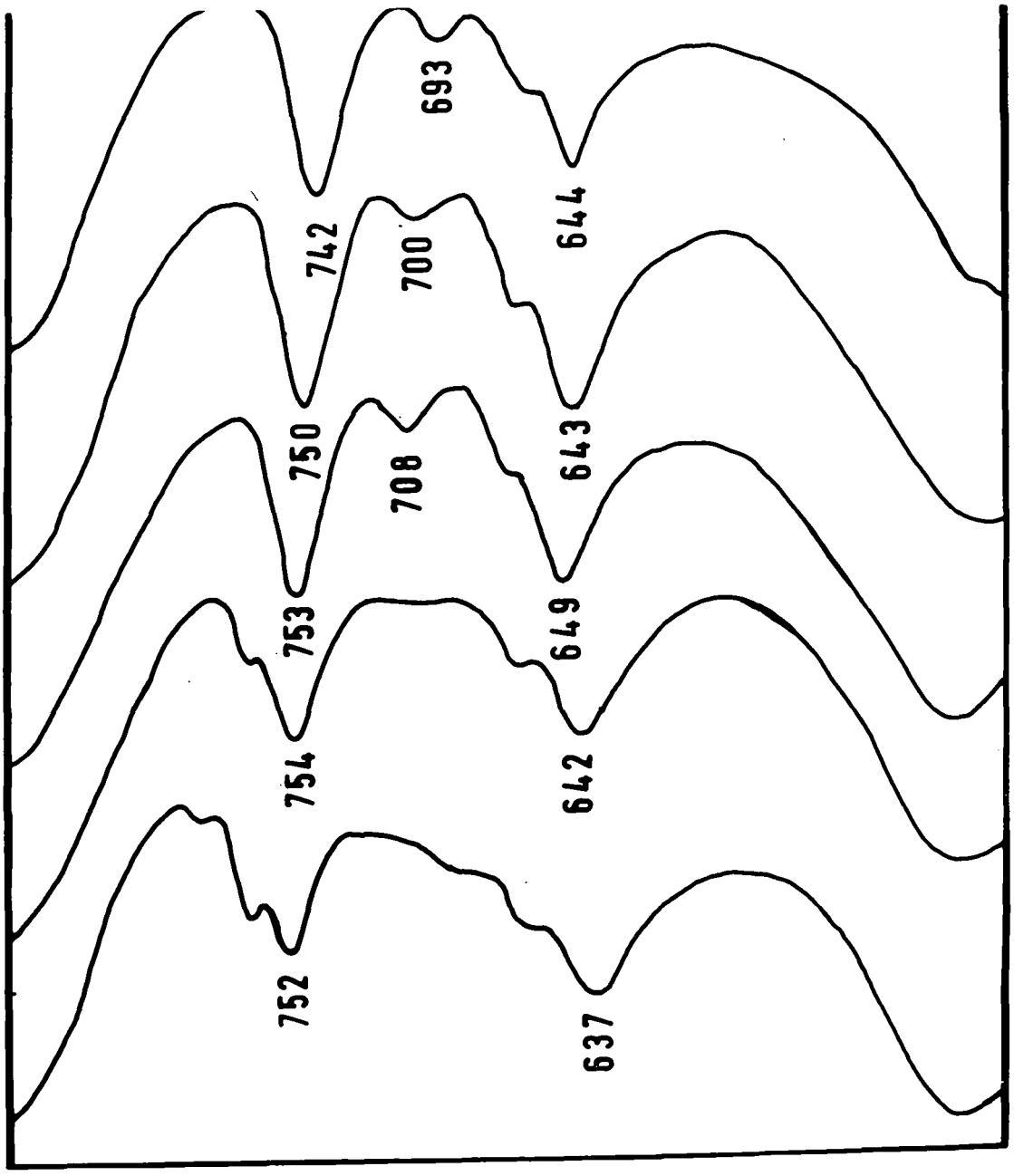

Fig. 8-7 Silicon - Oxygen bending frequencies of arfvedsonites from Nigeria and Greenland.

650 cm^{-1} (limit of spectrum) and are four in number. The magnesium rich varieties of this series possess a doublet peak between 695 and 675 cm^{-1} which is not present in the iron rich varieties (riebeckite).

8-2-3. Eckermannite-Arfvedsonite Series.

The present investigation is the first report on the infra-red absorption spectra for members of the eckermannite-arfvedsonite series.

Spectra for these minerals are shown in figure 8-6. In the magnesium-rich members of this group (eckermannite) there are four peaks in the silicon-oxygen stretching region whereas in the iron-rich varieties (arfvedsonites) there are three peaks, namely at 1140, 1078 and 963 cm^{-1}. The maximum absorption of the Si-O stretching frequency moves towards lower frequencies with increasing amounts of iron; 980 cm^{-1} for eckermannite and 960 cm^{-1} for the arfvedsonites. There is also a change in peak position to lower frequencies in the Si-O bending region.

Dr. V. C. Farmer determined the spectra of some riebeckite-arfvedsonites and arfvedsonites to reveal the position of one of the peaks in the 640 cm^{-1} region (Fig. 8-7). A large peak occurs at 644 cm^{-1} in an arfvedsonite from Ilímaussaq (D.U. 10951). This particular specimen also has peaks at 536, 444, and 416 cm^{-1}.

Discussion of the silicon-oxygen bending and stretching frequencies in the alkali amphiboles.

All the infra-red spectra of the alkali amphiboles are sufficiently different from sub-group to sub-group to utilise this method as a "fingerprint" technique.

In the Si-O stretching region (1150-850 cm^{-1}) there are seven peaks in the richterite spectrum, five in the glaucophane-riebeckite spectrum, four in the eckermannite spectrum and three in the arfvedsonite spectrum. These differences readily split them up into sub-groups. In

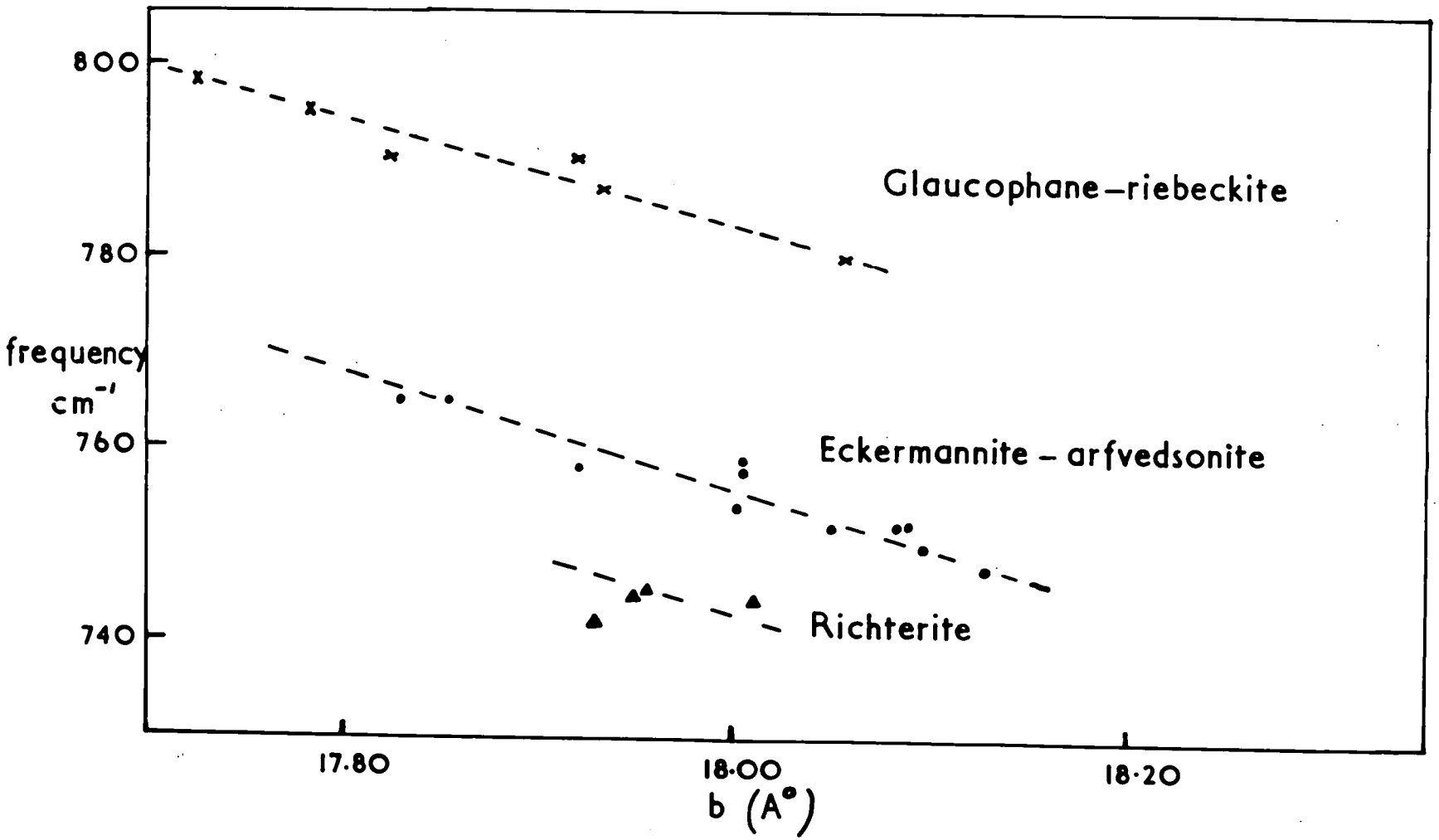

Fig.8–8. Variation in peak position (peak at 740–800 cm^{-1}) in the alkali amphiboles.

addition glaucophane possesses a peak at 890 cm^{-1} and a doublet peak at 698-678 cm^{-1} which are present in no other amphibole. The shift in maximum absorption of the Si-O stretching frequency of the eckermannite-arfvedsonite series has already been noted.

In the Si-O bending region the alkali amphiboles all have an absorption peak between 740-800 cm^{-1}, this appears to be the peak most susceptible to variation with changes in chemical composition.

Although this absorption peak changes with composition, it is difficult to assign it to a particular substitution. When the position of this peak is plotted against the b_o cell parameter, which has been shown to be sensitive to changes in composition, there are three curves corresponding to the three alkali amphibole sub-groups: glaucophane-riebeckite, eckermannite-arfvedsonite, and richterite (Fig. 8-8).

The above study indicates that it is possible to determine the type of alkali amphibole from a study of the infra-red spectra.

8-3. Infra-red absorption studies of the hydroxyl stretching frequency in alkali amphiboles.

To date there have been a series of infra-red studies by Burns et. al. who have worked upon the fundamental stretching frequency of the hydroxyl ion in clinoamphiboles.

Burns and Strens (1966) and subsequently Strens (1966), Burns and Prentice (1969), Burns and Law (1970), and Addison and White (1968) concentrated upon amphiboles with a vacant 'A' site. The present study confirms this work and, in addition, extends it to alkali amphiboles with partially or completely filled 'A' sites.

The hydroxyl ion (O(3) site) lies in a hole formed by the linking of Si_6O_{18} units and closed at each end by $(Mg,Fe^{2+})_3OH$ groups. The O-H bond projects towards the central void away from the metal ions

(Burns and Strens, 1966). The orientation of this bond was determined using microscopic techniques in conjunction with the overtone bands (7200 cm^{-1}) of the hydroxyl stretching frequency, and only applies to amphiboles with a vacant 'A' site (Burns and Strens ibid.).

The fundamental band of the hydroxyl stretching frequency shows a single sharp peak in iron-free tremolite (designated A by Burns and Strens). As the amount of iron increases additional peaks (B, C, and D) appear at lower frequencies; peak A decreasing in intensity simultaneously. Thus for the tremolite-ferrotremolite series the peaks A, B, C, and D are at 3673 cm^{-1}, 3660 cm^{-1}, 3648 cm^{-1} and 3625 cm^{-1} while in the cummingtonite-grunerite series they occur at 3665, 3650, 3635, 3615 cm^{-1} respectively.

The positions of these peaks depend upon the electronegativity of the element in the octahedral (M(1), M(3)) sites to which the hydroxyl is bonded. The magnesium ion has an electronegativity of 1·23 and ferrous iron 1·64, thus the ion with the lower electronegativity will form a weaker bond with the hydroxyl ion and therefore raise the frequency of the absorption band.

There are eight distinguishable ways of distributing Fe^{2+} and Mg over three inequivalent positions, reduced to six by the equivalence of the M(1) sites and further reduced to four by the pseudo-trigonal symmetry of the ($M_1M_1M_3$) OH sites (Burns and Strens, ibid.).

The four peaks have been designated by Burns and Strens (op. cit.) as follows:-

$$A = (MgMgMg)^1$$

$$B = (MgMgFe^{2+})^3 \text{ or } (MgMgFe^{2+})^1, (MgFe^{2+}Mg)^1, (Fe^{2+}MgMg)^1$$

$$C = (MgFe^{2+}Fe^{2+})^3$$

$$D = (Fe^{2+}Fe^{2+}Fe^{2+})$$

The superscripts refer to the number of indistinguishable

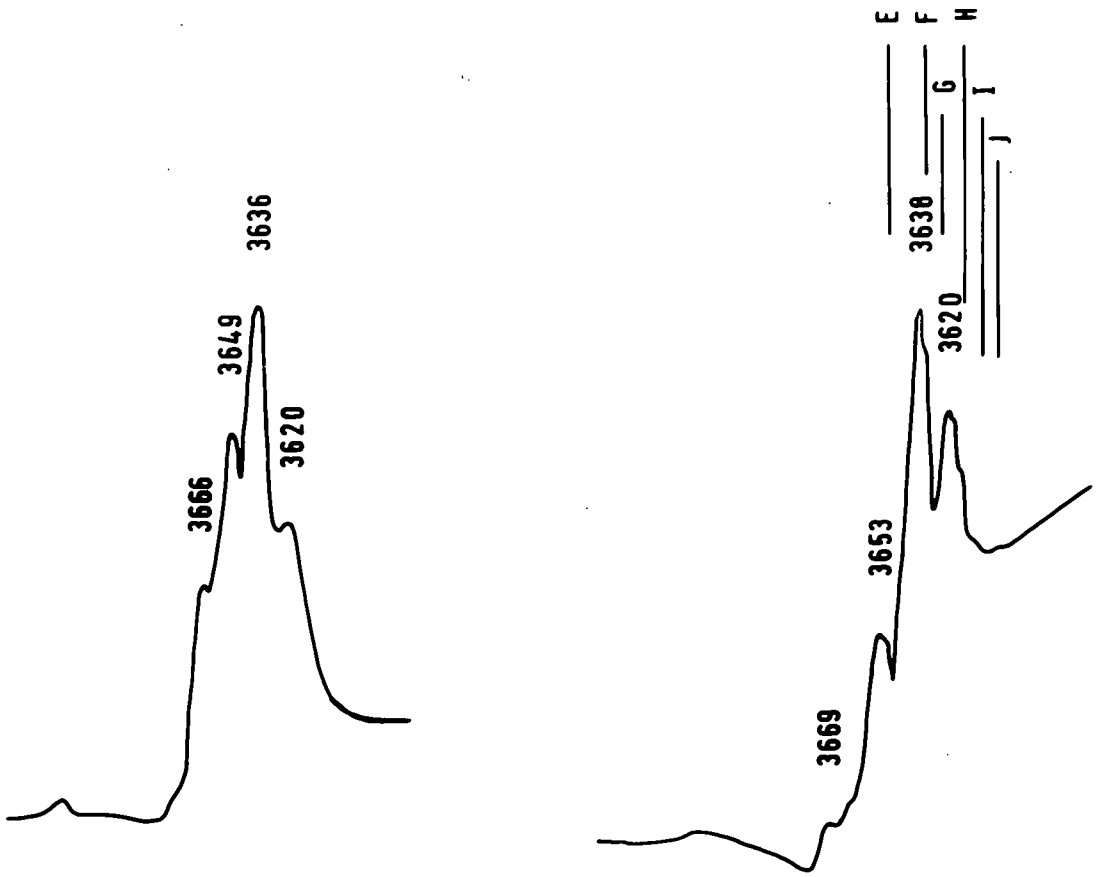

(a) Hydroxyl stretching frequency of Glaucophane (Valley Ford, California.).

(b) Hydroxyl stretching frequency of Riebeckite (W. Australia).

Fig.8-9 Fundamental hydroxyl stretching frequency of the Glaucophane–Riebeckite series.

distributions over the three sites bonded to the hydroxyl (M(1), M(3), M(1)) in the amphiboles.

When three cations are co-ordinated to OH there are ten different three-cation groups.(Burns and Prentice, 1969).

If the assumption of random mixing of two cations between three sites is made then the calculated relative absorbances of the various bands are given by:-

$$A = [\overline{Mg}]^3$$

$$B = 3[\overline{Mg}]^2[\overline{Fe}]$$

$$C = 3[\overline{Fe}]^2[\overline{Mg}]$$

$$D = [\overline{Fe}]^3$$

In section 8-3-2-2 the relative intensities of each peak in the natural minerals is calculated using the above formula for random mixing and then compared to the intensities and positions of the observed peaks.

8-3-1. Hydroxyl stretching frequency of the glaucophane-riebeckite series

The four major peaks for this series are shown in Fig. 8-9. The frequency of these bands occurs between those for the tremolite-ferrotremolite series and the cummingtonite-grunerite series. The major difference between these amphiboles is the M(4) occupant, calcium in tremolite, ferrous iron or magnesium in commungtonites and sodium in the glaucophane-riebeckite group. If the overall position is dependent upon the M(4) occupant (Burns and Strens op. cit.) then the intermediate position of glaucophane is correct.

Burns and Strens (op. cit.) have devised a method for determining the amount of ferrous iron and magnesium in M(1) and M(3) sites from the intensities of peaks A to D:

$$Fe(II) = 0.A + 1.B + 2.C + 3.D$$

$$Mg = 3.A + 2.B + 1.C + 0.D$$

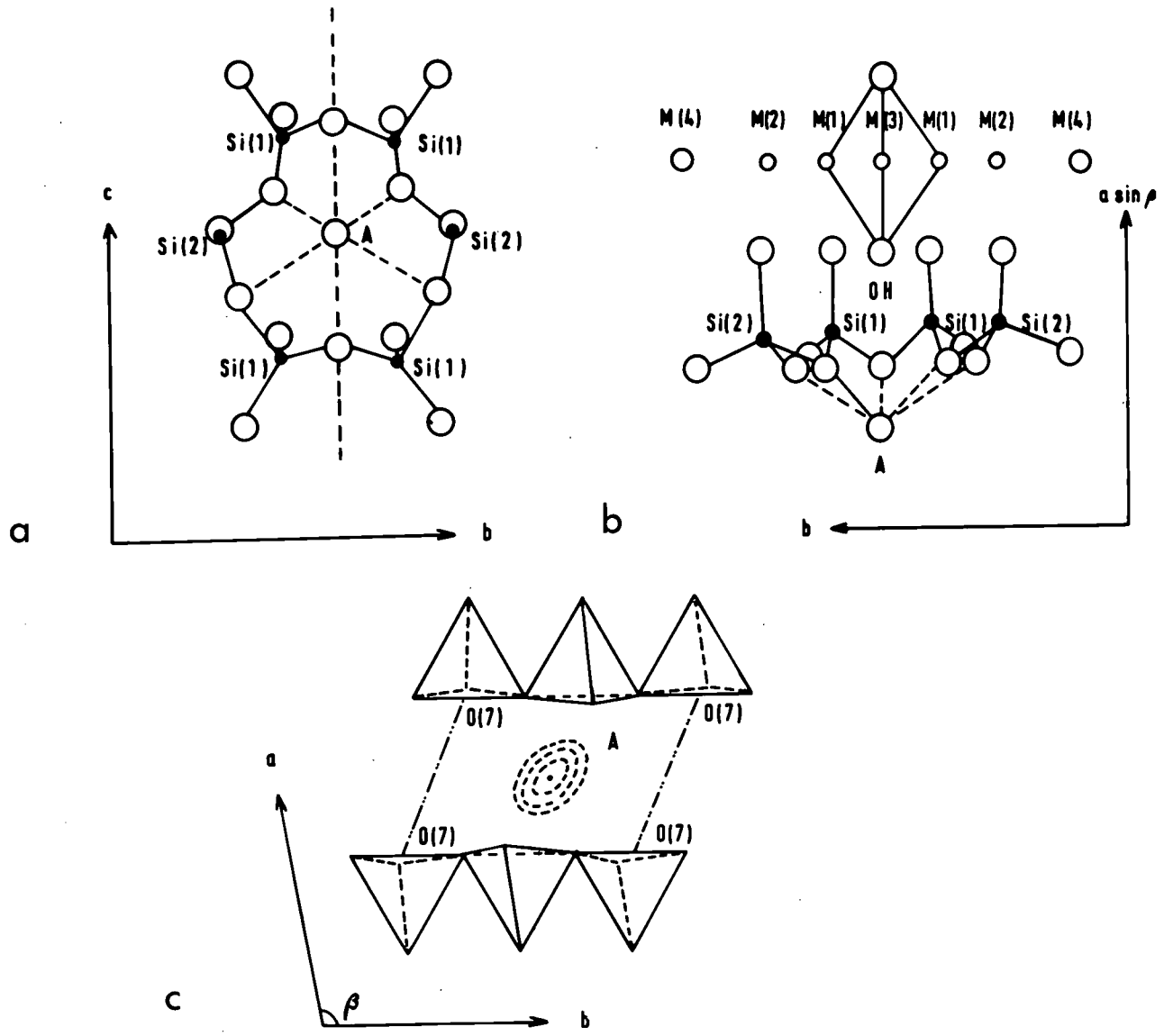

Fig.8-10 Position of the 'A' site in the amphibole structure.

This follows from the designations, given above, to each of these bands. Burns and Prentice (1968) determined the distribution of iron cations in riebeckite (crocidolite). They found that in addition to iron (II) and magnesium in M(1) and M(3), iron (III) also entered these sites to a lesser extent. The spectra for these riebeckites and glaucophanes are shown in figure 8-9 where the author's results are compared to those of Burns and Prentice. The additional bands E to J are the result of iron (III) replacing magnesium and iron (II) in M(1) and M(3).

8-3-2. Hydroxyl stretching frequency of alkali amphiboles with 'A' site occupancy

In the preceding section alkali amphiboles with no 'A' site occupancy were discussed, in the present section the author sets forward results for amphiboles with alkali ions (Na^+, K^+) in the 'A' site.

The 'A' site in the monoclinic amphiboles is surrounded by twelve oxygens (Ghose, 1961; Papike and Clark, 1968; and Papike, Ross and Clark, 1969) i.e. $4(A\text{-}O_5)$, $4(A\text{-}O_6)$, $4(A\text{-}O_7)$. The $A\text{-}O_7$ distances are divided into two short and two long bonds (Papike and Clark, op. cit.).

Papike et. al. (1969) conclude, from structural considerations, that sodium and potassium occupy slightly different locations in the 'A' site (hypothetical position at $\frac{1}{2}$, 0, 0). The electron density map of this site shows a distribution about $\frac{1}{2}$, 0, 0 as shown in Fig. 8-10c.

The 'A' site (Fig. 8-10a, b, c) is directly above the O(3) site which is occupied by a monovalent anion (OH^-, F^-, or possible Cl^-). The sheet silicates are similar to the amphiboles and Farmer and Russell (1964) studied the effect of introducing potassium into the talc structure to produce phlogopite where potassium ions lie directly

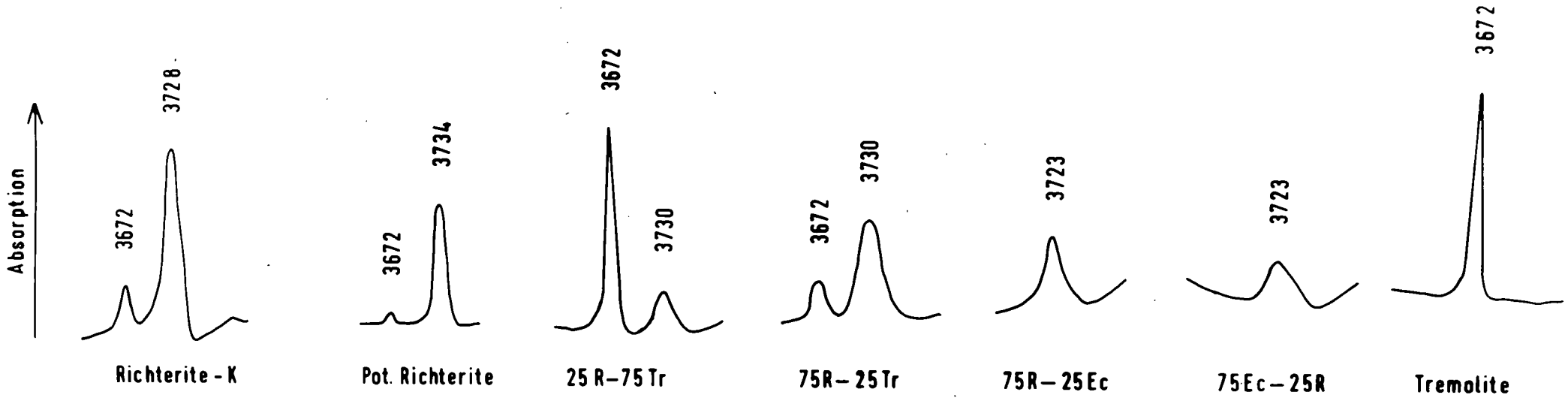

Fig.8-11 Fundamental stretching frequency of hydroxyl in synthetic alkali amphiboles.

above the hydroxyl ions. In talc the fundamental hydroxyl stretching frequency is at 3677 cm^{-1}, whereas in phlogopite it is at 3710 cm^{-1}. This increase in frequency would arise, according to Farmer and Russell (ibid.) because the hydroxyl would approach the alkali ions and move away from the octahedral cations. A similar situation would be expected for the amphiboles.

Several synthetic and natural alkali amphiboles have been studied and the results presented here:-

8-3-2-1 Synthetic amphiboles

(a) sodium richterite and potassium richterite.

(b) richterite-tremolite series.

(c) richterite-eckermannite series.

1(a) The richterite composition is particularly illustrative because one can study the effect of changing the 'A' site occupancy whilst keeping the octahedral cations (Mg) constant. In figure 8-11 the infra-red spectra for the region 4000-3000 cm^{-1} are shown for sodium richterite and potassium richterite. In both these specimens there is a small peak at 3672 cm^{-1}; in addition sodium richterite has a large peak at 3728 cm^{-1} while that of potassium richterite occurs at 3734 cm^{-1}.

1(b) Several members of the richterite-tremolite series were synthesized during the hydrothermal synthesis experiments. Members of this series have had their cell dimensions determined establishing that they are, in fact, of one phase and not a mixture of the two end-members. The substitution involved in changing composition from tremolite to richterite is, $\square\ Ca \rightleftharpoons NaNa$. This substitution involves only the M(4) and the 'A' sites, the latter being vacant in tremolite.

In figure 8-11 the hydroxyl bands are shown for the end-members richterite and tremolite together with two intermediate compositions.

The peak at 3672 cm^{-1} decreases in intensity from tremolite to richterite whilst the higher frequency peak at 3728 cm^{-1} increases. The peaks are very sharp indicating good ordering in the octahedral sites.

1(c) Two members of the richterite-eckermannite series were synthesized during the hydrothermal synthesis experiments. Unfortunately eckermannite yields a very poor infra-red spectrum and further work is needed on this composition. Spectra for the two intermediate compositions are shown in figure 8-11. The fundamental stretching frequency of the hydroxyl ion results in one peak at 3723 cm^{-1}. In addition there is a noticeable broadening of this peak as the amount of eckermannite component is increased. This peak broadening may be attributed to increased disorder in the M(1), M(3) sites due to the introduction of aluminium in octahedral co-ordination.

Discussion

The hydroxyl ion lies directly beneath the 'A' site thus as this site is filled, some effect upon the fundamental stretching frequency would be expected. The hydroxyl would approach the monovalent cation and deviate away from the octahedral cations at M(1) and M(3) thus raising the frequency of the vibration.

In the richterites there is a small peak at 3672 cm^{-1} which corresponds to unperturbed hydroxyl ion. The presence of this peak suggests incomplete filling of the 'A' site, despite careful preparation.

The higher frequency of the perturbed hydroxyl in potassium richterite (3734cm^{-1}) compared to sodium richterite (3728cm^{-1}) is due to its higher effective charge.

The theory outlined above is supported by the spectra for intermediate compositions between richterite and tremolite. The perturbed peak increases at the expense of the unperturbed peak with the proportion of richterite component in the composition. The

intermediate compositions between richterite and eckermannite, with completely filled 'A' sites, show only the perturbed peak.

8-3-2-2 Natural Minerals

(a) Juddite (manganoan-magnesioarfvedsonite) Mahdya Pradesh, India

The analysis of this mineral (appendix 3) indicates that the main occupants of the M(1) and M(3) sites are magnesium (2·73 atoms) and manganese (0·27 atoms) and the 'A' site contains 0·72 atoms of sodium plus potassium. In an infra-red spectrum of the region of the hydroxyl stretching frequency (fig. 8-12a) there are three peaks; 3671cm^{-1}, 3700cm^{-1}, 3727cm^{-1}.

The results of a calculation of the statistical frequency of occurrence of magnesium and manganese co-ordinated to the hydroxyl ions are as follows:-

$(Mg)^3$	75·3%
$3(Mg)^2(Mn)$	22·3%
$3(Mg)(Mn)^2$	2·2%
$(Mn)^3$	0·7%

If we assume random ordering of the ions in M(1) and M(3) and a partially occupied 'A' site then four peaks should appear in the spectrum. In the observed spectrum only three peaks appear, of which only one (3671cm^{-1}) can be assigned with any certainty to unperturbed hydroxyl co-ordinated to (MgMgMg).

(b) Winchite (manganoan-magnesioriebeckite) Netra, Mahdya Pradesh, India

The infra-red spectrum for winchite shows two peaks (3665cm^{-1} and 3693cm^{-1}) in the hydroxyl stretching region. The chemical composition (Appendix 3) indicates that magnesium (2·80 atoms) and manganese (0·20 atoms) occupy the M(1) and M(3) sites and sodium (0·41 atoms) and potassium (0·12 atoms) occupy the 'A' site.

A calculation of the relative intensities expected from the chemical analysis yields the following results:-

$(Mg)^3$ = 81·2%

$3(Mg)^2(Mn)$ = 17·4%

$3(Mg)(Mn)^2$ = 1·2%

$(Mn)^3$ = 0·2%

If the 'A' site contains 0·53 atoms of sodium and potassium we should expect four peaks in the hydroxyl stretching frequency region. Only two peaks are present in the spectrum of which the 3665cm^{-1} peak could be assigned to unperturbed hydroxyl co-ordinated to (MgMgMg).

(c) Tirodite, Tirodi, Madhya Pradesh, India

X-ray and chemical analyses of this mineral indicate that it is intermediate in composition between cummingtonite and richterite. The chemical analysis shows that ½ of the 'A' sites are occupied by sodium and potassium. Assuming that magnesium (2·59 atoms) and manganese (0·41 atoms) are the sole occupants of the M(1) and M(3) sites, the following calculation of the statistical frequency of occurrence ensues:-

$(Mg)^3$ = 64·59%

$3(Mg)^2(Mn)$ = 30·34%

$3(Mg)(Mn)^2$ = 4·82%

$(Mn)^3$ = 0·25%

We should therefore expect four peaks in the infra-red spectrum if 'A' site occupancy perturbs the hydroxyl stretching frequency. There are three peaks in the spectrum at 3659cm^{-1}, 3665cm^{-1}, and 3693^{-1}. The major peak at 3669cm^{-1} can be assigned to unperturbed hydroxyl co-ordinated to (MgMgMg). The shoulder at 3659cm^{-1} may possibly be due to a (MgMgMn) group of ions.

In these three magnesium rich clino-amphiboles with partial 'A' site occupancy we should expect a perturbed (MgMgMg) peak at ~3730cm^{-1} as in the synthetic samples. Only in the juddite is there a peak in this region (3727cm^{-1}) which could possibly be assigned to perturbed

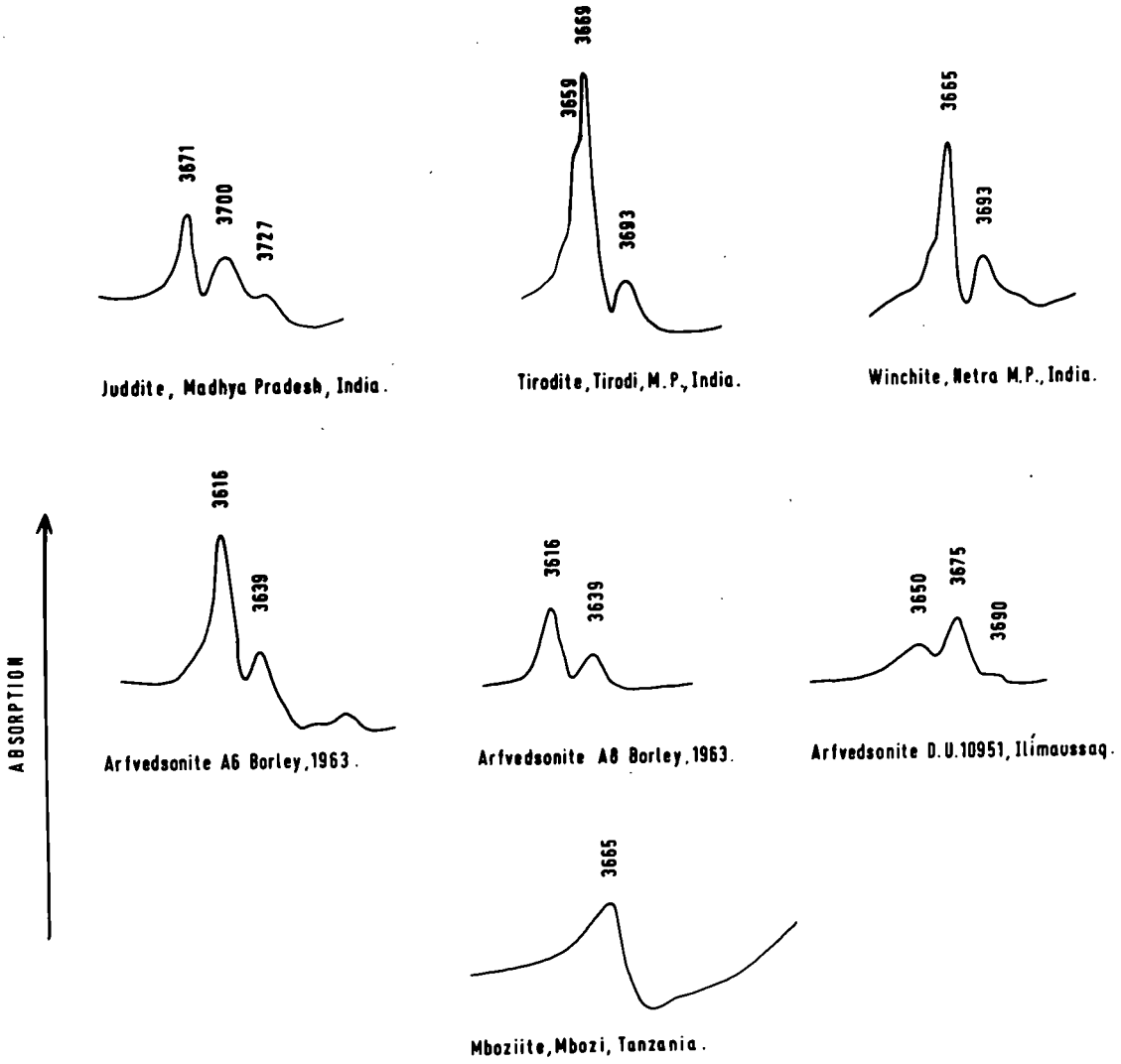

Fig. Fundamental hydroxyl stretching frequency of natural alkali amphiboles.

hydroxyl co-ordinated to (MgMgMg). It remains difficult to assign the peak at ~ 3695cm^{-1}.

(d) Riebeckite-arfvedsonite (Nigeria) and arfvedsonite (D.U.10951 Greenland)

Two of the samples are from Nigeria (A6, A8, Borley 1963) and the third (D.U. 10951) is an arfvedsonite from Ilímaussaq, S.W. Greenland. The Nigerian specimens contain very high fluorine concentrations (A6, 0·80 atoms, A8 1·16 atoms) whereas the Greenland sample contains only 0·16 atoms of fluorine. The main occupants of the M(1), M(3) sites are ferrous iron, ferric iron, and lithium. It is assumed that the amount of lithium in the M(1), M(3) sites is balanced by ferric iron according to the equation:-

$$Fe^{2+} + Fe^{2+} \rightleftharpoons Fe^{3+} + Li$$

A calculation of the statistical frequency of occurrence of Fe^{3+}, Fe^{2+}, and Li co-ordinated to hydroxyl groups is set out below in the order of expected appearance in the spectrum:-

	10951	A6	A8
$(Li)^3$	0·06%	0·27%	0·84%
$3(Li)^2(Fe^{2+})$	1·73%	4·23%	7·36%
$3(Li)^2(Fe^{3+})$	0·17%	0·82%	2·52%
$3(Li)(Fe^{2+})^2$	17·35%	21·77%	21·48%
$6(Li)(Fe^{2+})(Fe^{3+})$	3·47%	8·47%	14·72%
$3(Li)(Fe^{3+})^2$	0·17%	0·82%	2·52%
$(Fe^{2+})^3$	57·86%	37·32%	20·90%
$3(Fe^{2+})^2(Fe^{3+})$	17·35%	21·77%	21·48%
$3(Fe^{2+})(Fe^{3+})^2$	1·73%	4·23%	7·36%
$(Fe^{3+})^3$	0·06%	0·27%	0·84%

The octahedral (M(1) M(3)) occupants are as follows:-

$(Mg)^3$ = 0·2%

$3(Mg^2)(Fe^{2+})$ = 1·2%

$3(Mg)(Fe^{2+})^2$ = 17·4%

$(Fe^{2+})^3$ = 81·2%

The coupled substitutions $MgFe^{+++} \rightleftharpoons Fe^{++}Al$ and $MgAl \rightleftharpoons Fe^{++}Fe^{+++}$ do not appear to be important in this compositional cell.

In minerals of the richterite compositional cell none of the aforementioned substitutions appear to be important. The only substitution of importance is $\square Ca \rightleftharpoons Na(K)Na$ and it indicates a complete solid solution series between richterite and tremolite. Sodium and potassium are completely interchangeable in the 'A' sites of the richterites reaching the highest potassium contents in magnophorites (potassium richterites).

Many of the analyses cited in the literature and plotted onto various diagrams do not show the extent of substitution between the compositional cells. A useful way of representing amphiboles of intermediate composition has been found by using those substitutions in the Y sites which are balanced by substitutions in Z and X (designated YZX) and plotting these against Y atoms. When these substitutions are plotted against each other they reveal complete solid solution between riebeckite and arfvedsonite; magnesioriebeckite and magnesioarfvedsonite; and richterite and eckermannite.

A suggested nomenclature for these intermediate compositions could be:

A) riebeckite 2.00 - 1.60 YZX

riebeckite-arfvedsonite 1.60 - 1.20 YZX

arfvedsonite 1.20 - 0.80 YZX

These suggestions are in general agreement with those of Kovalenko (1968) except that Kovalenko accepts an upper limit in the A + X sites of 3.3 atoms and a lower limit of 1.5 atoms which are outside the limitation accepted by the author for a superior analysis.

B) magnesioriebeckite 2.00 - 1.40 YZX

magnesioarfvedsonite 1.40 - 0.80 YZX

The limits of these divisions are based upon the range of compositions of magnesioriebeckites from crystalline schists. An alternative suggestion could be similar to the riebeckite-arfvedsonites.

c) richterite 0.50 - 0 YZX

eckermannite 0.50 - 1.00 YZX

A survey of the possible substitutions within the alkali amphiboles has indicated that there are few areas of Phillips compositional space which do not have natural amphiboles within them. Two possible miscibility gaps can be found in the ferro-eckermannite and the miyashiroite fields. There is no available analysis closer to miyashiroite than $M_{60}Gl_{40}$. These may indicate two true gaps in possible amphibole compositions or that amphiboles of these compositions have yet to be found in nature.

The alkali amphiboles from the Ilímaussaq undersaturated nepheline syenite all plot in the arfvedsonite composition cell. The earliest alkali amphibole is close to katophorite in composition and the later amphiboles become more arfvedsonitic. The fluorine content of the amphiboles decreases with fractionation. This behaviour is in contradistinction to that of the amphiboles from the Kûngnât and Tugtutôq intrusions which show an increase in fluorine with differentiation. Apatite is an early crystallizing phase in Tugtutôq and Kûngnât and this will tend to take up fluorine. When apatite ceases to crystallize fluorine is then available to enter the amphibole lattice. Apatite is absent from the Ilímaussaq rocks and therefore fluorine can enter the amphibole lattice.

The main substitutions in the amphiboles from Ilímaussaq with increasing fractionation are: 1) $CaAl \rightleftharpoons NaSi$, 2) $CaFe^{++} \rightleftharpoons NaFe^{+++}$, 3) $Fe^{++}Fe^{+++} \rightleftharpoons LiFe^{+++}$, 4) $F^- \rightleftharpoons OH^-$. All the substitutions have been ascribed to decreasing temperature and increasing peralkalinity.

In the late stage lujavritic rocks the amphiboles contain high concentrations of potassium (up to 0.65 atoms). This element has been shown to be exchanged between amphibole and nepheline in these rocks. The main factor which may facilitate the transport of potassium between amphibole and nepheline is the high volatile content of these late stage rocks. This is the first natural example to support the evidence of alkali exchange in amphiboles noted by Huebner and Papike (1971) in synthetic richterites.

Lithium is considered to enter the M(1) and M(3) sites in these arfvedsonites and the charge deficiency made up by the introduction of a trivalent cation. Evidence for lithium entering M(1) and M(3) may be cited from a study of the hydroxyl stretching region of an amphibole from a lujavrite which shows a small perturbed peak at 3690 cm^{-1}. This peak is equivalent to that found by Addison and White (1968) in a Nigerian riebeckite-arfvedsonite.

The Ilímaussaq intrusion is an undersaturated syenite whereas Kûngnât and Tugtutôq are saturated syenite intrusions. The behaviour of these extreme examples is reflected in the amphibole compositions. Aluminium is available for incorporation into the amphiboles in the Ilímaussaq intrusions but in the saturated syenites quartz becomes an interstitial phase early in the differentiation sequence, hence the amphiboles will be low in tetrahedral aluminium. The main substitutions in the Tugtutôq dykes are: 1) $CaFe^{++} \rightleftharpoons NaFe^{+++}$, 2) $\square Ca \rightleftharpoons NaNa$, 3) $CaAl \rightleftharpoons NaSi$ (minor), 4) $OH^- = F^-$. These amphiboles in Tugtutôq are ferro-richterites and arfvedsonites with late stage development of riebeckite-arfvedsonite. These, therefore, define a trend in amphibole composition from saturated and oversaturated alkaline bodies whereas Ilímaussaq is typical of undersaturated compositions.

A study of all the cell parameters of synthetic amphiboles has shown that the variation of the b_o axis depends upon the occupancy of the M(4) and M(2) sites. This conclusion supports that originally put forward by Colville et. al. (1966), and contrary to the conclusions of Ernst (1968) who maintained that the occupant of M(2) controlled the b_o axis repeat and Forbes (1971) that M(2) and the 'A' site occupant affected the b_o axis. The role of the M(4) occupant is seen in the natural amphiboles where the calciferous amphiboles have b_o axes approximately 0.10 A^o longer than alkali amphiboles for the same M(2) site occupancy.

The $a_o \sin\beta$ dimension represents the unit repeat across facing chains and appears to be controlled by the occupants of the octahedral, and tetrahedral sites (Colville et. al., 1966) and the 'A' site (present study). Alkali amphiboles with sodium in the 'A' site have larger $a_o \sin\beta$ dimensions than those with vacant 'A' sites. Potassium substitution in the 'A' sites also increase this dimension (Huebner and Papike, 1970). The high potassium arfvedsonites from the Ilímaussaq intrusion have larger $a_o \sin\beta$ parameters than the other arfvedsonites.

Whittaker (1960) discussed the relationship between M(4) occupant and the β angle of monoclinic amphiboles. The β angle shows a strong positive correlation with calcium content but additional factors in the alkali amphiboles appear to be the magnesium content and potassium in the 'A' site both of which increase the β angle.

The variations in the c_o axis of alkali amphiboles are less than half the other parameters and in general the longest c_o axes are in amphiboles with high iron content, and the 'A' site fully occupied.

When the $a_o \sin\beta$ dimension is plotted against the β angle the amphiboles split up into their various groups. Indeed the $a_o \sin\beta$

parameter appears to be the most useful in determining to which series the alkali amphibole belongs when plotted against the total iron content of the mineral.

The main effects produced by the following substitutions in minerals of alkali amphibole composition are:

A) Minerals of richterite composition

1) □ Ca → NaNa, 2) Na → K, 3) Mn → Mg, and 4) $OH^- \rightarrow F^-$

a_o increases
b_o decreases
β decreases

a_o, b_o, c_o, β all increase

b_o increases a_o decreases

B) Minerals of glaucophane-riebeckite composition

1) Al → Fe^{+++}, 2) Mg → Fe^{++}, 3) MgAl → $Fe^{++}Fe^{+++}$

a_o, b_o, c_o, β increase

a_o, b_o, c_o increase
β decreases

a_o, b_o, c_o increase
β decreases

C) Minerals of eckermannite-arfvedsonite compositions.

The three substitutions in the glaucophane-riebeckite series produce the same effects in the eckermannite-arfvedsonite series.

1) □ $Fe^{+++} \rightarrow NaFe^{++}$, 2) Na → K, 3) $OH^- \rightarrow F^-$

a_o, β increase

a_o, β increase b_o decreases

Additional substitutions in the alkali amphiboles which affect cell parameters are CaAl → NaSi decreases b_o, c_o, and the β angle and NaMg → □Al produces a decrease in all the parameters.

It is possible to utilise infra-red spectroscopy to "fingerprint" the various alkali amphibole sub-groups. All the alkali amphiboles have a peak at $\sim$ 1150 cm^{-1} in the Si-O stretching region which calciferous amphiboles do not appear to have. The number of peaks within the Si-O stretching region appears to vary from sub-group to sub-group; seven in richterites, five in the glaucophane-riebeckite group, four in the eckermannite spectrum and three in the arfvedsonite spectrum. Glaucophane can be readily identified by the presence of a peak at 890 cm^{-1} and a doublet between 698-678 cm^{-1}, which no other alkali amphibole possesses.

The peak which appears most susceptible to compositional variation within these minerals is in the Si-O bending/stretching region between 740-800 cm^{-1}. There are three curves corresponding to the three alkali amphibole sub-groups.

The study of the OH^- stretching vibration of alkali amphiboles shows the peak positions (3673, 3660, 3648 and 3625 cm^{-1}) for tremolite-ferrotremolite indicated by Burns and Strens (1966) and ascribed by these authors to OH^- co-ordinated to Mg and Fe^{++}. Alkali amphiboles with 'A' site occupancy show OH^- stretching peaks at higher frequencies (3728 and 3734 cm^{-1}) than those with vacant 'A' sites. This frequency shift is probably due to the displacement of the OH^- group towards Na^+ or K^+ and away from the octahedral cations (displacement being greater for K^+ than Na^+). Natural amphiboles although they have high frequency bands between 3690-3710 cm^{-1} they are lower than the synthetic minerals. It is possible that weak absorption of hydroxyl perturbed by $(Na, K)^+$ in 'A' sites is due to preferential association of these cations with F^- or $O^=$ substituting for OH^-. These lower frequencies could arise in two ways: 1) a direct effect of trivalent cations in M(1) and M(3); 2) an indirect effect due to the displacement of Na^+ or K^+ due to F^- or $O^=$ substituting for OH^-. Evidence for trivalent cations in M(1) and M(3) is the interpretation of a high frequency peak in riebeckite-arfvedsonite from Nigeria (Addison and White, 1968) and present study.

APPENDIX I

Mineral separation

The rocks were ground in a Spex ball-mill and fractions were separated at: -90 +120; -120 +150; -150 +180. The alkali amphiboles were separated using one of two methods.

1) Cooke Isodynamic separator

Fractions were passed through separator until > 99% pure amphibole. If present iron oxides were removed using the electromagnet. The mafic fraction of minerals from alkaline rocks consisted mainly of amphibole and alkali pyroxene ± aenigmatite ± eudialyte ± astrophyllite etc.

Separator angles to separate alkali amphibole from other mafics:-

Longitudinal tilt	14°
Transverse tilt	12°
Amperage	0.4 amps.

2) Heavy liquid separation

Used when separator could not purify > 90% amphibole. This applied mainly to magnesium rich varieties. Liquids used were Bromoform (S.G. 2.89 gm/cc), Methylene Iodide (S.G. 3.325 gm/cc) with a diluent N.N. dimethylformamide (S.G. 0.948 gm/cc).

Eckermannite (Norra Kärr) separated using a density gradient consisting of methylene iodide and N.N. dimethylformamide.

SOLUTION A — NaOH fusion — SiO_2 (spect.) — Molybdenum blue complex at 650 mμ

SOLUTION B

acid digestion with HF/H_3PO_4

Group III ppt. w NH_4OH.	Na_2O, K_2O, Li_2O (flame photometer)	
	Al_2O_3 (spect.)	extraction by chloroform - 8-hydroxyquinoline complex at 410 mμ
	Fe_2O_3 (Total iron) (spect.)	2,2' dipyridyl complex solution at 522 mμ
	TiO_2 (spect.)	H_2O_2 complexing reagent at 410 mμ
Spect. = spectrophotometer	P_2O_5 (spect.)	Molybdenum blue complex at 650 mμ
	CaO, MgO titration	CaO-EDTA titration and indicator MgO-EDTA titration and indicator Eriochrome black T indicator
	FeO	titration against potassium permanganate.
	H_2O^+	(1) Penfield tube method (2) Riley furnace modified by R.C.O. Gill.

X-RAY FLUORESCENCE METHOD

All the major elements were determined using an automatic Philips 1212 X-ray fluorescence spectrometer. Standards comprised international rock standards and amphiboles of various compositions (supplied by various workers). The operating conditions were as set out in the table below:-

	Si	Al	Fe	Mg	Ca	Na	K	Ti	Mn
COLLIMATOR	Coa	Coa	Coa	Coa	Coa	Coa	Coa	Coa	Coa
CRYSTAL	P.E.	P.E.	LiF	K.A.P.	P.E.	K.A.P.	P.E.	P.E.	LiF
COUNTER	FLOW	FLOW	F+S	FLOW	FLOW	FLOW	FLOW	FLOW	SCINT
COUNTS	10^5	10^5	10^5	$3x10^4$	10^5	10^4	10^5	10^5	10^5
mA	8	24	8	20	8	20	8	8	8
KV	60	60	60	50	20	50	40	40	60
TUBE	Cr	Cr	Cr	Cr	Cr	Cr	Cr	Cr	W

Zn was also determined in amphiboles from the Ilímaussaq intrusion by X.R.F. methods using addition standards.

The samples and standards were made up into bricquettes by pressing the powder to 5 tons/sq. inch.

The results were computed using the method by Holland and Brindle (1966).

OPTICAL SPECTROGRAPHIC METHOD FOR THE DETERMINATION OF FLUORINE

Sample preparation

Three parts by weight of $CaCO_3$ added to four parts by weight of standard or sample.

Internal standard Cu added as CuO to sample/$CaCO_3$ mixture in the proportion 1 : 14 by weight.

Carbon powder added to sample/$CaCO_3$/CuO mixture in the proportions 9 : 14 by weight.

Conditions of operation

Stallwood Jet with Argon/oxygen atmosphere.

Seven Step sector.

Focus arc on slit.

Glass optics 4600 - 9600 A°

No pre-burn.

30 secs. burn.

Current 8 amps.

Plate Development:- Type Ilford H.P.3.

Developer PQ Universal.

Time of development 5 mins.

Measurement of Plates

CaF bandhead 5291 A°

Cu Int. Std. 5015 A°

Standards

Standards of synthetic amphibole composition were made up containing 4, 3, 2, 1, 0.5, 0.25% Fluorine as NaF.

Synthetic amphiboles contained SiO_2, Fe_2O_3, MgO, Na_2CO_3, NaF in various proportions. Standards were analysed in triplicate.

Samples

Duplicate samples made up as follows:-

0.2 gm	sample or standard
0.15 gm	$CaCO_3$
0.025 gm	Cu as CuO
0.225 gm	C as graphite

X-RAY DIFFRACTION

For the determination of amphibole cell parameters two methods were used:-

1) Powder camera (11.46 cm diameter)

Conditions

	Cu K$\bar{\alpha}$ radiation	Co K$\bar{\alpha}$ radiation
KV	40	34
mA	20	10
Exposure time of Ilford Ind 'B' film	24 hrs	48
Exposure time of Ilford Ind 'G' film	12 hrs	24

2) X-ray Diffractometer

Philips 1.KW generator.

The specimens were prepared as smear mounts using amyl acetate as the mounting medium. Quartz was used as an internal standard in the proportions 1 quartz : 4 sample.

Conditions

		Cu Kα radiation	Co Kα radiation
KV		40	34
mA		20	10
filter		Ni	Fe
2θ range		5-50°2θ	
Goniometer Speed		$\frac{1}{4}$°/min.	
Slit system	Divergence	1°	
	Receiving	.1	
	Antiscatter	1°	

Rate Meter		x 2
	Time constant	x 4
	multiplier	x 1
Chart Speed		x 10
Proportional Counter		1700 V
Discrimination used		

The specimen was irradiated three times and the average of the 2 values were taken. Peaks were measured at $^2/_3$ peak height, $\frac{1}{2}$ peak width. Indices for the reflections were obtained either by comparison with other amphiboles (ASTM Index File) or by generating a set of (hkl) reflections from an approximate cell size using a computer programme "Genstruck" by Marples and Shaw (UKAEA. Int report AERE R5210, 1966) on the S.R.C. "Atlas" computer at Didcot, Berks.

The cell parameters were calculated from the indices obtained using a least squares analysis programme "Cohen" - reference as above.

All the reflections were weighted equally because of the small range of 2θ and also because the most intense and most accurately measured peaks were in the lower range.

Within the programme a rejection level $(\sin^2\theta_{obs} - \sin^2\theta_{calc})$ can be set in steps of Δ Sin $^2\theta$ of 0.0004 between 0.004 and 0.0004. The rejection level was set at point 9 i.e. Sin $^2\theta$ 0.0008.

INFRA-RED SPECTROSCOPIC TECHNIQUE

1.5 mg of powdered amphibole was mixed with 1.00 gm of KBr. Enough of this mixture $\sim$ 400 mg is weighed to form a disc of a suitable thickness and then pressed in a vacuum die (30 tons/square inch).

The discs were then irradiated using either a Grubb Parsons "Spectromaster" double grating infra-red spectrometer or a Perkin Elmer 157 spectrometer, the former was used for high resolution.

The scan range was 4000 cm^{-1} to 400 cm^{-1} on the Grubb Parsons instrument and 4000 cm^{-1} to 650 cm^{-1} on the Perkin Elmer.

For determination of the hydroxyl stretching region of amphiboles the chart scale was changed from 1"/micron to 8"/micron; scale was expanded x3; and high resolution (2.5-3.0) was used. This procedure was necessary to resolve the separate OH^- peaks.

ELECTRON PROBE MICROANALYSIS

All electron probe microanalysis results were determined using the Durham University's Cambridge Instruments Geoscan Microprobe.

Conditions

KV	15
specimen current	20 μ amps
Counting time	20 secs

Pulse height analysis set up each time different element determined.

Elements:
- Na, Mg, Al, Si — KAP crystal
- K, Ca, Ti — Quartz crystal
- Fe, Mn — LiF crystal

Standards used are lodged in the Geology Department, Durham University.

Standards:
- P4 "amphibole" glass
- synthetic diopside
- jadeite
- AF 15 glass
- rutile
- manganese metal

The reduction of the electron probe data was performed using computer programmes written by Boyd, Finger, and Chayes (Ann. Rep Director Geophysical Laboratory, Yearbook 1967-68). These programmes were modified for the Geoscan electron probe by G.H. Gale (Ph.D. Thesis, Durham 1971).

Programme 1. "CONE"

This programme averages the counts, evaluates statistical parameters and makes instrumental corrections i.e. dead time and background. The output is the initial approximation to the composition.

Programme 2. "ABFAN"

This programme calculates the matrix corrections i.e. atomic number, stopping power, fluorescence, absorption, and backscatter and corrects the initial composition by iteration.

These programmes are written in Fortran IV for the IBM 360/67 Numac computer.

APPENDIX II

HYDROTHERMAL SYNTHESIS RESULTS

Abbreviations for Appendix II

R = Richterite, Ec = Eckermannite, Su = Sundiusite, Ts = Tschermakite,

Fo = Forsterite, En = Enstatite, Ab = Albite, Q = Quartz, T = Talc,

Na(-Ca)mont = montmorillonite, Tr = Tremolite, Ed = Edenite.

EXPERIMENTS OF GLAUCOPHANE COMPOSITION ($Na_2O.3MgO.Al_2O_3.8SiO_2$)

RUN NO.	STARTING MATERIAL	TEMP. (°C)	PRESS. (bars)	DURATION (hours)	RUN PRODUCTS
1	GEL	800	1000	85	Fo+En+Ab+Na mont.
2	"	800	"	85	"
3	"	800	"	85	"
4	"	800	"	80	"
5	"	800	"	80	"
8	"	750	"	168	"
9	"	750	"	168	"

EXPERIMENTS OF SUNDIUSITE COMPOSITION ($Na_2O.CaO.3MgO.2Al_2O_3.6SiO_2$)

RUN NO.	STARTING MATERIAL	TEMP. (°C)	PRESS. (bars)	DURATION (hours)	RUN PRODUCTS
17	GEL	800	1000	72	Su+Talc+Na-Ca.mont
19	"	840	"	162	" " "
23	"	880	"	108	" " "
25	"	880	"	84	" " "
27	"	870	"	70	" " "
29	"	875	"	188	" " "
31	"	880	"	92	" " "
33	"	875	"	30	" " "
39	"	875	"	92	" " "
45	"	885	"	68	" " "
48	"	950	"	24	" " "
52	"	1000	"	48	" " "
62	"	900	"	48	Su+Na-Ca.mont(No Talc)
77	"	1000	5000	24	Su+Talc+Na-Ca.mont
89	"	1000	"	24	" " "
91	"	870	"	68	" " "
93	"	870	"	68	" " "
104	"	870	"	68	" " "
107	"	770 910	"	20 21	" " "
108	"	770 910	"	20 21	" " "
122	"	770 910	"	20 21	" " "
129	"	1200 950	1000	$\frac{1}{2}$ 48	Su+Na-Ca.mont(No Talc)
130	"	1200 975	"	$\frac{1}{2}$ 48	" "
133	"	1200 900	"	$\frac{1}{2}$ 24	" "

EXPERIMENTS OF RICHTERITE COMPOSITION ($Na_2O.CaO.5MgO.8SiO_2$)

RUN NO.	STARTING MATERIAL	TEMP. (°C)	PRESS. (bars)	DURATION (hours)	RUN PRODUCTS
10	GEL	750	1000	192	Richterite
11	"	750	"	120	"
12	"	750	"	120	"
13	"	750	"	120	"
40	"	875	"	68	" (Richterite seeds)
42	"	885	"	20	Richterite
71	"	900	"	24	"
72	"	900	"	24	"
73	"	900	"	24	"
74	"	900	"	24	"
81	"	1000	5000	24	"
82	"	1000	"	24	"
95	"	870	"	67.5	"
96	"	870	"	67.5	"
106	"	870	"	67.5	"
111	"	770 910	"	20 21	"
112	"	770 910	"	20 21	"
113	"	770 910	"	20 21	"
125	"	1050	1000	24	"
126	"	1100	"	24	Fo+Dp+Q+Glass
134	"	1075	"	24	Richterite
168	"	925	5000	30	"

EXPERIMENTS OF MIYASHIROITE COMPOSITION ($3Na_2O.6MgO.3Al_2O_3.14SiO_2$)

RUN NO.	STARTING MATERIAL	TEMP. (°C)	PRESS. (bars)	DURATION (hours)	RUN PRODUCTS
15	GEL	800	1000	72	Na-montmorillonite
16	"	800	"	72	"
18	"	840	"	162	"
21	"	850	"	92	"
22	"	880	"	108	"
26	"	870	"	70	"
28	"	875	"	188	"
30	"	925 880	"	0.5 92	"
32	"	875	"	30	"
34	"	885	"	20	"
38	"	875	"	92	"
44	"	885	"	68	"
47	"	855	"	68	"
49	"	950	"	24	"
53	"	1000	"	48	"
61	"	1150 900	"	0.5 24	"
75	"	1000	5000	24	Fo+Na montmorillonite
78	"	1000	"	24	" "
90	"	1000	"	24	Fo+Na.mont+glass
92	"	870	"	67.5	Na.-mont.
94	"	870	"	67.5	"
123	"	1200 950	1000	0.5 48	"
124	"	1200 975	"	0.5 48	"
170	"	925	5000	30	"
183	"	925	"	30	"

EXPERIMENTS OF ECKERMANNITE COMPOSITION ($3Na_2O.8MgO.Al_2O_3.16SiO_2$)

RUN NO.	STARTING MATERIAL	TEMP. (°C)	PRESS. (bars)	DURATION (hours)	RUN PRODUCTS
14	GEL	800	1000	72	Ec + Talc
20	"	850	"	92	" "
24	"	880	"	84	" "
41	"	875	"	68	" "
43	"	885	"	20	" "
51	"	1000	"	48	" "
84	"	1000	5000	24	" "
100	"	870	"	67.5	" "
116	"	770 910	"	20 21	" "
127	"	1050	1000	24	" "
128	"	1100	"	24	" "
136	"	1075	"	24	" "
172	"	925	5000	30	" "

EXPERIMENTS OF MISCELLANEOUS COMPOSITIONS

RUN NO.	STARTING COMPOSITION	TEMP. (°C)	PRESS. (bars)	DURATION (hours)	RUN PRODUCTS
173	$.75Na_2O$-$1.25CaO$-$5MgO$-$8SiO_2$	900	5000	30	Amphibole - 75R-25Tr
176	$1.125Na_2O$-$.75CaO$-$4.75MgO$-$.125Al_2O_3$-$8SiO_2$	"	"	"	Amphibole - 75R-25Ec
178	$1.375Na_2O$-$.25CaO$-$4.25MgO$-$.375Al_2O_3$-$8SiO_2$	"	"	"	Amphibole - 25R-75Ec
180	$.25Na_2O$-$1.75CaO$-$5MgO$-$8SiO_2$	"	"	"	Amphibole - 25R-75Tr
182	$.75Na_2O$-$1.5CaO$-$5MgO$-$.25Al_2O_3$-$7.5SiO_2$	"	"	"	Amphibole - 50R-50Ed

Riebeckite - Arfvedsonites from Soda Granite Suite, Nunassuit, S.W. Greenland

OXIDE	NUN.1. WT.%	N.243 WT.%	GGU20626 WT.%	GGU20627 WT.%	NUN.2. WT.%	GGU31036 WT.%	GGU30875 WT.%	N.234 WT.%
SiO_2	50.84	51.68	50.17	49.68	49.55	49.47	49.24	49.81
Al_2O_3	0.76	0.60	0.64	0.99	0.93	1.00	0.91	1.09
Fe_2O_3	12.11	14.60	11.02	13.71	11.25	10.88	10.55	12.92
FeO	21.60	18.65	23.17	20.82	23.66	23.01	23.61	19.77
MnO	0.67	0.95	0.59	0.70	0.71	0.61	0.64	0.77
MgO	0.02	0.10	0.21	0.33	0.05	0.15	0.04	0.67
TiO_2	1.32	0.75	1.20	1.24	1.18	1.30	1.39	1.45
CaO	0.42	0.12	0.57	1.28	1.40	1.87	2.08	2.56
Na_2O	8.20	8.28	8.18	7.43	7.13	7.60	7.31	7.94
K_2O	1.68	2.23	1.69	1.52	1.53	1.56	1.64	0.84
H_2O^+	0.80	1.22	1.06	0.60	1.34	1.20	0.95	1.76
H_2O^-	0.06	0.04	0.05	0.11	0.20	0.08	0.08	0.05
F	1.22	0.97	1.11	2.31	1.15	1.25	1.47	0.70
Total	99.70	100.19	99.66	100.71	100.08	99.98	99.91	100.33
O F	0.51	0.41	0.47	0.97	0.49	0.53	0.62	0.30
Total	99.19	99.78	99.19	99.74	99.59	99.45	99.29	100.03

Recalculations of Analyses to 24 Oxygens

Si	8.06	8.07	7.98	7.84	7.86	7.85	7.86	7.74
Al^{IV}	nil	nil	0.02	0.16	0.14	0.15	0.14	0.20
Al^{VI}	0.14	0.11	0.10	0.02	0.03	0.04	0.03	nil
Fe^{3+}	1.44	1.71	1.32	1.63	1.34	1.30	1.27	1.51
Fe^{2+}	2.86	2.43	3.08	2.75	3.14	3.05	3.15	2.57
Mn	0.09	0.13	0.08	0.09	0.10	0.08	0.09	0.10
Mg	0.004	0.02	0.05	0.08	0.01	0.04	0.01	0.16
Ti	0.16	0.09	0.14	0.15	0.14	0.16	0.17	0.17
Ca	0.07	0.02	0.10	0.22	0.24	0.32	0.36	0.43
Na	2.52	2.51	2.52	2.27	2.19	2.34	2.26	2.39
K	0.34	0.44	0.34	0.31	0.31	0.32	0.33	0.17
OH	0.85	1.27	1.13	0.63	1.42	1.27	1.01	1.82
F	0.61	0.48	0.56	1.15	0.58	0.63	0.74	0.34

MISCELLANEOUS RIEBECKITE - ARFVEDSONITES

	Igaliko, S.W. Greenland		Jebel Sileitat, Sudan			Fukushin-Zan, Korea	Nigeria
	G.G.U.63702	G.G.U.43900	S.421	J.S.2(L.P.)	J.S.3(S.M.)	Heikolite	N.I.R.I.
OXIDE	WT.%	WT.%	WT.%	WT.%	WT.%	WT.%	WT.%
SiO_2	49.42	46.07	47.62	49.85	48.82	47.35	52.54
Al_2O_3	2.60	3.96	1.30	0.65	1.15	2.60	1.05
Fe_2O_3	12.00	12.51	8.20	9.46	9.34	10.85	15.57
FeO	22.18	19.32	25.97	24.81	24.90	21.17	16.40
MnO	0.99	1.84	0.59	0.69	0.62	1.26	0.72
MgO	0.56	1.88	nil	0.16	0.00	2.65	nil
TiO_2	0.92	2.43	1.76	1.90	1.52	1.23	1.07
CaO	0.76	2.26	3.33	1.53	2.54	4.34	nil
Na_2O	6.59	5.84	6.92	6.71	6.66	4.57	9.21
K_2O	1.52	1.74	1.50	1.49	1.55	1.64	1.73
H_2O^+	1.20	1.19	1.46	1.46	1.50	1.40	1.25
H_2O^-	nil	0.05	0.08	0.15	0.07	0.10	-
F	1.73	0.40	0.75	0.42	0.70	0.87	1.50
Total	100.47	99.49	99.48	99.28	99.57	100.03	101.04
O F	0.73	0.17	0.32	0.18	0.29	0.37	0.63
Total	99.74	99.32	99.16	99.10	99.28	99.66	100.41
			Recalculation to 24 Oxygens				
Si	7.73	7.31	7.67	7.94	7.80	7.46	8.03
Al^{IV}	0.27	0.69	0.25	0.06	0.20	0.48	nil
Al^{VI}	0.21	0.05	nil	0.06	0.02	nil	0.19
Fe^{3+}	1.41	1.49	0.99	1.13	1.12	1.29	1.79
Fe^{2+}	2.90	2.56	3.50	3.31	3.33	2.79	2.10
Mn	0.13	0.25	0.08	0.09	0.08	0.17	0.09
Mg	0.13	0.44	0.00	0.04	nil	0.62	nil
Ti	0.11	0.29	0.21	0.23	0.18	0.15	0.12
Ca	0.13	0.38	0.57	0.26	0.44	0.73	nil
Na	2.00	1.80	2.16	2.07	2.06	1.40	2.73
K	0.30	0.35	0.31	0.30	0.32	0.33	0.34
OH	1.25	1.26	1.57	1.55	1.60	1.47	1.27
F	0.86	0.20	0.38	0.21	0.35	0.43	0.73

Fibrous Riebeckites and Magnesioriebeckites

	Magnesioriebeckite S. Westland A.J.R.W.I.	Riebeckite (Medical R.C.) I.U.C.C.	Riebeckite Wittenoom W. Australia	Riebeckite Hamersley Ranges W. Australia - 10150	Riebeckite Koegas S. Australia - 12113
OXIDE	WT. %	WT. %	WT. %	WT. %	WT. %
SiO_2	56.41	51.32	54.67	53.68	51.50
Al_2O_3	1.82	0.52	0.53	0.53	0.53
Fe_2O_3	14.84	16.16	16.36	17.01	17.17
FeO	4.69	19.80	14.15	17.97	19.57
MnO	0.07	0.12	0.07	0.07	0.13
MgO	12.65	2.71	5.54	2.56	2.25
TiO_2	0.21	nil	0.11	0.02	0.06
CaO	nil	1.15	0.23	0.34	0.97
Na_2O	6.95	5.94	6.75	5.80	5.33
K_2O	0.49	0.07	0.04	0.05	0.08
H_2O^+	1.87	1.90	1.90	2.09	1.90
H_2O^-	n.d.	n.d.	n.d.	n.d.	n.d.
Total	100.00	99.69	100.35	100.12	99.49
		Recalculation of analyses to 24 Oxygens			
Si	8.00	7.90	8.09	8.08	7.94
Al^{IV}	nil	0.09	nil	nil	0.06
Al^{IV}	0.30	nil	0.09	0.09	0.03
Fe^{3+}	1.58	1.87	1.82	1.93	1.99
Fe^{2+}	0.56	2.55	1.75	2.26	2.51
Mn	0.01	0.02	0.01	0.01	0.02
Mg	2.67	0.62	1.22	0.57	0.52
Ti	0.02	nil	0.01	0.00	0.01
Ca	nil	0.19	0.04	0.05	0.16
Na	1.91	1.77	1.94	1.69	1.59
K	0.09	0.01	0.01	0.01	0.02
OH	1.77	1.95	1.88	2.10	1.95

APPENDIX IV CELL DIMENSIONS OF THE ALKALI AMPHIBOLES

A. Glaucophane - Riebeckite

Specimen Locality and Index No.	a(A°)	b(A°)	C(A°)	(°)	asin (A°)	vol(A°3)
Glaucophane, Piedmont, N. Italy (35)	9.563	17.769	5.312	103.60	9.295	877.3
Glaucophane, Tiburon, Pensn, California (36)	9.555	17.802	5.294	103.68	9.284	875.0
Gastaldite, Champ de Praz, Val D'Aosta, Italy (50)	9.543	17.726	5.302	103.72	9.271	871.3
Glaucophane, Susatal, Italy (77)	9.588	17.818	5.306	103.52	9.322	881.3
Glaucophane, Mustang Pass, California (82)	9.585	17.794	5.306	103.69	9.313	879.3
Glaucophane, X1172, Syros, Aegean (83)	9.588	17.801	5.299	103.66	9.317	878.8
Glaucophane (89)	9.550	17.783	5.306	103.62	9.281	875.8
Crossite, Berkeley, Almeda Co., California (84)	9.662	17.919	5.312	103.62	9.390	893.8
Riebeckite, Quincy, Massachusetts (21)	9.821	18.059	5.316	103.86	9.535	915.3
Riebeckite, Ras Zeit, Egypt (78)	9.856	18.070	5.334	103.77	9.573	922.7
Magnesioriebeckite, Grønnedal-Ika, Greenland (22)	9.781	17.984	5.294	103.88	9.495	904.0
Magnesioriebeckite, Sheep Creek, Montana (24)	9.711	17.935	5.281	103.92	9.426	892.8
Magnesioriebeckite, Gem Park, Colorado (54)	9.787	17.876	5.299	103.66	9.510	900.8
Magnesioriebeckite, Pinon Peak, Colorado (55)	9.804	17.855	5.292	103.86	9.519	899.4
Magnesioriebeckite, Green River (79)	9.826	17.927	5.299	103.69	9.547	906.9
Magnesioriebeckite, South Westland, New Zealand (71)	9.705	17.903	5.301	103.72	9.428	894.8

B. Riebeckite - Arfvedsonite

Specimen Locality and Index No.	a(A°)	b(A°)	c(A°)	(°)	asin (A°)	vol(A°3)
1) Ilimaussaq, S.W. Greenland						
D.U.10917 Pulaskite - Arfvedsonite (31)	9.979	18.159	5.336	104.37	9.667	936.7
D.U.10943 Sodalite Foyaite - Arfvedsonite (25)	9.974	18.132	5.349	104.32	9.664	937.3
D.U.10941 Naujaite - Arfvedsonite (37)	9.975	18.152	5.336	104.09	9.675	937.1
D.U.10942 Naujaite pegmatite - Arfvedsonite (29)	9.979	18.171	5.365	104.41	9.665	942.2
D.U.10931 Kakortokite(Black) - Arfvedsonite (73)	9.938	18.105	5.330	103.91	9.647	930.9
D.U.10933 " (Transitional) - Arfvedsonite (69)	9.904	18.151	5.253	103.70	9.622	917.5
D.U.10934 " (Red) - Arfvedsonite (33)	9.921	18.144	5.328	103.96	9.628	930.8
D.U.10936 " (Transitional) - Arfvedsonite (70)	9.920	18.075	5.328	103.96	9.627	927.1
D.U.10937 " (Pegmatite) - Arfvedsonite (72)	9.937	18.120	5.318	104.12	9.637	928.6
D.U.10957 Naujaite (Pegmatite) - Arfvedsonite (27)	9.944	18.154	5.339	104.17	9.641	934.5
D.U.12837 " (Pegmatite) - Arfvedsonite (86)	9.947	18.124	5.332	103.99	9.652	923.6
D.U.10930 Lujavrite - Arfvedsonite (23)	9.957	18.111	5.320	104.03	9.658	930.6
D.U. 10942a Lujavrite(Pegmatite) - Arfvedsonite (28)	9.961	18.019	5.326	104.03	9.664	927.4
D.U. 10951 " " (26)	9.992	18.070	5.318	104.01	9.695	931.6
D.U. 10919 Arfvedsonite granite - Arfvedsonite (32)	9.876	18.072	5.329	103.72	9.594	924.0
D.U. 10927 " " " (85)	9.901	18.095	5.320	103.74	9.618	925.9
2) Nunassuit, S.W. Greenland						
N.157 Soda granite (1)	9.817	17.990	5.321	103.81	9.531	912.4
N.243 " " (2)	9.840	18.013	5.312	103.69	9.560	914.8
N.1 " " (3)	9.845	18.031	5.311	103.71	9.565	915.9
N.2 " " (4)	9.845	18.083	5.314	103.81	9.560	918.7
N.75 " " (5)	9.888	18.128	5.318	103.88	9.599	925.4
N.88 " " (6)	9.911	18.118	5.313	104.09	9.613	925.3
N.30875 (G.G.U.) Soda granite (7)	9.878	18.113	5.308	103.81	9.592	922.3
N.20627 (G.G.U.) " " (66)	9.860	18.055	5.320	103.80	9.575	919.7
N.20626 (G.G.U.) " " (67)	9.878	18.061	5.312	103.62	9.599	920.9
N.31036 (G.G.U.) " " (68)	9.900	18.123	5.321	103.81	9.614	927.1
N.234 " " (74)	9.843	18.074	5.336	103.81	9.559	921.9

B. Riebeckite - Arfvedsonite (continued)

Specimen Locality and Index No.		a(A°)	b(A°)	c(A°)	(°)	asin (A°)	vol(A°3)
3) Other S.W. Greenland Intrusions							
D.U. 13170 Soda Granite, Kungnat	(13)	9.836	18.058	5.323	103.80	9.552	918.2
63702 (G.G.U.) Syenite, Igaliko	(14)	9.858	18.072	5.327	103.79	9.574	921.7
4) Kangerdlugsuaq, E. Greenland							
D.R.C.K. 1397	(38)	9.911	18.123	5.314	104.32	9.603	924.8
" 2046	(39)	9.883	18.096	5.309	103.94	9.592	921.5
" 4582	(40)	9.876	18.054	5.321	104.31	9.570	919.3
" 4666	(41)	9.864	18.033	5.326	103.84	9.578	919.9
" 4789	(Kempe)	9.875	18.004	5.302	104.23	9.572	913.7
5) Younger Granites, Nigeria							
P.B. 92 (Imperial College)	(15)	9.816	17.998	5.307	103.71	9.536	910.9
P.B. 63 " "	(16)	9.851	18.060	5.315	103.87	9.564	918.01
P.B. 20 " "	(17)	9.862	18.066	5.319	103.80	9.577	920.3
P.B. 37 " "	(18)	9.940	18.202	5.346	103.81	9.653	939.3
P.B. 30 " "	(19)	9.840	18.028	5.327	103.67	9.561	918.2
P.B. 50 " "	(20)	9.850	18.105	5.330	103.87	9.563	922.8
Riebeckite - Arfvedsonite (Warren Springs)	(46)	9.829	18.012	5.313	103.78	9.546	913.1
6) Jebel Sileitat, Sudan							
J.S.1	(8)	9.878	18.117	5.316	103.78	9.594	924.0
J.S.2	(9)	9.918	18.136	5.316	103.85	9.630	928.4
J.S.3	(10)	9.928	18.210	5.329	104.27	9.622	933.7
J.S.5	(11)	9.913	18.145	5.312	103.74	9.629	928.1

C. Richterite

Specimen Locality and Index No.	a(A°)	b(A°)	c(A°)	(°)	asin (A°)	vol(A°3)
Richterite, Wichita Meteorite (Olsen 1967) (7)	9.882	18.075	5.324	104.47	9.569	920.8
Richterite, Ravalli Co., Montana (51)	9.798	17.988	5.310	104.21	9.498	907.2
Richterite, Iron Hill, Colorado (52)	9.826	18.007	5.302	104.20	9.526	909.5
Richterite, Gem Park, Colorado (53)	9.846	17.944	5.291	104.10	9.548	906.5
Richterite, Iron Hill, Colorado (56)	9.847	17.928	5.290	103.99	9.555	906.3
Richterite, Langban, Sweden (59)	9.912	18.026	5.270	104.55	9.594	911.4
Winchite, Netra, Madhya Pradesh, India (60)	9.761	17.914	5.286	103.83	9.478	897.5
Richterite, Langban, Sweden (61)	9.914	17.985	5.276	104.37	9.604	911.3
Winchite, Tirodi, M.P., India (62)	9.886	18.016	5.282	104.43	9.574	911.1
Winchite, Kalijdongri, M.P., India (100)	9.834	18.062	5.300	104.45	9.521	911.4
Imerinite, Imeria, Malagasy (102)	9.783	17.943	5.287	104.07	9.472	898.6

D. Eckermannite - Magnesioarfvedsonite

Magnesioarfvedsonite, Grønnedal, Greenland (34)	9.843	17.915	5.289	103.88	9.556	905.4
Juddite, Chikla, India (49)	9.818	17.860	5.283	104.10	9.522	898.5
Eckermannite, Norra Karr, Sweden (63)	9.799	17.833	5.273	104.18	9.501	893.4
Juddite, Madhya Pradesh, India (64)	9.796	17.932	5.289	103.99	9.505	901.5
Juddite, Nagpur, M.P., India (81)	9.752	17.820	5.289	104.09	9.459	891.4

E. Miscellaneous Amphiboles

Specimen Locality and Index No.	a(A°)	b(A°)	c(A°)	(°)	asin (A°)	vol(A°3)
Tirodite, Tirodi, Madhya Pradesh, India (57)	9.799	17.994	5.289	103.89	9.512	905.3
Torendrikite, (type loc.) Malagasy (101)	9.801	17.988	5.235	104.98	9.468	891.6
Imerinite, Imeria, Malagasy (102)	9.783	17.943	5.287	104.07	9.473	898.7
Heikolite, Fukushin-Zan, Korea (103)	9.817	18.046	5.271	103.71	9.537	907.2
Mboziite, Mbozi, Tanzania (95)	9.902	18.052	5.356	104.70	9.578	926.1
Mboziite, Darkainle, Somalia (91)	9.947	18.062	5.348	104.73	9.620	929.3

F. Synthetic Amphiboles

Mineral composition	a(A°)	b(A°)	c(A°)	(°)	asin (A°)	vol(A°3)
Richterite - K	9.892	17.958	5.263	104.28	9.586	906.0
Eckermannite - K	9.762	17.892	5.284	103.17	9.505	898.6
Sundiusite - K	9.914	17.919	5.305	105.35	9.560	908.8
Tschermakite - K	9.823	17.921	5.272	105.51	9.456	894.3
Richterite 25 - Eckermannite 75	9.812	17.963	5.254	103.75	9.531	899.5
Richterite 75 - Eckermannite 25	9.869	17.971	5.272	104.14	9.570	906.7
Richterite 25 - Tremolite 75	9.812	18.010	5.237	104.69	9.500	896.02
Richterite 75 - Tremolite 25	9.895	17.985	5.259	104.40	9.584	906.5
Richterite 50 - Edenite 50	9.914	18.024	5.274	104.82	9.584	911.1
Fluor-Richterite	9.817	17.956	5.263	104.36	9.510	898.8

Standard deviations of all the cell parameters are less than the following:

$a_o \pm 0.010$ A° $\quad b_o \pm 0.010$ A° $\quad c_o \pm 0.006$ A° $\quad \pm 10'$

REFERENCES

Adamson, O. J. (1942) Eckermannite, a new Alkali Amphibole. Geol. Fören. Förh. 64, 329.

Adamson, O. J. (1944) The Petrology of the Norra Kärr district. Geol. Fören. Förh. 66, 113-255.

Addison, C. C., W. E. Addison, G. H. Neal, J. H. Sharp (1962) Oxidation of crocidolite. Journ. Chem. Soc. 1962, 1468-1471.

Addison, W. E., and A. D. White (1968) Spectroscopic evidence for the siting of lithium ions in a riebeckite. Min. Mag. 36, 743-745.

Addison, W. E., and A. D. White (1968) The oxidation of Bolivian crocidolite. Min. Mag. 36, 791-796.

Adler, H. H. (1963) Some basic considerations in the application of infrared spectroscopy to mineral analysis. Econ. Geol. 58, 558-568.

Ahlfeld, F. (1943) Los yaciementos de crocidolita en las Yungas de Cochabamba. Notas Mus. La Plata 8, 355 (ref. Min. Abs. 10, 242).

Ahrens, L. H. (1965) Significance of the chemical bond for controlling the geochemical distribution of the elements. Part I. Physics and Chemistry of the Earth vol. 5, 1-54.

Allaart, J. H. (1964) Review of the work on the Precambrian Basement (pre-Gardar) between Kobberminebugt and Frederiksdal, South Greenland. Rapp. Grønlands geol. Unders., No. 1.

Ames, L. L., and L. B. Sand (1958) Factors affecting the maximum hydrothermal stability in montmorillonites. Am. Min. 43, 476-480.

Aoki, K. (1963) Kaersutites and oxykaersutites from Japan. Journ. Petrology 4, 198-210.

Aoki, K. (1970) Petrology of Kaersutite - Bearing Ultramafic and Mafic Inclusions in Iki Island, Japan. Contr. Min. and Pet. 25, 270-283.

Appleman, D. E., F. R. Boyd, G. M. Brown, W. G. Ernst, G. V. Gibbs, and J. V. Smith (1966) Short course on chain silicates. Amer. Geol. Inst., Washington, D.C.

Bailey, E. H., W. P. Irwin, and D. L. Jones (1964) Franciscan and related rocks, and their significance in the geology of Western California. Bull. 183, Calif. Div. Mines and Geology.

Bailey, D. K. (1969) The stability of acmite in the presence of H_2O. Amer. J. Sci. (Schairer Vol.) 267-A, 1-16.

Bain, A. D. N. (1934) The younger intrusives of the Kudaru Hills, Nigeria. Quart. J. Geol. Soc. London 90, 201-215.

Bancroft, G. M., R. G. Burns, A. G. Maddock, and R. G. J. Strens (1966) Cation distribution in anthophyllite from Mössbauer and infrared spectrocopy. Nature 212, 913-915.

Bancroft, G. M., R. G. Burns, and A. G. Maddock (1967). Determination of the cation distribution in the cummingtonite-grunerite series by Mössbauer spectra. Amer. Min. 52, 1009-1026.

Banno, S. (1959) Notes on rock forming minerals (10). Glaucophanes and garnet from the Kotu Bizan district, Sikoku. Journ. Geol. Soc. Japan 65, 658-663.

Banno, S. (1964) Petrologic Studies on Sanbagawa Crystalline Schists in the Bessi-Ino district, central Sikoku, Japan. Tokyo Univ. Fac. Sci. Jour., sec. 2, 15, 203-219.

Barnes, V. E. (1930) Changes in hornblende at about 800°C. Am. Miner. 15, 393-417.

Bassett, W. A. (1960) Role of hydroxyl orientation in mica alteration. Bull. Geol. Soc. Am. 71, 449-455.

Bearth, P. (1959) Über Eklogite, Glaucophanschiefer, metamorphe Pillowlaven. Schweiz. Min. Pet. Mitt. 39, 268.

Beatty, S. V. D. (1950) X-ray diffraction patterns of asbestos. Amer. Min. 35, 579-589.

Beer, K. E. (1952) The petrography of some riebeckite-granites of Nigeria. Geological Survey and Museum, London. Rep. GSM/AED 116.

Berman, H. (1937) Constitution and classification of the natural silicates. Amer. Min. 22, 342.

Berman, H., and E. S. Larsen (1931) Compositions of alkali amphiboles. Amer. Min. 16, 140-144.

Berthelsen, A. (1965) On the geology of the country around Ivigtut, S.W. Greenland. Geol. Rdsch. 52, 269-280.

Berthelsen, A. and A. Noe-Nygaard (1965) The Precambrian of Greenland. In Rankama, K. (ed.) The Geologic Systems, The Precambrian, 2, 113-262.

Bilgrami, S. A. (1955) Manganese amphiboles from Sitasaongi Mine, Bhandara District, India. Min. Mag. 30, 633-647.

Bilgrami, S. A. (1956) Manganese silicate minerals from Chikla, Bhandara District, India. Min. Mag. 31, 236-244.

Binns, R. A. (1965) The mineralogy of metamorphosed basic rocks from the Willyama Complex, Broken Hill District, New South Wales. Part I, hornblendes. Min. Mag. 35, 306-325.

Black, P. M. (1970) Ferroglaucophane from New Caledonia. Amer. Min. 55, 508-512.

Bloxam, T. W. (1956) Jadeite-bearing metagraywackes in California. Amer. Min. 41, 488-496.

Bloxam, T. W. (1959) Glaucophane-schists and associated rocks near Valley Ford, California. Amer. J. Sci. 257, 95-112.

Bloxam, T. W. (1960) Jadeite rocks and glaucophane rocks from Angel Island, San Fransisco Bay, California. Amer. J. Sci. 258, 555-573.

Bloxam, T. W., and J. B. Allen. (1960) Glaucophane schist, eclogite and associated rocks from Knockormal in the Girvan-Ballantrae complex, S. Ayrshire. Trans. Roy. Soc. Edinburgh 64, 1-27.

Bøggild, O. B. (1906) On some minerals from Narsarsuk at Julianehaab, Greenland. Medd. om. Grønland 33, no. 5.

Borg, I. Y. (1956) Glaucophane schists and eclogites near Healdsburg, California. Amer. Min. 41, 488-496.

Borg, I. Y. (1967) Optical properties and cell parameters in the glaucophane-riebeckite series. Contr. Min. and Pet. 15, 67-92.

Borley, G. D. (1963) Amphiboles from the younger granites of Nigeria. Part I. Chemical classification Min. Mag. 33, 358-376.

Borley, G. D., and M. T. Frost (1963) Some observations on igneous ferrohastingsites. Min. Mag. 33, 646-662.

Borneman-Starynkevitch, I. D. (1960) Chemical formulae of minerals. IV Amphiboles. Mem. All-Union Min. Soc. 89, 236 (Translation by O. Bradley).

Bowden, P. (1966) Zirconium in younger granites of Nigeria. Geochim. Cosmochim. Acta 30, 985-993.

Bowden, P. (1970) Origin of the Younger Granites of Northern Nigeria. Contr. Min. and Pet. 25, 153-162.

Bowen, N. L., and J. F. Schairer (1935) Grunerite from Rockport Massachusetts and a series of synthetic fluor-amphiboles. Amer. Min. 20, 543-551.

Bown, M. G. (1966) A new amphibole polymorph in intergrowth with tremolite: clino-anthophyllite. Amer. Min. 51, 259-260.

Boyd, F. R. (1954) Amphiboles. Carnegie Inst. Washington. Ann. Rept. Director Geophys. Lab. 53, 116-117.

Boyd, F. R. (1955) Amphiboles. Carnegie Inst. Washington. Ann. Rept. Director Geophys. Lab. 54, 115-119.

Boyd, F. R. (1959) Hydrothermal Investigations of amphiboles, in Researches in Geochemistry ed. P. H. Abelson, vol. 1, 397-426.

Bridgewater, D. (1965) Isotopic age determinations from South Greenland and their geological setting. Medd. om Grønland 179, no. 4.

Brock, P. W. G., D. C. Gellatly, and O. von Knorring (o964) Mboziite, a new sodic amphibole end-member. Min. Mag. 33, 1057-1065.

Brothers, R. N. (1954) Glaucophane schists from North Berkeley Hills, California. Am. J. Sci. 252, 614-626.

Brummer, J. J., and E. L. Mann (1961) Geology of Seal Lake, Labrador. Bull. Geol. Soc. Am. 72, 1361-1382.

Buerger, M. J., G. E. Klein, and G. Donnay (1954) Determination of the crystal structure of nepheline. Amer. Min. 39, 805-818.

Burns, R. G. (1968) Crystal-field phenomena and iron enrichments in pyroxenes and amphiboles. Proc. International Mineralogical Association, 5th Gen. Meeting, Cambridge 1966, 170-183.

Burns, R. G., and G. M. Bancroft (1969) Correlations of Mössbauer and infrared spectral data in site population studies of amphiboles (abs.). Proc. Symp. on Amphiboles and Pyroxenes Virginia Poly. Blacksburg, Virginia 1969.

Burns, R. G., and F. J. Prentice (1968) Distribution of iron cations in the crocidolite structure. Amer. Min. 53, 770-776.

Burns, R. G., and R. G. J. Strens (1966) Infrared study of the hydroxyl bands in clinoamphiboles. Science 153, 890-892.

Burns, R. G., and A. D. Law (1970) Hydroxyl Stretching Frequencies in the Infrared Spectra of Anthophyllites and Gedrites. Nature, 226, 73-75.

Butler, J. R., and A. Z. Smith (1962) Zirconium and niobium in some alkaline rocks. Geochim. Cosmochim. Acta 26, 945-953.

Carmichael, I. S. E. (1967) The mineralogy and petrology of the volcanic rocks from the Leucite Hills, Wyoming. Contr. Min. and Petr. 15, 24-66.

Chapman, R. W., and C. R. Williams (1935) The evolution of the White Mountain magma series. Amer. Min. 20, 502-530.

Cilliers, J. J. Le (1967) The origin of crocidolite. Conference on Physics and Chemistry of Asbestos Minerals. Oxford, 1967 (abstract).

Cilliers, J. J. Le. and J. H. Genis (1964) The origin of the crocidolite deposits of South Africa in "Some Ore Deposits of Southern Africa". Vol. II. Geol. Soc. S. Africa.

Clark, J. R., and J. J. Papike (1968) Crystal chemical characterization of omphacites. Amer. Min. 53, 840-868.

Coleman, R. G. (1951) Riebeckite from St. Peters Dome, Colorado. Bull. Geol. Soc. Am. 62, 1517 (abs.).

Coleman, R. G. (1967) Glaucophane Schists from California and New Caledonia. Tectonophysics 4, 479-498.

Coleman, R. G., and D. H. Lee (1963) Glaucophane-bearing Metamorphic rock types of the Cazadero area, California. Journ. Petrology 4, 260-301.

Coleman, R. G., and J. J. Papike (1968) Alkali Amphiboles from the Blueschists of Cazadero, California. Journ. Petrology 9, 105-122.

Colville, A. A., and G. V. Gibbs (1965) Refinement of the crystal structure of riebeckite. Spec. Pap. Geol. Soc. Am. 82, 31.

Colville, A. A., W. G. Ernst, and M. C. Gilbert (1966) Relationships between cell parameters and chemical compositions of monoclinic amphiboles. Amer. Min. 51, 1727-1754.

Comeforo, J. E., and J. A. Kohn (1954) Synthetic asbestos investigations. I. Study of synthetic fluor-tremolite. Amer. Min. 39, 537-548.

Debron, G. (1965) Contribution à l'étude des reactions d'echange des ions alcalins et alcalin-terre dans les feldspathoides. Bull. Soc. franç. Min. Crist. 88, 69-96. (ref. Min. Abs. 17, 374).

Dengo, S. (1953) Geology of the Caracas region, Venezuela. Bull. Geol. Soc. Am. 64, 7-40.

Dietrich, R. V., and K. S. Heier (1967) Differentiation of quartz bearing syenite (nordmarkite) and riebeckite-arfvedsonite granite (ekerite) of the Oslo series. Geochim. Cosmochim. Acta 31, 275-280.

Drysdall, A. R., and A. R. Newton (1960) Blue asbestos from Lusaka, Northern Rhodesia (Zambia), and its bearing on the genesis and classification of this type of asbestos. Amer. Min. 45, 53-59.

Du Toit, A. L. (1945) The origin of the amphibole asbestos deposits of South Africa. Trans. Geol. Soc. S. Africa 48, 161-206.

Duke, D. A., and J. D. Stephens (1964) Infrared investigation of the olivine group of minerals. Amer. Min. 49, 1388-1406.

Dunn, J. A., and P. C. Roy (1939) Manganese amphiboles from Tirodi, Central Provinces. Rec. Geological Survey India 73.

Eckermann, H. von. (1968) A new contribution to the interpretation of the genesis of the Norra Kärr alkaline body, southern Sweden. Lithos 1, 76-88.

Emeleus, C. H. (1964) The Grønnedal-Íka alkaline complex, South Greenland. Medd. om Grønland 172, no. 3.

Emeleus, C. H., and W. T. Harry (1970) The Igaliko nepheline syenite Complex. Medd. om Grønland 186, no. 3.

Engel, A. E. J., and C. G. Engel (1962) Progressive metamorphism of amphibolite, northwest Adirondack Mountains, New York. In Petrologic Studies: A volume to Honour A. F. Buddington. Eds. A. E. J. Engel, H. L. James, and B. F. Leonard. Part II. Mineralogy. Geol. Soc. Am. 37-82.

Ernst, W. G. (1959b) Alkali Amphiboles. Carnegie Inst. Washington. Ann. Rept. Director Geophys. Lab. 58, 1958-1959, 121-126.

Ernst, W. G. (1960) Stability relations of magnesioriebeckite. Geochim. Cosmochim. Acta 19, 10-40.

Ernst, W. G. (1961) Stability relations of glaucophane. Am. J. Sci. 259, 735-765.

Ernst, W. G. (1962) Polymorphism in alkali amphiboles. Journ. Geophys. Res. 67, 3555-3556.

Ernst, W. G. (1962) Synthesis, stability relations, and occurrence of riebeckite and riebeckite-arfvedsonite solid solutions. Journ. Geol. 70, 689-736.

Ernst, W. G. (1963) Petrogenesis of Glaucophane schists. Journ. Petrology 4, 1-30.

Ernst, W. G. (1963a) Polymorphism in alkali amphiboles. Amer. Min. 48, 241-260.

Ernst, W. G. (1964) Petrochemical study of co-existing minerals from low grade schists, Eastern Sikoku, Japan. Geochim. Cosmochim. Acta 28, 1631-1668.

Ernst, W. G. (1965) Mineral parageneses in Franciscan metamorphic rocks, Panoche Pass, California. Bull. Geol. Soc. Am. 76, 879-914.

Ernst, W. G. (1966) Synthesis and stability relations of ferrotremolite. Am. J. Sci. 264, 37-65.

Ernst, W. G., and C. M. Wai (1969) Mössbauer, infrared, X-ray and optical study of cation ordering and dehydrogenation in natural and heat-treated sodic amphiboles. Proc. Symp. on Amphiboles and Pyroxenes Virginia Poly. Blacksburg, Virginia 1969.

Eskola, P., and G. Sahlstein (1930) On astrophyllite-bearing nepheline syenite gneiss found as a boulder in Kühtelysvaara, eastern Finland. Bull. Comm. géol. Finlande, 92, 77.

Essene, E. J., W. S. Fyfe, and F. J. Turner (1965) Petrogenesis of Franciscan glaucophane schists and associated metamorphic rocks, California. Beit. zür Min. und Pet. 11, 695-704.

Farmer, V. C. (1964) Infrared spectroscopy of silicates and related compounds. In "Chemistry of Cements", vol. 2. (Ed. H. F. W. Taylor, 289.

Farmer, V. C., and J. D. Russell (1966) The effects of particle size and structure on the vibrational frequencies of layer silicates. Spectrochim. Acta 22, 389.

Ferguson, J. (1964) Geology of the Ilímaussaq Alkaline Intrusion, South Greenland. Medd. om Grønland Bd 172, no. 4.

Ferguson, J. (1967) Geology of the Ilímaussaq alkaline intrusion, South Greenland. Unpublished Ph.D. thesis. University of Witwatersrand.

Fermor, L. L. (1909) The Manganese Ore Deposits of India. Mem. Geol. Survey India 37.

Finger, L. W. (1969) The crystal structure and cation distribution of a grunerite. Min. Soc. America Spec. Paper no. 2, 95-100.

Finger, L. W., and T. Zoltai (1967) Cation distribution in grunerite (abstr.). Trans. Amer. Geophys. Union 48, 233-234.

Fischer, K. F. (1966) A further refinement of the crystal structure of cummingtonite, $(Mg,Fe)_7(Si_4O_{11})_2(OH)_2$. Amer. Min. 51, 814-818.

Floor, P. (1966) Petrology of an aegirine-riebeckite gneiss-bearing part of the Hesperian massif: the Galiniero and surrounding areas, Vigo, Spain. Leidse Geol. Meded. 36, 1-204.

Freeman, A. G. (1966) The dehydroxylation behaviour of amphiboles. Min. Mag. 35, 953-957.

Freudenberg, W. (1910) Der Anophorit, eine neüe Hornblende vom Katzenbuckel. Neues Jahrb. Min. 1, 34-35.

Frost, M. T. (1963) Amphiboles from the Younger granites of Nigeria. Part II. X-ray data. Min. Mag. 33, 377-384.

Fyfe, W. S. (1960) Hydrothermal synthesis and determination of equilibrium between minerals in the subsolidus region. Journ. Geol. 68, 553-566.

Fyfe, W. S. (1962) On the relative stability of talc, anthophyllite, and enstatite. Am. J. Sci. 260, 460-466.

Garrod, R. I., and C. S. Rann (1952) Preliminary studies of crocidolite and amosite. Acta. Cryst. 5, 285.

Garson, M. S. (1960) Geology of Lake Chilwa area. Bull. Geol. Survey Nyasaland (Malawi) 12.

Gellatly, D. C., and G. Hornung (1968) Metasomatic nepheline-bearing gneisses from Darkainle, Somali Republic. Journ. Geol. 76, 678-691.

Gerasimovski, V. I., and S. Ya Kuznetsova (1967) The chemical composition of rocks of the Ilímaussaq alkaline massif. Geochemistry International 1968 (for 1967), 274.

Ghent, E. D. (1965) Glaucophane-schist facies metamorphism in the Black Butte area, northern California. Am. J. Sci. 263, 385-400.

Ghose, S. (1961) The crystal structure of a cummingtonite. Acta. Cryst. 14, 622-627.

Ghose, S. (1965) A scheme of cation distribution in the amphiboles. Min. Mag. 35, 46-53.

Ghose, S., and E. Hellner (1959) The crystal structure of grunerite and observations on the Fe-Mg distribution. Journ. Geol. 67, 691-701.

Gibbs, G. V. (1969) The crystal structure of protoamphibole. Min. Soc. Amer. Spec. Pap. 2, 101-110.

Gibbs, G. V., J. L. Miller, and H. R. Shell (1962) Synthetic fluor-magnesiorichterite. Amer. Min. 45, 75-82.

Gibbs, G. V., and C. T. Prewitt (1966) Amphibole cation site disorder (Cambridge I.M.A. meeting, 1966, abstract).

Gilbert, M. C. (1966) Synthesis and stability relations of the hornblende, ferropargasite. Am. J. Sci. 264, 698-742.

Gilbert, M. C. (1969) Reconnaissance study of the stability of amphiboles at high pressure. Carnegie Inst. Washington. Ann. Rept. Director Geophys. Lab. 67, 167-170.

Glagolev, A. A., and O. B. Beyseev (1965) Rhodusite concretions from South Minusinsk and Dzhezkazgan trough. Doklady Acad. Sci. Earth Sci. Sect. 157, 88 (ref. Min. Abs. 18 no. 2).

Goranson, R. W. (1931) Solubility of water in granite magmas. Amer. J. Sci. 22, 481.

Gordon, S. G. (1927) On arfvedsonite, riebeckite, and crocidolite from Greenland. Proc. Acad. Nat. Sci. Philad. 79, 193-205.

Gossner, B., and F. Spielberger (1929) Chemische und röntgeno-graphische Untersuchungen an Silikaten. Ein Beitrag zür Kenntnis der Hornblendegruppe. Zeit. Krist. 72, 111-142.

Green, J. (1959) Geochemical table of the elements for 1959. Bull. Geol. Soc. Am. 70, 1127-1184.

Greene-Kelly, R. (1952) Irreversible dehydration in montmorillonite. Clay Minerals Bulletin 1, 221-225.

Greenwood, H. J. (1963) The synthesis and stability of anthophyllite. Journ. Petrology 4, 317-351.

Greenwood, R. (1951) Younger intrusive rocks of plateau province Nigeria, compared with alkalic rocks of New England. Bull. Geol. Soc. Am. 1151-1178.

Grigoriev, D. P., and E. W. Iskull (1937) The regeneration of amphiboles from their melts at normal pressures. Amer. Min. 22, 169-177.

Grigorjeva, R. F., O. G. Chigarova, and A. D. Fedoseev (1967) Synthetic fibrous fluoro-amphiboles and their properties. Conference on Physics and Cehmistry of Asbestos Minerals Oxford, 1967 (abstract).

Gross, E. B., and E. Wm. Heinrich (1965) Petrology and Mineralogy of the Mount Rosa Area, El Paso and Teller Counties, Colorado. I. The Granites. Amer. Min. 50, 1273-1294.

Gross, E. B., and E. Wm. Heinrich (1966) Petrology and Mineralogy of the Mount Rosa Area, El Paso and Teller Counties, Colorado. II. Pegmatites. Amer. Min. 51, 299-323.

Grozdanov, L. (1969) A crystallochemical and X-ray diffraction study of amphiboles in the Svidnya intrusion. Izv. Geol. Inst. Bulg. Akad. Nauk. 18. (ref. Chemical Abstracts 73, 68409).

Hahn, T., and M. J. Buerger (1955) The detailed structure of nepheline $KNa_3Al_4Si_4O_{16}$. Zeit. Krist. 106, 308.

Hallimond, A. F. (1943) On the graphical representation of the calciferous amphiboles. Amer. Min. 28, 65-89.

Hamilton, D. L. (1961) Nephelines as crystallization temperature indicators. Journ. Geol. 69, 321-329.

Hamilton, E. I. (1964) The geochemistry of the northern part of the Ilimaussaq intrusion, S. W. Greenland. Medd. om Grønland 162, no. 10.

Hanisch, K. (1966) Messung des Ultrarot - Pleochroism von Minerolen VI OH Streck frequenz in Riebeckit. Neues Jahr. Min. Mn. 109-112.

Harry, W. T. (1950) Aluminium replacing silicon in some silicate lattices. Min. Mag. 29, 142-149.

Harry, W. T., and C. T. R. Pulvertaft (1963) The Nunassuit intrusive complex, South Greenland. Medd. om Grønland 169, no. 1.

Hayashi, H., and K. Oinuma (1965) Relationship between infrared absorption spectra in the region of 450-900 cm^{-1} and chemical composition of chlorite. Amer. Min. 50, 476-483.

Heinrich, E. Wm., and D. H. Dahlem (1966) Carbonatites and Alkalic rocks of the Arkansas River area, Fremont County, Colorado. Min. Soc. India, IMA vol. 1966, 38-44.

Heinrich, E. Wm., and D. H. Dahlem (1967) Carbonatites and Alkalic Rocks of the Arkansas River Area, Fremont County, Colorado. 4. The Pinon Peak Breccia Pipes. Amer. Min. 52, 817-831.

Hellner, E., Th. Hinrichsen, and F. Seifert (1965) The study of mixed crystals of minerals in metamorphic rocks, 155-168. In "Controls of metamorphism", eds. W. S. Pitcher and G. W. Flinn.

Hellner, E., and K. Schürmann (1966) Stability of metamorphic amphiboles: the tremolite-actinolite series. Journ. Geol. 74, 322-331.

Heritsch, H. (1965) Der Natrium-Amphibol aus dem Glasbochgraben bei Schlaining Burgenland. Tschermaks Min. Pet. Mitt. 10, 209.

Heritsch, H., and E. Kahler (1960) Strukturuntersuchung an zwei Kluft-Karinthinen. Ein Beitrag zur Karinthinfrage. Tschermaks min. pet. Mitt., ser. 3, 7, 218-234.

Heritsch, H., and L. Reichert (1960) Strukturuntersuchung an einer basaltischen Hornblende von Cernosin, CSR. Tschermaks min. pet. Mitt., ser. 3, 7, 235-245.

Heritsch, H., P. Paulitsch., and E. M. Walitzi (1957) Die Struktur von Karinthin und einer basaltischen Hornblende. Tschermaks min. pet. Mitt., ser. 3, 6, 215-225.

Heritsch, H., G. Bertoldi, and E. M. Walitzi (1960) Strukturuntersuchung an einer basaltischen Hornblende von Kuruzzenkogel südlich Fehring, Steiermark. Tschermaks min. pet. Mitt., ser. 3, 7, 210-217.

Himmelberg, G. R., and J. J. Papike (1969) Coexisting amphiboles from Blueschist facies metamorphic rocks. Journ. Petrology, 10, 102-114.

Hodgson, A. A. (1965) The thermal decomposition of miscellaneous crocidolites. Min. Mag. 35, 291-305.

Hodgson, A. A. (1965) Fibrous silicates. Royal Inst. Chem. Lec. Ser., 4.

Hodgson, A. A., A. G. Freeman, and H. F. W. Taylor (1965) The thermal decomposition of crocidolite from Keogas, South Africa. Min. Mag. 35, 5-30.

Hofmann, U., and J. Endell (1939) The cation exchange and swelling of montmorillonite as a function of preheating. Angew. Chemie 52, 708-709.

Hofmann, U., and R. Klemen (1950) Verlust der Austauschfahigkeit vom Lithiumionen an Bentonit durch Erhitzung. Zeit. Anorg. Chem. 262, 95-99.

Holgate, N. (1951) On crossite from Anglesey. Min. Mag. 29, 792-798.

Huang, W. T. (1958) Riebeckite granite in the Wichita Mountains, Oklahoma. Bull. Geol. Soc. Am. 69, 1191-1192.

Huebner, J. S., and J. J. Papike (1969) Synthesis and sodium-potassium exchange in the richterite series $(K,Na)CaNaMg_5Si_8O_{22}(OH)_2$ Proc. Symp. on Amphiboles and Pyroxenes. Virginia Poly. Blacksburg, Virginia 1969.

Hunt, J. M., M. P. Wishert, and L. C. Bonham (1950) Infrared absorption spectra of minerals and other inorganic compounds. Anal. Chem. 22, 1478-1497.

Hytönen, K., and A. Heikinnen (1967) Alkali amphibole from Otanmaki, Finland. Bull. Comm. Geol. Finlande no. 222, 145-156.

Iiyama, J. T. (1963) The system Na_2O-MgO-Al_2O_3-SiO_2-H_2O. Compte Rendu Acad. Sci. (Paris) 256, 966-967.

Inoue, T. (1950) Amphiboles and biotites from the Fukushin-zan alkaline complex, Korea. Journ. Geol. Soc. Japan 56, 71.

Ivanov, I. P., and G. A. Sidorenko (1965) Richterite asbestos. Zap. Vses. Min. Obshch. 94, 497-506 (ref. Min. Abs. 17, 691).

Iwasaki, M. (1960a) Colourless glaucophane and associated minerals in quartzose schists from eastern Sikoku, Japan. Journ. Geol. Soc. Japan 66, 566-574.

Iwasaki, M. (1960b) Barroisitic amphibole from Bizan in eastern Sikoku, Japan. Journ. Geol. Soc. Japan 66, 625-630.

Iwasaki, M. (1963) Metamorphic rocks of the Kotu-Bizan area, eastern Sikoku. Tokyo Univ. Fac. Sci. Journ., sec 2, 15, 1-90.

Jacobson, R. R. E., W. N. Macleod, and R. Black (1958) Ring-complexes in the younger granite province of N. Nigeria. Geol. Soc. London, Mem. 1.

Jaffe, H. W., W. O. J. Graenveld Meyer, and D. H. Selchow (1961) Manganoan cummingtonite from Nsuta, Ghana. Amer. Min. 46, 642-653.

Jaffe, W. H., P. Robinson, and C. Klein (1968) Exsolution lamellae and optic orientation of clinoamphiboles. Science 160, 776-778.

Kanehira, K. (1967) Sanbagawa crystalline schists in the Iimori district Japan. Japan Journ. Geol. Geog. 38, 109.

Kawahara, A. (1963) X-ray studies on some alkaline amphiboles. Miner. Journ. (Japan) 4, 30-40.

Keil, K. (1967) The Electron Microprobe X-Ray Analyzer and its application in Mineralogy. Fortschr. Miner. 44, 4-66.

Kempe, D. R. C. (1969) The cell parameters of the arfvedsonite-eckermannite series, with observations on the MgO and total iron content of amphiboles. Min. Mag. 37, 317-332.

Kerr, P. F., J. L. Kulp, and P. K. Hamilton (1949) Differential Analysis of reference clay mineral specimens. Prelim. report 3 of "Reference Clay Minerals, A.P.I. Research Project 49". American Petroleum Institute.

Ketellaar, J. A. A. (1953) Chemical Constitution.

Kilpady, S. (1964) Winchite from Ponia, Balaghat District, Madhya Pradesh, India. Journ. Geol. Soc. Univ. Nagpur 1, 1-7.

King, B. C., and D. S. Sutherland (1960) Alkaline rocks of eastern and southern Africa. Part II Petrology. Science Progress 48, 504-524.

King, D. (1961) The occurrence and comparative mineralogy of S. Australian magnesian crocidolites (rhodusites). Trans. Roy. Soc. S. Austr. 84, 119-128.

Kisch, H. J. (1969) Magnesiocummingtonite - $P2_1/m$: A Ca- and Mn- poor clino-amphibole from New South Wales. Contr. Min. Pet. 21, 319-331.

Klein, C. (1964) Cummingtonite - Grunerite Series: A chemical, optical and X-ray study. Amer. Min. 49, 963-982.

Klein, C. (1968) Coexisting amphiboles. Journ. Petrology, 9, 281-330.

Klein, C. (1966) Mineralogy and Petrology of the metamorphosed Wabush Iron Formation, Southwestern Labrador. Journ. Petrology, 7, 246-305.

Klein, C. (1968) Two-amphibole assemblages in the system actinolite - hornblende - glaucophane. Amer. Min. 54, 212-237.

Klein, C., and D. R. Waldbaum (1967) X-Ray crystallographic properties of the cummingtonite - grunerite series. Journ. Geol. 75, 379-392.

Kohn, J. A., and J. E. Comeforo (1955) Synthetic asbestos investigations. II X-ray and other data on synthetic fluor-richterite,-edenite, - boron-edenite. Amer. Min. 40, 410-421.

Korzhinskü, D. S. (1950) Differential mobility of components and metasomatic zoning in metamorphism. Int. Geol. Cong. 18th session, Great Britain 1948, Pt. III, 65-80.

Korzhinskü, D. S. (1965) The theory of systems with perfectly mobile components and processes of mineral formation. Amer. J. Sci. 263, 193-205.

Kovalenko, V. I. (1968) On the chemical composition, properties, and mineral paragenesis of riebeckite-arfvedsonite. Proc. International Mineralogical Association, 5th Gen. Meeting, Cambridge 1966, 261-284.

Kulish, L. I. (1966) Alkaline metasomatism of ore bearing series in the Lesser Khingan. Miner. Fatsü Granitoidov, Ikh Rhudonos., Akad. Nauk. S.S.S.R., Sib. Otd., Dol'-nevost. Geol. Inst. (ref. Chem. Abs. 66, 8214).

Kunitz, W. (1930) Die Isomorphieverhältnisse in der Hornblende-gruppe. Neues Jahrb. Min. 60, A, 171-250.

Kupletsky, B. M. (1930) Über zwei Alkalihornblenden vom Urma-Waraka (Kola). Trans. Mus. Min. Acad. Sci. U.R.S.S. 4, 10. (ref. Min. Abst. 5, 34).

Lacroix, A. (1923) Mineralogie de Madagascar, 3, 1-328.

Larsen, E. S. (1942) Alkalic rocks of Iron Hill, Gunnison County, Colorado. U.S. Geol. Survey Prof. Paper 197-A, 1-64.

Laudermilk, J. D., and A. O. Woodford (1930) Soda-rich anthophyllite asbestos from Trinity County, California. Amer. Min. 15, 259-262.

Launer, P. J. (1952) Regularities in the infrared absorption spectra of silicate minerals. Amer. Min. 37, 764-784.

Layton, W. (1964) Factors governing the natural and synthetic occurrences of members of the amphibole group of minerals. Neues Jahrb. Mineralogie Monatsh. no. 5, 135-147.

Layton, W., and R. Phillips (1960) The cummingtonite problem. Min. Mag. 32, 659-663.

Lazarev, A. N., and F. F. Tenisheva (1962) Infrared spectra of amphiboles. Optika Spectrosk. 12, 115.

Leake, B. E. (1962) On the non existence of a vacant area in the Hallimond calciferous amphibole diagram. Jap. Journ. Geol. Geogr. 33, 1-13.

Leake, B. E. (1965) The relationship between composition of calciferous amphibole and grade of metamorphism. In"Controls of Metamorphism", eds. W. S. Pitcher and G. W. Flinn, 299-318.

Leake, B. E. (1965a) The relationship between tetrahedral aluminium and the maximum possible octahedral aluminium in natural calciferous and subcalciferous amphiboles. Amer. Min. 50, 843-851.

Leake, B. E. (1968) A catalog of analyzed calciferous and subcalciferous amphiboles together with their nomenclature and associated minerals. Geol. Soc. Am. Spec. Pap. 98.

Lee, D. E., R. G. Coleman, H. Bastron, and V. C. Smith (1966) A two-amphibole glaucophane schist in the Fransiscan Formation, Cazadero Area, Sonoma County, California. U.S. Geol. Surv. Prof. Paper 550-C, C148-C157.

Linthout, K., and C. Kieft (1970) Preliminary note: a mboziite of metamorphic origin. Min. Mag. 37, 629-630.

Lyon, R. J. P. (1963) Evaluation of infrared spectrophotometry for compositional analysis of Lunar and Planetary soils. Stanford Research Institute, Final Report. N.A.S.A. Note D-1871.

Lyon, R. J. P. (1968) Infrared absorption spectroscopy. In "Determinative Mineralogy" (Ed. J. Zussman) 371-403.

Lyon, R. J. P., W. M. Tuddenham, and C. S. Thompson (1959) Quantitative mineralogy in 30 minutes. Econ. Geol. 54, 1047-1055.

Luth, W. C., and O. F. Tuttle (1963) Externally heated cold-seal pressure vessels for use to 1000 bars and 750°C. Amer. Min. 48, 1401-1403.

Macdonald, R. (1966) Petrological studies of some alkalic and peralkalic dyke rocks from the Tugtutôq-Narssaq area. Grønlands Geol. Unders. Rapp. 11. 1966, 44-47.

Macdonald, R. (1969) The Petrology of alkaline dykes from the Tugtutôq area, South Greenland. Medd. fra Dansk. Geol. For. 19, 257-282.

McKee, B. (1962) Widespread occurrence of jadeite , lawsonite and glaucophane in central California. Am. J. Sci. 260, 596-610.

McKie, D. (1967) Fenitisation in "Carbonatites" eds. Tuttle and Gittins.

McLachlan, G. R. (1951) The aegirine-granulites of Glen Lui, Braemar, Aberdeenshire. Min. Mag. 29, 476-494.

Magnusson, N. H. (1930) Långbans Malmtakt. Sveriges. Geol. Undersökning ser Ca, 23, 1-111.

Makarova, T. A., E. N. Korytkova, and A. D. Fedoseev (1967) The synthesis of fibrous amphiboles under hydrothermal conditions. Conference on Physics and Chemistry of Asbestos Minerals, Oxford, 1967 (abstract).

Marmo, V. (1967) On granites, a revised study. Bull. Comm. Geol. Finlande, 227.

Matsuo, N., T. Katsutoshi, and K. Tsuyoshi (1969) Kôzulite, a new alkali amphibole, from Tanohata Mine, Iwate Prefectine, Japan. Min. Journ. (Japan) 12, 311-312.

Michel-Lèvy, M. C. (1957) Premiers stades du métamorphisme artificiel d'une dolomie siliceuse: formation de tremolite et diopside. Bull. Soc. franç. Min. Crist. 80, 297.

Miles, K. R. (1942) The blue asbestos-bearing banded iron formation of the Hammersley Range, Western Australia. W. Australian Geol. Surv. Bull. 100 Pt. I.

Milton, C., and H. P. Eugster (1959) Mineral assemblages of the Green River formation, in Abelson, P.H., ed., Researches in Geochemistry vol. I.

Mitchell, J. T., F. D. Bloss, and G. V. Gibbs (1969) A refinement of the structure of actinolite. Proc. Symp. on Amphiboles and Pyroxenes. Virginia Poly. Blacksburg, Virginia 1969.

Mitchell, J. T., F. D. Bloss, and G. V. Gibbs (1971) Examination of the actinolite structure and four other C2/m amphiboles in terms of double bonding. Zeits. Krist. 133, 273-300.

Miyashiro, A. (1957) The chemistry, optics and genesis of the alkali amphiboles. Journ. Fac. Sci. Univ. Tokyo, Sect II, 11, 57.

Miyashiro, A. (1967) Chemical compositions of rocks in relation to metamorphic facies. Jap. Journ. Geol. Geog. 38, 149-157.

Miyashiro, A., and T. Miyashiro (1956) Nepheline syenites and associated alkalic rocks of the Fukushin-zan area, Korea. Journ. Fac. Sci. Univ. Tokyo sect. II 10, 1-64.

Miyashiro, A., and M. Iwasaki (1957) Magnesioriebeckite in crystalline schists of Bizan in Sikoku, Japan. Journ. Geol. Soc. Japan 256, 97-110.

Miyashiro, A., and S. Banno (1958) Nature of Glaucophanitic Metamorphism. Am. Journ. Sci. 256, 97-110.

Morozewicz, J. (1925) Über einige Eisenalkaliamphibole. Tschermaks Min. Pet. Mitt. 38, 210-222.

Morozewicz, J. (1930) Der Mariupolit und seine Blutsverwandten. Tschermaks Min. Pet. Mitt. 40, 335-436.

Mueller, R. F. (1967) Tremolite-ferroactinolite series - a discussion. Journ. Geol. 75, 234-236.

Murakami, N. (1964) Ferraedenite and ferrorichterite in the Metasomatic syenites from Utsugiono, Yamaguchi Prefecture, Japan. Journ. Jap. Assoc. Min. Petr. & Econ. Geol. 51, 77-87.

Nash, W. P., I. S. E. Carmichael, and R. W. Johnson (1969) The Mineralogy and Petrology of Mount Suswa, Kenya. Journ. Petrology 10, 409-439.

Nayak, V. K. (1961) Juddite from Kajlidongri Manganese Mine, Jhabua District, Madhya Pradesh, India. Min. Mag. 32, 736-737.

Nayak, V. K., and K. J. Neuvonen (1963) Some manganese minerals from India. Comptes Rend. Soc. Geol. Finlande 35, 27-37.

Nayak, V. K., and K. J. Neuvonen (1964) Some manganese minerals from India. Bull. Comm. Geol. Finlande 221, 27.

Nicholls, G. D., and J. Zussman (1955) The structural formula of a hydrous amphibole. Min. Mag. 30, 717-722.

Nicholls, J., and I. S. E. Carmichael (1968) Peralkaline acid liquids: A petrological study. Contr. Min. and Pet. 20, 268-294.

Nickel, E. H., and E. Mark (1965) Arfvedsonite and aegirine-augite from Seal Lake, Labrador. Can. Mineral. 8, 185-197.

O'Connor, D. J., and J. H. Patterson (1967) Thermal studies of Wittenoom crocidolite in vacuum. Conference on Physics and Chemistry of Asbestos Minerals. Oxford, 1967 (abstract).

Olsen, E. (1967) Amphibole: First occurrence in a meteorite. Science 156, 61-62.

Orville, P. M. (1967) Unit cell parameters of the microcline - low albite and the sanidine - high albite solid solution series. Amer. Min. 52, 55-86.

Papike, J. J., and J. R. Clark (1967) Crystal-chemical role of potassium and aluminium in a hornblende of proposed mantle origin. Geol. Soc. Amer. Prog. 1967 Ann. Meeting, New Orleans (Geol. Soc. Amer. Spec. Pap. 115, 171 (1968)).

Papike, J. J., and J. R. Clark (1968) The crystal structure and cation distribution of glaucophane. Amer. Min. 53, 1156-1173.

Papike, J. J., and M. Ross (1969) Gedrites; crystal structures and intracrystalline cation distrubutions. Proc. Symp. on Amphiboles and Pyroxenes. Virginia Poly., Blacksburg, Virginia 1969.

Papike, J. J., M. Ross, and J. S. Huebner (1968) Potassic richterite, $KNaCaMg_5Si_8O_{22}(OH)_2$: crystal chemistry and sodium-potassium exchange (abstr.). Geol. Soc. Amer. Prog. 1968 Ann. Meeting, Mexico City. (Geol. Soc. Amer. Spec. Pap. 121, 230).

Papike, J. J., M. Ross, and J. R. Clark (1969) Crystal-chemical characterization of clino-amphiboles based on five new structure refinements. Min. Soc. Amer. Spec. Pap. 2, 117-136.

Parker, R. B. (1961) Rapid determination of the approximate composition of amphiboles and pyroxenes. Amer. Min. 46, 892-900.

Patterson, J. H. (1965) Thermal disintegration of crocidolite in air and vacuum. Min. Mag. 35, 31-37.

Patterson, J. H., and D. J. O'Connor (1966) Chemical studies of amphibole asbestos. Aust. Journ. Chem. 19, 1155-1164.

Peacock, M. A. (1928) The nature and origin of the amphibole asbestos of South Africa. Amer. Min. 13, 241-285.

Phemister, J., C. O. Harvey, and P. A. Sabine (1950) The riebeckite-bearing dykes of Shetland. Min. Mag. 29, 359-373.

Phillips, R. (1963) The recalculation of amphibole analyses. Min. Mag. 33, 707-711.

Phillips, R. (1966) Amphibole compositional space. Min. Mag. 35, 945-952.

Phillips, R., and W. Layton (1964) The calciferous and alkali amphiboles. Min. Mag. 33, 1097-1109.

Phillips, R., and G. Rowbotham (1968) Studies on synthetic alkali amphiboles. Proc. International Mineralogical Association, 5th Gen. Meeting. Cambridge 1966, 249-254.

Polovinkina, Y. Ir. (1953) Cummingtonite and alkali amphiboles from Krivoi Rog, Ukraine. Mineral. Sbornik, Lvov Geol. Soc. N. 7, 167-186 (Ref. Min. Abstr. 13, 1956).

Poulter, N. W. (1967) The crocidolite bearing rock of Cape Province, South Africa. Conference on Physics and Chemistry of Asbestos Minerals. Oxford, 1967 (abstract).

Prider, R. T. (1939) Some minerals from the leucite-rich rocks of the west Kimberley, Western Australia. Min. Mag. 25, 373-387.

Pulvertaft, T. C. R. (1968) The Precambrian stratigraphy of Western Greenland. XXIII International Geol. Congress, Prague 1968, 4, 89-107.

Puustinen, K. (1970) The Carbonatite of Sülinjärvi in the Pre-Cambrian of Eastern Finland. Lithos 3, 89-92.

Rabbitt, J. C. (1948) A new study of the anthophyllite series. Amer. Min. 33, 263-323.

Ravier, J. (1951) Sur une nouvelle variété d'amphibole: l'eckrite. Bull. Soc. franç. Min. Crist. 74, 10-19.

Raychaudhuri, B. (1964) Relation of atomic constitution to lattice parameters in some hornblendes from the Black Hills, South Dakota. Amer. Min. 49, 198-206.

Ridge, J. D. (1959) The unual manganese-iron deposits of Långban, Sweden. Min. Industries (Penn. State Univ.) 29, no. 3.

Rimskaya-Korsakova, O. M., and E. P. Sokolova (1964) Iron-magnesium micas with reversed absorption. Zap. Vses. Min. Obshch. (Mem. All-Union Min. Soc.) 93, 411-423 (ref. Min. Abs. 17, 504).

Robie, R. A. (1966) Thermodynamic properties of minerals, in Handbook of Physical Constants, Mem. Geol. Soc. Am. 97, 428-480.

Robie, R. A., P. M. Bethke, and K. M. Beardsley (1967) Selected X-ray crystallographic data, malar volumes and density of minerals and related substances. Bull. U.S. Geol. Survey 1248.

Robinson, K., G. V. Gibbs, and P. H. Ribbe (1969) A refinement of the crystal structure of pargasite. Proc. Symp. on Amphiboles and Pyroxenes. Virginia Poly., Blacksburg, Virginia 1969.

Robinson, P., W. H. Jaffe, C. Klein, and M. Ross (1969) Equilibrium coexistence of three amphiboles. Contr. Min. Pet. 22, 248-258.

Roever, W. P. de., and H. J. Nijhuis (1963) Plurifacial Alpine metamorphism in the Eastern Betic Cordillera (S.E. Spain). Geol. Rundschau 53, 324-336.

Ross, M., W. L. Smith, and W. H. Ashton (1968) Triclinic talc and associated amphiboles from Gouveneur Mining District, New York. Amer. Min. 53, 751-769.

Ross, M., J. J. Papike, and P. W. Weiblen (1968) Exsolution in clinoamphiboles. Science 159 (3819), 1099-1102.

Ross, M., J. J. Papike, and K. W. Shaw (1969) Exsolution textures in amphiboles as indicators of subsolidus thermal histories. Min. Soc. America Spec. Paper no. 2, 275-299.

Roy, S., and P. K. Purkait (1968) Mineralogy and Genesis of the Metamorphosed Manganese Silicate Rocks (Gondite) of Gowari Wadona, Madhya Pradesh, India. Contr. Min. and Pet. 20, 86-114.

Roy, S., and F. N. Mitra (1964) Mineralogy and genesis of gondites associated with metamorphosed manganese ore bodies of Madhya Pradesh and Maharashtra, India. Proc. Nat. Inst. Sci. India 30A, 395-438.

Sabine, P. A. (1960) Geology of Rockall. Bull. Geol. Survey Great Britain 16, 156.

Saether, E. (1958) The alkaline rock province of the Fen area in southern Norway. Norske Videnske Selsk. skr. no. 1 (for 1957).

Sahama, Th. G. (1956) Optical anomalies in arfvedsonite from Greenland. Amer. Min. 41, 509-512.

Saito, H. (1963) Synthesis of asbestos by isomorphous replacement in fluor-richterite, $NaCaNaMg_5Si_8O_{22}F_2$. Journ. Chem. Soc. Japan (Ind. Chem. Sect.) 66, 18-21. (ref. Min. Abs. 17, 669).

Saito, H., and K. Ogasawara (1959) Synthesis of various types of fluor-amphibole by isomorphic substitution. Journ. Chem. Soc. Japan (Ind. Chem. Sect.) 62, 976-978. (ref. Min. Abs. 15, 219).

Schreyer, W., and F. Seifert (1966) Synthetic amphiboles in the system Na_2O-MgO-SiO_2-H_2O and their significance for the chemistry of natural amphiboles. Proc. International Mineralogical Association, 5th General Meeting, Cambridge 1966 (abstract).

Segeler, C. G. (1951) First U.S. occurrence of manganoan cummingtonite, tirodite. Amer. Min. 46, 751-769.

Seki, Y. (1958) Glaucophanitic regional metamorphism in the Kanto Mountains, Japan. Jap. Journ. Geol. Geogr. 29, 233-258.

Serratosa, J. M., A. Hidalgo, and J. M. Vinas (1962) Orientation of hydroxyl bands in kaolinite. Nature 195, 486.

Shell, H. R., J. E. Comeforo, and W. Eitel (1958) Synthetic asbestos investigations: synthesis of fluoramphiboles from melts. U.S. Buer. Mines, Rept. Inves. 5417.

Shoda, T. (1954) On the anomalous optical properties of heikolite. Min. Journ. (Japan) 1, 69-83.

Shoda, T. (1956) Dependence of the optical absorption on the crystallographic orientation in heikolite. Min. Journ. (Japan) 2, 39-47.

Simpson, E. S. (1929) Contributions to the mineralogy of Western Australia, ser V. Riebeckite, Hamersley Range, N.W. Div. Proc. Roy. Soc. W. Australia 16, 25-40.

Sinclair, W. E. (1957) The Kliphius crocidolite deposits. Trans. Inst. Min. Metal. London, 66, 69-78.

Sipovskii, D. P., T. A. Makarova, and A. D. Fedoseev (1966) Crystallisation of fibrous amphiboles during hydrothermal synthesis. Zap. Vses. Min. Obshch. 95, 436 (ref. Min. Abs. 18.2).

Slaughter, M. (1966) Chemical binding in silicate minerals. Parts I-III. Geochim. Cosmochim. Acta 30, 299-339.

Smith, J. V. (1959) Graphical representation of amphibole compositions. Amer. Min. 44, 437-440.

Sørenson, H. (1958) The Ilímaussaq batholith. A review and discussion. Medd. om. Grønland. 162, no. 3.

Sørenson, H. (1960) On the agpaitic rocks. Rep. Int. Geol. Cong. 21st Session, Norden, pt. 13, 319-327.

Sørenson, H. (1962) On the occurrence of steenstrupine in the Ilímaussaq massif, Southwest Greenland. Medd. om Grønland, 167, no. 1.

Sørenson, H. (1966) On the magmatic evolution of the alkaline province of South Greenland. Rapp. Grønlands geol. Unders. no. 7.

Sørenson, H., J. Hansen and E. Bondesen (1969) Preliminary account of the geology of the Kvanefjeld area of the Ilímaussaq intrusion, South Greenland. Rapp. Grønlands geol. Unders. 18.

Steinfink, H. (1962) The crystal structure of a trioctahedral mica: phlogopite. Amer. Min. 47, 886-896.

Strauss, C. A., and F. C. Truter (1951) The alkaline complex at Spitzkop, Sekukuniland, eastern Transvaal. Trans. Geol. Soc. S. Africa 53, 81-130.

Strens, R. G. J. (1966) Infrared study of cation ordering and clustering in some (Fe,Mg) amphibole solid solutions. Chemical Communications no. 15, 1966, 519-520.

Strens, R. G. J. (1967) Spectroscopic studies of cation ordering in amphiboles. Conference on Physics and Chemistry of Asbestos Minerals. Oxford, 1967 (abstract).

Stubican, V., and R. Roy (1961) Infrared spectra of layer lattice silicates. J. Amer. Ceram. Soc. 44, 625.

Sundius, N. (1945) The position of richterite in the amphibole group. Geol. För. Förh. 67, 266-270.

Sundius, N. (1945) The Composition of eckermannite and its position in the amphibole group. Sveriges Geol. Unders. Årsbok 39, No. 8.

Sundius, N. (1946) The classification of the hornblendes and the solid solution relations in the amphibole group. Sveriges Geol. Unders. Årsbok 40, no. 4.

Sutherland, D. S. (1969) Sodic amphiboles and pyroxenes from Fenites in East Africa. Contr. Min. and Petr. 24, 114-135.

Sveshnikova, E. V., E. I. Lomeiko, Z. P. Ershova, and A. M. Usenko (1966) Fluorine containing magnesio-arfvedsonites from alkaline rocks of the Enisei Ridge. Tr. Mineral. Muz. Akad. Nauk S.S.S.R. 17, 224-228 (ref. Chemical Abstracts 1967, 1104780).

Sweatman, T. R., and J. V. P. Long (1969) Quantitative Electron-Probe Microanalysis of Rock-Forming Minerals. Journ. Petrology 10, 332-379.

Switzer, G. (1951) Mineralogy of the California glaucophane schists. Bull. Calif. Div. Mines and Geology 161, 51-70.

Taliaferro, N. L. (1943) The Franciscan-Knoxville problem. Bull. Am. Assoc. Petrol. Geol. 27, 109-219.

Taylor, S. R. (1966) The application of trace element data to problems in petrology. Physics and Chemistry of the Earth vol. 6, 133-213.

Temple, A. K., and R. M. Grogan (1965) Carbonatite and related alkalic rocks at Powderhorn, Colorado. Econ. Geol. 60, 672-692.

Thompson, J. B. (1947) Role of aluminium in rock forming silicates. Bull. Geol. Soc. Am. 58, 1232.

Thompson, J. B. (1959) Local Equilibrium in metasomatic processes, in "Researches in Geochemistry" vol. 1, 427-457 (ed. Abelson).

Tugarinov, A. I., V. B. Naumov, and E. Chang (1963) Experimental study of alkali-carbonate metasomatism. Geochemistry International 6, 584-595.

Tuttle, O. F. (1949) Two pressure vessels for silicate-water systems. Bull. Geol. Soc. Am. 60, 1727-1729.

Upton, B. G. J. (1960) The alkaline igneous complex of Kûngnât Fjeld, South Greenland. Medd. om Grønland 123, no. 4.

Upton, B. G. J. (1962) Geology of Tugtutôq and neighbouring islands, South Greenland. Part I. Medd. om Grønland 169, no. 8.

Upton, B. G. J. (1964) Geology of Tugtutôq and neighbouring islands, South Greenland. Part II. Medd. om Grønland 169, no. 2.

Ussing, N. V. (1912) Geology of the country around Julianehaab, Greenland. Medd. om Grønland 38.

Van der Plas, L. (1959) Petrology of the northern Adula region, Switzerland. Leidse Geol. Mededelingen 24, 418-598.

Van der Plas, L., and Th. Hügi (1961) A ferrian sodium-amphibole from Vals, Switzerland. Schweiz. Min. Petr. Mitt. 41/2 371-391.

Velde, B. (1967) A chloritoid and glaucophane mica-schist on Isle de Groix, Morbihan. Bull. Soc. franç. Min. Crist. 90, 265-266.

Verhoogen, J. (1962) Distribution of titanium between silicates and oxides in igneous rocks. Am. J. Sci. 260, 211-220.

Vermass, F. H. S. (1952) The amphibole asbestos of South Africa. Trans. Geol. Soc. S. Africa 55, 199-229.

Villiers, J. E., de (1949) Note on an unusual amphibole from Zesfontein, South-West Africa. Trans. Geol. Soc. S. Africa 51, 77-80.

Viswanathan, K., and S. Ghose (1965) The effect of Mg^{2+}-Fe^{2+} substitution on the cell dimensions of cummingtonites. Amer. Min. 50, 1106-1112.

Vlasov, K. A. (1964) The periodic law, isomorphism and paragenesis of minerals. Dokl. Acad. Sci. U.S.S.R. Earth Sci. Sect. 155, 162-164.

Vlasov, K. A., M. Z. Kuz'menko, and E. M. Eskova (1966) The Lovozero Alkali Massif.

Vogt, T. (1966) Amphibole group constitution and classification. K.G.L. Norske Vidensk. Selsk. Skr. no. 7, 1-55.

Wade, A., and R. T. Prider (1940) The leucite-bearing rocks of the west Kimberley area, Western Australia. Quart. J. Geol. Soc. London 96, 39-98.

Wahlstrom, E. E. (1940) Ore deposits at Camp Albion, Boulder County, Colorado. Econ. Geol. 35, 477-500.

Warren, B. E. (1929) The structure of tremolite $H_2Ca_2Mg_5(SiO_3)_8$. Zeit. Krist. 72, 42-57.

Warren, B. E. (1930) The crystal structure and chemical composition of the monoclinic amphiboles. Zeit. Krist. 72, 493-517.

Watson, K. D. (1955) Kimberlite at Batchelor Lake, Quebec. Amer. Min. 40, 565-579.

Wegmann, C. E. (1938) Geological investigations in southern Greenland. Part I. On the structural divisions of southern Greenland. Medd. om Grønland 113, no. 2.

White, A. J. R. (1962) Aegirine-riebeckite schist from south Westland, New Zealand. Journ. Petrology 3, 38-48.

Whitfield, H. J., and A. G. Freeman (1967) Mössbauer study of amphiboles. Conference on Physics and Chemistry of Asbestos Minerals. Oxford, 1967 (abstract).

Whittaker, E. J. W. (1949) The structure of Bolivian crocidolite. Acta. Cryst. 2, 312-317.

Whittaker, E. J. W. (1960) The crystal chemistry of amphiboles. Acta. Cryst. 13, 291-298.

Whittaker, E. J. W. (1967) The structure and chemistry of asbestos minerals. Conference on Physics and Chemistry of Asbestos Minerals. Oxford, 1967 (abstract).

Whittaker, E. J. W. (1968) Classification of the amphiboles. Proc. International Mineralogical Association, 5th General Meeting, Cambridge 1966, 232-242.

Whitten, E. H. T. (1954) Two arfvedsonitic rhyolite intrusions from Cloghaneely, Co. Donegal. Min. Mag. 30, 393-399.

Wilkins, R. W. T. (1968) The hydroxyl-stretching region of the biotite mica spectrum. Min. Mag. 36, 325-333.

Williams, D. W. (1966) Externally-heated cold-seal pressure vessels for use to 1200°C at 1000 bars. Min. Mag. 35, 1003-1012.

Winchell, A. N. (1945) Variations in the compositions and properties of the calciferous amphiboles. Amer. Min. 30, 27-50.

Winchell, H. (1963) Clinoamphibole regression studies. I. Regressions of optical properties and density on composition. Min. Soc. America. Spec. Paper 1, 267-277.

Wittels, M. (1951) Structural transformations in amphiboles at elevated temperatures. Amer. Min. 36, 851-858.

Wittels, M. (1952) The structural disintegration of some amphiboles. Amer. Min. 37, 28-36.

Witte, P., K. Langer, F. Seifert, and W. Schreyer (1969) Synthetische Amphibole mit OH-Überschuss in System Na_2O-MgO-SiO_2-H_2O. Die Naturwissenschaften 85, 114-115.

Woodard, H. H. (1957) Diffusion of chemical elements in some naturally occurring silicate inclusions. Journ. Geol. 65, 61-84.

Woolley, A. R. (1969) Some aspects of fenitisation with particular reference to Chilwa Island and Kanganku nde, Malawi. Bull. Brit. Mus. (Nat. Hist.) Min. 2, no. 4.

Wright, T. L. and D. B. Stewart (1968) X-ray and optical study of alkali feldspar: I. Determination of composition and structural state from refined unit-cell parameters. Amer. Min. 53, 38-87.

Wymond, A. P., and R. B. Wilson (1951) An occurrence of crocidolite near Robertstown, S. Australia. Trans. Roy. Soc. S. Australia 74, 44-48.

Yagi, K. (1953) Petrochemical Studies on the alkaline of the Morotu district, Sakhalin. Bull. Geol. Soc. Am. 64, 759-810.

Yoder, H. S. (1950) High-low quartz inversion up to 10,000 kg/cm^2. Trans. Amer. Geophys. Union 31, 827-835.

Zemann, J. (1968) Measurement and interpretation of infra-red pleochroism in minerals. Proc. International Mineralogical Association, 5th General Meeting, Cambridge 1966, 20-22.

Zussman, J. (1955) The crystal structure of an actinolite. Acta. Cryst. 8, 301-308.

Zussman, J. (1959) A re-examination of the structure of tremolite. Acta. Cryst. 12, 309-312.

Zwaan, P. C., and van der Plas (1958) Optical and X-ray investigation of some pyroxenes and amphiboles from Nagpur, Central Provinces, India. Proc. Koninkl. Ned. Akad. Wetenschap 61B, 265-277.

References which have only been derived from Deer, Howie, and Zussman 'Rock Forming Minerals" vol. II, Longmans, 1963, have been omitted from this reference list.

Addenda to the References

Papike, J.J. and J.R. Clark (1966). Crystal structure of glaucophane (Abstract). Geol. Soc. Amer. Meeting, 1965.

Ramberg, H. (1952). The origin of metamorphic and metasomatic rocks. University of Chicago Press, Chicago.

Whittaker, E.J.W. (1969). The structure of the orthorhombic amphibole holmquistite. Acta. Cryst., B25, 394-397.

CHEMICAL COMPOSITION OF MAGNESIUM RICH ALKALI AMPHIBOLES

	Winchite, Netra, India	Juddite, Madhyha Pradesh, India	Tirodite, W. Tirodi, Madhyha Pradesh, India	Richterite(1) Langban, Sweden	Richterite(2) Langban, Sweden	Richterite(3) Langban, Sweden
OXIDE	WT.%	WT.%	WT.%	WT.%	WT.%	WT.%
SiO_2	55.80	55.68	55.84	54.53	55.87	55.05
Al_2O_3	1.59	1.05	0.86	1.49	0.85	0.91
TiO_2	0.78	1.66	0.71	1.01	0.43	0.54
Fe_2O_3	10.92	10.88	7.08	2.35	2.08	2.26
FeO	0.51	tr.	tr.	tr.	tr.	tr.
MnO	1.71	2.29	8.38	2.96	3.17	3.47
MgO	17.14	15.67	17.34	22.87	21.69	22.38
CaO	2.02	2.19	2.78	6.70	7.22	6.67
Na_2O	6.72	7.72	3.92	4.64	4.44	4.64
K_2O	0.72	1.44	1.00	2.43	2.23	2.41
H_2O^+	2.09	2.02	1.98	1.02	2.02	1.66
H_2O^-	n.d.	0.05	0.10	-	-	-
F	tr.	tr.	n.d.	n.d.	n.d.	n.d.
Li_2O	n.d.	n.d.	n.d.	n.d.	n.d.	n.d.
Total	100.00	100.65	99.99	100.00	100.00	100.00
O F						
Total	100.00	100.65	99.99	100.00	100.00	100.00

Recalculated to 24 Oxygens

Si	7.81	7.83	7.92	7.74	7.82	7.77
Al^{IV}	0.19	0.17	0.08	0.25	0.14	0.15
Al^{VI}	0.07	-	0.06	-	-	-
Fe^{3+}	1.15	1.15	0.76	0.25	0.22	0.24
Ti	0.08	0.18	0.08	0.11	0.05	0.06
Fe^{2+}	0.06	-	-	-	-	-
Mn^{2+}	0.20	0.27	1.00	0.36	0.38	0.41
Mg^{2+}	3.58	3.28	3.67	4.84	4.53	4.71
Li	n.d.	n.d.	n.d.	n.d.	n.d.	n.d.
Ca	0.30	0.33	0.42	1.02	1.08	1.01
Na	1.82	2.10	1.08	1.28	1.21	1.27
K	0.13	0.26	0.18	0.44	0.40	0.43
OH	1.95	1.89	1.87	0.97	1.89	1.56
F	tr.	tr.	n.d.	n.d.	n.d.	n.d.

Those compositions which have been normalised to 100% have been determined mainly by X.R.F. methods (Holland and Brindle, 1966).

	Magnesioriebeckite, S. Westland, New Zealand	Glaucophane(1) 302-143-I Valley Ford, California	Glaucophane(2) 302-143-II Valley Ford, California	Magnesioarfvedsonite 27282 Grønnedal Ika, Greenland
	WT.%	WT.%	WT.%	WT.%
	56.41	58.24	57.06	54.20
	1.82	9.00	10.31	0.98
	0.21	0.02	0.27	0.01
	14.84	5.05	3.54	11.39
	4.69	7.38	11.02	4.24
	0.07	0.19	0.11	0.26
	12.65	11.21	9.29	16.29
	0.00	1.14	0.00	1.51
	6.95	5.85	6.50	7.85
	0.49	0.04	0.01	1.51
	1.87	1.88	1.89	0.71
	n.d.	n.d.	n.d.	0.10
	n.d.	n.d.	n.d.	2.35
	100.00	100.00	100.00	101.40
				100.41
	8.00	8.02	7.94	7.77
	-	-	0.06	0.17
	0.30	1.46	1.63	-
	1.58	0.52	0.37	1.23
	0.02	0.00	0.03	0.00
	0.56	0.85	1.28	0.51
	0.01	0.02	0.01	0.03
	2.67	2.23	1.93	3.48
	n.d.	n.d.	n.d.	n.d.
	0.00	0.17	0.00	0.23
	1.91	1.56	1.75	2.18
	0.09	0.01	0.00	0.28
	1.77	1.73	1.75	0.68
	n.d.	n.d.	n.d.	1.07

APPENDIX III CHEMICAL ANALYSES

Alkali Amphiboles from Ilimaussaq Intrusion, S.W. Greenland

	Pulaskite		Sodalite Foyaite		Naujaite		
	D.U.10917	D.U.10925	D.U.10943	D.U.10941	D.U.10942	D.U.10957	D.U.12837
OXIDE	WT.%	WT.%	WT.%	WT.%	WT.%	WT.%	WT.%
SiO_2	43.74	50.37	46.16	45.07	47.57	46.58	46.39
Al_2O_3	4.16	1.29	3.10	3.48	2.47	2.97	2.76
Fe_2O_3	8.43	11.58	9.24	8.38	11.92	11.20	8.47
FeO	27.52	22.74	25.02	26.41	23.00	22.66	26.30
MnO	0.76	0.59	0.83	0.64	0.50	0.60	0.57
ZnO	n.d.	0.18	0.08	0.07	0.07	0.07	0.06
MgO	0.20	0.26	0.00	0.13	0.00	0.85	0.10
Li_2O	n.d.	0.20	0.25	0.23	n.d.	0.20	0.25
TiO_2	n.d.	1.18	1.18	1.80	0.86	0.79	0.77
CaO	5.11	1.49	2.78	2.64	1.99	2.59	2.66
Na_2O	4.26	6.49	7.07	6.85	7.40	7.74	7.27
K_2O	1.37	1.49	1.86	1.69	1.75	1.48	1.81
H_2O^+	1.95	1.26	1.34	1.75	1.90	1.40	1.10
H_2O^-	n.d.	0.07	0.08	0.05	n.d.	0.15	0.00
F	n.d.	0.85	0.90	0.35	n.d.	1.47	0.30
Total	97.50	100.04	99.89	99.54	99.43	100.75	98.81
O F	n.d.	0.36	0.38	0.15	n.d.	0.62	0.13
Total	97.50	99.68	99.51	99.39	99.43	100.13	98.68

Recalculation of Analyses to 24 Oxygens

Si	7.23	7.91	7.43	7.27	7.57	7.37	7.59
Al^{IV}	0.77	0.09	0.57	0.66	0.43	0.55	0.41
Al^{VI}	0.04	0.15	0.02	nil	0.03	nil	0.12
Fe^{3+}	1.05	1.37	1.12	1.02	1.43	1.33	1.04
Fe^{2+}	3.80	2.99	3.37	3.56	3.06	3.00	3.60
Mn	0.11	0.08	0.11	0.09	0.07	0.08	0.08
Zn	n.d.	0.02	0.01	0.01	0.01	0.01	0.01
Mg	0.05	0.06	0.00	0.03	0.00	0.20	0.02
Li	n.d.	0.13	0.16	0.15	n.d.	0.13	0.16
Ti	n.d.	0.14	0.14	0.22	0.10	0.09	0.09
Ca	0.90	0.25	0.48	0.46	0.34	0.44	0.47
Na	1.36	1.98	2.21	2.14	2.28	2.38	2.31
K	0.29	0.30	0.38	0.35	0.36	0.30	0.38
OH	2.15	1.32	1.44	1.88	2.02	1.48	1.20
F	n.d.	0.42	0.46	0.18	n.d.	0.74	0.16
A	0.71	0.53	1.07	1.07	1.02	1.32	1.27
X	2.00	2.00	2.00	2.00	2.00	2.00	2.00
Y	3.96	3.72	3.83	3.91	3.54	3.79	4.56
YZX	1.08	1.25	1.13	1.09	1.33	1.16	0.45
Z	8.00	8.00	8.00	7.93	8.00	7.93	8.00
OH	2.00	2.00	2.00	2.00	2.00	2.00	2.00

	Kakortokite				Lujavrite			Alkali Granite	
	D.U.10931	D.U.10933	D.U.10936	D.U.10937	D.U.10930	D.U.10951	D.U.10942a	D.U.10919	D.U.10927
	WT.%	WT.%	WT.%	WT.%	WT.%	WT.%	WT.%	WT.%	WT.%
	47.53	48.05	47.85	45.68	50.52	49.76	49.52	49.81	49.65
	3.09	2.93	3.01	3.33	1.72	1.34	1.39	1.38	1.06
	9.89	10.69	10.63	8.59	10.83	12.68	12.15	12.20	8.59
	23.78	22.32	22.48	25.42	21.78	20.30	20.99	20.27	25.39
	0.85	0.81	0.74	0.65	1.31	1.28	1.11	0.95	0.97
	0.06	0.09	0.07	0.08	0.10	0.10	0.10	0.15	0.14
	0.48	0.39	0.66	0.85	0.00	0.04	0.00	0.39	0.09
	0.25	0.25	0.27	0.20	0.33	0.39	n.d.	0.23	0.20
	0.70	0.83	0.84	1.23	0.71	0.94	0.80	2.10	2.20
	1.70	1.37	1.76	3.58	0.10	0.21	0.24	0.67	0.94
	7.49	8.09	7.65	6.33	7.61	7.95	8.69	8.58	8.03
	1.87	2.04	1.91	1.56	3.07	3.25	2.87	1.42	1.32
	1.30	1.46	1.09	1.06	1.10	1.69	2.12	0.72	0.50
	0.12	0.07	0.10	0.25	0.16	0.10	0.14	0.10	0.12
	0.43	0.40	1.16	1.16	0.70	0.33	0.30	1.46	1.28
	99.54	99.79	100.22	99.97	100.04	100.36	100.42	100.43	100.48
	0.18	0.17	0.49	0.49	0.30	0.14	0.13	0.62	0.54
	99.36	99.62	99.73	99.46	99.74	100.22	100.29	99.81	99.94
	7.61	7.63	7.59	7.37	7.99	7.82	7.77	7.84	7.93
	0.39	0.37	0.41	0.63	0.01	0.18	0.24	0.14	0.07
	0.19	0.18	0.15	nil	0.31	0.07	0.02	0.12	0.12
	1.19	1.28	1.27	1.04	1.29	1.50	1.43	1.44	1.03
	3.18	2.96	2.98	3.43	2.88	2.67	2.75	2.67	3.39
	0.12	0.11	0.10	0.09	0.18	0.17	0.15	0.13	0.13
	0.01	0.01	0.01	0.01	0.01	0.01	0.01	0.02	0.02
	0.11	0.09	0.16	0.20	nil	0.01	nil	0.09	0.02
	0.16	0.16	0.17	0.13	0.21	0.25	n.d.	0.15	0.13
	0.08	0.10	0.10	0.15	0.08	0.11	0.09	0.25	0.26
	0.29	0.23	0.30	0.62	0.02	0.04	0.04	0.11	0.16
	2.33	2.49	2.35	1.98	2.34	2.42	2.64	2.62	2.49
	0.38	0.41	0.39	0.32	0.62	0.65	0.57	0.29	0.27
	1.39	1.55	1.15	1.14	1.16	1.77	2.22	0.76	0.53
	0.22	0.20	0.58	0.59	0.35	0.16	0.15	0.73	0.65
	1.00	1.13	1.04	0.97	0.97	1.11	1.63	1.01	1.03
	2.00	2.00	2.00	2.00	2.00	2.00	2.00	2.00	2.00
	4.13	3.96	3.91	4.20	4.01	3.75	3.55	3.74	4.52
	0.91	1.02	1.05	0.80	0.97	1.17	1.16	1.18	0.48
	8.00	8.00	8.00	8.00	8.00	8.00	8.00	8.00	8.00
	2.00	2.00	2.00	2.00	2.00	2.00	2.00	2.00	2.00

T136 MICROGRANITE

	PHENOCRYST 1			PHENOCRYST 2		PHENOCRYST 3			
SiO_2	49·75	49·09	49·52	48·10	48·86	49·28	49·18	50·04	51·58
Al_2O_3	0·58	0·42	0·61	1·27	1·02	0·70	0·70	0·66	0·36
Fe_2O_3	36·68	35·75	36·54	36·78	35·68	37·79	38·01	36·28	36·45
MnO	0·61	0·54	0·66	0·74	0·67	0·67	0·57	0·58	0·63
MgO	-	-	-	0·24	0·09	0·01	0·01	0·01	0·01
CaO	0·81	0·55	1·06	3·68	2·09	1·53	1·50	1·39	0·07
Na_2O	7·52	7·39	7·17	6·71	7·45	6·61	6·79	7·49	8·10
K_2O	1·00	1·21	1·11	0·90	1·34	1·08	1·08	1·22	1·24

TABLE 6 - 9 COMPOSITION OF LATE-STAGE ALKALI AMPHIBOLES IN SODA GRANITES

	AMPHIBOLES FROM RIEBECKITE GRANITE, N.HANTS, D.U.13170.				AMPHIBOLES FROM RIEBECKITE GRANITE SHEET GGU 86163		AMPHIBOLES FROM RIEBECKITE MICRO GRANITE DYKE (GRORUDITE) GGU 86157					
	CORE	RIM	CORE	RIM	1	2	3	4	1	2	3	4
SiO_2	46·42	48·68	46·65	46·75	49·95	50·84	51·00	50·64	50·99	51·79	51·29	51·19
Al_2O_3	1·20	1·09	1·04	0·61	0·81	0·92	0·80	0·70	0·20	0·13	0·18	0·46
TiO_2	0·64	0·28	0·60	0·33	-	-	-	-	-	-	-	-
Fe_2O_3	40·26	39·33	39·78	38·75	37·58	38·57	38·34	37·94	34·74	34·82	34·81	34·78
MnO	0·99	0·80	0·98	0·69	0·29	0·31	0·36	0·28	1·33	1·50	1·61	1·41
MgO	0·19	0·25	0·21	0·19	0·04	0·03	0·03	0·04	0·04	0·08	0·08	Tr.
CaO	2·47	0·23	2·45	0·27	0·46	0·18	0·34	0·74	0·06	0·10	0·06	0·50
Na_2O	6·06	6·42	6·05	6·84	7·45	7·75	7·44	7·14	8·04	7·86	7·32	6·47
K_2O	0·50	0·98	0·43	1·23	1·29	1·17	1·12	1·28	1·85	2·08	2·03	1·82

T.306

	1	2	3	4	5	6	7	8	9
SiO_2	51·41	51·37	50·78	49·66	50·64	51·59	50·80	51·42	51·02
Al_2O_3	0·46	0·53	4·39*	0·24	0·79	0·93	0·61	0·11	0·61
Fe_2O_3	36·97	39·11	37·20	38·53	37·05	38·33	37·16	36·47	37·44
MnO	0·66	0·94	0·92	0·78	0·94	1·00	0·97	1·14	1·28
MgO	0·48	0·30	0·49	0·36	0·90	0·55	0·64	0·68	0·65
CaO	1·79	3·16	4·03	3·21	4·30	2·46	3·14	4·44	2·67
Na_2O	6·21	4·37	3·98	4·40	3·69	3·46	4·43	3·83	6·56
K_2O	0·55	0·36	0·38	0·78	0·74	0·51	0·44	0·09	0·51

T142

	1		2	3	4	5	6	
SiO_2	50·59	48·33	48·76	47·39	47·59	50·67	49·71	51·08
Al_2O_3	0·53	0·97	1·32	1·27	1·18	0·92	0·71	0·35
Fe_2O_3	37·26	34·81*	35·21	34·74	33·73	35·00	35·47	38·38
MnO	0·97	0·72	0·64	0·63	0·55	0·57	0·73	0·87
MgO	0·33	1·09	1·37	1·30	1·16	1·42	1·24	0·51
CaO	3·64	4·95	5·44	6·67	5·76	5·02	4·59	3·94
Na_2O	3·98	4·91	4·78	2·74	3·84	4·39	5·17	4·18
K_2O	1·19	1·07	1·31	1·18	1·25	1·18	0·94	0·46

TABLE 6 - 6 COMPOSITIONS OF CO-EXISTING GLAUCOPHANE AND HORNBLENDE, N. SYROS. (X1172)

	GLAUCOPHANE	HORNBLENDE	GLAUC.	HORN.	GLAUC.	HORN.	GLAUC.	HORN.
SiO_2	56·51	53·01	55·58	53·17	57·18	53·25	56·18	53·59
Al_2O_3	8·32	4·46	7·88	4·96	7·94	4·85	8·12	4·22
Fe_2O_3	12·99	13·35	13·58	13·46	13·72	13·36	13·06	12·43
MgO	13·65	16·70	13·48	16·09	12·34	16·27	13·16	16·94
CaO	0·55	7·43	1·74	7·23	1·21	7·18	1·90	7·65
Na_2O	6·09	3·19	5·78	3·22	5·67	3·17	5·64	3·30